

**The Spectroscopic Characterization of
Mitochondrial Porin in Membrane Mimetic Systems**

by

Denice C. Bay

A Thesis Submitted to the Faculty of Graduate Studies of

The University of Manitoba

in partial fulfilment of the requirements of the degree of

DOCTOR OF PHILOSOPHY

Department of Microbiology

University of Manitoba

Winnipeg

Copyright © 2006 by Denice C. Bay

Thesis Abstract

Voltage-dependent anion-selective channels (VDAC), or mitochondrial porins, regulate the flow of metabolites across the mitochondrial outer membrane. They presumably span the membrane as β -barrels, but the residues forming the individual β -strands are unknown. This information is essential for understanding the structure and function of the protein. Using *Neurospora* VDAC as a template, published data were reassessed to delineate a unified model for porin structure Bay and Court 2002, which was subsequently refined in collaboration with Greg Runke Runke *et al.* 2006.

The focus of this work was the development and analysis of systems for maintaining high levels of folded porin for the acquisition of high resolution data needed for model testing. The conformation of hexahistidinyI-tagged *Neurospora* porin in detergent was probed by fluorescence, near-UV circular dichroism and ultraviolet absorption spectroscopy. Derivatives of tryptophan and tyrosine were also examined by fluorescence spectroscopy and UV absorbance spectroscopy to model the interactions between the detergents and the amino acid side chains in the protein. Detergent-specific levels of β -strand and tyrosine exposure were observed. In all cases, the two tryptophan residues reside in weakly asymmetric, hydrophobic environments, suggesting transient tertiary interactions. Porin solubilized in these detergents forms functional channels in liposomes and membrane insertion is accompanied by increased levels of β -strand and loss of protease sensitivity.

These data were used to develop mixed detergent folding systems. A mixture of SDS and dodecyl- β -D-maltopyranoside (DDM) supports a β -strand rich conformation at high protein concentrations. The tertiary contacts and protease resistance of the SDS/DDM-

solubilized porin are very similar to those of the protein following reconstitution into liposomes.

Finally, the role of sterols in porin folding was examined, as the addition of sterols to detergent-solubilized VDAC is required for channel formation in artificial membranes. Sterols do not alter the secondary structure of VDAC, and subtle alterations to tertiary interactions were detected, suggesting that sterols do not promote an insertion-competent structure, but rather facilitate insertion into artificial bilayers. In summary, this analysis of the folded states of detergent-solubilized porin has revealed a system that maintains high concentrations of mitochondrial porin in a state that is very promising for structural studies.

Acknowledgements

I would first like to acknowledge the funding that made the work presented in this thesis possible. This work was supported by Discovery Grants from the Natural Sciences and Engineering Research Council (NSERC) to Drs. D. Court and J.D.O'Neil, funds from the University of Manitoba Research Grants Program (D.A.C.) and a Manitoba Health Research Council Graduate Fellowship to D. Bay.

I would especially like to thank Deb for permitting me work in her lab. Through her infinite wisdom, guidance, support, and boundless patience I was able to produce work we could both be proud of. I would also like to thank, my laboratory co-hort and friend, Matt Young for his continued encouragement and support during these studies. I cannot put into words how much you both have helped me out during the tenure my studies and without their wonderful comedic timing I probably would have gone crazy. Thanks so very much!

Thank you to Drs. G. Hausner and I. Oresnik for all the advice and generous support they have given me during my studies. Also a special thank you to the members my examining committee Drs. J.D. O'Neil and E. Worobec for their support throughout this project. I would like to thank L. Chen, A. Tran, and W.A.T. Summers for excellent technical assistance as well as G. Runke, S. Theriault, M. Li, J. Galka, and D. Manley for valuable discussions and advice.

A very special thank you to my family (my Mom, Dad, Mark and Darlene, my siblings, Allan (and Dianne), Nicole, Diane, and Nicholas, and my aunt Wendy and nephews Marshall and Luke) my friends (Ian and Melissa), the makers of coffee, and to metal music. Without all of their support I would not have made it this far.

Table of contents	
Thesis Abstract	II
Table of Contents	V
List of Tables	IX
List of Figures	X
List of Copyrighted Material for Which Permission has Been Obtained	XII
List of Abbreviations	XIII
CHAPTER 1 Literature review	1
1.1 Mitochondrial porin function	1
1.2 Bacterial porins: conceptual models for VDAC	7
1.3 Circular dichroism spectropolarimetry of native and recombinant VDAC	11
1.4 Electron microscopy of two-dimensional VDAC arrays	14
1.5 What do predictive and experimental data tell us about the VDAC β-barrel?	16
1.6 Experimental contributions to the elucidation of VDAC structure	24
1.6.1 N-terminus	27
1.6.2 β -Barrel	28
1.6.3 Residues 21–46	28
1.6.4 Residues 47–104	29
1.6.5 Residues 105–135	30
1.6.6 Residues 136–212	32
1.6.7 Residues 213–283	34
1.7 VDAC Folding in vivo: relevance to bacterial porin folding?	37
1.7.1 Sorting Signals	37
1.7.2 Transport into the intermembrane/ periplasmic space	38
1.7.3 Integration into the outer membrane	40
1.8 OmpA folding in vitro: a β-barrel folding archetype	41
1.9 VDAC folding in vitro: self catalyzed oriented insertion	49

1.10 Thesis Objectives	50
CHAPTER 2 Spectroscopic analysis of the conformations of mitochondrial porin solubilized in detergent	52
2.1 Abstract	52
2.2 Introduction	53
2.3 Materials and Methods	59
2.3.1 Lipids, detergents, and amino acid derivatives	59
2.3.2 Expression and purification of His ₆ -porin	59
2.3.3 Solvent and detergent solubilization of His ₆ -porin	60
2.3.4 Liposome stock preparation	60
2.3.5 Proteoliposome preparation and swelling assays	61
2.3.6 Reconstitution of detergent-solubilized His ₆ -porin in liposome for spectroscopic analysis	62
2.3.7 Isolation of <i>N. crassa</i> mitochondria	63
2.3.8 Protease digestions of isolated mitochondria and His ₆ -porin reconstituted liposomes	64
2.3.9 Western blots of liposomes and <i>N. crassa</i> mitochondria	65
2.3.10 Fluorescence spectrophotometry	66
2.3.11 Ultraviolet (UV) absorption spectroscopy	67
2.3.12 Circular dichroism (CD) spectropolarimetry	67
2.4 Results	69
2.4.1 Solubility of His ₆ -porin in detergent systems	69
2.4.2 Reconstitution of His ₆ -porin into liposomes	70
2.4.3 Protease sensitivity of mitochondrial porin and detergent-solubilized His ₆ -porin reconstituted into liposomes	75
2.4.4 Characterization of His ₆ -porin reconstituted into liposomes by far-UV CD	80
2.4.5 Characterization of detergent-solubilized His ₆ -porin by far-UV CD	84
2.4.6 Fluorescence of tryptophan model compounds in detergent	90
2.4.7 Tryptophan fluorescence of His ₆ -porin in detergent	96
2.4.8 Tryptophan fluorescence of His ₆ -porin reconstituted into liposomes	99
2.4.9 Fluorescence of tyrosine model compounds in detergent	101
2.4.10 Tyrosine Fluorescence of His ₆ -porin in detergent	102
2.4.11 Tyrosine exposure in detergent-solubilized His ₆ -porin	104
2.4.12 Near-UV CD of His ₆ -porin in detergent and in liposomes	109
2.5 Discussion	112
2.5.1 Porin solubility	112
2.5.2 His ₆ -porin reconstituted into liposomes	114
2.5.3 The folded states of His ₆ -porin reconstituted into liposomes	117
2.5.4 Detergent-promoted folded states	119
2.5.5 Amino acid model compounds	122

CHAPTER 3 Two-step folding of recombinant mitochondrial porin in detergent	125
3.1 Abstract	125
3.2 Introduction	126
3.3 Materials and Methods	130
3.3.1 Detergents and amino acid derivatives	130
3.3.3 Detergent solubilization of His ₆ -porin	131
3.3.4 Liposome preparation and swelling assays	131
3.3.5 Protease digestions of isolated mitochondria and His ₆ -porin reconstituted into liposomes or solubilized in mixed detergents	133
3.3.6 Western blots of liposomes and <i>N. crassa</i> mitochondria	134
3.3.7 Fluorescence spectrophotometry	134
3.3.8 UV absorption spectroscopy	135
3.3.9 Circular dichroism spectropolarimetry	136
3.4 Results	137
3.4.1 Characterization of mixed detergent-solubilized His ₆ -porin by far-UV circular dichroism spectropolarimetry	137
3.4.2 Fluorescence of tryptophan model compounds in mixed-detergent systems	142
3.4.2 Fluorescence of tryptophan model compounds in mixed-detergent systems	139
3.4.3 Fluorescence of tyrosine model compounds in mixed-detergent systems	148
3.4.4 Tryptophan fluorescence of His ₆ -porin in detergent	149
3.4.5 Tyrosine fluorescence of His ₆ -porin in detergent	151
3.4.6 SDUV analysis of tyrosine exposure in detergent-solubilized His ₆ -porin	152
3.4.7 Near-UV circular dichroism spectropolarimetry	157
3.4.8 Reconstitution of SDS/DDM-His ₆ -porin into liposomes	163
3.4.9 Protease sensitivity of mitochondrial porin and SDS/DDM-solubilized His ₆ -porin reconstituted into liposomes	163
3.5 Discussion	170
CHAPTER 4 The influence of sterols on the conformation of recombinant mitochondrial porin in detergents and liposomes	177
4.1 Abstract	177
4.2 Introduction	178
4.3 Materials and Methods	181
4.3.1 Lipids, sterols, detergents, and amino acid derivatives	181
4.3.2 Expression and purification of His ₆ -porin	181
4.3.3 Sterol-detergent solubilization of His ₆ -porin.	182
4.3.4 Liposome stock preparation	183
4.3.5 Liposome swelling assays	183

4.3.6 Reconstitution of SDS-solubilized His ₆ -porin in ergosterol-containing liposomes for spectroscopic analysis	185
4.3.7 Fluorescence spectrophotometry	185
4.3.8 Circular dichroism (CD) spectropolarimetry	186
4.3.9 Protease digestions of His ₆ -porin reconstituted into ergosterol-liposomes	187
4.3.10 Western blots of His ₆ -porin-ergosterol-liposomes	188
4.4 Results	188
4.4.1 Liposome swelling assays of His ₆ -porin in the presence of ergosterol	188
4.4.2 Protease digestion of His ₆ -porin in ergosterol-liposomes	196
4.4.3 Characterization of detergent-sterol-solubilized His ₆ -porin and His ₆ -porin-ergosterol-liposomes by far-UV circular dichroism spectropolarimetry	197
4.4.4 Near-UV circular dichroism spectropolarimetry of detergent-sterol-solubilized His ₆ -porin	209
4.4.5 Tryptophan fluorescence of His ₆ -porin in detergent-sterol and sterol-liposomes	213
4.5 Discussion	220
4.5.1 The influence of sterols on His ₆ -porin conformation in detergents	220
4.5.2 His ₆ -porin reconstituted into liposomes in the presence of ergosterol	224
5.1 CONCLUSIONS	231
5.2 FUTURE DIRECTIONS	233
6. APPENDIX Protein and gene structures of mitochondrial porins	238
6.1 Introduction	238
6.2. Materials and Methods	242
6.2.1 Database searches for porin protein and gene sequences	242
6.2.2. PRALINE Alignment of porin sequences	243
6.3 Results and Discussion	244
6.3.1 VDAC alignments using PRALINE and secondary structure predictions	244
6.3.2. Comparison of VDAC gene structure	273
6.3.3 Intron location with respect to functional and structural motifs of VDAC	282
6.4 Conclusions	282
REFERENCES	284

List of Tables

Table 1.1	Secondary structure content of bacterial porins and VDAC	12
Table 2.1	Solubility of His ₆ -porin in detergent or solvents	71
Table 2.2	Far-UV CD analysis of His ₆ -porin solubilized in urea or detergents	89
Table 2.3	Summary of fluorescence spectroscopy of His ₆ -porin in detergents and solvents	93
Table 2.4	SDUV analysis of His ₆ -porin and model compounds	105
Table 3.1	Far-UV CD analysis of His ₆ -porin in mixed detergent systems	140
Table 3.2	Summary of fluorescence spectroscopy of His ₆ -porin in mixed detergents	147
Table 3.3	SDUV analysis of His ₆ -porin and model compounds in mixed detergents	156
Table 4.1	Summary of swelling data for His ₆ -porin proteoliposomes	193
Table 4.2	Summary of liposome swelling assay data	200
Table 4.3	Summary of fluorescence spectrophotometry maxima at excitation wavelength of 296 nm of His ₆ -porin in various detergents in the prescence or absence of sterol	216
Table 6.1	Characteristics of mitochondrial porin isoforms	240

List of Figures

Figure 1.1 Mitochondrial porin interactions with various compounds and proteins	4
Figure 1.2 The β -barrel of OmpF, as determined by X-ray diffraction	8
Figure 1.3 Predicted TM β -strands in <i>Neurospora crassa</i> VDAC	19
Figure 1.4 Models of NcVDAC	21
Figure 1.5 Cartoon diagram summarizing OmpA intermediates during insertion and folding into artificial membranes	46
Figure 2.1 Runke model for the TM arrangement of <i>Neurospora</i> mitochondrial porin	54
Figure 2.2. Swelling assays of SDS-His ₆ -porin proteoliposomes	73
Figure 2.3 Protease sensitivity of mitochondrial porin	77
Figure 2.4 Far-UV CD analysis and thermal denaturation of porin reconstituted from SDS into liposomes	81
Figure 2.5 Far-UV CD spectra of His ₆ -porin in detergent	86
Figure 2.6 Fluorescence analysis of amino acid compounds and His ₆ -porin	97
Figure 2.7 SDUV absorption analysis	106
Figure 2.8 CD spectropolarimetry of His ₆ -porin in the near UV region	110
Figure 3.1. Far-UV CD analysis of 5 μ M His ₆ -porin in mixed detergent systems	141
Figure 3.2. Thermal denaturation of His ₆ -porin as followed by far-UV CD	144
Figure 3.3 Fluorescence of His ₆ -porin in mixed detergent systems	153
Figure 3.4 Near-UV analysis of 33 μ M His ₆ -porin in mixed systems	159
Figure 3.5 Thermal denaturation of His ₆ -porin in SDS and SDS _{3.5} DDM ₁₈₀	161
Figure 3.6 Liposome swelling assays. SDS/DDM-His ₆ -porin liposomes	164

Figure 3.7 Protease susceptibility of porin in mitochondria, liposomes and detergent	167
Figure 3.8 Summary of the folded state of His ₆ -porin in SDS/DDM systems.	172
Figure 4.1 Swelling assays of proteoliposomes in the presence of sterols	189
Figure 4.2 Protease sensitivity of His ₆ -porin in ergosterol-containing liposomes	198
Figure 4.3 Far-UV CD of detergent-solubilized His ₆ -porin in the presence of sterols	201
Figure 4.4 Far-UV CD spectra of His ₆ -porin in ergosterol-liposomes	206
Figure 4.5 Near-UV CD of detergent-solubilized His ₆ -porin in the presence of sterols	210
Figure 4.6 Fluorescence analysis of His ₆ -porin in detergent-sterol systems	214
Figure 4.7 Fluorescence spectra of His ₆ -porin reconstituted into ergosterol-liposomes	218
Figure 5.1 Cartoon diagram summarizing the various conformational states of His ₆ -porin in detergents and liposomes	235
Figure 6.1. PRALINE alignment and secondary structure predictions of eukaryotic porin sequences	245
Figure 6.2. Summary of the secondary structure prediction and analysis	270
Figure 6.3. Analysis of mitochondrial porin gene structure	274

List of copyrighted material for which permission has been obtained

Bay, D. C. and D. A. Court. 2002. *Biochemistry and Cell Biology*. 80 (5): 551-562) with permission from the NRC Press

Runke, G., E. Maier, et al. 2006. *Biophysical Journal* 90 (9): 3155-64 with permission from the *Biophysical Journal*

List of Abbreviations

Å	angstrom
α	tyrosine exposure
αNcPor-N	rabbit antibodies directed against residues 7- 20 of <i>N. crassa</i> mitochondrial porin
A_{280 nm}	absorbance at 280 nm
A_{400 nm}	absorbance at 400 nm
ADP	adenosine diphosphate
ATP	adenosine triphosphate
ATR-FTIR	attenuated total reflection-Fourier transform infrared spectroscopy
BAK	Bcl-2-antagonist/killer protein
BAX	Bcl-2-associated protein X
Bcl-2	B-cell lymphoma protein 2
Bcl-XL	B-cell lymphoma protein XL
Bid	BH3 interacting domain protein
BLB	black or planar lipid bilayers
BOC-Y-OMe	N-t-butyloxycarbonyl-L-D-tyrosine-methyl ester
Cα	alpha carbon
CCA	convex constraint algorithm
CD	circular dichroism spectropolarimetry
CDL40	tumor necrosis factor (ligand) superfamily member 5
cDNA	reverse transcribed messenger ribonucleic acid into deoxyribonucleic acid
CMC	critical micelle concentration
cm	centimetre
CT	chymotrypsin
C-terminus	carboxyl terminus
CTXIII	cardiolipotoxin analogue III protein
DEC	dielectric constant
deg	degree
DDM	dodecyl-β-D-maltopyranoside
DNA	deoxyribonucleic acid
dmol	decimole
DPC	dodecyl phosphocholine
ε	extinction co-efficient
EDTA	ethylenediamine-tetraacetic acid
EG	ethylene glycol
FhuA	ferrichrome-iron uptake porin A
FT	freeze-thaw
g	gram
g	gravity
GLK	glycine-leucine-lysine
GFP	green fluorescent protein
H¹-NMR	proton nuclear magnetic resonance spectroscopy

His₆-porin	hexahistidinyl tagged recombinant <i>Neurospora crassa</i> mitochondrial porin
HsVDAC	<i>Homo sapien</i> voltage-dependant anion channel
HT	high tension
IM	inner membrane
I_{M1}	OmpA first membrane bound folding intermediate
I_{M2}	OmpA second membrane bound folding intermediate
I_{M3}	OmpA third membrane bound folding intermediate
IMS	innermembrane space
INS	insertion
Int_{max}	fluorescence intensity at λ_{\max}
I_w	OmpA water-soluble intermediate
kb	kilobase
kDa	kiloDalton
L	litre
LamB	lactam activated maltoporin B
LDAO	lauryl dimethylamine oxide
λ	wavelength
λ_{ex}	excitation wavelength
λ_{\max}	wavelength at which fluorescence emission or ellipticity is at maximum value
λ_{\max} Tyr	wavelength at which tyrosine-derived fluorescence emission is at maximum value
λ_{\max} Trp	wavelength at which tryptophan-derived fluorescence emission is at maximum value
λ_{\min}	wavelength at which ellipticity is at minimum value
LPS	lipopolysacharide
LUV	large unilamellar vesicle
M	molecular weight
mdeg	millidegree
min	minute
μg	microgram
mg	milligram
μL	microlitre
mL	millilitre
MLV	multilamellar vesicles
μM	micromolar
mM	millimolar
MRE	mean residue ellipticity
M	molar
mV	millivolt
N	OmpA native folded state
NADH	nicotinamide adenine dinucleotide
NAc-Y-NH₂	N-acetyl-tyrosine amide
NAc-W-NH₂	N-acetyl-tryptophan amide
NAc-W-OEth	N-acetyl-L-tryptophan ethyl ester

NcVDAC	<i>Neurospora crassa</i> voltage-dependant anion selective channel
Ni-NTA	nickel nitrolotriactic acid
nm	nanometre
nM	nanomolar
NMR	nuclear magnetic resonance spectroscopy
nS	nanoSeimens
N-terminus	amino terminus
OG	<i>n</i> -octyl- β -D-glucopyranoside
OM	outer membrane
Omp85	protein import channel outer membrane porin 85
OmpA	outermembrane porin A of <i>Escherichia coli</i>
OmpF	outermembrane porin F of <i>Escherichia coli</i>
OmpX	outermembrane porin X of <i>Escherichia coli</i>
PAGE	polyacrylamide gel electrophoresis
PC	phosphatidyl choline
PhoE	phosphoporin E of <i>Escherichia coli</i>
PMSF	Phenyl methylsulphonyl fluoride
PorA	<i>Neisserial meningitidis</i> porin A
PorB	<i>Neisserial meningitidis</i> porin B
pS	picoSiemen
PTP	permeability transition pore
θ	ellipticity
r	ratio of the depths of the tryptophan-derived fluorescence minima near 340 nm and 359 nm in SDF plots
RMSD	root mean square deviation
s	second
ScVDAC	<i>Saccharomyces cerevisiae</i> voltage-dependant anion channel
SDUV	second derivative of UV absorption spectrum
SDS	sodium dodecyl sulphate
SDS-PAGE	sodium dodecyl sulphate-polyacrylamide gel electrophoresis
SDS-UREA-PAGE	sodium dodecyl sulphate-urea-polyacrylamide gel electrophoresis
Sec	bacterial protein secretory complex in inner membrane
SEM	sorbitol, ethylenediamine-tetraacetic acid, MOPS buffer
SON	sonication
SUV	small unilamellar vesicle
T	trypsin
TBS	tris buffered saline
TM	transmembrane
TNF-α	tumor necrosis factor portein- α
TOM	translocase of the outer membrane
Tob	Topology of the outer membrane β -barrel protein
TROSY-NMR	transverse relaxation optimized spectroscopy-nuclear magnetic resonance spectroscopy
Trp	tryptophan
Tyr	tyrosine
U	OmpA unfolded state

UV	ultraviolet
VDAC	voltage-dependant anion selective channel
VDAC1	voltage-dependant anion selective channel isoform 1
VDAC2	voltage-dependant anion selective channel isoform 2
VDAC3	voltage-dependant anion selective channel isoform 3

CHAPTER 1 Literature review

Some of the material presented in this literature review has been published previously, and has been updated for the purpose of this review. In particular, sections 1.1 to 1.6.0, Table 1.1, and Figures 1.2-1.4 are taken from (Bay, D. C. and D. A. Court. 2002. *Biochemistry and Cell Biology*. 80 (5): 551-562) with permission from the NRC Press.

Sections 1.6.1 to 1.6.7 and Figure 1.4 panel D also contain material published in (Runke, G. Maier, E. Summers, W. A. Bay, D. C. Benz, R. Court, D. A. 2006. *Biophysical Journal*. 90 (9): 3155-3164), with permission from the Biophysical Journal. My contributions to this work were the construction of the genes encoding three porin variants studied, work on circular dichroism and fluorescence assays with W.A.T. Summers, and participation in figure generation and manuscript writing.

1.1 Mitochondrial porin function

The mitochondrial outer membrane (OM) is a semi-permeable barrier between the mitochondrion and the cytosol that allows the intracellular exchange of molecules, including products and substrates for the electron transport chain and oxidative phosphorylation, cofactors for mitochondrial enzymes, nucleotides for RNA and DNA synthesis, and cytoplasmically synthesized proteins. While mitochondrial protein transport across the OM depends on the TOM complex (translocase of the outer membrane; reviewed in Paschen and Neupert 2001), the remaining molecules traverse the membrane through water-filled channels formed by members of a family of small (around 30 kDa) pore-forming molecules. These proteins have been labelled voltage-dependent anion-selective channels (VDAC) (Colombini 1980), or mitochondrial porins (Freitag *et al.* 1982), by analogy with the pore-forming proteins in bacterial OMs.

Pore-forming proteins were first isolated from the mitochondrial OM of *Paramecium aurelia* by Schein and colleagues (1976). These proteins were introduced into “black lipid bilayers”, planar artificial membrane systems in which the conductive properties and ion selectivity of transmembrane (TM) channels can be determined. The resulting pores displayed what are now recognized as the classical features of mitochondrial porin. First, insertion of each channel into the membrane created a distinct increase in conductivity across the lipid layer. The conductivity of the channels could be decreased upon the application of voltage of at least 20 mV across the membrane. This voltage-dependent gating converted the pores from an open state of about 4 nanoSiemens (nS) conductivity to a partially closed state of less than 2 nS. In the open state, the pores were slightly anion selective, while in the closed state, they were more cation selective.

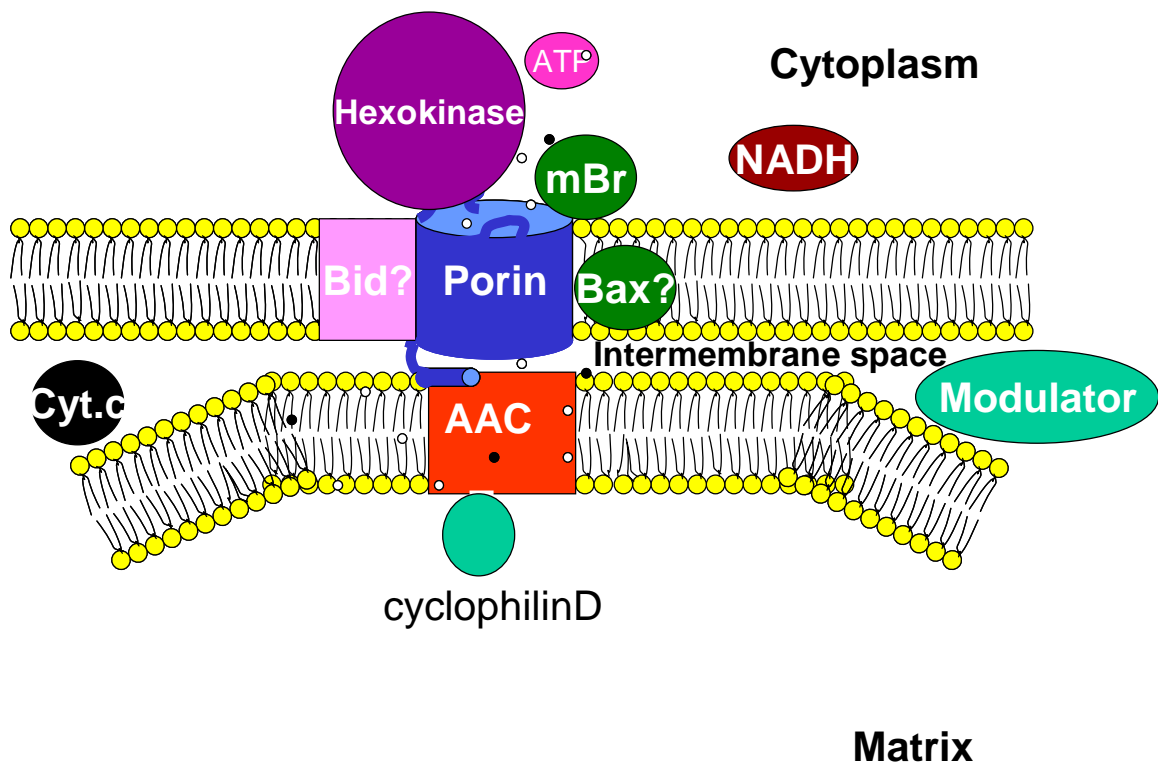
Multiple isoforms of porin have been detected in many organisms, particularly in fungi (for example Blachly-Dyson *et al.* 1997), insects (for example, Aiello *et al.* 2004, Graham and Craigen 2005) vertebrates (for example, Blachly-Dyson *et al.* 1993, Blachly-Dyson *et al.* 1994, Sampson *et al.* 1996, Sampson *et al.* 1997, Xu *et al.* 1999, Messina *et al.* 1999, Cesar Mde and Wilson 2004) and plants (for example, Heins *et al.* 1994, Elkeles *et al.* 1995, Abrecht *et al.* 2000, Al Bitar *et al.* 2003, Wandrey *et al.* 2004, also see Appendix 1 (Young, Bay, Hausner and Court, submitted)). Where channel forming activity has been assayed, at least one isoform forms pores with the features characteristic of classical VDACs. These isoforms generally are referred to as VDAC1 or porin (Blachly-Dyson *et al.* 1993), and unless otherwise indicated, these VDAC1s are the focus of the following discussion.

VDAC interacts with various substrates, such as ATP (Rostovtseva and Colombini 1996) and NADH (Zizi *et al.* 1994), and soluble and membrane-bound polypeptides. Proteins

such as hexokinase and creatine kinase have enhanced access to substrates by complexing with VDAC (Brdiczka *et al.* 1990; Brdiczka 1990, Brdiczka *et al.* 1994). VDAC and the adenosine nucleotide transporter form a complex at the contact sites between inner and outer membranes (Beutner *et al.* 1996) and with the addition of an 18-kDa ligand binding protein form the peripheral benzodiazepine receptor (McEnery 1992 see Fig. 1.1).

One of the most intriguing roles of porin is its proposed participation in the initiation of apoptosis. VDAC, the ADP/ATP carrier of the inner membrane, and cyclophilin D comprise the large permeability transition pore (PTP, Crompton *et al.* 1998, Woodfield *et al.* 1998). Interactions of VDAC with pro and anti-apoptotic members of the Bcl-2 family, appear to regulate the PTP, but the mechanism is currently unresolved. Shimizu and colleagues (Shimizu *et al.* 1999, Shimizu *et al.* 2000, Shimizu *et al.* 2000) propose that the pro-apoptotic protein Bax interacts with VDAC to form the PTP through which cytochrome *c* can be released, thereby triggering apoptosis. This interaction has not been replicated by Rostovstesa *et al.* (Rostovtseva *et al.* 2004) who have detected pore closure induced by the pro-apoptotic protein Bid, leading to the hypothesis that release of cytochrome *c* results from rupture of the mitochondrial membrane. Alternatively, Vander Heiden *et al.* (Vander Heiden *et al.* 2001) have evidence supporting an interaction between Bcl-XL and VDAC that promotes increased permeability of the outer membrane. Furthermore, interactions between an isoform of mammalian porin, VDAC2, and BAK, but not BAX, may regulate apoptosis by increasing

Figure 1.1 Cartoon diagram summarizing mitochondrial porin interactions with various compounds and proteins. Mitochondrial porin (blue cylinder) within the outer membrane is shown to interact with a variety of proteins and compounds from the cytosol, intermembrane space, inner membrane and matrix of the mitochondrion. Interacting proteins shown are as follows, hexokinase (purple circle) Bid (light pink rectangle), Bax (green oval), mitochondrial benzodiazepine receptor (green oval), ATP/ADP nucleotide carrier (red rectangle), cytochrome c (black circles), and VDAC modulator (light blue oval) and compounds ATP (pink oval), NADH (brown oval) and cyclophilin D (light blue oval). Small black and white filled circles represent small anionic and cationic species that diffuse through porin.



the susceptibility of BAK to proteolysis, thereby downregulating apoptosis (Cheng *et al.* 2003). Finally, cytochrome *c* release from porin-containing vesicles lacking Bcl-family proteins has been demonstrated, suggesting that porin oligomerization is responsible for PTP formation (Zalk *et al.* 2005). VDAC interactions with other compounds such as reactive oxygen species (Madesh and Hajnoczky 2001), may play an important role in regulating apoptosis by controlling the release of cytochrome *c* from the inter membrane space and may also act as a global regulator for the cell (as reviewed by Kim *et al.* 2006, Shoshan-Barmatz *et al.* 2006, Lemasters and Holmuhamedov 2006 see Fig.1.1).

From the first reports of the primary sequence of VDAC (Mihara and Sato 1985, Kleene *et al.* 1987), there has been great interest in the topology of the protein across the membrane. An understanding of the structure of the pore is essential for further investigation of its roles in protein complexes and of the mechanisms by which it gates and generates the characteristic anion selectivity. A variety of predictive and experimental methods have led to the conclusion that VDAC forms a β -barrel in the OM. A large body of data has been obtained to elucidate the precise structure of the barrel; experiments have used VDAC from several species, in environments ranging from detergent micelles to intact mitochondria. In this review, I will apply these results to VDAC from *Neurospora crassa* in an attempt to generate a unified model.

This review will also examine mitochondrial and bacterial porin folding both *in vivo* and *in vitro*, which is essential information for preparing the mitochondrial protein in forms amenable to structural analysis.

1.2 Bacterial porins: conceptual models for VDAC

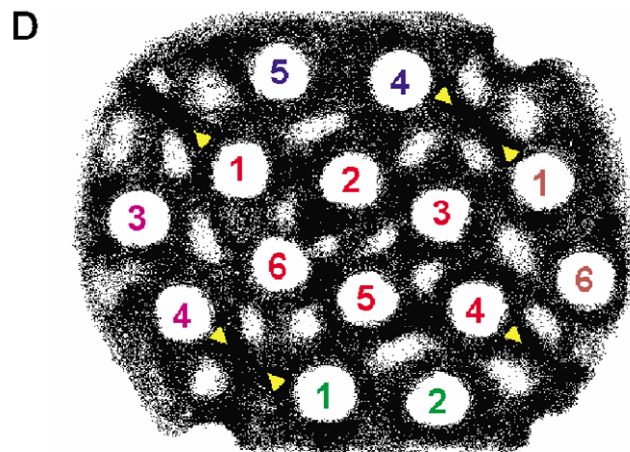
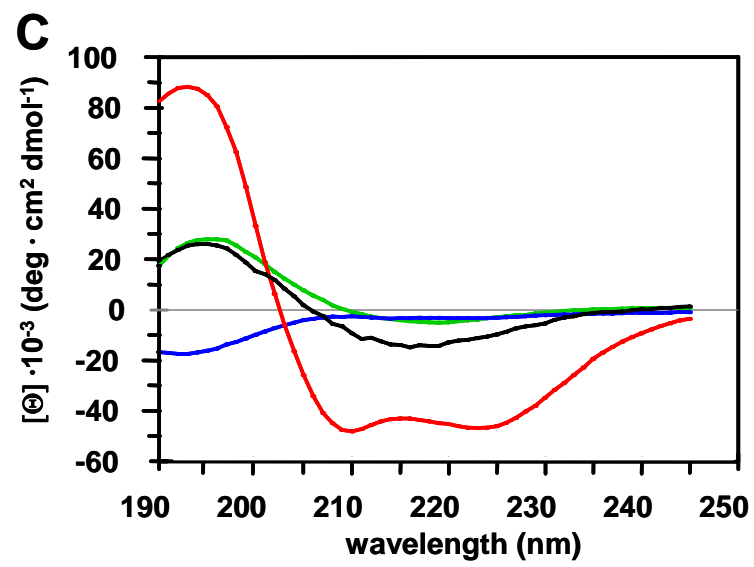
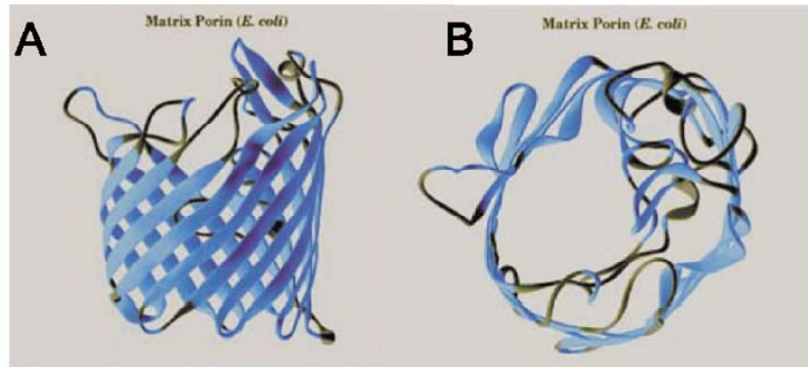
Bacterial porins have served as references for pore forming mitochondrial proteins that display high β -strand content, including the OM protein import pore (TOM40; Künkele *et al.* 1998) and VDAC, as will be discussed herein. Bacterial porins are useful for comparison due to the availability of a large number of high-resolution crystal (for example Weiss *et al.* 1991, Cowan *et al.* 1992, Cowan *et al.* 1995, Ferguson *et al.* 1998, Pautsch and Schulz 1998, Forst *et al.* 1998, Przybylski *et al.* 1996) and NMR (for example Fernández *et al.* 2001, Fernández *et al.* 2001, Arora *et al.* 2001, Tamm *et al.* 2003, Fernández *et al.* 2004) structures from members of each of the six bacterial porin families. Bacterial porin structure will be summarized briefly; for in-depth reviews of these structures, see Jap and Walian (1996) and Koebnik *et al.* (2000).

X-ray diffraction of bacterial porins reveals β -barrel channels (see Figs. 1.2A and 1.2B) that are composed of antiparallel amphipathic TM β -strands tilted at angles between 35 and 60° (Jap and Walian 1996, Koebnik *et al.* 2000). The β -barrels are composed of 8–24 TM β -strands that are present in multiples of two to satisfy hydrogen bonding requirements and twisting stresses (Murzin *et al.* 1994, Jap and Walian 1996, Koebnik *et al.* 2000). The typical bacterial porin surface diameter is 3.4 nm (*Escherichia coli* OmpF and PhoE and *Rhodobacter capsulatus* porin), but the pore diameter decreases at various points throughout the channel due to the presence of loops within the barrel (Fig. 1.2B), restricting transport to molecules of 600 Da or less (Jap and Walian 1996). Some bacterial β -barrel proteins are substrate specific, including LamB, a maltose

Figure 1.2 The β -barrel of OmpF, as determined by X-ray diffraction (Cowan *et al.* 1992).

A) Side and **B)** top views were obtained from files S3D00196 and S3D00195, respectively, from SWISS-3DIMAGE, accession No. P02931. In Fig. 1.1**A**, the extracellular face is on the top of the figure. In these diagrams, β -strands are indicated by thick ribbons and loops and turns by narrow cords. In Fig. 1.1**B**, note latching loop 2 extending away from the “left” side of the barrel and loop 3, which rests inside the lumen.

C) Sample CD spectrum, generated by D. Bay, of recombinant NcVDAC solubilized in 1% Genapol X-80. The spectrum was obtained as described in Runke *et al.* (2000) and deconvoluted using the convex constraint algorithm (CCA; Perczel *et al.* 1992) and the membrane protein data set of Park *et al.* (1992). The experimental data (black curve) and the deconvoluted data representing α -helix (red curve), β -strand (green curve), and random coil (blue curve) components are presented. Note that the experimental and β -strand curves are very similar in the diagnostic regions of 190–200 and 215–220 nm, indicative of the high β -strand content of NcVDAC. **D)** Schematic representation of two-dimensional NcVDAC arrays. This model is based on the data presented by Guo and Mannella (1993). Numbered open circles indicate low-density lumens of channels arranged in a six-member array; each array is identified by numbers of the same colour. Electron-dense protein arms extending between channels in adjacent arrays are indicated by pairs of yellow arrowheads aligned along the length of the arm or by single arrowheads directed away from the central array. Reproduced from Bay and Court (2002), with permission from NRC press.



and maltodextrin uptake porin, and FhuA, an iron–siderophore complex uptake channel. In contrast, OmpF is a general diffusion pore (Koebnik *et al.* 2000).

The β -strands in bacterial porins are connected by either short turns or long extracellular loops (Fig. 1.2), with each loop playing a specific role in channel gating, ion selectivity, size restriction, or structural support. Loop 3, for example, folds into the porin lumen in OmpF (Fig. 1.2B), creating a network of salt bridges and hydrogen bonding contacts to the barrel. In this constriction zone, charged residues contribute to the ion selectivity of the channel. Alterations to salt bridges and hydrogen bonding regions in loop 3 have been speculated to cause channel gating, making this loop a crucial structure for porin function (Koebnik *et al.* 2000). Loop 2, the shorter “latching” loop in OmpF, plays a more structural role by linking adjacent porin monomers together through hydrogen bonding and hydrophobic interactions leading to the formation of a trimer (Jap and Walian 1996, Koebnik *et al.* 2000).

Highly stable homotrimers, such as those of LamB and OmpF, are the characteristic quaternary structures of bacterial porins, making the OM resilient to changes within a harsh environment. Experimentally, porin trimers are resistant to denaturants such as 5 M guanidium hydrochloride and 2% sodium dodecyl sulfate (SDS) at 70°C. In addition, monomeric β -barrel proteins, such as OmpA, OmpX, and FhuA, and homodimers, such as phospholipase A (PldA), have also been identified (Koebnik *et al.* 2000). Mitochondrial porin homo-oligomers have been demonstrated by SDS-polyacrylamide gel electrophoresis (PAGE) of “water soluble” porin (Pfaller *et al.* 1985) and by chemical cross-linking of porin in artificial bilayers (Zalk *et al.* 2005). However, its native oligomeric state within the OM

has not been identified, and it has been suggested to vary depending on cellular conditions (as reviewed by Shoshan-Barmatz *et al.* 2006).

Critical differences exist between mitochondrial and bacterial porins. Mitochondrial porins are more readily denatured by urea (Popp *et al.* 1997), heat, and detergents like SDS (Shao *et al.* 1996). In addition, the environments of the bacterial and mitochondrial OM are very different, perhaps placing different constraints on pore structure. Finally, as discussed in this review, the presence of a short amino-terminal α -helix is unique to the mitochondrial porins. In spite of these differences, bacterial β -barrel proteins do provide a conceptual framework for the analysis of mitochondrial porin structure.

1.3 Circular dichroism spectropolarimetry of native and recombinant VDAC

Circular dichroism (CD) spectropolarimetry studies of native VDAC (isolated directly from mitochondrial OM) or of recombinant VDAC (prepared from *E. coli* over-expressing VDAC cDNA) support the hypothesis that VDAC spans the membrane as a series of β -strands (Mihara and Sato 1985, Kleene *et al.* 1987, Forte *et al.* 1987) (see Fig. 1.2C and Table 1.1 and references therein). VDAC from *N. crassa* and *Saccharomyces cerevisiae* have been examined in detail using this method. Native VDAC resuspended in a variety of detergents and reconstituted into artificial phospholiposomes generates CD spectra indicative of high β -strand content in the range of those of bacterial porins (30–70%; Table 1.1). Within the limits of this method, the β -strand content of recombinant “His₆-tagged” porin is the same as that of the native protein, demonstrating that these forms are comparable with those isolated from mitochondria and therefore will be very useful experimental tools (Popp *et al.* 1996, Koppel *et al.* 1998).

Table 1.1 Secondary structure content of bacterial porins and VDAC estimated from circular dichroism, X-ray diffraction and ATF-FTIR. All CD data presented were collected in the far-UV region.

Porin/VDAC	Secondary Structure (%)			References
	β-strand	α-helix [¶]	other [*]	
<i>N. crassa</i>				
VDAC _(native)	62 ^{a§} , 63 ^{b§} , 45 ^{b#}	30 ^{a§} , 7 ^{b§} , 12 ^{b#}	8 ^{a§} , 31 ^{b§} , 37 ^{b#}	Shao <i>et al.</i> 1996 Koppel <i>et al.</i> 1998
pH 4-4.5	38 ^{a§} , 30 ^{b#}	28 ^{a§} , 27 ^{b#}	34 ^{a§} , 45 ^{b#}	Shao <i>et al.</i> 1996 Koppel <i>et al.</i> 1998
65°C ^{a§}	0	30	70	Shao <i>et al.</i> 1996
His ₆ VDAC	45 ^{b#} , 47 ^{c¥} , 22 ^{b□}	12 ^{b#} , 31 ^{c¥} , 28 ^{b□}	37 ^{b#} , 22 ^{c¥} , 51 ^{b□}	Koppel <i>et al.</i> 1998 Runke <i>et al.</i> (2000)
residues 1-20	--	40-50 [£] , 30 ^b , 0 ^c	--	Guo <i>et al.</i> 1995
<i>S. cerevisiae</i>				
VDAC1 _(native) ^{b#}	30	27	37	Koppel <i>et al.</i> 1998
His ₆ VDAC1 ^{b#}	35	20	45	Koppel <i>et al.</i> 1998
Pea root plastid				
His ₆ porin ^b	70 [¥] , 10 [□] , 25 ^c	20 [¥] , 40 [□] , 35 ^c	10 [¥] , 50 [□] , 40 ^c	Popp <i>et al.</i> 1996
<i>Phaseolus vulgaris</i> - ATR-FTIR				
VDAC31 [¥]	50	14	39	Abrecht <i>et al.</i> 2000
VDAC32 [¥]	53	9	46	
<i>Rb. capsulatus</i> porin				
CD	70 ^a , 29 ^b , 30 ^c	18.5 ^a , 12 ^b , 27 ^c	11.5 ^a , 40 ^b , 44 ^c	Park <i>et al.</i> 1992
X-ray diffraction	57	6	37	Weiss <i>et al.</i> 1991

*Includes values for β -turn secondary structures

¶Includes values for α -helix secondary structures.

CD spectral data deconvoluted by:

^aYang's method (Chang *et al.* 1978, Yang *et al.* 1986)

^bVariable Selection method (Manavalan and Johnson 1987, Johnson 1990),

^cConvex Constraint Algorithm method (Perczel *et al.* 1992).

CD spectra collected in:

[§]2% octyl- β -glucoside (β -OG) pH 7,

[#]1% lauryl dimethylamine oxide (LDAO) pH 8,

[¥]1-2% Genapol X-80 pH 7,

[£]trifluoroethanol,

^bmethanol,

^cwater,

[□]1% sodium dodecyl sulfate (SDS)

Reproduced from Bay and Court 2002 with permission from the NRC press.

In contrast with the high overall β -strand character of porin, a synthetic peptide encoding the first 20 residues of *N. crassa* VDAC (NcVDAC) displays a high α -helical content (Guo *et al.* 1995; Table 1.1), as predicted (Mihara and Sato 1985, Kleene *et al.* 1987, Forte *et al.* 1987). In this respect, VDAC differs significantly from some bacterial porins, in which the N-terminus forms part of a β -strand (reviewed in Jap and Walian 1996).

Unfortunately, the CD data are not of sufficient precision to be used alone in creating or testing secondary structural models. There are several factors that contribute to variability in the percentage of β -strand detected. First, there are differences that result from the choice of detergent used to solubilize these membrane proteins in aqueous solution. For example, the structure of native VDAC from *Neurospora* is estimated to contain 63% β -strand when in OG but only 45% when the protein is in lauryl dimethylamine oxide (LDAO) (Table 1.1). This observation highlights the uncertainty regarding the ability of different detergents to mimic conditions in the OM. In addition, many detergents tend to interfere with data collection in the far-UV region, limiting the precision of the method. A more biologically-relevant system involves VDAC reconstitution into phospholiposomes, where protein function and structural composition can be determined (Shao *et al.* 1996). However, as with detergents, liposomes are not suitable for secondary structure estimations from CD spectra, due to light scattering at wavelengths below 200 nm and the low amounts of protein that can be incorporated within the membranes (Shao *et al.* 1996, Bathori *et al.* 1993).

Predicted secondary structure compositions also vary with the deconvolution methods and reference data set used. For example, the α -helical content of NcVDAC folded in OG varies from 7 to 30%, depending on the deconvolution algorithm (Table 1). Furthermore, as demonstrated for experiments involving *R. capsulatus*, the β -strand content determined by

CD analysis (30–70%; Park *et al.* 1992) does not precisely reflect the data obtained by X-ray diffraction (57%; Weiss *et al.* 1991).

In spite of these difficulties, CD is extremely valuable for comparing porins with respect to structural stability under different conditions (Shao *et al.* 1996, Koppel *et al.* 1998, this thesis). For example, experiments involving fungal VDAC reconstituted in OG or liposomes demonstrated a reversible loss of β -strand content and an increase in α -helical content at low pH (Table 1.1). In addition, this approach may provide information about conformational changes that can occur within the channel that may contribute to gating.

In summary, although CD spectropolarimetry is a valuable technique for obtaining general structural information, it fails to provide the precise data needed to construct an accurate model of VDAC. However, it is an excellent technique for examining conformational changes in VDAC under various conditions.

1.4 Electron microscopy of two-dimensional VDAC arrays

Two-dimensional VDAC arrays suitable for electron cryomicroscopy can be produced by phospholipase A2 treatment of isolated OM fractions (Mannella and Frank 1984, Mannella 1989). Electron microscopic analysis of NcVDAC arrays at 1–3 nm resolution shows unit cells composed of six VDAC, with protein extensions between channels in adjacent unit cells (Guo and Mannella 1993) (see Fig. 1.2D). Distinct pore-like structures are observed in which circular, stain-filled lumens of low density are surrounded by high-density protein walls (Mannella and Frank 1984, Mannella 1989). These analyses did not reveal the structural details of the channels but did show an irregular topology of the pore wall at the membrane surface, including slight extensions past the barrel wall (Mannella 1989, Thomas *et al.* 1991). Modelling of the NcVDAC C α backbone predicts a lumen diameter of 2.8 ± 0.1

nm with a ring thickness between 0.3 and 0.5 nm, which is in agreement with the diameters of 3–4 nm estimated by liposome swelling assays and 2 nm as determined by single channel conductance experiments in artificial bilayers (Colombini 1980, Freitag *et al.* 1982). It should be noted that the latter values are approximations, as they were calculated with the assumption of a perfectly cylindrical pore.

Subsequent attempts to refine the two-dimensional arrays of NcVDAC in the presence of amphipathic polyanions resulted in the loss of the protein “extensions” due to protein lattice contractions in the membrane crystals suggesting that the proteins adopt a compact conformation (Guo and Mannella 1993). It remains unclear whether the extensions are the N-termini involved in protein–protein contacts between adjacent channels or regions of a single pore that undergo conformational changes due to tighter channel packing (Mannella *et al.* 1992, Guo and Mannella 1993, Guo *et al.* 1995).

Three-dimensional analysis of the NcVDAC structure by applying Fourier reconstruction methods to aurothioglucose-embedded crystal arrays again predicted grooves and regions of uneven height and pore thickness and major protrusions of the pore above the surface of the phospholipid membrane (Guo *et al.* 1995). An irregular pore surface has also been visualized in phospholipid crystal arrays of human VDAC (HsVDAC). The pores in these arrays are 5.1–5.8 nm in diameter, between 4.0 and 4.6 nm in height, with 0.3–0.4 nm ring thickness (Dolder *et al.* 1999). These dimensions are slightly larger than those measured in fungal VDAC arrays but were obtained at lower resolution (5 nm) (Guo *et al.* 1995, Dolder *et al.* 1999). The use of phospholipids to construct the arrays led to membrane layer stacking effects that resulted in altered orientations of channels within the (x, y) plane of the array, making it difficult to resolve a higher quality structure of the channel (Dolder *et al.* 1999).

Refinements in crystallization techniques and the analytical approaches to the data for VDAC are being developed and are expected to result in higher resolution of the existing arrays (Verschoor *et al.* 2001). However, caution must be taken in drawing conclusions from these results, since VDAC was crystallized in alternating orientations and in an artificial membrane, not in mitochondrial OM fractions.

Attenuated total reflection-Fourier transform infrared spectroscopy (ATR-FTIR) was used to investigate the structure of *Phaseolus vulgaris* VDAC (Abrecht *et al.* 2000). In addition to providing independent estimates of β -strand content (Table 1.1), this method was able to demonstrate that the β -strands in the membrane are tilted at a 45° angle with respect to the axis of the barrel.

To date, X-ray diffraction (Cowan *et al.* 1992), Raman spectroscopy (Vogel and Jahnig 1986), and more recently solution state three-dimensional transverse relaxation optimized spectroscopy TROSY-NMR (Arora *et al.* 2001, Fernández *et al.* 2001, Fernández *et al.* 2004) of bacterial porins have been the best methods to precisely identify residues within TM regions and therefore should represent the next step in the structural analysis of VDAC.

1.5 What do predictive and experimental data tell us about the VDAC β -barrel?

Given the limitations of CD analysis and electron microscopy of VDAC arrays, other techniques such as primary sequence analysis, comparative algorithm-based computer analysis, immunolocalization methods, site-directed mutagenesis, and biotinylation experiments have been used to probe VDAC TM structure (see references in the following discussion).

There are a large number of deduced primary sequences for channels that display the characteristic properties (voltage dependency, anion selectivity) of VDAC (Mihara and Sato 1985, Kleene *et al.* 1987, Kayser *et al.* 1989, Troll *et al.* 1992, Ha *et al.* 1993, Blachly-Dyson *et al.* 1993, Blachly-Dyson *et al.* 1994, Heins *et al.* 1994, Fischer *et al.* 1994, Elkeles *et al.* 1995, Elkeles *et al.* 1997, Xu *et al.* 1999, Abrecht *et al.* 2000). These sequences show regions of alternating hydrophobic and hydrophilic residues, as expected for TM β -strands in a wall that surrounds an aqueous lumen (Benz 1994) (Fig. 1.3A). However, assignment of TM β -strands based solely on amphipathic sequences can be unreliable, as was demonstrated for bacterial porins (see Cowan *et al.* 1992).

Computer-based structural prediction algorithms have been developed and are based on comparisons of bacterial porin sequences with the corresponding resolved structures. Alignment of bacterial and eukaryotic porins by their hydropathy profiles has been one method of assigning TM regions in VDAC (Rauch and Moran 1994) (Fig. 1.3A, boxed residues, and Fig. 1.4A). By applying Kyte–Doolittle hydropathy index values in a moving window of residues, TM regions are predicted using a set of rules in which β -strands can be broken by residues with high potential for turn conformation (P, G, N, D, W) and the influence of strong turning residues is considered (see Rauch and Moran 1994, Fasman 1989, Kyte and Doolittle 1982). Using this approach, human, fungal (*S. cerevisiae*, *N. crassa*), and slime mold (*Dictyostelium discoideum*) VDAC were predicted to contain 16 TM β -strands (Fig. 1.4A) (Rauch and Moran 1994), reminiscent of OmpF (Figs. 1.2A and 1.2B) (Cowan *et al.* 1992).

A multiple alignment algorithm, the Gibbs sampler, has also been applied to VDAC primary sequences (Mannella *et al.* 1996). This technique determines residue frequencies in

motifs characteristic of TM β -strands in bacterial porin sequences of known structure and then uses the derived bacterial motifs to screen mitochondrial membrane proteins. The bacterial TM β -motif determined using the Gibbs sampler is an 11-residue sequence comprising alternating polar and nonpolar residues at the lipid–water interface of the lumen of the barrel. In this motif, charged residues are predicted to occur at high frequency at positions 1 and 10, aromatic groups occur at positions 11 and, less frequently, 3 and 9, and glycines are commonly found within central regions of the motif (positions 6 and 8) (Mannella *et al.* 1996). Position 11 is notable, as these residues contribute to the “girdle” of aromatic amino acids found at the interface between the outer leaflet of the membrane and the aqueous surroundings (discussed in Koebnik *et al.* 2000). Significant matches were made with bacterial motifs in three regions of yeast VDAC (ScVDAC); the corresponding regions of NcVDAC are indicated in Fig. 1.3A. This method could not exclude the possibility that more β -strands exist outside these regions, since it typically discovered fewer than half of the β -strand sequences in bacterial porins of known structure (Mannella *et al.* 1996).

Another forecasting technique utilizes a Neural Network, trained on bacterial OM proteins, to predict regions facing the periplasm and extracellular space as well as TM strands (Diederichs *et al.* 1998). The Neural Network calculates z -coordinates of $C\alpha$ backbone atoms, in the (x, y, z) plane, from the true membrane protein sequence. Periplasmic turns and loops have z values between 0.2 and 0.4 and extracellular loops have z values between 0.6 and 1.0 (Diederichs *et al.* 1998). We have used this program to analyze the NcVDAC primary sequence, assuming that the cytosolic and intermembrane space (IMS) segments are equivalent to extracellular and periplasmic regions in bacterial OM proteins. Excluding

Figure 1.3 **A)** *Neurospora crassa* VDAC primary sequence identifying experimentally examined regions of the protein and predicted TM β -strands. Boxed residues indicate β -strands predicted using the algorithm developed by Rauch and Moran (1994). Underlined amino acids highlight β -strands predicted by the hydropathy plot of (Benz 1994). Blue lines indicate β -strands estimated by the Gibbs sampler (Mannella *et al.* 1996). Red lines indicate β -strands predicted by the transFold web server (Waldispuhl *et al.* 2006). Pink lines define regions of VDAC bound by antibodies on the cytosolic side (cytosol+) or after OM lysis (cytosol-) from experiments performed by Stanley *et al.* (1995). Residues used in dual biotinylation studies (Song *et al.* 1998, Song *et al.* 1998) are labelled in red with the residue number of the second amino acid and its relative position (*cis/trans*) indicated in green below. **B)** Neural Network plot (Diederichs *et al.* 1998) predicting *N. crassa* VDAC secondary structure from its protein sequence. Peaks between z values of 1 and 0.6 indicate residues involved in β -turns or loops that face the cytosol, z values within 0.6–0.4 suggest regions that compose TM β -strands, and z values below 0.4 predict turns or loops facing the IMS. Residues at the apex of each strong peak or valley are labelled. **C)** Alignment of NcVDAC and ScVDAC primary sequences. Conserved residues are underlined in the yeast sequence. Residues indicated in red and green were replaced with amino acids of opposite charge (see text for details); red indicates replacements that did alter ion selectivity, while those shown in green did not (Blachly-Dyson *et al.* 1990, Peng *et al.* 1992, Thomas *et al.* 1993). Residue numbers are given above and below the NcVDAC and ScVDAC sequences, respectively. Reproduced from Bay and Court (2002), with permission from NRC press.

MAVPAFS₇DIAKSANDLLNKDFYH₂₃LAAGTIEVKSNTPN₃₈VAFKVTGKSTHDKVT₅₃

Cytosol - cisT53 transT69

SGALEGKFTDKP₆₈NGLT₆₉VTQTWNTANA₇₉LETKVEMADNLAKGLKAE₉₀GI FSFLPATN

cisS190 transT53 cisT53

ARGAKFNLHF₁₀₈FKQSNFHG₁₁₆RAFFDL₁₁₉LKGP₁₂₆T₁₃₅ANIDAIVG₁₄₃HEGFLAGASAGY₁₅₂D₁₅₆VQKA

cisT53 cisT53

AITGYSAAVGYHAPTYS₁₆₄AAITAT₁₇₈DNLSVFS₁₈₄S₁₉₀ASYV₁₉₂HKVNSQVEA₁₉₅GS₂₀₉KATWNSKGTGN₂₁₅

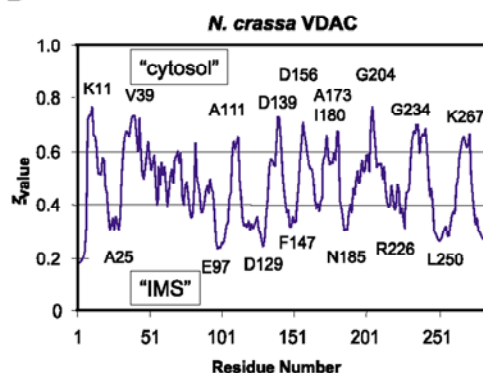
cisT69 Cytosol -

TVGLEVATKYRID₂₁₆DP₂₂₉VSVFKGKIN₂₃₈DR₂₄₀GVAAIAYN₂₄₁VLLREGVT₂₄₉LVGVGASFD₂₅₇D₂₆₄TQKLD

cisT53 Cytosol + cisT53

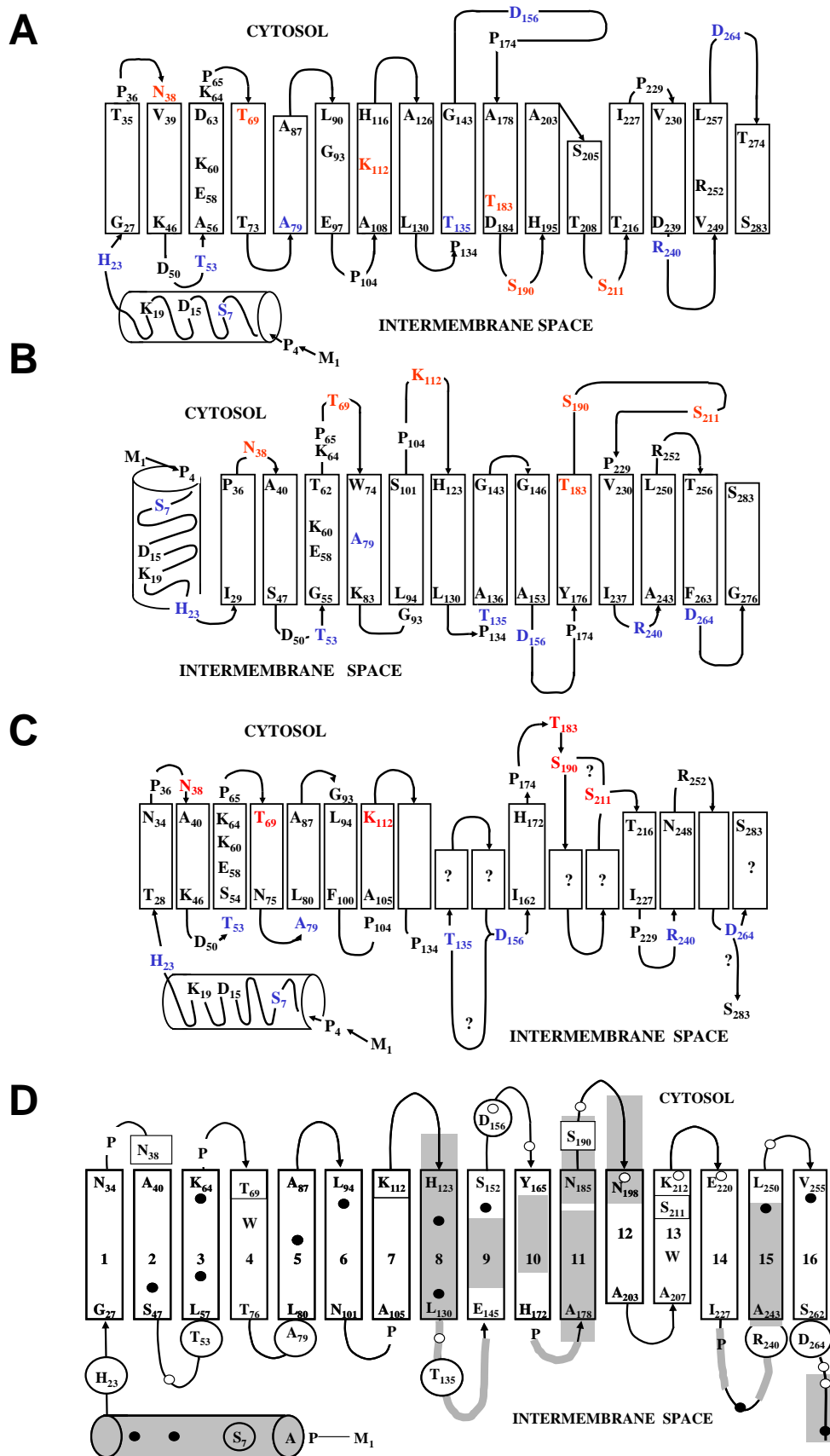
QATHKVGTSFTFES₂₇₄

Cytosol -



1 11 21 31 41 51
 Nc MAVPAFSDIKASANDLLN KDFY HLAAGT IE VKSNT PNNVAFKV TGK S--THDKVTSG
 Sc MS PPVYSDIS RNINDLL **N**KDFY HAT PAA **F**VDVQTT TANG I KFS LKA**K**QPV**K**DGP LST
 1 61 11 71 21 81 31 91 41 101 51 111
 Nc ALEGKFT DKPNGLTVTQTWNTANALETKEVMADNLAKGLKAEGI FSFLPATNARGAK
 Sc NVEA**K**LND**K**Q**T**GLGL**G**TQGSWNTNNLQ**T****K**LE F A N-L TP GL**K**NEL I TSLTPGV-A**K**SAV
 61 71 81 91 101 111
 Nc FNLHFKQSNFHFGRFA FDL--LKGPTANI DAIV GHEGFLAGA SAGYDVQKAA ITGYS A
 Sc LNTTFT E PFF T A**R**GAF**D**LC**L****K** SP**T**F VGDLTMAHEG IVGGA**E**F GY**D**I SA GS IS**R**YAM
 121 131 141 151 161
 Nc AVGYHAP T YSAA I TATDNL SVFS AS YYHKVN SQVEAG S KA T--WNSKTGN--TV GL
 Sc AL **S**YF **A**K**D** YS**L**GATLN--NEQITTV**D**F FQN **V**NAF LQVA--**K**A TMMNC**K**LPN SNVN I
 171 181 191 201 211
 Nc EVATKYR IDPVSF VKGK INDRGVAAIAYNVLLRE GVTLGVGASFDTQKLD QATHKV
 Sc **E**FATR YLPDASSQ**V****K**A**K**VSDSGI VTLAY **K**QL**L****R**PGV**T**LG**V**GS **S**FDAL**K**LS E PVH**K**L
 221 231 241 251 261 271
 Nc GT SFTFE S
 Sc GWSLS FDA

Figure 1.4 Models of NcVDAC. The models proposed by **A)** Rauch and Moran (1994) and **B)** Song *et al.* (Song *et al.* 1998) have been simplified to indicate the locations of residues discussed in the text. **C)** A proposed model of Bay and Court (2002) based on predictive and experimental evidence of *N. crassa* VDAC topology within the OM. The data were insufficient to predict structures for sections between T135-D156, S190-S211, and D264-S283; therefore, two possible conformations are presented and are indicated by question marks. **D)** The model of Runke *et al.* (2006) refining the predictions for the C-terminus region of NcVDAC. Deletions created by Runke *et al.* (2006) and by Popp *et al.* (1996) are shown by grey shaded regions. In all panels, cylinders indicate amino acids that compose the N-terminal α -helix. Arrows represent turns or loops between the indicated residues and TM β strands represented by rectangles. Red or circled residues indicate amino acids determined to be on the cytosolic side of the membrane to blue or squared residues using biotinylation assays (Song *et al.* 1998, Song *et al.* 1998) (see Fig. 1.3A). Small solid and open circles indicate residues shown by Blachly-Dyson *et al.* (1990) that either influence or do not influence the ion selectivity of the pore. Panels A-C were reproduced from Bay and Court (2002), with permission from NRC press and panel D was reproduced from Runke *et al.* (2006) with permission from the Biophysical Journal.



the C-terminus, where overlapping windows of sequence for analysis obviously do not exist, eight cytoplasmic and seven IMS loops are easily identified (Fig. 1.3B). This would suggest a β -barrel composed of at least 14 β -strands. This method of prediction may be better suited for identifying residues involved in turns or loops, since it cannot delineate individual β -strands in a long stretch of hydrophobic or amphipathic sequence, for example, residues 30–90 in NcVDAC (see Figs. 1.3A and 1.3B).

Another program referred to as transFold, has recently been developed to predict TM arrangement of β -barrel proteins and the interstrand residue interactions directly from primary sequence (Waldispuhl *et al.* 2006, Waldispuhl *et al.* 2006). Since integral β -barrel membrane protein structures are limited to bacterial outer membrane porins, this program uses pairwise interstrand residue statistical potentials derived from globular or cytoplasmic proteins to predict the secondary structure of TM β -barrel proteins (Waldispuhl *et al.* 2006). This approach differs from other available structure prediction programs because it does not require a training phase on known TM β -barrel structures, is the first to explicitly capture and predict long-range interactions, and can resolve smaller membrane proteins (≤ 200 residues) along with larger proteins. The web-version of transFold (Waldispuhl *et al.* 2006) was used to predict a β -strand TM topology of NcVDAC (Fig. 1.3A). Interestingly, this prediction algorithm identified a total of 18 potential TM β -strands, failed to identify the α -helical N-terminus, and instead predicted a β -strand in this region. In many cases this program also predicted β -turns of 2 residues, which are in poor agreement with bacterial porin β -turns that consist of generally three or more residues. 17 of the predicted 18 β -strands overlap with TM regions predicted using a simple hydropathy plot (Benz 1994), a feature that is part of the transFold algorithm (Waldispuhl *et al.* 2006, Waldispuhl *et al.* 2006). Thus, this new program

appears unable to predict a reasonable secondary structure arrangement for mitochondrial porins.

All of these prediction methods have three problems: (i) statistically, the prediction is only as good as the number of solved structures used for comparison, (ii) eukaryotic porins differ from most bacterial β -barrel proteins due to the presence of an α -helical N-terminus (Guo *et al.* 1995) and the lack of detectable loop regions within channel lumen (Mannella *et al.* 1992, Guo and Mannella 1993), and (iii) the predictions do not agree completely with experimentally obtained data determining the locations of residues in the OM, as discussed below.

1.6 Experimental contributions to the elucidation of VDAC structure

Experimentally obtained data from channel modifications, porin variants, or immunolocalization studies are critical to support or contradict secondary structure estimations for VDAC proteins. *Neurospora crassa* VDAC has been examined in the most detail (Stanley *et al.* 1995, Song *et al.* 1998, Song *et al.* 1998, Runke *et al.* 2006) due to the large amounts of intact mitochondria that can be easily isolated from this organism, facilitating isolation of the protein and *in organello* analysis. On the other hand, genetic tools for use in *S. cerevisiae* have been available for more than 10 years, allowing the *in vivo* expression of mutant VDAC genes that were generated by site-directed mutagenesis (Blachly-Dyson *et al.* 1990, Thomas *et al.* 1991, Peng *et al.* 1992, Zizi *et al.* 1995, Wandrey 2004). In the following sections, these methods will be briefly introduced, and a model of VDAC structure will be developed, based on the data accumulated for NcVDAC. Data obtained from yeast VDAC mutants will be discussed in relation to the *Neurospora* sequence, as most of the residues investigated in the yeast system are conserved in the *Neurospora*

protein (Fig. 1.3C). Caution must be taken when directly applying data obtained from the yeast system to *Neurospora* because not all residues are conserved and they may not share similar functions.

Site-directed mutagenesis has been used to generate yeast VDAC variants to identify residues involved in barrel or loop regions (Blachly-Dyson *et al.* 1990, Peng *et al.* 1992, Thomas *et al.* 1993). The underlying assumption in these studies is that replacing charged residues in the barrel, but not in exposed loops or turns, with ones of opposite charge should alter the ion selectivity of the channel.

Another approach to localizing particular residues utilizes cysteines in VDAC, either native residues in ScVDAC (Zizi *et al.* 1995) or those engineered into NcVDAC (Song *et al.* 1998, Song *et al.* 1998), which normally does not contain this amino acid. These cysteines can be covalently linked to biotin and the purified protein inserted into artificial bilayers. The effect of adding streptavidin, a biotin-binding moiety, to either the *cis* or *trans* side of the membrane, with respect to the side of porin addition, is then determined (Zizi *et al.* 1995). Assuming that most VDAC molecules assemble into the bilayer in the same orientation, the binding of the relatively bulky 60-kDa streptavidin molecule can only occur when the biotinylated cysteine residue is exposed to the side of the membrane to which streptavidin is added. Residues in the interior of the membrane can only be labelled if they are exposed to the aqueous phase and are physically accessible to streptavidin. The orientation of VDAC in the membrane has not been correlated with that in intact mitochondria, so residues can only be localized with respect to each other. This approach led to the development of the model shown in Fig. 1.4B.

CD has also proven to be effective in combination with fluorescence spectrophotometry and BLB experiments for characterizing the secondary structure of detergent solubilized His-tagged NcVDAC variants which harbour small deletions within potential membrane spanning segments (Runke *et al.* 2006). By combining calculated secondary structure composition, information concerning Trp residue environments in detergent-solubilized VDAC, and channel forming ability in BLBs, three classes of porin variants were determined. The first class produced large, stable pores, indicating deletions likely outside of β -strands. The members of the second class of porin variants had minimal pore-forming ability, indicating disruptions in key β -strands or β -turns and the third class of porins formed small unstable pores with a variety of gating and ion-selectivity properties (Runke *et al.* 2006).

By combining information determined from the model proposed in Bay and Court (2002) (Bay and Court 2002), and the data described in Runke *et al.* (2006) (Runke *et al.* 2006), TM arrangements within central and C-terminal portions of the protein have been refined and are discussed below (see Fig. 1.4 for models). The Runke *et al.* (2006) porin model was refined based on three assumptions: first, the variants with limited pore-forming ability lack at least part of a region normally in a β -strand or β -turn conformation that contributes to channel formation. Second, the assignment of strands based on the effects of single residue replacements on ion selectivity of yeast VDAC1 (Blachly-Dyson *et al.* 1990) uses the assumption that residues contributing to ion selectivity line the barrel, but residues in exposed loops or turns could also influence ion selectivity. Finally, the last consideration in model building was that the five proline residues in porin could not be included in β -strands because these residues disrupt secondary structure (Rauch and Moran 1994).

1.6.1 N-terminus

The location of the N-terminus (residues 1–20) of VDAC has been a source of debate. Initially, it was argued that it folds into an amphipathic α -helix that forms part of the barrel (Mihara and Sato 1985, Kleene *et al.* 1987, Forte *et al.* 1987). However, as described below, more recent evidence supports an IMS location for this part of the protein.

Electrophysiological characterization of ScVDAC mutants has been used to investigate the location of aspartate 15 and lysine 19 of ScVDAC, which are conserved in the *Neurospora* protein (see Fig. 1.3C). Site-directed mutagenesis of the yeast gene to convert D15 to a lysine (D15K) and K19 to glutamate (K19E) led to the production of channels with altered selectivity (Blachly-Dyson *et al.* 1990). The interpretation of these results is that the N-terminus is within the membrane and participates, along with a mobile “voltage sensor”, in the ion selectivity of the channel (Peng *et al.* 1992). It is important to note that residues outside the β -barrel could also contribute to ion selectivity, and therefore, the results do not necessarily dictate a membranous location for the N-terminus.

Immunolabelling experiments have also been used to address the orientation of the N-terminus. Extensive labelling of rat heart (Konstantinova *et al.* 1994, Konstantinova *et al.* 1995) and *Neurospora* (Stanley *et al.* 1995) mitochondria with antibodies against the N-terminal part of the corresponding VDAC only occurred after the OM had been ruptured, supporting an IMS location for the N-terminus.

Biotinylation experiments involving residue S7C of NcVDAC also indicate that the N-terminus is not embedded in the membrane. When biotinylated, this residue could be bound by streptavidin from either side of an artificial bilayer, suggesting that the N-terminus is flexible and may participate in gating activity (Song *et al.* 1998). Deletion of this segment

does not prevent pore formation in artificial bilayers (Popp *et al.* 1996, Koppel *et al.* 1998). Further, the addition of an N-terminal His-tag to NcVDAC (Court *et al.* 1996) or a green fluorescence protein to the N-terminus of mouse and human VDAC (Zaid *et al.* 2005, Schwarzer *et al.* 2002) does not prevent the assembly of these proteins into the mitochondrial OM. Taken together, these studies suggest that the N-terminus is likely external to the OM and exposed to the IMS (Figs. 1.4C and 1.4D).

1.6.2 β -Barrel

TM β -strand assignment is much more complicated than that of the N-terminus, due to the lack of consistent experimental evidence for central portions of the sequence. To facilitate the following discussion, it is much simpler to address sections of residues as opposed to identifying each TM β -strand individually, since there are several possible assignments that fit the experimental data. The following discussion refers to the models in Figs. 1.4C and 1.4D.

1.6.3 Residues 21–46

The putative α -helical region of the N-terminus extends to residue H23. This leaves a three- or four-residue turn, resulting in the first β -strand spanning residues T28 to N34 in NcVDAC (Rauch and Moran 1994). This assignment will result in a turn occurring from T35 to N38. After biotinylation of residue H23C, streptavidin binding occurred only on the side of VDAC addition to the membrane (*cis*) and created a channel with “type 2 conductance”, where the channel exists in the closed state and shows no voltage dependence (Song *et al.* 1998). These results support the previously described experimental data indicating that the N-terminus is mobile and furthermore indicate that it is in close proximity to the barrel opening.

The data obtained for residue N38, however, are less clear; membranes containing multiple N38C mutant channels are able to bind streptavidin from both sides. This produces “type 1 conductance”, where channel conductance is decreased compared with the wild-type, but voltage-induced gating is still observed, indicating that N38 is not required for the latter process (Song *et al.* 1998). In contrast, a single N38C VDAC is able to interact with streptavidin only from one side of the membrane, suggesting that the *cis/trans* nature of binding to multiple channels results from insertion of this variant in both orientations across the membrane. Based on the presence of the IMS-localized N-terminus, and β -strand breaking P36 in the centre of a predicted β -rich region (residues 27–46), we placed the first β -strand (β 1) from G27 to N34, N38 in a cytosolic loop, followed by a β -strand (β 2) continuing to K46 (Bay and Court 2002). This placement agrees well with Neural Network assignments of a cytosolic loop including N38 (Fig. 1.3B).

1.6.4 Residues 47–104

Residues S47 to V52 are not predicted to form a β -strand. The presence of T53 in an IMS turn fits well with biotinylation data placing both residues T53 and H23 facing the IMS (Song *et al.* 1998). Replacement of the ScVDAC residue corresponding to D50 in NcVDAC with a lysine created a pore with normal anion selectivity, as expected if this residue does not contribute to the charged nature the of barrel (Blachly-Dyson *et al.* 1990).

The next β -strand (β 3) could extend from S54 to K64 based on hydropathy alignment profiling (Rauch and Moran 1994). This assignment is supported by labelling of bovine VDAC E72 (corresponding to NcVDAC E58) with the hydrophobic compound dicyclohexylcarbodiimide, indicating that this residue is embedded in the membrane (De Pinto *et al.* 1993). Also, replacement of the ScVDAC equivalent of K60 and K64 in

NcVDAC produced less anion-selective pores, as expected for β -barrel residues (Blachly-Dyson *et al.* 1990). P65 is predicted to be associated with the short turn needed prior to the next putative β -strand (β_4), extending from T69 to N75 (Bay and Court 2002, Runke *et al.* 2006). The placement of T69 and T53 on opposite sides of the OM is supported by *trans* streptavidin binding to the double mutant T53C/T69C (Song *et al.* 1998). Using the same approach, it was shown that A79 and T53 reside on the same side of the membrane (Song *et al.* 1998), supporting the proposal of a turn between residues N75 and A79.

Residues L80 to F100 are estimated to form two β -strands (β_5 - β_6); however, the location of a short turn between the two strands is not uniformly predicted by the hydropathy plot (Benz 1994), the Neural Network (Fig. 1.3B), and the prediction algorithm of Rauch and Moran (1994) (see Fig. 1.3A). It is proposed that G93 is part of a turn, as glycine tends to end β -strands (Rauch and Moran 1994, Kyte and Doolittle 1982). Placement of the second β -strand in this region is supported by replacement of K95 with E in the *Neurospora* and yeast proteins (Runke *et al.* 2000, Blachly-Dyson *et al.* 1990). In both cases, a cation-selective channel was produced, as expected if a charged residue within the lumen is altered. Finally, P104 would act as an effective barrier to β -strand extension past L103. At this point a total of six β -strands are predicted and there is some general agreement between experimental data and predicted models (Figs. 1.4C, and 1.4D) (see Bay and Court 2002, Runke *et al.* 2006).

1.6.5 Residues 105–135

A single β -strand (β_7) from residues A105 to K112 follows the loop starting at S101 (Bay and Court 2002, Runke *et al.* 2006). This β -strand placement is contradicted by the observation that ScVDAC variant K108E does not display altered ion selectivity, as might be expected if K108E (K109 in NcVDAC) is in the barrel lumen (Blachly-Dyson *et al.* 1990). It

is important to note, however, that not every charged residue in the barrel lumen is expected to have a large-scale impact on ion selectivity.

One or two β -strands may form between residues K112 and L130 (see Fig. 1.3A) (Rauch and Moran 1994, Benz 1994, Mannella *et al.* 1996). Dual biotinylation experiments show that T53C and T135C bind streptavidin in a *cis* fashion, placing them on the same side of the membrane (Stanley *et al.* 1995, Song *et al.* 1998) and arguing against the presence of two β -strands between K112 and L130. Furthermore, K112 is *trans* to T53 (Song *et al.* 1998).

A single β -strand (β 8) between H123 to L130 is also supported based on the characteristics of the deletion variants 126porin and 120porin, which lack residues 126-136 and 120-143, respectively (Runke *et al.* 2006). β 8 partially overlaps a β -strand predicted by Benz (Benz 1994) and Rauch and Moran (Rauch and Moran 1994). These deletion variants were engineered with two glycyl residues at the junction of the deletions to compensate for the lack of flexibility that may arise if all of the residues separating two β -strands are deleted. 126porin and 120porin have very limited pore forming ability, suggesting that β -strands were disrupted in those variants (Runke *et al.* 2006). β 8 was positioned in these models to include R125 and R129 that influence ion selectivity and exclude K132 that does not (Blachly-Dyson *et al.* 1990). Its presence also maintains the relative orientations of K112 and T135 (Song *et al.* 1998). In contrast, a large extramembrane loop (S120 to H144) was predicted in this region by Casadio *et al.* (Casadio *et al.* 2002).

Together, these data support the placement of two β -strands, β 7 between A105 to K112 and β 8 between H123 to L130, followed by a turn including P134 (Fig. 1.4D).

1.6.6 Residues 136–212

Limited data were available for the segment A136 to S211, making it very difficult to identify regions of β -strand propensity (Bay and Court 2002). Dual biotinylation mutant T53C/D156C was *cis* for streptavidin binding, assigning D156 to either a turn or the end of a β -strand on the same side of the membrane as H23, T53, A79, and T135. Hydropathy data (Benz 1994) support the latter placement. Furthermore, ScVDAC residue D156 (also D156 in NcVDAC) is speculated to sit outside the barrel, since the yeast D156K variant did not display altered channel selectivity (Blachly-Dyson *et al.* 1990, Peng *et al.* 1992). This leaves us with two possibilities (Fig. 1.4C). Either the same large IMS loop includes T135 and D156 or two very short β -strands separate these two residues.

Deletion variants were analyzed to help resolve this dilemma (Runke *et al.* 2006). 147porin, lacking residues 147–151, does not form pores, suggesting that the ninth β -strand includes some or all of residues 147–151. β 9 (E145 to S152) places D156 outside the membrane where it would not contribute to ion selectivity, and D152 in the membrane (Blachly-Dyson *et al.* 1990). However, D156 is likely on the same side of the membrane as T135, suggesting its placement in the IMS (Song *et al.* 1998). To reconcile these data, a long loop in the IMS that spans T135 to D156 could be introduced and the assumption made that only D152 interacts with the channel in a way that regulates ion selectivity. However, this arrangement would leave only residues 157–164 to create a short β -strand and a loop to connect to β 10 (see below). Therefore, D156 is placed in a loop in the Runke *et al.* model, where it could be accessible from the IMS (Runke *et al.* 2006).

T183 and S190 are *trans* to T53 and exposed to the cytosol. T183 is eight residues to the C-terminal side of P174; accordingly, we predicted a β -strand from approximately I162 to

H172 (Bay and Court 2002), which combines segments of two β -strands predicted by hydropathy analysis (Benz 1994). Another region of uncertainty includes S190 to S211, both of which rest on the cytosolic side of the membrane, as demonstrated by biotinylation assays (Song *et al.* 1998). Again, this arrangement can be achieved through prediction of one large loop or two short β -strands. Antibodies directed against residues 195–210 of NcVDAC do not bind intact mitochondria (Stanley *et al.* 1995), arguing against a large cytosolic loop. The possibility remains, however, that such a large loop interacts strongly with the barrel lumen, leaving it inaccessible to the antibody. Replacements in ScVDAC that correspond to NcVDAC S192 (D192K; Blachly-Dyson *et al.* 1990), K206 (K205E), and K212 (K212E; Thomas *et al.* 1993) do not change ion selectivity, supporting the absence of a membrane-bound segment in this region.

A β -strand in the position of β 10 (Y165 to H172) is predicted by all algorithms, except that of Rauch and Moran (Rauch and Moran 1994) (Fig. 1.4A) and is supported by the limited pore formation of deletion variant 166porin, lacking residues 166-170, (Runke *et al.* 2006). β 10 has been placed to expose R164 to the cytosol, as this residue is not involved in ion selectivity, and to position P174 outside of the β -strand. Support for a second β -strand within this region (β 11) (A178 to N185) is the limited pore formation by the nested deletion variants 173porin (173-184) and 177porin (177-182) (Runke *et al.* 2006). The deletion in 173porin is predicted to disrupt β 11 and the turn between β 10 and β 11 (Fig. 1.4D), and this variant also has a significantly increased level of random sequence, which likely contributes to its inability to form pores. This region contains a predicted β -strand that is proposed by all models except that of Casadio *et al.* (Casadio *et al.* 2002). In the current transmembrane

arrangement, $\beta 11$ is also needed to maintain S190 on the same side of the membrane as N38, T69, and K112 (Runke *et al.* 2006).

The placement of two β -strands ($\beta 12$ -13) within this region is supported by the lack of pore formation by 195porin, lacking residues 195-198, and the likelihood that W209 resides in a hydrophobic environment, as shown by Trp fluorescence of the detergent-solubilized His₆-porin (Runke *et al.* 2006). The two strands must arrange S190 and S211 on the same side of the membrane, and keep N198 (E198 in yeast) and K212 in positions where they do not participate in ion selectivity. Finally, at least some of residues 195–210 must be exposed to the IMS. Given the number of residues available in this region, $\beta 12$ and $\beta 13$ are proposed to be only six residues long, the minimum needed to span the membrane (Koebnik *et al.* 2000).

1.6.7 Residues 213–283

All or part of $\beta 14$ is predicted by all algorithms (Rauch and Moran 1994, Benz 1994, Casadio *et al.* 2002, Bay and Court 2002), and spanning residues from T216 to I227 (Fig. 1.3A and 1.4). In the Runke *et al.* model, $\beta 14$ is placed between residues E220 and I227, leaving P229 in the IMS. Replacement of E220 does not affect ion selectivity; if it resides in $\beta 14$, it must be in a position that limits its contribution to ion selectivity. The presence of P229 places a turn in the IMS. Dual biotinylation results indicating that T53 and R240 are *cis* with respect to streptavidin binding suggest that this loop also includes R240 (Song *et al.* 1998). A loop spanning 228-242 is also predicted from the deletion variants 228porin and 238porin which formed large pores, suggesting that residues 228–232 and 238–242 are not involved in β -strand formation (Runke *et al.* 2006). Within this region, K234 contributes to

ion selectivity; this observation is compatible with a large loop that can enter the pore and contribute to the charge characteristics of the channel. 228porin forms a cation-selective pore, and the deleted segment includes D228, whose absence would decrease the net negative charge in the region, and therefore would be unlikely to directly shift the ion selectivity toward cations. Therefore, residues 228–232 are not direct determinants of ion selectivity, but perhaps interact with a region of the protein that is. P229 is also absent in 228porin, which may alter the topology of the loop that contains it, perhaps interrupting interactions responsible for gating. K234 and K236, which are required for the stable assembly of yeast VDAC1 into the mitochondrial OM (Smith *et al.* 1995), are also within this proposed loop.

A hydrophobic region separates R240 and D264, both of which are *cis* to T53 (Song *et al.* 1998). Part of this region is predicted to form a β -strand (Rauch and Moran 1994, Benz 1994); however, two strands must exist to place both R240 and D264 on the IMS side of the membrane. The N-terminal segment of this region is not amphipathic, but it could reside in the barrel, with lumen-facing hydrophobic residues interacting with another part of VDAC or another protein. By exchanging K248 with E in ScVDAC (N248 in NcVDAC), a channel with altered ion selectivity was created, supporting the placement of this residue in the barrel (Thomas *et al.* 1993). In contrast, the ion selectivity of ScVDAC R252E (Blachly-Dyson *et al.* 1990) is not changed, placing this residue outside the barrel.

The deletion variant 242porin (242–248) results in formation of unstable pores (Fig. 2, Runke *et al.* 2006) suggesting that β 15 occurs from residues A243 to L250. This β -strand placement would be necessary to place at least some of segment 251–268 facing the cytosol, where it would be accessible to antibody binding (Stanley *et al.* 1995) (Fig. 1.3A). Placing a β -strand between residues A243 and L250 places N248 (K248 in yeast) inside and R252

outside of the membrane, as predicted in Blachly-Dyson *et al.* (Blachly-Dyson *et al.* 1990). β 15 was not predicted by Benz (Benz 1994) or Song *et al.* (Song *et al.* 1998).

In the Runke model, β 16 (V-255 to S-262) places V255 in the membrane (Blachly-Dyson *et al.* 1990) and D264 on the same side of the membrane as R240. A β -strand at the position of β 16 is predicted in all models (Fig. 1.3 and residues E253 to D264 in Mannella *et al.* (Mannella *et al.* 1996)). Finally, all of the models presented in the literature (for examples, see Figs. 1.3A, 1.4A, and 1.4B) predict that the region spanning residues K273 to S283 forms a β -strand. ScVDAC variant D282K displays altered ion selectivity, further supporting a membranous location for the C terminus (Thomas *et al.* 1993). However, this putative β -strand cannot be accommodated in the TM arrangement because it would create an odd number of β -strands. The truncation variant Δ Cporin lacking residues 269–283 forms pores in artificial bilayers (Court *et al.* 1996), supporting the absence of a β -strand in this region. Finally, an epitope between 272 and 283 is accessible in mitochondria with ruptured outer membranes, suggesting that this segment resides in the IMS (Stanley *et al.* 1995). This prediction is also compatible with the fact that K267 and K274 do not contribute to ion selectivity. A role for E282 (D282 in yeast) in the process is possible if the C-terminus interacts with the channel, as may be suggested by fluorescence analysis (Fig. 1.4D) (Runke *et al.* 2006). In these studies, deletion of the C-terminus increases Trp fluorescence, suggesting that the C-terminal segment interacts with one or both of the two Trp residues, thereby quenching fluorescence of the detergent-solubilized protein. It is noteworthy that the amino and carboxyl termini of two β -barrel proteins of the outer membrane protein import machinery TOM40 (Künkele *et al.* 1998), and Tob55/Omp85 (Gentle *et al.* 2004) are also likely exposed to the IMS.

1.7 VDAC Folding *in vivo*: relevance to bacterial porin folding?

Understanding the *in vivo* assembly of integral β -barrel proteins into the outer membrane of gram-negative bacteria or mitochondria will provide a basis for analyzing the folded state of isolated porins, which in turn is essential for accurately determining the structure of the protein. In the following sections, the basic steps of transport and assembly of mitochondrial and bacterial porins into their respective outer membranes will be compared and contrasted.

1.7.1 Sorting Signals

In bacteria, integral outer membrane protein import has been best characterized for *E. coli* PhoE porin, and to a lesser extent for OmpF and OmpA. The precursor bacterial porin protein is translated in the cytoplasm with a cleavable, hydrophobic N-terminal signal sequence (Freudl *et al.* 1988) and targeted to the inner membrane secretory (Sec) protein complex (Manting and Driessen 2000). Additional C-terminal sorting information has been identified in *E. coli* PhoE. A variant PhoE protein, $\Delta F330$, lacking the C-terminal Phe residue demonstrated slower insertion kinetics than did wild-type PhoE, suggesting that this residue is required for directing porin insertion into the OM (Jansen *et al.* 2000).

In contrast, mitochondrial porin is synthesized outside of the organelle, in the cytosol (Mihara *et al.* 1982, Freitag *et al.* 1982). Poorly defined sorting information is located in the C-terminal portion (residues 269-283) of the *Neurospora* protein as deletion of this region prevents import into isolated mitochondria (Court *et al.* 1996). Further, Lys residues at positions 234 and 236 in *Saccharomyces* VDAC1 are required for assembly in the outer membrane (Smith *et al.* 1995, Angeles *et al.* 1999).

1.7.2 Transport into the intermembrane/ periplasmic space

In bacteria, the precursor porin traverses the cytoplasmic membrane via the Sec complex, to enter the periplasmic space. In contrast, VDAC import into the outer membrane first involves transport across the translocase of the outer mitochondrial membrane complex (TOM complex), into the inter-membrane space (reviewed by Rapaport 2005). The TOM complex is composed of the core Tom40 protein and subunit proteins Tom22, Tom7, Tom6, and Tom5. The signal required for targeting to the TOM complex is unknown, but apparently does not include the first 20 residues of the putative N-terminal α -helix (Court *et al.* 1996). Like many mitochondrial precursor proteins, mitochondrial porins targeted to the Tom20 complex (Schleiff *et al.* 1997, Schleiff *et al.* 1999) are sorted by the core TOM complex (Sherman *et al.* 2005, Sherman *et al.* 2006). Competitive import assays of porin into isolated yeast and *Neurospora* mitochondria, with intact or proteolytically-cleaved receptors, indicated that besides Tom20, mitochondrial porin insertion is dependent on the central receptor Tom22, and other components of the core complex, Tom5 and Tom7 (Krimmer *et al.* 2001). The *Neisseria* porin PorB can also utilize this import pathway, emphasizing that both bacterial porin and mitochondrial porin share signals recognized by the TOM complex (Muller *et al.* 2000, Muller *et al.* 2002).

Within the periplasmic space, bacterial porin begins to fold into an assembly-competent form that is possibly assisted by the chaperones Skp (Harms *et al.* 2001) and SurA (Lazar and Kolter 1996). Although chaperone-bacterial porin interactions have been demonstrated *in vitro*, the extent of chaperone assisted folding *in vivo* is uncertain since lipopolysaccharide (LPS) involvement has also been shown to assist OmpF assembly (Traurig and Misra 1999). However, even the LPS interaction with OmpF is not essential,

suggesting a variety of folding and assembly chaperones may be involved preparing porin for insertion into the OM (Visudtiphole *et al.* 2005).

As with bacterial porins, mitochondrial porins reside between two membranes before final assembly into the OM. Chaperone-mediated folding of mitochondrial porin within the intermembrane space has been proposed to involve the hetero-oligomeric components TIM8/13 which transport precursors from the TOM complex to the TIM23 translocase complex in the mitochondrial inner membrane (IM) (reviewed by Rapaport 2005). Yeast mutants lacking either TIM8 or TIM13 demonstrated reduced levels of β -barrel protein import, including that of VDAC suggesting that these proteins to play a dual role in protein import to the OM and to the IM (Hoppins *et al.* 2004). Homology between TIM8/13 and bacterial chaperones Skp and SurA protein has not been demonstrated to date.

Other possible VDAC chaperones that have been identified from two-hybrid screens involving human VDAC1 are the interacting proteins: dyenin light chain Tctex-1 and mitochondrial heat-shock protein 70/peptide-binding protein 74 (PBP74). Both proteins modulate mitochondrial channel forming activity in BLB experiments and co-localized with enhanced green fluorescence protein –human VDAC1 fusion proteins in HeLa cells (Schwarzer *et al.* 2002). The relevance of these findings is not clear, as mt-hsp70 is localized to the matrix, and not the intermembrane space (Schmidt *et al.* 2001, Voos and Rottgers 2002) and Tctex-1 is a cytoplasmic homodimeric protein that plays a role in actin remodelling within the cytosol (Chuang *et al.* 2005) and dyenin-cargo delivery from the post-Golgi to the plasma membrane (Yeh *et al.* 2006). Additionally, an as yet unannotated 54-kDa protein referred to as the VDAC modulator has been isolated from the IMS and alters porin channel formation and conductance in BLB experiments, suggesting that it may also

participate in VDAC assembly into the OM (Liu and Colombini 1991, Liu and Colombini 1992, Liu and Colombini 1992, Liu *et al.* 1994).

1.7.3 Integration into the outer membrane

VDAC is assembled into the outer membrane by the topogenesis of mitochondrial outer-membrane β -barrel proteins (TOB-SAM) complex (reviewed by Paschen *et al.* 2005). The TOB-SAM complex is a hetero-oligomer composed of the core component Tob55, as well as Tob37 and Tob38. *In organello* import of radiolabelled mitochondrial porin into mitochondria demonstrated that precursor porin is associated with His-tagged Tob55, supporting a role for Tob55 in porin topogenesis in the outer membrane (Paschen *et al.* 2003). Although the TOB-SAM complex appears similar to the chloroplast Toc complex based on β -barrel structure and function, only Tob55 has primary sequence homology to bacterial Omp85 (reviewed by Paschen *et al.* 2005), an essential protein involved in outer membrane protein assembly (Voulhoux *et al.* 2003, Gentle *et al.* 2004). Inactivation of the *omp85* gene in *Neisseria meningitidis* resulted in the accumulation of precursor PorA and PorB within the periplasm, indicating that Omp85 plays an important role in porin assembly into the bacterial OM (Voulhoux *et al.* 2003).

In summary, it appears that both bacterial and mitochondrial porins have similar mechanisms for importing and assembling into the OM, an observation that supports the endosymbiont theory of mitochondrial evolution (Paschen *et al.* 2003). However, unlike mitochondrial porin, all bacterial porins must undergo translocation across the inner membrane before assembling into the OM, creating a requirement for cleavable N-terminal targeting sequences not needed for VDAC precursor protein. Perhaps the α -helical N-terminus has some distant relationship to these bacterial Sec targeting sequences, although

the observation that deletion of the N-terminal 20 residues does not prevent import into isolated organelles suggests that a targeting function has been lost (Court *et al.* 1996). However, the amino-terminal sequences of fungal mitochondrial porins are one of the most highly conserved parts of the protein, suggesting that this segment has gained other functional relevance (Young *et al.* submitted). Similarities in porin folding, particularly at the OM assembly stage, likely will direct future studies into the *in vivo* assembly and folding of bacterial and mitochondrial porins.

1.8 OmpA folding in vitro: a β -barrel folding archetype

Given the complexities of the *in vivo* systems, many of the folding studies of bacterial porin have been carried out *in vitro*. Bacterial porin folding in detergents and artificial bilayers has been well characterized using a variety of biophysical techniques. *Escherichia coli* OmpA has been used extensively as a model for β -barrel folding. This protein has two functional domains; the first 171 residues of the N-terminus comprise the eight transmembrane β -stand barrel domain and the last 154 residues of the C-terminus form a globular periplasmic domain that interacts with peptidoglycan (Koebnik 1995). Structural characterization of this protein has primarily focused on the truncated N-terminal β -barrel region and a three-dimensional structure has been determined by X-ray diffraction (Pautsch and Schulz 1998) as well as by NMR spectroscopy (Arora *et al.* 2001) techniques. The β -barrel fragment of OmpA has served as a useful archetype for folding studies, both in detergents and lipid bilayers, due to its relatively small size, its monomeric state, and the availability of a well characterized three-dimensional structure. To simplify the discussion below, this N-terminally truncated variant will be referred to as OmpA.

Most detergent-based folding experiments involving OmpA utilize urea-denatured protein, which like many porins, has the ability to refold in a variety of detergents following isolation from inclusion bodies (Kleinschmidt and Tamm 1996, Kleinschmidt *et al.* 1999). Denatured OmpA refolds only in the presence of zwitterionic or non-ionic detergents with minimum acyl chain lengths ranging from C₈-C₁₂, which meet the requirement for detergent packing around the hydrophobic perimeter of the β -barrel. OmpA refolding is also influenced by the micellar state of the detergent; refolding could only be demonstrated at or above the critical micelle concentration of each detergent (Kleinschmidt *et al.* 1999). The precise mechanism for this detergent-induced OmpA refolding is not clear. OmpA refolding in the Kleinschmidt *et al.* experiments appears to occur as a two-state folding transition proceeding from random structure in monomeric detergent to β -strand in micellar detergent concentrations (Kleinschmidt *et al.* 1999).

The first instance of using mixed systems to refold OmpA denatured by urea or SDS was performed by the Henning lab, where denatured OmpA was diluted into Triton X-100 in the presence of LPS, resulting in refolded protein (Schweizer *et al.* 1978). The refolding process was described as spontaneous since the refolded protein was observable immediately after detergent-LPS addition. Similar experiments performed by Dornmair *et al.* (Dornmair *et al.* 1990) also demonstrated spontaneous re-folding of OmpA. The protein was extracted from the outer membrane, boiled in SDS and then diluted into the non-ionic detergent octyl- β -glucoside (OG). In this case, refolding occurred without LPS addition (Dornmair *et al.* 1990). To determine the requirements for re-folding in detergent, SDS-denatured OmpA was refolded in the presence of different concentrations of OG. Protein refolding occurred above an OG weight fraction (X_{OG}) of 0.7 (Ohnishi *et al.* 1998, Ohnishi and Kameyama 2001).

Based on this system, a pathway of refolding involving four kinetic phases was deduced from the three experimentally obtained rate constants (Ohnishi and Kameyama 2001). These rate constants were derived from OmpA CD and fluorescence spectra monitored over a period of days as the weight fraction of OG was increased. The spectral profiles were used to calculate the re-folding kinetics of OmpA in the detergent mixtures. The experimentally derived equations indicated the logarithmic dependence of OmpA re-folding on the weight fraction of OG and suggested that two potential folding intermediates may occur along the detergent refolding pathway during the spontaneous refolding of OmpA in detergent (Ohnishi and Kameyama 2001).

The characterization of the folded and unfolded states of OmpA along with other Omps in both detergents and membranes has been facilitated by monitoring the shift in apparent molecular mass when the proteins are electrophoresed through SDS-polyacrylamide gels. Schweizer *et al.* (1978) first demonstrated that unboiled OmpA migrated through, or electrophoresed through the gels with an apparent molecular mass of 30 kiloDaltons (kDa) whereas the boiled species had an apparent mass of 35 kDa. The folded state of the 30 kDa species of OmpA on SDS-PAGE could be correlated to channel activity in BLB experiments, since only protein isolated from these bands had demonstrated gating activity (Arora *et al.* 2000). Refolded OmpA can also be identified by its protease resistance since the 35 kDa species demonstrate higher susceptibility to degradation by proteases on SDS-PAGE gels (for examples see Dornmair *et al.* 1990, Kleinschmidt and Tamm 1996, Kleinschmidt *et al.* 1999).

Although, OmpA appears to spontaneously refold in detergents, OmpA membrane insertion and folding mechanisms have been examined in much greater detail. As in detergent-OmpA refolding experiments, urea-denatured protein also inserts and refolds

within artificial phosphatidyl choline-based lipid bilayers (Surrey and Jahnig 1992, Surrey and Jahnig 1995). In experiments similar to those first described for bacteriorhodopsin and UDP-glucuronosyltransferase (Scotto and Zakim 1988), OmpA spontaneously inserts into liposomes from a urea-denatured state but only at temperatures of 30°C and above (Surrey and Jahnig 1992). Three transitions along the OmpA *in vitro* folding pathway were identified and two intermediates, a misfolded water-soluble form and a partially folded, membrane-inserted form, were detected (Surrey and Jahnig 1995, Kleinschmidt and Tamm 1996). This three step mechanism of OmpA refolding within liposomes has been refined further through the application of time-resolved Trp fluorescence quenching (Kleinschmidt *et al.* 1999, Kleinschmidt and Tamm 1999, reviewed in Kleinschmidt 2003, Tamm *et al.* 2004, Kleinschmidt 2006 see Fig. 1.5). In the first, most rapid step (occurring within seconds to minutes), the urea solubilized protein is unfolded (U) and upon dilution in water rapidly becomes a hydrophobically collapsed water-soluble intermediate (I_W). The slower second stage (taking minutes to hours) involves three membrane bound intermediates, where the first intermediate is formed when I_W associates with the membrane (I_{M1}) in an aggregated arrangement characterized by disordered Trp residues. This aggregated form proceeds to the second intermediate (I_{M2}) where β -structure begins to develop but lacks tertiary contacts; this form has been termed a “molten disk”. The β -hairpin loops within I_{M2} translocate to the centre of the lipid bilayer and lack correct tertiary arrangements forming the final “molten globule” intermediate (I_{M3}) that proceeds to the native state (N).

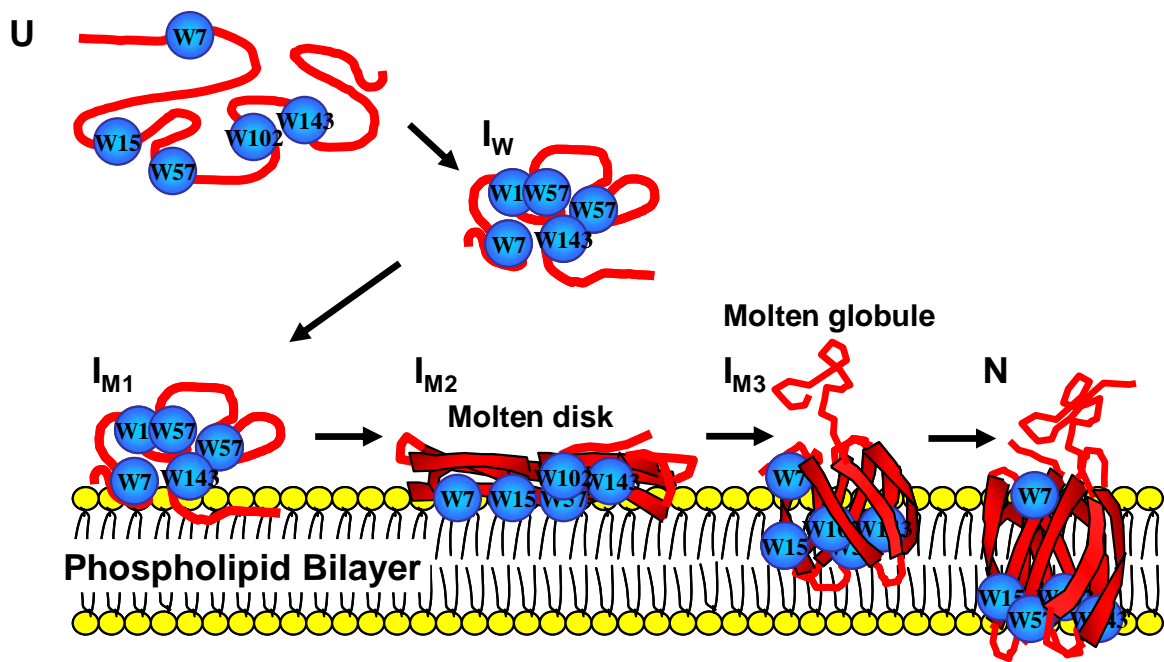
This kinetic folding mechanism of OmpA is influenced by a variety of factors such as membrane thickness, elasticity, and curvature, which affect both the kinetics and refolding of OmpA (Kleinschmidt and Tamm 1996, Kleinschmidt *et al.* 1999, Kleinschmidt and Tamm

2002, Marsh *et al.* 2006, Pocanschi *et al.* 2006). From these studies OmpA insertion occurred spontaneously only into highly curved SUVs, whereas spontaneous insertion into unstrained LUVs required phospholipid chain lengths of 12 C atoms only (Kleinschmidt and Tamm 1996, Kleinschmidt *et al.* 1999, Kleinschmidt and Tamm 2002).

A folding pathway parallel to that described for OmpA has recently been determined for a larger β -barrel porin, FomA of *Fusobacterium nucleatum*. FomA is composed 14 TM antiparallel β -strands and is assembled in artificial bilayers via a mechanism similar to the three step kinetic folding mechanism shown for OmpA (Pocanschi *et al.* 2006). Overall, the insertion and folding kinetics of FomA were much slower than those of OmpA. The insertion kinetics of both proteins were dependent on membrane thickness and lipid bilayer content. Since the elasticity and curvature of liposomes containing varying phosphatidylcholine lipid head groups influenced the insertion and folding kinetics of both OmpA and FomA, the folding of larger porins may have a greater dependence on particular lipid composition than does OmpA (Pocanschi *et al.* 2006).

To complicate the application of the OmpA folding studies described above to *in vivo* folding studies, two conformations of full length OmpA, have been suggested to form *in vitro* and possibly *in vivo*. The first is a two-domain 171-residue, 8-TM β -barrel with 154 residue periplasmic C-terminus and the second is a minor form that exists as a single β -barrel domain consisting of all 325 residues (Sugawara and Nikaido 1992, Sugawara and Nikaido 1994, Arora *et al.* 2000). A single domain β -barrel conformation of OmpA is proposed to occur *in vivo* based on the detection of OmpA C-terminal epitopes on the cell surface by antibodies against peptides within the OmpA C-terminus domain which is proposed to reside within the

Figure 1.5 Cartoon diagram summarizing OmpA intermediates during insertion and folding into artificial membranes as determined by time-resolved Trp fluorescence quenching (TDFQ) experiments (reviewed by Tamm *et al.* 2004, Kleinschmidt 2006). The unfolded state (U), water-collapsed intermediate (I_W), three membrane bound intermediates (I_{M1} , I_{M2} , and I_{M3}), and the native conformation (N) of OmpA are shown in the diagram. Trp residues W7, W57, W102, and W143 examined by TDFQ experiments are indicated by blue circles. Red lines with or without connecting red filled rectangles (β -strand) represent OmpA protein in the various stages of folding. Black arrows indicate each stage during OmpA insertion and folding into the phospholipid bilayer.



periplasm (Martin *et al.* 1993, Rawling *et al.* 1995, Singh *et al.* 2003). Planar lipid bilayer experiments involving full length OmpA protein at room temperature have also demonstrated two populations of channels: a major subset of small pores with conductances of 50-80 picoSiemens (pS) and a minor set of larger pores with 260-320 pS (Arora *et al.* 2000). Larger pores could not be demonstrated in BLB experiments using N-terminal domain OmpA protein suggesting that both domains are required to produce the both small and large channels (Arora *et al.* 2000). The channel size of full length OmpA appears to be influenced by temperature since small, low conductance channels are formed at temperatures of $\leq 21^{\circ}\text{C}$ (Zakharian and Reusch 2003, Zakharian and Reusch 2005) and upon incubation at higher temperatures channels could be converted to larger pores with increased conductance. Characterization of this transition revealed that it was irreversible, as incubation of full length OmpA large pores at physiological temperatures ($\geq 26^{\circ}\text{C}$) produced greater numbers of large pores with high channel conductance. At 37°C only large pores were observed (Zakharian and Reusch 2005). These large pores could only be converted back to small pores in the presence of denaturants such as SDS or urea. Based on these findings a two-domain OmpA structure may represent a partially-folded intermediate that is kinetically stable only at or below room temperature and will be converted to a one-domain β -barrel at higher temperatures (Zakharian and Reusch 2005). However, this one-domain OmpA state has not been structurally characterized apart from these experiments.

Overall, examination of the folding of C-terminally truncated OmpA in liposomes reveals that similar steps in the folding mechanism may apply to its folding in mixed detergent systems and that can be used to reflect the folding of much larger porins. The three

step folding mechanism of OmpA contrasts the three-stage mechanism proposed for integral α -helical membrane proteins (Engelman *et al.* 2003).

1.9 VDAC folding in vitro: self catalyzed oriented insertion

Unlike OmpA, the folding mechanism of mitochondrial porins has not been characterized in detail. Folding studies involving mitochondrial porins have primarily focused on its channel forming ability and orientation in black lipid bilayer experiments. The first studies that focused on mitochondrial porin insertion and orientation within these artificial bilayers were examined by Zizi *et al.* (1995). These experiments utilized two yeast VDAC variants (E145K or E152K), both with asymmetric voltage-dependence, meaning that gating could be induced only when the electric field was oriented in one direction across the membrane. Since the asymmetry was observed in the presence of a single channel or hundreds of channels, it was assumed that all channels were inserted in the same orientation. However, the initial channel orientation was random and the orientation of subsequent channels depended on the orientation of the pre-inserted VDAC within each membrane. This phenomenon was referred to as “auto-directed insertion”.

Studies by Xu *et al.* (Xu and Colombini 1996, Xu and Colombini 1997) expanded on this phenomenon by using native *Neurospora crassa* VDAC to characterize the folding ability of mitochondrial porin in various denaturing and non-denaturing solvents, prior to insertion into the artificial bilayers. In these BLB experiments, membranes were prepared from phospholipids and detergent-solubilized VDAC was added to one side of the compartment (the *cis* chamber). Perfusion of one chamber or the other with 2 M guanidinium chloride or 2 M urea in the presence of VDAC resulted in bursts of channel insertion; all channels were oriented in the same way. When urea solubilized porin was perfused in the

trans chamber, channel insertion increased by 10-60 fold in comparison to perfusion of the *cis* chamber. In contrast, when chambers were perfused with VDAC solubilized in sarcosine, a natural N-methyl derivative of glycine, channel insertion did not occur, suggesting that the denaturants enhance an insertion competent conformation of the protein (Xu and Colombini 1996). In bilayers devoid of inserted VDAC, perfusion with 5 M urea or 0.001 % Triton X100 solubilized VDAC resulted in a longer delays (240 sec) in channel formation than when added to the opposite side of initial channel addition/ insertion (14 sec) (Xu and Colombini 1997). This suggests that porin insertion is self-catalyzed by previously inserted VDAC and that this insertion is enhanced by denaturing solvents added to the opposite side of initial VDAC insertion.

Even though mitochondrial porins appear to possess self-catalyzed auto-directed insertion ability, questions such as how the initial porin channels form within these artificial membranes and how their orientation is determined still remain. Additionally, the concentrations of denaturing solvents used in the experiments by Xu *et al.* (1996, 1997) were exceedingly high in comparison to those in the OmpA folding studies, where maximum urea concentrations were in the mM range. However, as for bacterial porins, these experiments demonstrate that mitochondrial porins solubilized in detergents or denaturing solvents can insert and form conductive channels in artificial bilayers.

1.10 Thesis Objectives

As discussed in the above sections, the precise topology of mitochondrial porins within mitochondrial OM remains elusive. It is clear that structural analysis that goes beyond determining the secondary structure of mitochondrial porin is crucial to the understanding of the structure and function of this protein. Thus, the overall objective of this study is to

investigate the folded states of mitochondrial porins in membrane mimetic systems.

Ultimately, these results obtained from this work may reveal a detergent-based system able to promote a stable, β -rich, folded arrangement of mitochondrial porins suitable for analysis by NMR spectroscopy. Recombinant His₆-tagged *Neurospora crassa* porin (His₆-porin) was used as the starting material, and detergent systems were chosen for porin folding, as they have been used successfully for studies of bacterial β -barrel proteins.

Three specific approaches were used:

- i) To examine the folded state of His₆-porin in several single detergent systems.
- ii) To identify mixed detergent systems capable of promoting a β -rich folded state of His₆-porin.
- iii) To examine the role of sterols on porin arrangement in detergent and lipid-based systems.

The tools used in these investigations were circular dichroism spectropolarimetry in the near and far UV regions, fluorescence spectrophotometry, and ultraviolet (UV) absorbance spectroscopy. Additionally, liposome-embedded His₆-porin was probed by proteolytic digestion, and its channel forming ability measured through liposome swelling assays. These approaches also required the examination of model compounds in detergent, as such reference data were not available. This thesis presents the first extensive characterization of mitochondrial porins in detergent and liposomes, and provides the first system for generating a detergent-folded state of the protein that has strong similarities to the membrane-embedded form.

CHAPTER 2 Spectroscopic analysis of the conformations of mitochondrial porin solubilized in detergent.

The material presented in chapter 2 was written with the intent to submit to the Biophysical Journal in parallel with the material in Chapter 3. I completed all of the experiments outlined in this chapter. The data were analyzed and the manuscript was written with guidance and feedback from my advisor and Dr. J. O'Neil, who are co-authors on the manuscript.

2.1 Abstract

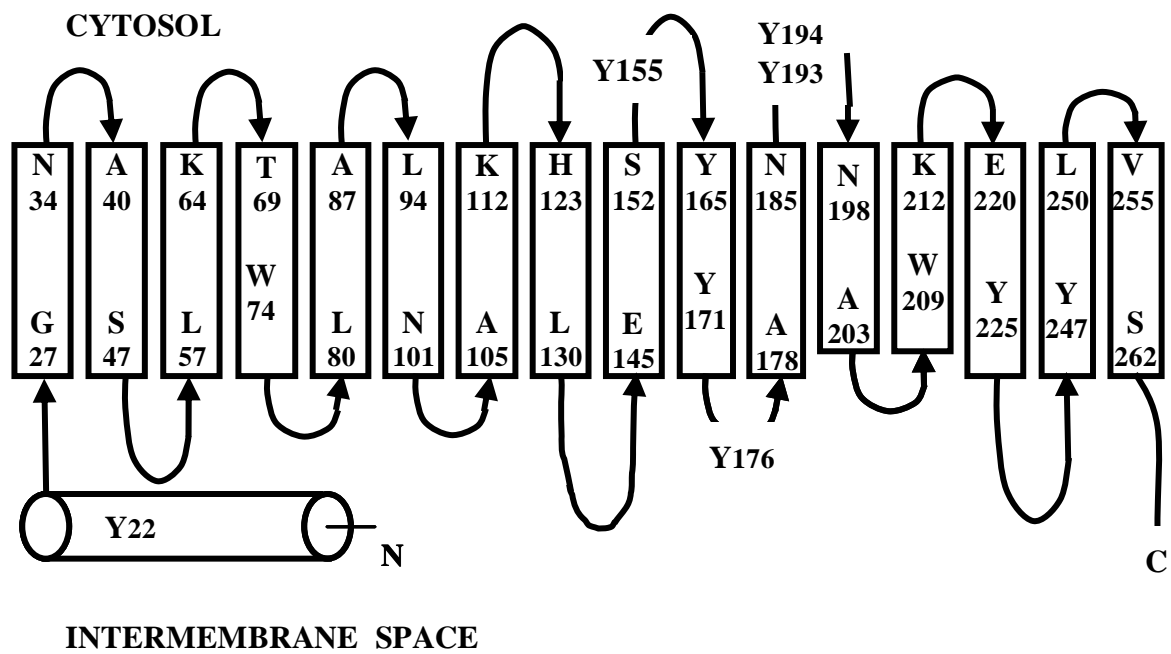
Far-UV circular dichroism (CD) spectropolarimetry has been the predominant tool for direct structural analysis of mitochondrial porins. In this study, the conformation of detergent-solubilized hexahistidinyI-tagged *Neurospora crassa* porin was probed by fluorescence, near-UV CD and UV absorption spectroscopy. N-acetyl and O-alkyl-ester derivatives of tryptophan and tyrosine were examined to model the interactions between the detergents and the amino acid side chains in the protein. Lauryl dimethylamine oxide (LDAO) promotes a β -sheet rich conformation, with most of the tyrosine residues in the hydrophobic interior of the protein-detergent complex. Sodium dodecyl sulfate (SDS) and dodecyl phosphocholine (DPC) promote different amounts of α -helix and β -strand, and tyrosine exposure is higher in SDS. In all three detergents, the two tryptophan residues in porin reside in hydrophobic environments that are weakly asymmetric, suggesting transient tertiary interactions. Porin solubilized in these detergents can be incorporated into liposomes by freeze-thaw methods, and form functional channels. Membrane insertion is accompanied by increased levels of β -strand and loss of protease sensitivity. Analysis of these partially-

folded states that are competent for membrane insertion provided the starting point for mixed detergent folding systems described in Chapter 3.

2.2 Introduction

Porins, the most abundant proteins in the mitochondrial outer membrane (for example see Mayer *et al.* 1993), are predicted to span the lipid bilayer as β -barrels (Fig. 2.1), as do their bacterial namesakes (Mihara and Sato 1985, Kleene *et al.* 1987, reviewed in Bay and Court 2002). The resulting channels permit the mitochondrial entry and exit of molecules, including substrates and products of the electron transport chain and oxidative phosphorylation, cofactors for mitochondrial enzymes, nucleotides for RNA and DNA synthesis, and cytoplasmically synthesized proteins (reviewed in Blachly-Dyson and Forte 2001). Interactions with many of these solutes are known to regulate the pore behaviour in black lipid bilayers, and presumably they have *in vivo* regulatory activity (Blachly-Dyson and Forte 2001). Furthermore, mitochondrial porin interacts with cytosolic hexokinase (Arora *et al.* 1993), and intermembrane space enzymes including creatine kinase (Brdiczka *et al.* 1994). Together with the inner membrane ADP/ATP carrier and cyclophilin-D, porin is believed to be a component of the permeability transition pore that may be the conduit for cytochrome *c* release upon initiation of apoptosis (reviewed by Crompton *et al.* 2002). Interaction partners in the outer membrane such as the pro- and anti-apoptotic regulators of the Bcl-2 family (Shimizu *et al.* 1999, Shimizu *et al.* 2000, Vander Heiden *et al.* 2001, Rostovtseva *et al.* 2004) further implicate porin in the regulation of apoptosis, which in turn is critical to key processes such as development, aging and the destruction of abnormal or virally-infected cells (Jacotot *et al.* 2000, Jacotot *et al.* 2001, Tsujimoto and Shimizu 2002). To

Figure 2.1. Model for the transmembrane arrangement of *Neurospora* mitochondrial porin (Bay and Court 2002, Runke *et al.* 2006). The N-terminus is at the left and proposed to reside in the intermembrane space. Potential β -strands are indicated by filled rectangles, and loops and turns by thin lines between them. The putative limits of the β -strands are indicated; it should be noted that neither the number of strands nor the precise position of any one strand has been confirmed by high resolution methods. Proteases trypsin (cleave protein at K and R residue sites) and chymotrypsin (cleaves protein at W, Y, and F residues sites) have 28 and 29 predicted cut sites respectively located throughout this protein sequence.



understand the abilities of this protein to form a gated, ion-selective pore and its roles in many important cellular processes, high-resolution structural information is required.

Numerous approaches have been taken to investigate the activity and structure of mitochondrial porin (see Chapter 1, reviewed by Bay and Court 2002). These studies have relied on detergent-solubilized porin, initially isolated from mitochondria in Triton X-100 (Colombini 1980, Roos *et al.* 1982), Freitag *et al.* 1982), lauryl dimethylamine oxide (LDAO; Aljamal *et al.* 1993), or Genapol X-080 (Troll *et al.* 1992). Detergent-solubilized native porin inserts into black lipid bilayers upon the application of voltage and forms conductive channels (Colombini 1980; Freitag *et al.* 1982). The pores are anion-selective in their high conductance open state, but are converted to a slightly cation-selective partially-closed state with increased voltage, leading to their alternative designation as voltage-dependent anion channels (VDAC, Colombini 1980). Detergent resuspended mitochondrial porins reconstituted into liposomes have also demonstrated channel forming activity (Colombini 1980, Colombini *et al.* 1987). These liposome-based systems have been useful for the characterization of pore forming ability by porin and its isoforms (Xu *et al.* 1999, Shao *et al.* 1996, Komarov *et al.* 2004), and to determine influences on channel formation and substrate diffusion of other interacting molecules (Bathori *et al.* 2006, Colombini *et al.* 1987, Madesh and Hajnoczky 2001) or proteins (Shimizu *et al.* 1999, Shimizu *et al.* 2000, Shimizu and Tsujimoto 2000, Gonzalez-Gronow *et al.* 2003).

More recent work has utilized recombinant mitochondrial porins that are isolated from inclusion bodies in *E. coli* and renatured in detergents; these proteins, following pre-incubation with ergosterol or cholesterol, can also be inserted into black lipid bilayers, where they form channels functionally indistinguishable from those of porin isolated from

mitochondria (Popp *et al.* 1996; Popp *et al.* 1997; Koppel *et al.* 1998). Far-UV CD spectropolarimetry has confirmed that the native and recombinant porins from fungal mitochondria and pea root plastid, dissolved in LDAO or Genapol X-080, all have high β -strand content (40-70%; Koppel *et al.* 1998, Popp *et al.* 1997, Runke *et al.* 2000, Runke *et al.* 2006). *N. crassa* mitochondrial porin embedded in liposomes is also β -strand rich, suggesting that the protein in detergent forms β -strands similar to those found in the membrane (Shao *et al.* 1996). However, the tertiary conformations of the protein in these detergents or in liposomes have not been examined and it is not known whether the protein exists as a molten globule under detergent conditions or forms tertiary arrangements expected for membrane reconstituted porins.

X-ray crystallography has been used to investigate the structures of numerous bacterial porins (summarized in Popot and Engelman 2000), and the structures of bacterial outer membrane protein X (OmpX, Fernández *et al.* 2001, Fernández *et al.* 2004) and the transmembrane domain of OmpA (Arora *et al.* 2001) have been determined recently by nuclear magnetic resonance (NMR) spectroscopy. The inherent stability of folded bacterial porins (for example see (Dornmair *et al.* 1990)) aids the acquisition of high (mM) concentrations of folded protein needed for these studies. These approaches have not been applied to mitochondrial porins, likely due in part to difficulties resulting from the conformational instability of the protein in the detergent systems used (Shao *et al.* 1996, Bay and Court, unpublished results). In addition, mitochondrial porins are significantly larger (~30 kDa) than the bacterial porins studied by NMR (~20 kDa).

For mitochondrial porins, spectroscopic analysis of detergent and membrane associated proteins is the first essential step toward determination of the folded state.

Secondary structure predictions and in vitro analyses of wild-type and variant porins have led to models for the transmembrane arrangement of porin (see Fig. 2.1 for one example), but cannot reveal the precise positions of the membrane-spanning segments, loops and termini in the folded protein (reviewed in Bay and Court 2002). Therefore, in this study, mitochondrial porin of *N. crassa* was solubilized in a collection of detergents to examine the conformation of the protein, with the goals of characterizing the folded states of porin solubilized in commonly used detergents and following reconstitution in artificial membranes (liposomes). The ultimate goal is to identify a system suitable for solubilization of high concentrations of folded protein for structural analysis by NMR spectroscopy. The detergents chosen (Genapol X-080 (Troll *et al.* 1992), LDAO (Koppel *et al.* 1998), DPC (Arora *et al.* 2001), OG (Shao *et al.* 1996), DDM (Ahting *et al.* 1999), and SDS (Popp *et al.* 1997) have been used successfully in electrophysiological or structural studies of bacterial or mitochondrial β -barrel proteins.

Several approaches to investigating mitochondrial porin in detergents and artificial membranes were used in this study: secondary structure content and tertiary interactions involving tryptophan and tyrosine were investigated by CD in the far and near UV regions, respectively. CD and fluorescence spectroscopy of membrane-bound porin was used, although there were some limitations due to light scattering by liposomes. Exposure of tyrosine residues to the aqueous environment was estimated by second derivative analysis of UV spectra and the hydrophobicity of the environment surrounding tryptophan residues was determined by fluorescence. Model tyrosine and tryptophan compounds were also investigated in the same detergents, to form a reference dataset useful for the present and future studies of membrane proteins in detergent. Taken together, these studies represent the

first characterization of detergent-solubilized amino acid model compounds and mitochondrial porin by fluorescence and UV absorption, and the first investigation of tertiary interactions in mitochondrial porin reconstituted in detergents and liposomes.

2.3 Materials and Methods

2.3.1 Lipids, detergents, and amino acid derivatives

Egg yolk L- α -phosphatidyl choline, egg lecithin L- α -phosphatidic acid, NAc-W-NH₂, NAc-Y-NH₂, SDS, ethylene glycol, urea and NAc-W-OEtH were obtained from Sigma (St. Louis, MO), DPC, DDM, OG and LDAO from Anatrace (Maumee, OH). BOC-Y-OMe (FLUKA, Oakville, ON) and Genapol X-080 from Caledon Laboratories (Georgetown, ON). CMCs of single detergents in 50 mM sodium phosphate pH 7 (Table 1) were measured for this study using the method of dye solubilization (Kleinschmidt *et al.* 1999).

2.3.2 Expression and purification of His₆-porin

The cloning of the cDNA for *N. crassa* mitochondrial porin into the pQE-9 vector (Qiagen, Toronto, ON), which encodes an N-terminal His₆-tag has been described previously (Popp *et al.* 1996). Protein expression was carried out using the QIAexpress *E. coli* M15 [pREP4] strain from Qiagen.

The recombinant His₆-porin used in this study was expressed in *E. coli* and purified in 8 M urea, using the procedure described in (Runke *et al.* 2000), with the exception that protein expression was induced with 0.5 mM isopropyl- β -D-thiogalactopyranoside. The yield of His₆-porin was 2-5 mg/L. Porin was eluted from immobilized nickel nitrotriacetic acid (Ni-NTA) in 8 M urea, 0.1 M EDTA, 0.1 M Na₂HPO₄, 10 mM Tris•Cl pH 6.8, followed by overnight dialysis in the same buffer lacking EDTA. The protein concentration was

determined using the calculated extinction coefficient at 280 nm of $24,050 \text{ M}^{-1} \text{ cm}^{-1}$. Protein purity was monitored by sodium dodecyl sulfate-polyacrylamide gel electrophoresis and was estimated to be at least 95%.

2.3.3 Solvent and detergent solubilization of His₆-porin

Dialyzed His₆-porin was acetone-precipitated and the dried pellets were resuspended either in 8 M urea or in aqueous detergent solutions buffered in 50 mM sodium phosphate pH 7. Washing the pellet in acetone to remove urea following the initial precipitation greatly reduced the solubility of the protein; a requirement for low levels of denaturant for re-folding the bacterial porin OmpGm has also been reported (Conlan and Bayley 2003). The resuspended samples were mixed by repeated inversion overnight at room temperature (22°-25°C), centrifuged at 10,000 *g* for 15 minutes, and the optically-cleared supernatants were collected. Where indicated, protein samples were concentrated by ultrafiltration through Centricon™ columns (MW cutoff 10,000; Amicon, Inc., Beverly, MA).

2.3.4 Liposome stock preparation

His₆-porin was reconstituted into small unilamellar vesicles (SUV) using modifications of the procedures described by (Shao *et al.* 1996). Briefly, a 10:1 (w/w) mixture of egg yolk L- α -phosphatidyl choline and egg lecithin L- α -phosphatidic acid phospholipid was dissolved in chloroform and evaporated in a fumehood at room temperature (22-25°C) overnight. Evaporated lipids were resuspended in 50 mM sodium phosphate buffer at pH 7 or stored at -20°C in a dessicator until needed. The resulting milky suspension was diluted 1:1 with phosphate buffer pH 7 and sonicated on ice until the microtip (Fisher Scientific Sonifier Model 300) could clearly be observed through the haze to yield the stock

SUV suspension. As described in Traikia *et al.* 1997; Traikia *et al.* 2000, the unsonicated stock solution of dried lipids resuspended in buffer constitutes multilamellar vesicles (MLV) with diameters usually varying from 1-10 μm . This solution was sonicated to form the stock SUV solution, which should contain SUVs 30- 60 nm in diameter. Freeze-thaw treatment of the stock SUV solution would then generate fragile large unilamellar vesicles (LUV) that tend to break apart and reform SUVs (Traikia *et al.* 1997; Traikia *et al.* 2000). Thus, the proteoliposomes described in this study are mainly SUVs.

2.3.5 Proteoliposome preparation and swelling assays

Proteoliposomes were prepared based on a modified procedure for Type B (CD grade) liposomes as described by (Shao *et al.* 1996). In short, the sonicated 20 mg/ml stock phospholipid was diluted 1:1 with a 1 in 2 dilution of detergent-solubilized His₆-porin in 50 mM sodium phosphate buffer pH 7. Initial detergent concentrations were 3.5 mM SDS, 2 mM DPC, or 7.5 mM LDAO and initial His₆-porin concentrations ranged from 0.015 – 0.030 mg/ml (0.5 to 1 μM). The resulting suspension was subjected to three cycles of freezing in liquid nitrogen for 1 min and thawing for 20 min at room temperature. Upon the last thawing in the freeze-thaw cycle, samples were diluted with 1.5 volumes of 50 mM sodium phosphate pH 7 resulting in a cloudy solution and contained 6.6 mg/ml of total phospholipid. Final concentrations of detergent in the swelling assay samples were 0.58 mM SDS, 0.33 mM DPC, and 1.25 mM LDAO, which are below their CMC values (Table 2.1). Final concentrations of His₆-porin ranged from 2.5 – 5.0 $\mu\text{g/ml}$ (80- 166 nM). Negative controls for liposome swelling experiments were prepared with detergents only and lacked His₆-porin.

Liposome swelling (Shao *et al.* 1996) was measured on an Ultrospec 3100 pro spectrophotometer at an absorbance of 400 nm. Liposome samples prepared as described

above were diluted 1/100 into 50 mM sodium phosphate pH 7 buffer to a final volume of 0.5 ml and measured in a 1 cm quartz cuvette. After 300-400 seconds, liposomes were initially diluted with 40 μ l of the iso-osmotic phosphate buffer pH 7, followed by an addition of 40 μ l of the hyperosmotic 1 M sucrose after 600-700 seconds. Liposome re-swelling, is indicated by a gradual decrease in $A_{400\text{nm}}$ according to Bangham's Law described by the equation $A = k/V$ where UV absorbance (A) is inversely proportional to liposome volume (V) based on the refractive index of lipid particles (k) (Bangham *et al.* 1978). Liposome re-swelling was followed for 1200 or 1800 seconds after sucrose addition.

Swelling assays were also performed to assess the ability of urea and detergent-solubilized His₆-porin to insert into liposomes as described for *E. coli* OmpA (Surrey and Jahnig 1995). Liposomes for porin insertion experiments were prepared as described above for liposome swelling except that the stock 20 mg/ml SUV suspension was diluted 1: 1 with 50 mM sodium phosphate buffer pH 7. After the three freeze-thaw cycles, 0.25 volumes of detergent-resuspended porin and 1.25 volumes of 50 mM sodium phosphate pH 7 were added, to create a final 1:1.5 dilution. To encourage insertion, samples were incubated at room temperature, 30°C, and 42°C overnight.

2.3.6 Reconstitution of detergent-solubilized His₆-porin in liposome for spectroscopic analysis

His₆-porin was resuspended in detergent at concentrations (3.5 mM SDS, 2 mM DPC, and 7.5 mM LDAO) that upon 1:3 or 1:4 dilution in phosphate buffer resulted in final detergent concentrations near the CMC (0.9-1.0 mM SDS, 0.6-1.2 mM DPC, and 3.1-3.8 mM LDAO). His₆-porin concentrations varied from 5-10 μ M in the different detergents. The protein was diluted into liposomes (2 mg/ml) buffered in 50 mM sodium phosphate pH 7.

Liposome-detergent-His₆-porin mixtures were then subjected to one of three methods for reconstituting His₆-porin: freeze-thaw, sonication, and insertion. The freeze-thaw procedure was essentially as described for liposome swelling. Porin incorporation by sonication of the liposomes/protein/detergent mixture was achieved by sonication on ice in four 1 minute bursts and 30 second rests between bursts until the sample was optically clear. Insertion-type liposomes were created as described above. Following treatment, the resulting proteoliposomes were placed on a rotating mixer overnight at room temperature (22-25°C), followed by centrifugation at 10,000 g for 10 min to remove any precipitated material. Following centrifugation, the pelleted material was resuspended in 8 M urea and measured by UV absorption spectroscopy at 280 nm to determine the amount of insoluble protein, which was then used to estimate the final concentration of His₆-porin in the supernatant. In some cases, following spectroscopic analysis, liposome swelling assays of these samples were performed with samples diluted to 0.66 mg/ml phospholipid.

2.3.7 Isolation of *N. crassa* mitochondria

Mitochondria were isolated from *N. crassa* 97-20 *mus his⁻* (Ninomiya *et al.* 2004) strain according to the method described by Harkness *et al.* 1994 (Harkness *et al.* 1994). Briefly, *N. crassa* conidia were used to inoculate Vogel's medium supplemented with (0.2 g/L) histidine and grown at 30°C for 14-16 hrs. Mycelia were filtered out from the media and ground with a mortar and pestle, with 2 ml of SEM (250 mM sucrose, 1 mM EDTA, 9 mM MOPS pH 7.5) and 1.5 g quartz sand added per g of filtered mycelia for 1 min on ice.

Ground *Neurospora* mycelia were centrifuged in a Sorvall SS34 rotor (Mandel, Guelph, ON) at 4,000 rpm, 4°C for 10 min to pellet cell debris and the supernatant was centrifuged at 12,000 rpm for 12 min, at 4°C to pellet mitochondria. Mitochondrial pellets

were resuspended in 1 ml of chilled SEM and brought to 20 ml SEM and centrifugation steps described above were repeated. The final mitochondrial pellet was resuspended in SEM to final concentration of 1 mg/ ml mitochondrial protein as determined by a Bradford assay (Sigma).

2.3.8 Protease digestions of isolated mitochondria and proteoliposomes

Isolated mitochondria (1 mg/ml) in SEM were used directly or microcentrifuged for 3 min at 4°C at 13,000 rpm to pellet mitochondria, which were then resuspended into an identical volume of detergent (3.5 mM SDS, 20 mM DPC, or 50 mM LDAO) buffered at pH 7 with sodium phosphate. Mitochondrial digestions contained 0.5 mg/ml of mitochondria and detergent concentrations of 1.75 mM SDS, 25 mM LDAO, and 10 mM DPC. All samples were digested with 0.15 mg/ml trypsin or chymotrypsin for 10 or 30 min intervals at room temperature.

His₆-porin reconstituted in liposomes was digested after spectroscopic examination. Each liposome sample was digested as described for mitochondria and contained 0.008-0.015 mg/ml (0.25- 0.5 μ M) His₆-porin and 1 mg/ml phospholipid.

Detergent-solubilized His₆-porin samples were digested with trypsin and chymotrypsin under the same conditions as for mitochondria except that times were 30 or 60 minutes. The final concentration of His₆-porin was 0.075 mg/ml (2.5 μ M) and the detergent concentrations were 1.75 mM SDS, 25 mM LDAO, and 10 mM DPC. All protease digestions were arrested by adding phenylmethylsulfonylfluoride to a final concentration of 20 mM and 4:1 dilution into Laemmli buffer (Laemmli 1970) containing 8 M urea. All reactions were stored at -20°C until loaded onto SDS-PAGE gels containing 2 M urea, which

was necessary to aid migration of the protein into the gel in the presence of high concentrations of lipid.

2.3.9 Western blots of proteoliposomes and *N. crassa* mitochondria

All protease digested samples were loaded onto 0.1 % SDS- 3 M urea- 14% PAGE gels and electrophoresis was performed with the Mini-Protean[®] II system (Bio-Rad Laboratories, Hercules, CA). Gel loading was as follows: 5 µl of 0.5 mg/ml mitochondria in SEM or detergent, 10 µl of 7.5- 15 µg/ml His₆-porin in 1 mg/ml phospholipids, and 1 µl 75 µg/ml His₆-porin in detergent. Gels were blotted with a Trans-Blot[®] Cell system (Bio-Rad) onto nitrocellulose 0.45 µm membranes (Bio-Rad) overnight at 4°C and stained with Ponceau S (Sigma) to visualise the Benchmark protein ladder (Invitrogen, Burlington, ON).

Immunoblotting was carried out at room temperature using rabbit antibodies directed against residues 7- 20 of *N. crassa* mitochondrial porin (αNcPor-N, generated by R. Lill, at Universität München). Membranes were blocked for 30 minutes with a 5 % (w/v) skim milk/ 10 mM Tris-Cl, 0.15 mM NaCl, pH 7.5 (TBS) and incubated in 5 % (w/v) skim milk/ TBS with a 1: 1000 dilution of anti 7- 20 *N. crassa* mitochondrial porin antiserum for 1 hour. Membranes were washed twice with 0.1 % (v/v) Triton X-100/ TBS for 30 minutes each and twice with TBS for 10 minutes each before soaking in 5 % (w/v) skim milk / TBS with 1: 5000 dilution of anti-rabbit alkaline phosphatase (Sigma) antibody for 1 hour. Blots were washed twice with 0.1 % (v/v) Triton X-100/ TBS and TBS as described above. Membranes were soaked in detection buffer (0.1 M NaCl, 0.1 M Tris-Cl pH 9.5) for 2 minutes and soaked in 1: 100 dilution of CDP-star (Roche Diagnostics, Indianapolis, IN) in detection buffer (100 mM Tris-Cl pH 9.5, 100 mM NaCl) for 1 minute. Blots were placed in plastic and exposed

for 1- 2 hrs on X-Omat Blue XB-1 Scientific Imaging film (Kodak, Rochester, NY) before image development.

2.3.10 Fluorescence spectrophotometry

Fluorescence spectroscopic analyses of urea-, ethylene glycol-, and detergent-solubilized model compounds and His₆-porin were performed using a Shimadzu RF-1501 fluorometer or a JASCO-810 (FMO-427S) spectropolarimeter/fluorometer. All emission spectra were measured in a 1-cm path length quartz cuvette after excitation at 275 nm or 296 nm. Detergent- solubilized His₆-porin samples were measured at A_{280 nm} of 0.01, which corresponds to a protein concentration of 0.42 μ M. All His₆-porin-liposome samples were diluted 1:10 in 50 mM sodium phosphate buffer pH 7 to a final liposome concentration of 0.2 mg/ml and His₆-porin concentrations ranging from 0.1-0.2 μ M. His₆-porin-liposome samples were normalized to a concentration of 0.42 μ M with reference to His₆-porin in urea. Two sets of model compounds were used: NAc-W-NH₂ and NAc-Y-NH₂, which have been characterized in solvents of varying polarity (Cowgill 1967, Garcia-Borrón *et al.* 1982, Nayar *et al.* 2002) and BOC-Y-OMe and NAc-W-OEt, which are more hydrophobic and therefore are more likely to partition into the hydrophobic interior of the detergent micelles. His₆-porin contains two tryptophan and nine tyrosine residues. Samples of individual model compounds, and 2:9 Trp:Tyr mixtures, were prepared at molar concentrations close to those of the individual residues in porin and all of the protein and model compound fluorescence spectra were normalized with reference to His₆-porin in urea. The sums of the spectra obtained from the individual components equalled those from the 2:9 mixtures, indicating a lack of interaction between the fluorophores (for example see Fig. 2.3).

Fluorescence scans were repeated three times and the averaged spectra were used for analysis. Increased light scatter prevented accurate determination of higher wavelength regions 15-20 nm from the excitation wavelength. To determine tyrosine emission maxima in solutions containing both tyrosine and tryptophan, the second derivatives of the averaged spectra were obtained with Jasco Spectra Analysis Software, Version 1.53.04, using data at 1-nm intervals and a window of 9-13 nm, depending on the noise in the spectrum. This analysis was used to aid the determination of $\lambda_{\text{max}}\text{Tyr}$ and $\lambda_{\text{max}}\text{Trp}$ in the porin spectra (Table 2.3; Garcia-Borron *et al.* 1982)

2.3.11 Ultraviolet (UV) absorption spectroscopy

UV absorption spectra were obtained on an Ultrospec 4000 spectrophotometer, using a 1-cm path length cell and a porin concentration of 5 μM . Six spectra were obtained for each sample and averaged for further analysis. The second derivatives of the averaged spectra were obtained as described above, using data at 0.5 nm intervals and a window of 6.5 nm. Tyrosine exposure (α) was calculated using the method described by (Ragone *et al.* 1984), where r is the ratio of short (283 nm) to long (~ 291 nm) wavelength trough depths. For a given detergent, $\alpha = (r_n - r_a)/(r_u - r_a)$ where, $r_n = r$ for the protein in that detergent, $r_a = r$ for the 2:9 mixture of NAc-W-NH₂/NAc-Y-NH₂ in EG, and $r_u = r$ for the unfolded protein (in urea). Light scattering in the UV spectrum from 200-270 nm prohibited accurate measurements of the absorption spectra of liposome-His₆-porin samples.

2.3.12 Circular dichroism (CD) spectropolarimetry

CD spectra were acquired on a JASCO J-810 spectropolarimeter-fluorometer calibrated with (+)-10-camphorsulfonic acid and purged with N₂ at 20 L/min (Manley and

O'Neil 2003). CD spectra of 1.5 μM detergent-solubilized His₆-porin samples and porin-liposome samples containing 0.5-2.0 μM His₆-porin were measured in the far UV region (190-250 nm) using 0.05-0.10-cm path length quartz cuvettes at 22°C, a scan rate of 10 nm/min and a response time of 8 s. Examination of all porin liposome samples by CD determined that high initial concentrations of His₆-porin in SDS were necessary to maintain 1-2 μM of protein in the SUV samples after centrifugation. CD spectra were corrected by baseline subtraction and were converted to mean residue ellipticity (MRE) according to the formula: $[\theta]_M = M\theta / \{(10)(l)(c)(n)\}$ where $[\theta]_M$ is 10^{-3} deg cm² dmol⁻¹, M is the molecular weight of His₆-porin (31 402 g/mol), θ is the measured ellipticity in millidegrees, l is the path length of the cuvette in cm (0.1 cm), c is the protein concentration in g /L, and n is the number of amino acid residues in the protein (295). Detergent-solubilized His₆-porin spectra were deconvoluted with the CONTINLL algorithm (Provencher and Glockner 1981, van Stokkum *et al.* 1990) in the DichroWeb package (Whitmore and Wallace 2004). Light scattering by the liposome samples prevented reliable acquisition of spectra below 200 nm and thus prohibited deconvolution with secondary structure prediction algorithms.

Temperature was controlled during thermal denaturation experiments of detergent-solubilized His₆-porin using the Peltier device in the spectropolarimeter. These experiments were carried out with a 1°C / min ramp speed; θ (in mdeg) was monitored at 208 or 216 nm at 1°C intervals, and full spectra were collected at 5°C intervals. Liposome sample experiments were monitored at 217 nm at 1°C intervals, and full spectra were collected at 10°C intervals. Using the program *Mathematica*TM, the resulting denaturation curves were

fitted to the equation
$$Y_{obs} = \frac{Y_f + m_f T + (Y_u + m_u T) \bullet e^{(-\Delta H + T\Delta S)/(RT)}}{1 + e^{(-\Delta H + T\Delta S)/(RT)}} \quad (\text{Privalov and Potekhin 1986,})$$

Lopez-Llano *et al.* 2004) where Y_{obs} is the observed ellipticity, Y_f and Y_u are the ellipticities of the low and high temperature forms of the protein, respectively, m_f and m_u are the slopes of the curves at low and high temperatures, respectively, R is the gas constant, and ΔH and ΔS are the enthalpy and entropy of unfolding. The equation fits the thermal dependence of the ellipticity to a two-state unfolding transition. $T_m = \Delta H / \Delta S$, where T_m is the midpoint of the transition and the concentrations of folded and unfolded protein are equal. T_m serves as a quantitative indicator of the thermal stability of the protein, as the unfolding reactions are, in most cases, irreversible.

Near-UV (245-330 nm) CD spectra of 33 μ M His₆-porin in detergent were measured with a JASCO J-810 spectropolarimeter-fluorometer in a 1-cm path length jacketed quartz cuvette at room temperature, with a scan rate of 2 nm/min, and a response time of 8 s. Spectra of His₆-porin reconstituted in liposomes were measured in a 5-cm path length jacketed quartz cuvette at room temperature with a scan rate of 10 nm/min, and a response time of 8 seconds. Scans were measured in triplicate for averaging to reduce noise. Molar ellipticity was calculated from the baseline corrected spectra according to the formula: $[\theta] = M\theta / \{(10)(l)(c)\}$ where $[\theta]$ is the molar ellipticity in degrees cm² dmol⁻¹, θ is the measured ellipticity in millidegrees, l is 1 cm or 5 cm, and c is the protein concentration in g/L.

2.4 Results

2.4.1 Solubility of His₆-porin in detergent systems

To obtain high concentrations of folded recombinant porin, a practical system for purification and detergent solubilization is needed. Highly purified His₆-porin can be recovered from inclusion bodies at high concentrations (> 1 mg/mL) by extraction from *E.*

coli in urea or guanidinium chloride followed by Ni-NTA affinity chromatography (Popp *et al.* 1996, Koppel *et al.* 1998). Urea was used in this study, owing to the difficulty of spectroscopic analysis of proteins dissolved in guanidinium salts. Given the cost of many detergents, it is impractical to exchange the urea for detergent by dialysis, so the protein was precipitated from urea with acetone, and the resulting pellet dissolved in sodium-phosphate buffered detergent solution. Six detergents, namely SDS, an ionic detergent, LDAO and DPC, zwitterionic detergents, and Genapol X-080, OG, and DDM, non-ionic detergents, were examined for their ability to solubilize acetone-precipitated porin. The results are presented in Table 2.1, along with the measured CMCs of each of the detergents. The highest concentrations of His₆-porin (750 μ M) were obtained with SDS. At high concentrations, DPC and LDAO solubilize His₆-porin to concentrations of about 66 μ M and 25 μ M, respectively; further concentration of the protein by ultrafiltration was not possible due to precipitation of detergent/protein complexes and concentration of the detergent. His₆-porin is least soluble in the non-ionic detergents Genapol X-080, OG, and DDM (\sim 2 μ M; Table 2.1); increased concentrations of these detergents do not solubilize higher concentrations of protein. Instability has been reported for bacterial porins dissolved in Genapol X-080 (Conlan and Bayley 2003) and recombinant mitochondrial porins in OG (Koppel *et al.* 1998). DDM- and OG-solubilized His₆-porin rapidly form a visible precipitate during ultrafiltration, suggesting that the protein exists as soluble aggregates in these detergents. Therefore, the non-ionic detergents were not used further in this study.

2.4.2 Reconstitution of His₆-porin into liposomes

Modified type B liposomes (Shao *et al.* 1996) were used for osmotic swelling assays to determine if any of the detergent-solubilized porins studied herein were capable of forming

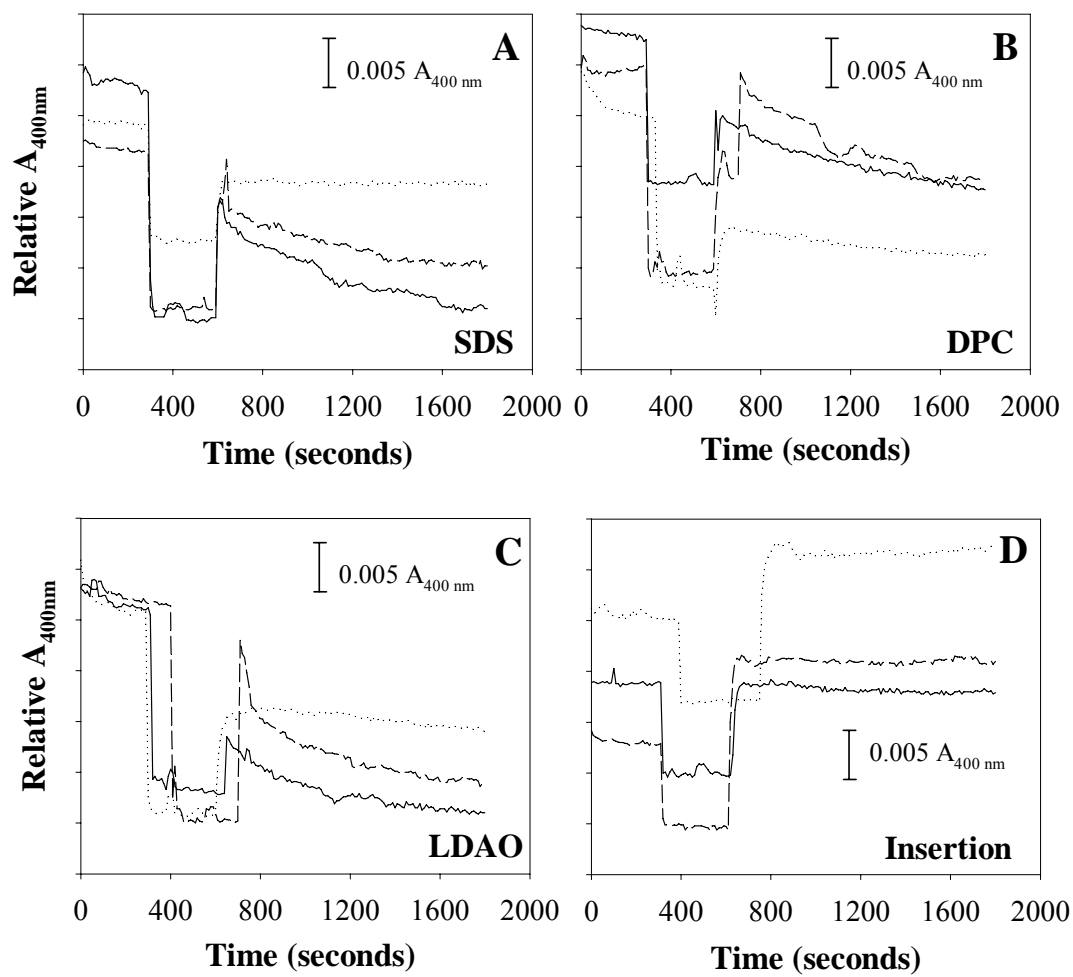
Table 2.1. Solubility of acetone-precipitated His₆-porin after resuspension in single detergents or solvents in 50 mM sodium phosphate pH 7. The protein concentrations indicated were determined from optically clear samples obtained after centrifugation.

Detergent / Solvent	CMC (mM) in 50 mM sodium phosphate	Concentration (μM) of solubilized His₆-porin
8 M urea		> 1 000
3.5 mM SDS	0.9 - 1.0	66
75 mM SDS	0.9 - 1.0	750
15 mM DM	0.9 - 1.9	2
50 mM OG	12.5 - 15.0	2
18 mM Genapol X-080	0.7 - 1.4	2
50 mM LDAO	3.1 - 3.8	5
300 mM LDAO	3.1 - 3.8	25
10 mM DPC	0.6 - 1.2	5
100 mM DPC	0.6 - 1.2	66

channels in membranes. Following freeze-thaw treatments, all detergent-solubilized His₆-porin preparations were capable of forming pores in liposomes (Fig. 2.2), despite differences in secondary structural content when the protein was solubilized in detergents alone (see below). Liposomes that incorporated His₆-porin in SDS (SDS-His₆-porin-liposomes) demonstrated the most rapid osmotic response to sucrose, with a change of -0.01 A_{400 nm} over 20 min. Different batches of SDS-His₆-porin-liposomes had the most reproducible swelling patterns of all detergent-solubilized His₆-porin samples examined (data not shown), which may indicate that SDS maintains more protein in a conformation amenable for incorporation into artificial membranes. Heating proteoliposomes to 42°C (data not shown) or 65°C (Fig. 2.2A) did not abolish osmotic shrinkage but did reduce the swelling phase (to -0.006 A_{400 nm} over 20 min), which agrees with previous experiments that used liposomes containing mammalian and fungal porins (Bathori *et al.* 1993, Shao *et al.* 1996). Heating SDS-His₆-porin-liposomes to 100°C produced non-swelling response patterns (Fig. 2.5A) indistinguishable from SDS-liposomes lacking His₆-porin (data not shown). DPC-His₆-porin-liposomes were also osmotically responsive and heating of these proteoliposomes to 65°C resulted in partial loss of the swelling response (Figs. 2.2B). Swelling rates of LDAO-His₆-porin-liposomes were not consistent between batches. In cases where osmotically-responsive liposomes were generated, heating to 65°C, enhanced the re-swelling phase (Fig. 2.2C), suggesting that increased temperature either drives pore formation by membrane-associated protein, or increases the activity of existing pores. Heating of both DPC- and LDAO-His₆-porin-liposomes to 100°C eliminated swelling.

Urea-solubilized *E. coli* OmpA assembles into the membrane upon dilution into a liposome suspension (Surrey and Jahnig 1995). Therefore, swelling assays were also

Figure 2.2. Liposome swelling assays. SDS-His₆-porin-liposomes were prepared by the freeze-thaw method (**A-C**) or the insertion method (**D**). Swelling was measured either directly (solid line) or following heating of the proteoliposomes to 65°C (dashed lines) or 100°C (dotted lines). Liposomes were diluted within 300-400 s by addition of 40 µl of the iso-osmotic phosphate buffer, causing a decrease in $A_{400\text{ nm}}$. Addition of 40 µl of hyperosmotic 1 M sucrose at 600-700 s resulted in liposome shrinkage, and a sharp increase in $A_{400\text{ nm}}$. Reswelling of osmotically responsive proteoliposomes is detected as a gradual decrease in optical density. Relative $A_{400\text{ nm}}$ values were plotted, on the same scale, to allow the individual plots to be clearly discernable from each other.



performed to determine if urea- or detergent- solubilized His₆-porin possesses the capacity to insert into liposomes in the absence of membrane disruption by freeze-thaw or sonication. However, urea-solubilized His₆-porin did not produce detectable channels in liposomes and porin was recovered with insoluble material following centrifugation of the sample (data not shown). Swelling was not observed at increased concentrations of His₆-porin (9 µg/ml or 0.3 µM) or increased temperature (30 or 42°C). Incubation of detergent-solubilized porin with preformed liposomes also did not generate osmotically-responsive proteoliposomes.

2.4.3 Protease sensitivity of mitochondrial porin and detergent-solubilized His₆-porin reconstituted into liposomes

Protease sensitivity is frequently used as a criterion for refolding of bacterial porins, such as OmpG in detergent (Conlan and Bayley 2003) or OmpA following reconstitution into artificial membranes (Dornmair *et al.* 1990, Kleinschmidt and Tamm 1996). *Neurospora* mitochondrial porin assembled in the outer membrane also displays resistance to high levels of protease (Freitag *et al.* 1982). Therefore, protease sensitivity of native mitochondrial porin, and detergent-solubilized His₆-porin prior to and following reconstituting into liposomes was examined. Immunoblotting was performed to allow detection of the low amounts of His₆-porin (< 2 µM) maintained in liposomes and of porin in the mixture of mitochondrial proteins. Trypsin (T) and chymotrypsin (C) were also detected as 24 or 25-kDa bands on the blots due to sequence similarity between T and C and the porin peptide (residues 7-20) used to generate antibodies for this study.

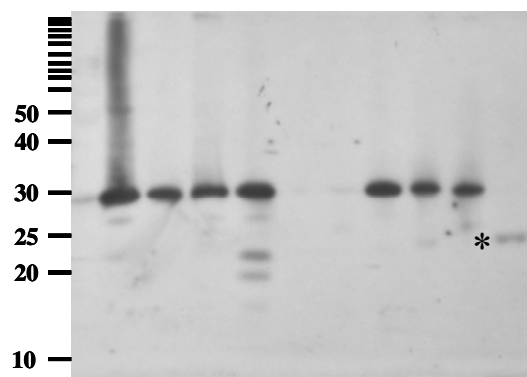
Western blots of undigested *N. crassa* mitochondria in SEM show an intense band of intact porin at 30 kDa (Fig. 2.3A); the weak band at 28 kDa likely arises from slight

proteolysis of porin during isolation or incubation at room temperature in the absence of added protease. The full-length protein is highly resistant to digestion with T or C (Fig. 2.3A). Following a 30 min digestion with 0.15 mg/ml T or C the intensity of the 30-kDa band is unchanged (Fig. 2.3A). Undigested 3.5 mM SDS solubilized mitochondria gave rise to four bands; the major one of 30 kDa corresponds to intact monomeric porin and the minor 28 kDa, 21 kDa and 20 kDa bands are proteolytic fragments resulting from the activity of mitochondrially-associated proteases during the 30-min incubation at room temperature (Fig. 2.3A). The presence of these fragments only in the SDS-solubilized mitochondrial preparations suggests that porin is arranged in a more protease sensitive conformation in this detergent. This is confirmed by the complete absence of the 30 kDa band after 30 min of digestion by T and C (Fig. 2.3A). Western blots of undigested or T or C digested mitochondria resuspended in either 50 mM LDAO (data not shown) or 20 mM DPC (Fig. 2.3A) also demonstrated a single band at the molecular mass of 30 kDa when immunoblotted with α NcPor-N. Longer digestions with T or C did not reduce the intensity of the 30 kDa band (data not shown).

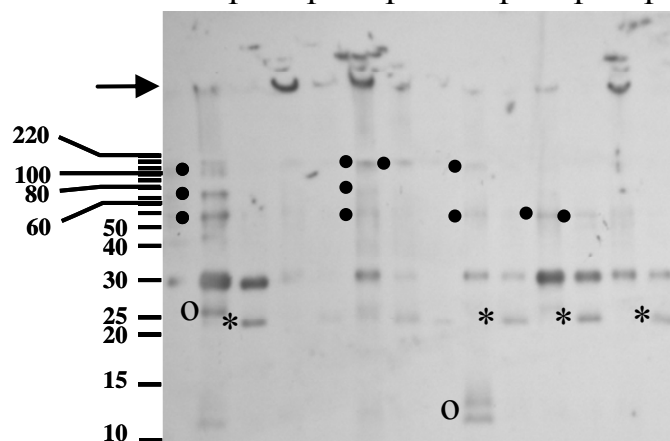
Protease-sensitivity of His₆-porin in liposomes was also investigated. His₆-porin migrates more slowly than mitochondrial porin (30 kDa) and has an apparent molecular mass of 32 kDa. A small amount of a 28-kDa proteolytic fragment was also seen. Remarkably, undigested FT SDS-His₆-porin-liposomes also contained two additional species of molecular masses of approximately 90 and 65 kDa (Fig. 2.3B), suggestive of trimers and dimers of the protein. Following digestion with trypsin, the majority of the full-length protein remained, but the putative oligomers were no longer detectable. Similar results were obtained for FT

Figure 2.3. Protease sensitivity of mitochondrial porin. **A)** *N. crassa* mitochondria (2.5 µg/lane) were resuspended in buffer alone (SEM), 3.5 mM SDS or 20 mM DPC and incubated at room temperature for 30 min in the absence (-) or presence of 0.75 µg of trypsin (T) or chymotrypsin (C). The last lane contains trypsin only, which is indicated by an asterisk. Following electrophoresis through urea-SDS-PAGE gels, samples were immunoblotted and probed with αNcPor-N antibodies. **B)** His₆-porin in liposomes. His₆-porin was solubilized in either SDS or DPC and incorporated into liposomes by freeze-thaw (FT), insertion (IN) or sonication (SO), as described in Materials and Methods. Samples were incubated in the absence (-) or presence (+) of 7.5 µg trypsin for 30 min prior to analysis as described in A). Arrow, position of wells in the gel; filled circles, multimers of His₆-porin, open circle, minor degradation product of His₆-porin; asterisks, cross-reacting trypsin. **C)** Detergent-solubilized His₆-porin. His₆-porin was solubilized in 3.5 mM SDS, 20 mM DPC or 50 mM LDAO and subjected to trypsin digestion as described for panels A and B. An image of the Coomassie Blue stained urea-SDS-PAGE gel is shown. In all panels, the positions of the marker proteins in the BenchmarkTM ladder (Invitrogen) are indicated to the left of each panel.

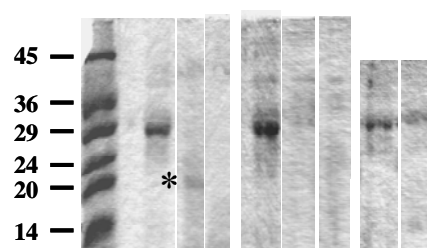
A Mitochondria
 SEM SDS DPC
 - T C - T C - T C T



B Liposomes
 SDS DPC
 FT IN SO FT IN SO
 - T - T - T - T - T - T



C Detergent
 SDS DPC LDAO
 - T C - T C T C



DPC-His₆-porin-liposomes, except that the band intensity was about half of that of the SDS-containing samples, likely due to accumulation of protein in the wells during electrophoresis (Fig. 2.3B). In addition, the 90-kDa band species was present in lower amounts in the DPC-dissolved protein.

Analysis of His₆-porin protease resistance by immunoblotting of INS and SON SDS-His₆-porin-liposomes proved difficult due to the high amount of His₆-porin retained in the wells of the gel (Fig. 2.3B). In both samples, some of the 32 kDa His₆-porin band remained following digestion with either trypsin or chymotrypsin (Fig. 2.3B). Immunoblots of undigested INS and SON DPC-His₆-porin-liposomes showed bands at molecular masses of 65 and 32 kDa, corresponding to dimeric and monomeric forms of His₆-porin (Fig. 2.3B). Interestingly, the 90 kDa band was not observed in undigested DPC-His₆-porin-liposome samples but this may be due to a reduced amount of His₆-porin that entered the gel. T and C digestion of INS and SON DPC-His₆-porin-liposomes resulted in two signals on the blot, an intense 32-kDa His₆-porin band and a minor 28-kDa species (Fig. 2.3B). Similar results were obtained for INS and SON LDAO-His₆-porin liposomes (data not shown). Thus, at least some of the protein in both the INS and SON LDAO- and DPC-His₆-porin-liposomes acquires protease-resistance upon introduction following incubation with liposomes in the presence or absence of sonication.

The ability to maintain high concentrations of His₆-porin in detergent alone enabled protease digests to be examined on Coomassie blue stained SDS-PAGE gels. Undigested His₆-porin solubilized in 3.5 mM SDS, 20 mM DPC and 50 mM LDAO resulted in a single band at 32 kDa (Fig. 2.3C). High molecular weight bands at 90 or 65 kDa were not observed on these gels and subsequent western blots also lacked these bands (data not shown). The 32-

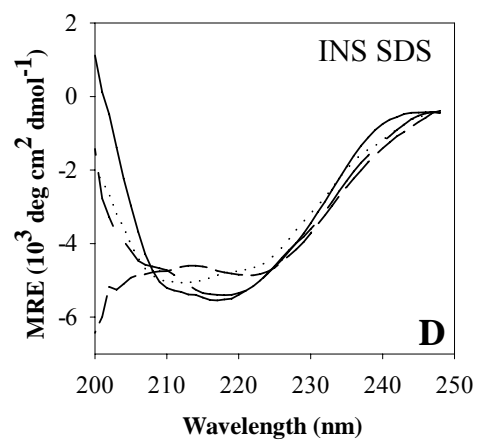
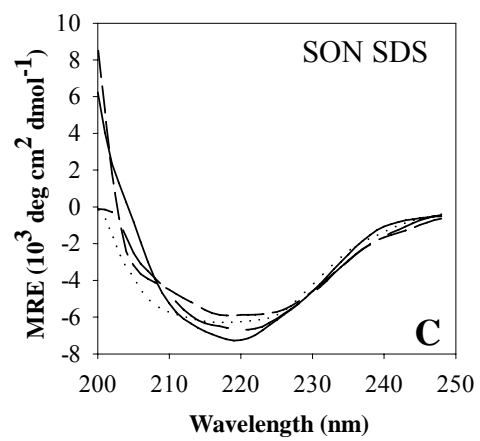
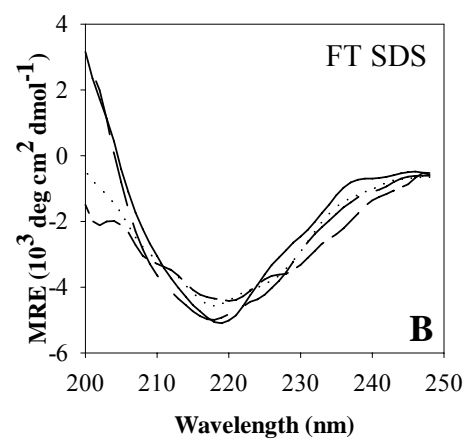
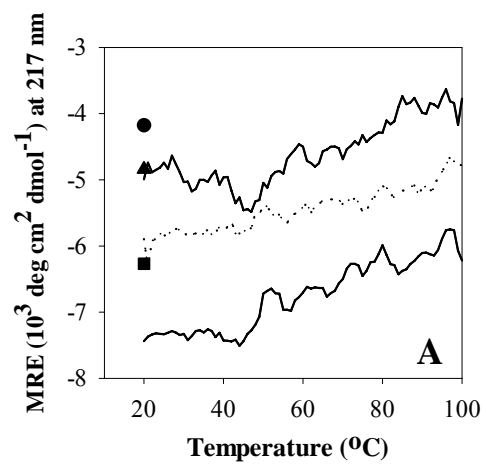
kDa band was retained in LDAO-solubilized His₆-porin samples following digestion with T or C after 0.5, 1, and 2 hrs (data not shown). 20 mM DPC- and 3.5 mM SDS-solubilized His₆-porin was highly sensitive to proteolysis by both T and C (Fig. 2.3C).

2.4.4 Characterization of His₆-porin reconstituted into liposomes by far-UV CD

Circular dichroism spectropolarimetry in the far UV region (200-250 nm; Fig. 2.4) was used to determine the secondary structural content of His₆-porin reconstituted by several different methods into liposomes. CD spectropolarimetry measures differences in absorption of left handed versus right handed circularly polarized light by asymmetric molecules. In the far UV region, the chromophore is the peptide bond and characteristic CD spectra arise for protein folded in secondary structures (Johnson 1990). SDS-His₆-porin liposomes were the only ones to maintain a high enough concentration of protein for examination by CD spectropolarimetry. Although light scattering by the liposomes prohibited collection at wavelengths below 200 nm, SUVs similar to those used here have been shown to minimize distortions from differential light scattering and absorption flattening observed in CD spectra of membrane suspensions (Wallace and Mao 1984, Mao and Wallace 1984).

The far-UV CD spectrum of FT SDS-His₆-porin-liposomes indicated that the protein was rich in β -strands, based on the sharp λ_{\min} at 217 nm (Fig. 2.4B). This spectrum was similar to that obtained from native *N. crassa* mitochondrial porin reconstituted into liposomes (Shao *et al.* 1996). CD spectra of SDS-His₆-porin-liposomes prepared by INS and SON had broader λ_{\min} values also centred around 217-218 nm (Fig. 2.4C and 2.4D), which may reflect differences in β -strand arrangements since the latter preparations were incapable of producing pores by osmotic swelling assays.

Figure 2.4. Far-UV CD analysis and thermal denaturation of porin reconstituted from SDS into liposomes. Proteoliposomes were prepared as described in Materials and Methods. His₆-porin concentrations ranged from 1-2 μ M in final concentrations of 0.9 mM SDS. **A)** Thermal denaturation of FT (upper solid line), INS (dotted line) and SON (lower solid line) type SDS-His₆-porin-liposomes was followed at MRE of 217 nm. Filled symbols indicate the MRE following cooling of the sample to 20°C: SON, square; INS, circle; FT, triangle. **B-D)** Full CD spectra obtained during the experiments shown in A). Spectra were taken at 20°C (solid line), 60°C (short dashed line), and 90°C (long dashed line) and following cooling back to 20°C (dotted line). **B)** FT, **C)** SON and **D)** INS-type proteoliposomes were used for these experiments.



The significant conformational alterations from the α -helical (λ_{\min} at 208 nm with a shoulder at 220 nm) spectra in SDS (Fig. 2.5A) to high β -strand content (λ_{\min} at 217 nm) in liposomes (Fig. 2.6) indicates that His₆-porin underwent a massive conformational change upon interaction with the artificial membrane. The role of the lipid in this change is further supported by the observation that dilution of His₆-porin in 3.5 mM SDS with phosphate buffer to an SDS concentration of 0.9 mM resulted in precipitation of porin, not β -strand formation. Also, CD spectra of His₆-porin FT liposomes prepared in the presence of 3.5 mM

SDS produced spectra characteristic of those from porin in SDS alone (with λ_{\min} at 208 nm, data not shown). Hence, the presence of phospholipid and detergent at or below the CMC, are required for development of β -strands. Thermal unfolding of SDS-His₆-porin-liposomes was performed to assess the stability of the protein secondary structure within the membrane. Thermal denaturation of FT-SDS-His₆-porin-liposomes produced a gradual increase in ellipticity at temperatures above 50°C and the ellipticity did not change upon cooling from 100°C to room temperature (Fig. 2.4A and 2.4B). CD spectra (200- 250 nm) of FT-SDS-His₆-porin-liposomes did not change upon heating from 20°-50°C (Fig. 2.4B). The CD spectra measured at 60°C and above demonstrated gradual broadening at the λ_{\min} with slight reductions in negative ellipticity at the λ_{\min} and larger decreases at wavelengths below 210 nm. Despite λ_{\min} broadening and spectrum flattening, it appears that β -strand content was maintained at high temperatures (90°C, Fig. 2.4B). As observed for thermal denaturation curves monitored at 217 nm, the full length CD spectrum of 20°C cooled FT SDS-His₆-porin-liposomes was very similar to the spectrum obtained at 100°C except at wavelengths < 205 nm and indicates that heating the protein results in some irreversible alterations to secondary structure content.

Thermal denaturation profiles monitored at 217 nm of SON-SDS-His₆-porin-liposomes (Fig. 2.4C) resemble those of the FT-SDS-His₆-porin-liposomes where ellipticity values remain unchanged upon heating to 45°C and heating the protein above 50°C results in a gradual reduction in negative ellipticity (Fig. 2.4D). A constant gradual decrease in negative ellipticity was observed for INS-SDS-His₆-porin-liposomes upon heating from 20°C to 100°C (Fig. 2.4D). Irreversible changes in conformation occurred at high temperatures since ellipticity values did not change upon cooling of both SON- and INS-SDS-His₆-porin-liposomes to 20°C (Fig. 2.4A). Above 40°C, CD spectra of SON-SDS-His₆-porin-liposomes were broader around λ_{\min} and a small shoulder appeared at 205 nm (Fig. 2.4C). In contrast, CD spectra of INS-SDS-His₆-porin-liposomes demonstrated this 205 nm shoulder at temperatures above 30°C and a shift in the λ_{\min} from 217 to 209 nm occurred above 70°C (Fig. 2.4D), indicating an alteration to a more α -helical type conformation. Cooling both SON- and INS- SDS-His₆-porin-liposome preparations to 20°C resulted in CD spectra intermediate to the 60°C and the 90°C spectra of each preparation (Fig. 2.4C and 2.4D).

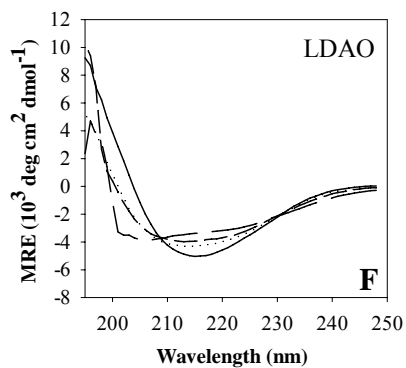
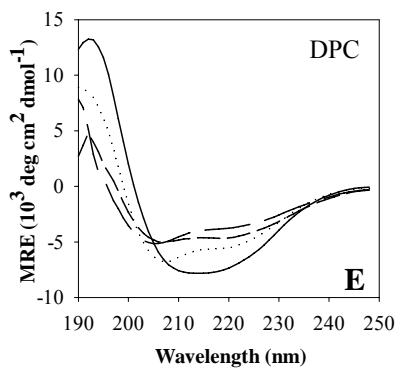
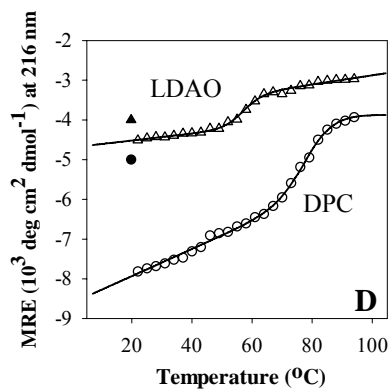
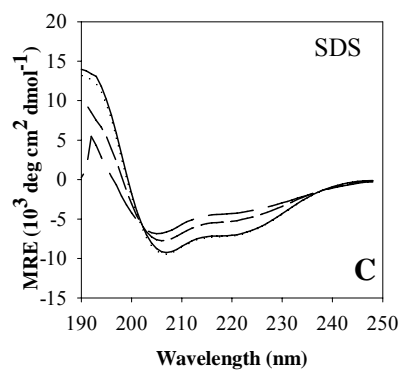
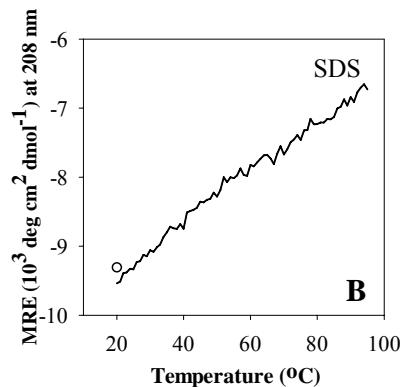
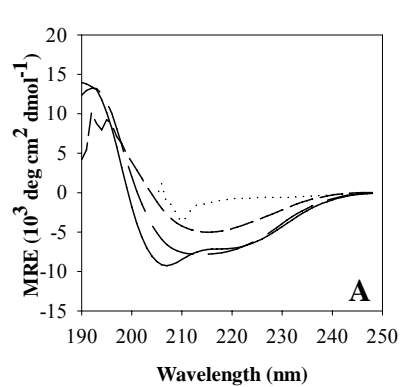
Overall, CD spectra of His₆-porin reconstituted into liposomes by freeze-thaw have sharp λ_{\min} and curves characteristic for high β -strand content. CD spectra of SON and FT SDS-His₆-porin-liposomes maintain β -strand rich curves at high temperatures in comparison to spectra of INS SDS-His₆-porin-liposomes. Combined with swelling data, these observations suggest that FT His₆-porin-liposomes contain temperature-tolerant β -barrels.

2.4.5 Characterization of detergent-solubilized His₆-porin by far-UV CD

Circular dichroism spectropolarimetry in the far UV region (190-250 nm; Fig. 2.5) was used to compare the secondary structures of His₆-porin dissolved in urea and in each of the detergents with those in liposomes. The results presented in Table 2 were obtained by

deconvolution of the CD spectra with CONTINLL and similar values were obtained using SELCON3, CDSSTR (Whitmore and Wallace 2004) and the convex constraint algorithm (CCA, Perczel *et al.* 1992) (data not shown). As expected in a denaturing system, the CD spectrum of His₆-porin in 8 M urea (Fig. 2.5A) shows little or no ellipticity above 210 nm, indicating a lack of secondary structure in the protein; this spectrum was not amenable to deconvolution. In contrast, significant secondary structure was observed in the detergent-solubilized porins. His₆-porin dissolved in 3.5 mM SDS (Fig. 2.5A) and in 50 mM SDS (data not shown) exhibit the characteristic α -helical spectrum with a minimum near 208 nm and a shoulder near 222 nm as reported by others (Shao *et al.* 1996, Popp *et al.* 1997, Koppel *et al.* 1998). Deconvolution of the spectrum yields 23% α -helix and 20% β -strand, with the remainder existing as β -turns and unordered structure (Table 2.2). The stability of the SDS-solubilized protein was assessed by thermal unfolding (Fig. 2.5B and 2.5C). Upon heating to 95°C, a linear increase in ellipticity at 208 nm was observed, indicating that a cooperative unfolding process did not occur (Fig. 2.5B). Slight shifts in the entire far UV CD spectrum were observed as temperature increased (Fig. 2.5C), and deconvolution revealed a small loss of α -helix (23% to 17%) with a concomitant increase in random structure, and little change in β -sheet content at 60°C, but not at 95°C (Table 2.2). Upon cooling back to 20°C, the MRE at 208 nm returned to its original value (Fig. 2.5B), and the CD spectrum was indistinguishable from that obtained prior to heating (Fig. 2.5C), indicating that the protein regained its original structure (Table 2.2). Overall, the protein had greater temperature stability in liposomes than in detergent, as λ_{\min} of ~ 217 nm was maintained at high temperatures (Fig. 2.4D) and only a slight linear increase in ellipticity at the minimum was observed (Fig. 2.4A).

Figure 2.5. Far-UV CD spectra of His₆-porin in detergent. **A)** Spectra were obtained, at 20°C, from 1.5 µM samples of porin solubilized in 8 M urea (dotted), 50 mM LDAO (short dashed), 20 mM DPC (long dashed), and 3.5 mM SDS (solid line). Melting curves for 1.5 µM His₆-porin in **B)** 3.5 mM SDS or **D)** 50 mM LDAO (open triangles) or 20 mM DPC (open circles) were generated by following the MRE at 208 nm in **B)** or 216 nm in **D)**. The solid lines in **D)** are corresponding thermal denaturation curves obtained as described in Materials and Methods. The circle in **B)** and the filled triangle and circle in **D)** indicate the MRE at the indicated wavelength upon cooling of the protein from 95°C to 20°C. **C)** Spectra of the SDS-solubilized protein at 20°C (solid line), 60°C (short dashed), 95°C (long dashed), following cooling to 20°C (dotted) are presented. **E)** and **F)** Spectra of the DPC- and LDAO-solubilized protein. Lines indicate the same temperatures as in **C)**, except that the short dashed line in **D)** represents 80°C.



The spectra of the protein solubilized in 10-20 mM DPC exhibit a broad minimum extending from 214 to 218 nm (Fig. 2.5A), whereas in 100 mM DPC, the spectrum has the characteristic minima of an α -helical rich protein (data not shown). However, deconvolution of the spectra suggests that both preparations contain the same α -helix content (16-17%) but that at low detergent concentrations there is a small increase in β -sheet content (30%) compared to higher detergent concentrations (26%).

To determine the stability of the protein in 20 mM DPC thermal denaturation was followed at 216 nm. The sigmoidal melting curve suggests a two-state cooperative transition and curve-fitting as described in Materials and Methods yields a T_m of 79.0°C (Fig. 2.5D and 2.5E). Deconvolution of the spectra showed a loss of α -helix and a concomitant increase in random structure; β -sheet content was unchanged. Protein precipitation occurred during heating; a visible precipitate was observed at the end of the experiment and an increase in absorption, indicating light scattering was noted near 90°C. The heat denaturation was not completely reversible; the protein refolded to a conformation similar to that at the midpoint of the denaturation curve (Fig. 2.5; Table 2.2). At the conclusion of the experiment, precipitated protein was removed by centrifugation and $A_{280\text{ nm}}$ measurements indicated that approximately 2/3 of the protein remained in solution.

The CD spectra of porin dissolved in LDAO exhibit a single broad minimum at 216 nm, characteristic of proteins with predominantly β -strand secondary structure (Fig. 2.5F). Deconvolution of the spectrum confirmed that in 75 mM LDAO the β -strand is highest (39%). Higher LDAO concentrations appear to promote more β -structure than do lower concentrations (Table 2.2). During thermal unfolding, the CD spectra of the LDAO-

Table 2.2. Analysis of His₆-porin solubilized in urea or detergents. Far-UV CD spectropolarimetry was performed on 1.5 μ M porin samples; the resulting spectra were deconvoluted with CONTINLL (Whitmore et al 2004). The CD spectra collected at 20°C were repeated at least three times and the standard deviations were less than 1%. The average value is presented. The thermal denaturation CD experiments were carried out once.

Detergent / Solvent	Temp (°C)	α -helix (%)	β -strand (%)	turn & unordered (%)
8 M urea	20°C	n/d	n/d	n/d
50 mM LDAO	20°C	16	32	53
75 mM LDAO	20°C	19	39	42
3.5 mM SDS	20°C	23	20	56
	60°C	17	23	59
	95°C	24	19	64
	95→20°C	24	20	57
50 mM SDS	20°C	31	21	48
10 mM DPC	20°C	16	30	54
100 mM DPC	20°C	17	26	57
20 mM DPC	20°C	20	29	52
	80°C	10	34	57
	95°C	11	29	60
	95→20°C	17	25	58
n/d, not determined				

solubilized protein undergo a small change in MRE at 216 nm, and the spectrum broadens in this region, indicating a decrease in ordered structure. As in DPC, the melting curve was sigmoidal, indicating a two-state cooperative transition, but in LDAO the T_m was lower (57°C). High temperature spectra were not deconvoluted because data could not be collected to 190 nm, likely due to increased light scattering. Unlike the case with DPC, a visible precipitate was not observed after heating but nonetheless, the folding is irreversible, and the spectrum after cooling resembles that observed near the midpoint in the denaturation curve (60°C).

2.4.6 Fluorescence of tryptophan model compounds in detergent

Fluorescence spectrophotometry probes the environments surrounding both tyrosine and tryptophan residues in protein. Initially, to determine the influence of detergent headgroups and acyl chains on fluorescence of His₆-porin, Trp and Tyr model compounds were examined. The fluorescence properties of the model compounds reflect their partitioning among the microenvironments in an aqueous detergent solution, namely water, the micelle surface, and the hydrophobic interior (Spyroacopoulos and O'Neil 1994). Compounds of differing hydrophobicities were used, individually, and in the 2:9 molar ratio that is present in mitochondrial porin. Pairs of model compounds were chosen, with differing hydrophobicities, to probe different microenvironments in the detergent solutions. The amide compounds NAc-Y-NH₂ and NAc-W-NH₂ are commonly used as models for aromatic amino acids in proteins (for example Cowgill 1968, Garcia-Borron *et al.* 1982, Lee and Ross 1998, Nayar *et al.* 2002, Noronha *et al.* 2004, Guzow *et al.* 2005). BOC-Y-OMe (N-t-butyloxycarbonyl-D-tyrosine-methyl ester) and NAc-W-OEt (N-Acetyl L-tryptophan ethyl ester) are more hydrophobic than the standard N-acetyl derivatives and therefore were chosen

as better probes of the interiors of detergent micelles. As seen in Table 2.3 and discussed below, each pair of model compounds had similar fluorescence properties in phosphate buffer and the commonly used solvents ethylene glycol and methanol hence comparisons between the two model compounds can be made.

Tryptophan fluorescence following excitation at 296 nm will be described first, with respect to the classification system devised by Burstein and colleagues to describe the microenvironments of Trp in proteins (Burstein *et al.* 1977, Burstein *et al.* 1973, Reshetnyak *et al.* 2001). Tryptophan in a highly hydrophobic environment without any possibility for hydrogen bonding exhibits highly quenched fluorescence at about 307-308 nm (Class A). Tryptophan in a slightly more polar environment exhibiting more flexibility and hydrogen bonded in a 1:1 exiplex fluoresces at 316 nm (Class S), whereas Trp hydrogen-bonded in a 2:1 exiplex fluoresce at about 331 nm (Class I), with higher efficiency. Tryptophans that are partially exposed to solvent in flexible regions of a protein fluoresce near 342 nm (Class II) and tryptophan in model compounds and unfolded proteins that are highly exposed to bulk water fluoresce at 347-352 nm (Class III).

Phosphate buffered aqueous solutions were used by Cowgill for the fundamental series of experiments characterizing Trp and Tyr model compounds and protein fluorescence (for example Cowgill 1966, Cowgill 1967, Cowgill 1968, Cowgill 1968, Cowgill 1970). Eight molar urea is commonly used to unfold proteins and expose their constituent amino acids to the surrounding aqueous environment (Cowgill 1966), although recent work has demonstrated that transient structure may exist under these conditions (Whittington *et al.* 2005). Both Trp model compounds display class III fluorescence in phosphate buffer with λ_{max} Trp of 350-351 nm, similar to that in urea (Table 2.3). The relative fluorescence of the

model compounds in urea is about twice as high as that in phosphate buffer; increases have been reported by others (14-20% increase, Eftink 1994, McGuire and Feldman 1973). In both solvents, N-Ac-W-OEtH fluorescence is about half of that of N-Ac-W-NH₂. Cowgill (Cowgill 1970) reported reduced fluorescence efficiency of N-acetyltryptophan methyl ester (0.5) compared to N-acetyltryptophan (1.4), although no data for N-Ac-W-NH₂ were provided.

Ethylene glycol is frequently used to mimic the hydrophobic interior of a protein (DEC ~ 38.7; Havel 1996 and methanol is commonly used to measure the effects of a nonpolar solvent on model compounds (DEC ~33; Lee and Ross 1998. λ_{max} Trp of the model compounds is blue-shifted in both solvents (338-344 nm, Class II) compared to that in urea and phosphate buffer. The blue-shift of λ_{max} Trp is slightly greater in methanol, compared to EG, as expected for a less polar solvent, but relative emission in EG is higher, perhaps due to effects of solvent viscosity on fluorescence quenching, as has been observed for tyrosine (Noronha *et al.* 2004. In methanol and EG, the fluorescence intensities of both model compounds are very similar to each other whereas in urea, there is a two-fold difference in intensity.

Comparisons of the fluorescence spectra of the model compounds in the solvents described above to those of detergent-solubilized compounds provide information regarding both the hydrophobicity of the microenvironment surrounding the molecule, and the quenching of fluorescence by detergent moieties. In both 50 mM LDAO and 20 mM DPC, λ_{max} Trp (337-343 nm) was in the range observed for both compounds in methanol and EG (338-344 nm), indicating that N-Ac-W-OEtH and N-Ac-W-NH₂ partitioned significantly into the hydrophobic interiors of the detergent micelles. In these detergents the λ_{max} Trp of N-Ac-

Table 2.3. Summary of fluorescence data collected for His₆-porin and amino acid model compounds solubilized in various detergents or solvents. Intensity data were normalized to that of His₆-porin in 8 M urea.

Detergent or Solvent	His ₆ -porin or Model Compound	Fluorescence			
		Tyr (Ex 275 nm)		Trp (Ex 296 nm)	
		λ_{\max}	Int _{max}	λ_{\max}	Int _{max}
8 M Urea	His ₆ -porin	299	nd*	348	0.06
	NAc-Y-NH ₂	300	0.18		
	BOC-Y-OMe	300	0.21		
	NAc-W-NH ₂			350	0.17
	NAc-W-OEth			351	0.10
	W-NH ₂ + Y-NH ₂ †	301	nd	350	0.02
	W-Oeth + BOC-Y‡	301	nd	352	0.13
Phosphate buffer	NAc-Y-NH ₂	301	0.07		
	BOC-Y-OMe	300	0.08		
	NAc-W-NH ₂			351	0.11
	NAc-W-OEth			351	0.04
	W-NH ₂ + Y-NH ₂	302	nd	350	0.10
	W-Oeth + BOC-Y	300	nd	350	0.05
Ethylene glycol	NAc-Y-NH ₂	302	0.68		
	BOC-Y-OMe	302	0.54		
	NAc-W-NH ₂			344	0.28
	NAc-W-OEth			344	0.20
	W-NH ₂ + Y-NH ₂	301	nd	345	0.30
	W-Oeth + BOC-Y	300	nd	343	0.24
Methanol	NAc-Y-NH ₂	301	0.25		
	BOC-Y-OMe	300	0.21		
	NAc-W-NH ₂			341	0.07
	NAc-W-OEth			338	0.07
	W-NH ₂ + Y-NH ₂	301	nd	339	0.13
	W-Oeth + BOC-Y	300	nd	338	0.09

continued on next page

Table 2.3, continued

3.5 mM SDS	His ₆ -porin	303	nd	336	0.03
	NAc-Y-NH ₂	301	0.13		
	BOC-Y-OMe	299	0.12		
	NAc-W-NH ₂		0.26	351	0.11
	NAc-W-OEth		0.10	347	0.04
	W-NH ₂ + Y-NH ₂	301	0.29	350	0.12
	W-Oeth + BOC-Y	300	0.15	346	0.06
50 mM SDS	His ₆ -porin	302	0.09	336	0.03
	NAc-Y-NH ₂	299	0.10		
	BOC-Y-OMe	301	0.10		
	NAc-W-NH ₂		0.15	345	0.07
	NAc-W-OEth		0.07	341	0.03
	W-NH ₂ + Y-NH ₂	300	0.16	345	0.07
	W-Oeth + BOC-Y	301	0.10	342	0.04
50 mM LDAO	His ₆ -porin	bd§	bd	333	0.08
	NAc-Y-NH ₂	302	0.12		
	BOC-Y-OMe	299	0.02		
	NAc-W-NH ₂		0.36	349	0.23
	NAc-W-OEth		0.26	345	0.17
	W-NH ₂ + Y-NH ₂	301	0.40	351	0.25
	W-Oeth + BOC-Y	300	0.27	345	0.17
20 mM DPC	His ₆ -porin	299	0.26	343	0.06
	NAc-Y-NH ₂	301	0.19		
	BOC-Y-OMe	301	0.16		
	NAc-W-NH ₂		0.43	348	0.25
	NAc-W-OEth		0.35	343	0.22
	W-NH ₂ + Y-NH ₂	301	0.43	350	0.24
	W-Oeth + BOC-Y	301	0.37	343	0.22
<hr/>					
Liposomes	Method				
SDS	Deterget Alone	303	nd	336	0.03
SDS	FT	hs ¶	hs	329	0.04
SDS	SON	hs	hs	334	0.07
SDS	INS	hs	hs	335	0.09

* nd, not determined due to overlapping Tyr and Trp emission

† W-NH₂ + Y-NH₂, 2:9 molar mixtures of NAc-W-NH₂ and NAc-Y-NH₂

‡ W-Oeth + BOC-Y, 2:9 molar mixtures of NAc-W-OEth and BOC-Y-OMe.

§ bd, Tyr fluorescence below detection levels

¶ hs, high scatter at low wavelengths prevented analysis of Tyr fluorescence

W-OEtH (337-339 nm) was shifted further to the blue than that of the amide compound (342-343 nm), indicating that this model compound resides on average in a more hydrophobic environment and interacts with both the hydrophobic interior of the detergent micelle and the solvent (intermediate between Classes I and II fluorescence). Based on these observations, N-Ac-W-OEtH appears to be a better model for Trp in protein folded in zwitterionic-detergent. The relative fluorescence intensity of the model compounds in both detergents is similar to that in methanol, indicating a lack of quenching by the LDAO and DPC micelles, and further suggesting that the viscosity of the microenvironments in the micelles of both of these detergents is more similar to that of methanol than EG.

In contrast, the lack of a blue-shift in $\lambda_{\text{max}}\text{Trp}$ for both model compounds (347-351 nm; Class III) in 3.5 mM SDS indicates that neither N-Ac-W-NH₂ nor N-Ac-W-OEtH spends much time in the hydrophobic interior of the detergent micelle. However, in 50 mM SDS, these compounds display Class II fluorescence ($\lambda_{\text{max}}\text{Trp}$ 341-345 nm; Table 2.3), indicating increased exposure to a hydrophobic environment. The blue-shift is the greatest for N-Ac-W-OEtH, indicating that, as in DPC and LDAO, it partitions into a more hydrophobic environment than N-AcW-NH₂. At both SDS concentrations, the fluorescence of both model compounds is similar to that observed in phosphate buffer, indicating a lack of quenching.

Mixtures of either the amide or the alkylester model compounds were prepared in the 2:9 ratio present in His₆-porin. $\lambda_{\text{max}}\text{Trp}$ was unchanged by the addition of a Tyr model compound to the solution (Table 2.3); generally the fluorescence intensities at $\lambda_{\text{max}}\text{Trp}$ were slightly higher in the mixtures, likely due to overlapping Tyr fluorescence.

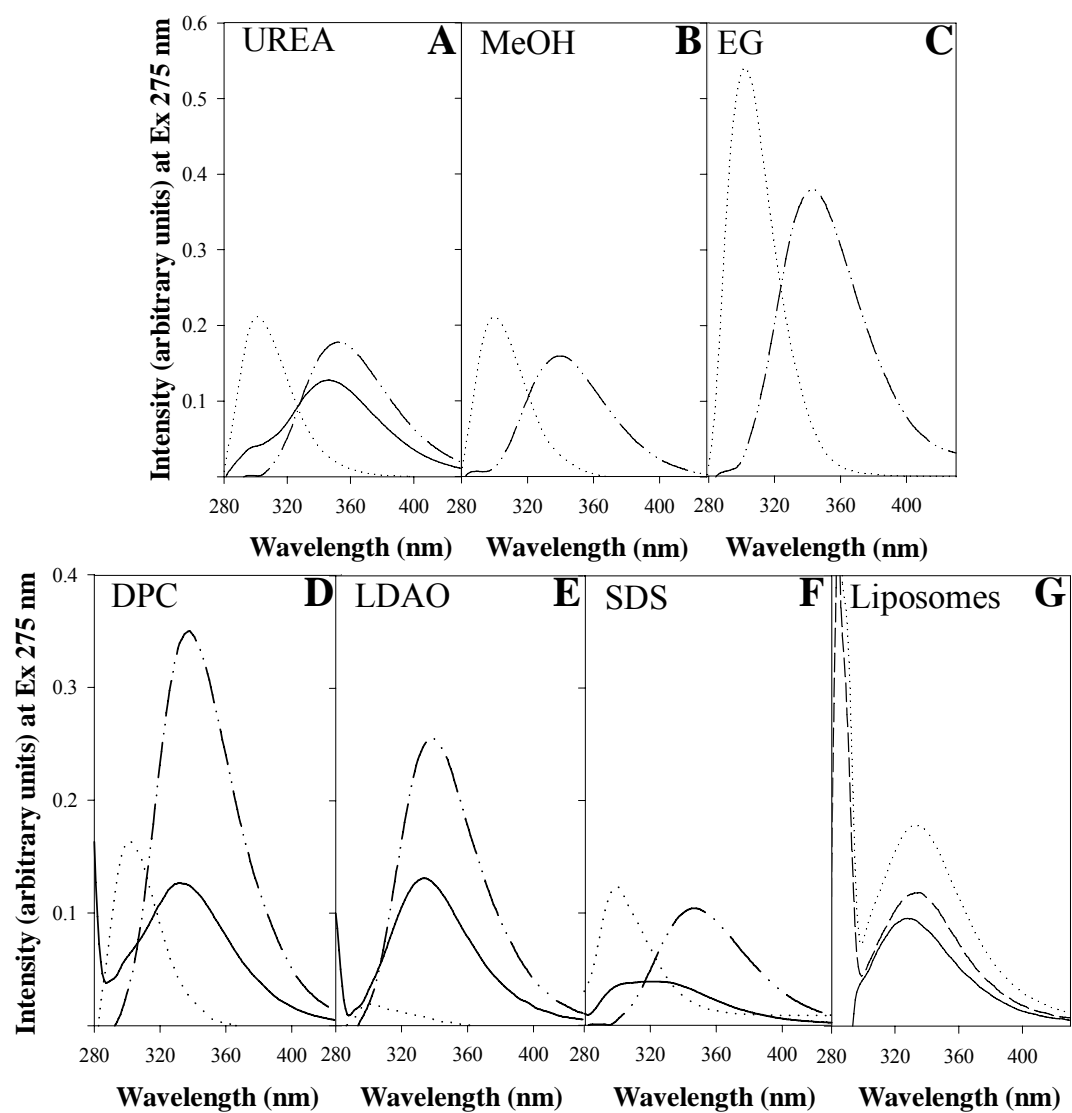
2.4.7 Tryptophan fluorescence of His₆-porin in detergent

In most models for porin structure, both tryptophan residues reside in membrane-spanning β -strands, one Trp residue is located near the centre of each half of the protein (reviewed by Bay and Court 2002; see Fig. 2.1 for example). Given the hydrophobic character of Trp and secondary structure predications that place them in β -strands, it would be expected that these residues would be involved in hydrophobic interactions with either adjacent β -strands or the lipids surrounding the β -barrel; without structural data these interactions cannot be identified. Likewise, in detergent-solubilized porin Trp residues could interact with other hydrophobic regions of the protein or with the interior of the detergent micelle.

Trp fluorescence dominates the spectra of urea-solubilized His₆-porin following excitation at 275 nm (Fig. 2.6A). $\lambda_{\text{max}}\text{Trp}$ is near 348 nm, as determined following excitation at 296 nm (see Table 2.3), and is characteristic of tryptophan residues exposed to an aqueous environment (Class III). Data from His₆-porin in phosphate buffer, EG and methanol is not available, as the protein is insoluble in these solvents. Therefore, porin fluorescence is compared to that of the urea-solubilized model compounds. In urea, $\lambda_{\text{max}}\text{Trp}$ of His₆-porin is similar to that of both tryptophan model compounds, but the fluorescence intensity is at least 40% lower than that of both NAc-W-NH₂ and NAc-W-OEt in urea (Table 2.3), likely due to quenching by peptide carbonyl groups in the unfolded protein (Cowgill 1967).

The fluorescence spectra of His₆-porin in 20 mM DPC and in 50 mM LDAO (see Fig. 2.6D and 2.6E) are also dominated by the tryptophan signal. $\lambda_{\text{max}}\text{Trp}$ is blue-shifted to 337 and 333 nm, respectively (Table 2.3), which suggests Class I fluorescence in DPC and

Figure 2.6. Fluorescence analysis. Fluorescence spectra were obtained following excitation at 275 nm of 0.42 μ M His₆-porin (solid line), BOC-Y-OMe (dotted line) , and NAc-W-OEth (dash-dot-dot line) solubilized in **A)** 8 M urea **B)** methanol (MeOH) **C)** EG **D)** 20 mM DPC **E)** 50 mM LDAO or **F)** 3.5 mM SDS. **G)** Fluorescence of His₆-porin in proteoliposomes prepared by the freeze thaw (solid line), insertion (dotted line) or sonication (dashed line) methods. λ_{ex} was 275 nm. All emission values were corrected for protein concentration. Note that the y-axis scale for panels A-C is larger than that for panels D-G.



fluorescence intermediate between Classes I and II in LDAO. Thus, LDAO and DPC promote folded states in which the Trp residues are in environments of similar polarity, although the environment in LDAO appears slightly more hydrophobic. Relative Trp fluorescence intensity is similar in both detergents, indicating that the folded states of the protein do not place the Trp residues in close proximity to quenching groups.

The fluorescence spectrum obtained following excitation of SDS-solubilized His₆-porin at 275 nm is striking in that overall fluorescence emission is very low and intensity at $\lambda_{\text{max}}\text{Trp}$ and $\lambda_{\text{max}}\text{Tyr}$ are very similar. Excitation at 296 nm reveals that His₆-porin Trp fluorescence in SDS is strongly blue-shifted, ($\lambda_{\text{max}}\text{Trp} \sim 336 \text{ nm}$; Class I/ Class II) and indicates that both tryptophan residues have very limited solvent exposure (Table 2.3). The intensity at $\lambda_{\text{max}}\text{Trp}$ is reduced at least 50% compared to that in urea, DPC, and LDAO (Table 2.3). This strong quenching of porin fluorescence in SDS is likely due to a combination of the low dielectric of the micelles, and quenching by the sulfate head groups of the detergent and/or by the side chains of nearby moieties in the SDS-folded protein, such as protonated aspartate (14 residues in His₆-porin), glutamate (10 residues), histidine (14 residues), phenylalanine (17 residues) (Ladokhin 2000). His₆-porin fluorescence is unchanged at higher SDS concentrations (Table 2.3), supporting the conclusion that, unlike the model compounds, His₆-porin resides within the micelle at both high and low SDS concentrations.

2.4.8 Tryptophan fluorescence of His₆-porin reconstituted into liposomes

Fluorescence spectroscopy of Trp residues in bacterial porins (OmpF and OmpA) reconstituted into lipid vesicles has been employed to monitor protein refolding and membrane insertion events (Surrey and Jahnig 1995, Surrey *et al.* 1996). To ascertain the environment of Trp residues of His₆-porin in artificial membranes, fluorescence emission

spectra were collected for each of the three preparations (FT, SON, and INS) of SDS-solubilized His₆-porin-liposomes following excitation at 275 nm (Fig. 2.6G), 280 nm, and 296 nm (Table 2.3). Precise examination of Tyr fluorescence was not possible due to the high degree of scatter of lower wavelength light by liposomes.

The emission spectrum of FT SDS-His₆-porin-liposomes following excitation at 275 nm had a sharp λ_{max} Trp of 330 nm and relative intensity of 0.1 (Table 2.3, Fig. 2.6G). This spectrum was striking in comparison to SDS-solubilized His₆-porin where the λ_{max} Trp is broad spanning the region of 315-335 nm and the relative intensity is 0.03 (Table 2.3, Fig. 2.3F). Following excitation at 296 nm, λ_{max} Trp of FT SDS-His₆-porin-liposomes was 329 nm, significantly blue-shifted from that of porin in detergent alone (336 nm); the relative fluorescence intensities were similar (Table 2.3; Fig. 2.6G). The emission spectra of SON and INS SDS-His₆-porin-liposomes following excitation at 275 nm have increased relative intensities compared to that of FT SDS-His₆-porin-liposomes (Table 2.3). λ_{max} Trp of SON SDS-His₆-porin-liposomes (λ_{ex} 296 nm) was slightly red-shifted compared to that of both INS and FT SDS-His₆-porin-liposomes, but was very similar to that of SDS-solubilized His₆-porin (Table 2.3, Fig. 2.6F).

Overall, the increased relative intensities at λ_{max} Trp in each emission spectrum of SDS-His₆-porin-liposomes in comparison to the spectrum of SDS solubilized His₆-porin support Trp location in an environment of increased hydrophobicity and/or reduced quenching by SDS headgroups. In general, the emission spectra for each preparation of SDS-His₆-porin-liposomes lacked the low intensity and broad λ_{max} Trp observed for SDS-solubilized His₆-porin, indicating that quenching by the detergent has been relieved. The higher relative intensity of the INS SDS-His₆-porin-liposomes emission spectrum, relative to that of the FT

liposomes, may also indicate that the Trp residues reside in a more hydrophobic environment. This observation is consistent with a β -barrel conformation in the osmotically-responsive FT liposomes, where Trp residues could be solvent-exposed in the channel (reduced intensity) and a collapsed β -structure in the INS liposomes (increased intensity).

2.4.9 Fluorescence of tyrosine model compounds in detergent

The detergent environments surrounding the Tyr model compounds were also investigated with fluorescence spectrophotometry following excitation at 275 nm. λ_{max} Tyr falls within the 299-302 nm range in all of the solvents and detergents tested (Fig. 2.6, Table 2.3). Given the ± 3 nm precision of the fluorometer, these values can be considered to be the same. However, there are striking differences in the relative intensities of fluorescence that reflect the environments in which the model compounds reside.

The intensities of NAc-Y-NH₂ and BOC-Y-OMe fluorescence are similar in 8 M urea, and both are reduced by about 65% in phosphate buffer. The enhanced fluorescence intensity of both model compounds in urea is unexpected, as the quantum yield of NAc-Y-NH₂ reported by others is similar in water and in urea (Lee and Ross 1998). A minor ($\sim 10\%$) contribution to this effect may result from the use of an excitation wavelength of 275 nm, which is the λ_{max} excitation for tyrosine in urea, while that in water is 273.5 nm (Lee and Ross 1998). Solvent viscosity may also contribute to the increased Tyr emission in urea (Noronha *et al.* 2004); the viscosity of 8 M urea is 1.66 times that of water (Kawahara and Tanford 1966). Relative to that in phosphate buffer, increased fluorescence intensity was observed for both model compounds in the hydrophobic solvents methanol and EG; the increase was two-to-three fold greater in EG. As discussed above, the large differences in

intensity in these two solvents may reflect their relative viscosities (0.6 cP for methanol, 19.9 cP for ethylene glycol).

In DPC, the high fluorescence intensity of both model compounds (0.16-0.19) indicates that they are exposed to an environment more similar to that in methanol (0.21-0.25) than to that in phosphate buffer (0.07-0.08). In striking contrast, Tyr fluorescence of BOC-Y-OMe is very strongly quenched in LDAO (0.02), suggesting close proximity of this model compound to quenching groups, most likely the headgroups of the detergent. In contrast, there is much less quenching of N-Ac-Y-NH₂ fluorescence (0.12), indicating that the moieties on the carboxyl and/or amino groups of the Tyr compounds promote different interactions of the model compounds with the detergent headgroups. For both model compounds, the fluorescence intensity in SDS, either at 3.5 or 50 mM, is similar to that in phosphate buffer, indicating little interaction between the model compounds and the hydrophobic regions of the SDS micelles. ¹H-NMR (data not shown) confirms that neither compound resides in the micelle in 3.5 mM SDS and that there is a small increase in the relative time that the hydrophobic BOC-Y-OMe spends in the interior of the micelle in 50 mM SDS, but this effect is not detectable by fluorescence.

2.4.10 Tyrosine Fluorescence of His₆-porin in detergent

Following excitation at 275 nm, fluorescence spectra of proteins are the result of both tyrosine and tryptophan emissions, and in most cases, are dominated by the tryptophan-derived signal (see Fig. 2.6). Second derivative analysis was used to estimate $\lambda_{\text{max}}^{\text{Tyr}}$ of His₆-porin in 8 M urea, DPC, LDAO and SDS; in all cases $\lambda_{\text{max}}^{\text{Tyr}}$ falls within the 299-303 nm range noted for the model compounds (Table 2.3). Both Trp and Tyr fluorescence contribute to intensity at $\lambda_{\text{max}}^{\text{Tyr}}$ (Fig. 2.6); therefore, only, general trends can be noted

regarding the relative Tyr fluorescence intensities. Data from His₆-porin in phosphate buffer, EG and methanol are not available, as the protein is insoluble in these solvents.

The intensity of Tyr fluorescence in His₆-porin is very different from that of the model compounds. In urea, the intensity of the tyrosine fluorescence produced by His₆-porin is only about 10% of that of NAc-Y-NH₂ or BOC-Y-OMe in the same solvent (Fig. 2.6A, Table 2.3). Quenching of Tyr fluorescence in a protein can result from interactions with tryptophan and ionized carboxylates on glutamate and aspartate residues and interactions with other quenched tyrosine residues (Cowgill 1968). These interactions could reflect local backbone structure in urea (Whittington *et al.* 2005), random collisions between the tyrosine residues, and the quenching moieties, and/or resonance energy transfer (with Trp residues). Since the arrangement of His₆-porin in urea is highly unordered based on its far UV CD spectrum (Fig. 2.5A), resonance energy transfer is unlikely as it would require a stable conformation in which the residues are in close proximity.

Far-UV CD analysis demonstrated unique conformations of porin in DPC and LDAO; this conclusion is borne out by the differences in the Tyr microenvironments promoted by these detergents. Fluorescence of His₆-porin at $\lambda_{\text{max}}^{\text{Tyr}}$ is similar in 20 mM DPC (Fig. 2.6D) and 8 M urea (Fig. 2.6A), and lower than that of the model compounds in methanol (Fig. 2.6E), suggesting that, in DPC, the Tyr residues are either not exposed to a hydrophobic environment, or that Tyr fluorescence is quenched. In contrast, Tyr fluorescence in 50 mM LDAO (Fig. 2.6E) is negligible, likely due to quenching by detergent headgroups, as was seen for BOC-Y-OMe in LDAO. Weak fluorescence was obtained from His₆-porin in 3.5 mM SDS (Fig. 2.6F), as discussed with respect to Trp fluorescence above. The highly-quenched, blue-shifted Trp fluorescence contributes to the signal at $\lambda_{\text{max}}^{\text{Tyr}}$; nonetheless the

fluorescence intensity at $\lambda_{\text{max}}^{\text{Tyr}}$ is low, suggesting that, in the SDS-promoted conformation, the tyrosine residues are likely solvent-exposed and may be in close proximity to quenching moieties.

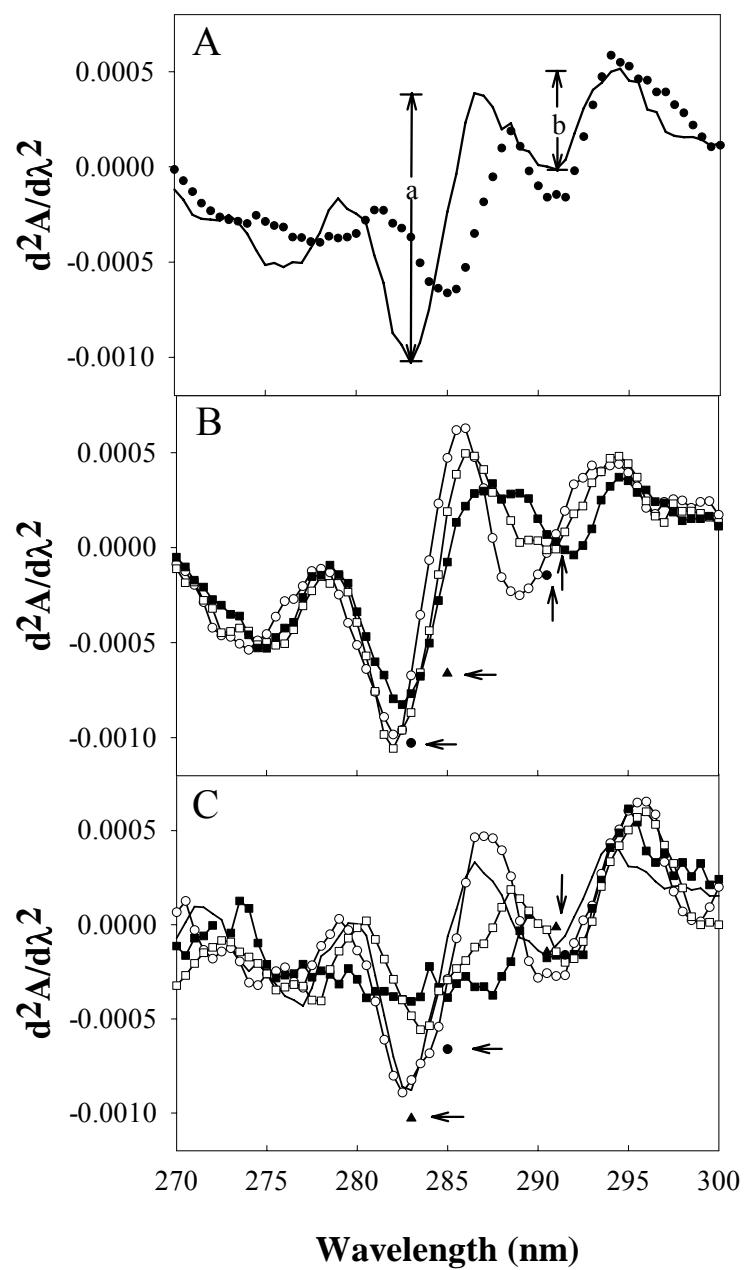
2.4.11 Tyrosine exposure in detergent-solubilized His₆-porin

Conclusions regarding Tyr environments cannot be made from fluorescence data alone, as reduced Tyr fluorescence can reflect increased solvent exposure or increased fluorescence quenching. To discern between these two possibilities, UV absorption data were used to estimate tyrosine exposure to the aqueous environment (Table 2.4; Ragone *et al.* 1984). The Tyr and Trp components of the absorption spectra can be separated by second derivative analysis (SDUV; Ragone *et al.* 1984), in which the tyrosine and the tryptophan absorbance both contribute to a peak in the range of 280-285 nm, while a second peak derived from Trp absorbance is near 291 nm (Fig. 2.7A). The absorption maximum of Tyr varies with the polarity of the surrounding environment and is red-shifted and of a lower magnitude in a non-polar environment, such as EG, while the positions of both tryptophan-derived components remain unchanged as they are derived from the $^1\text{L}_b \leftarrow ^1\text{A}$ transition, which is insensitive to polarity (Ragone *et al.* 1985). A red-shift in Tyr absorption decreases the signal at 283 nm relative to that at 291 nm; the ratio of these values, r , therefore reflects the hydrophobicity of the Tyr environment. For example, in Table 2.4, r for both NAc-Y-NH₂ and BOC-Y-OMe in EG is 0.56-0.58, while in the polar solvent urea the values are higher: 2.55 and 1.77, respectively (see Fig. 2.7A and B). r is high (2.24-2.91) for the amide model compound mixtures in LDAO, DPC and 3.5 mM SDS (Fig. 2.7B), in agreement with the fluorescence data that indicated that NAc-Y-NH₂ is not partitioned into the hydrophobic

Table 2.4. SDUV analysis of His₆-porin and model compounds. r and Y_{exp} values were calculated as described in Materials and Methods. His₆-porin was insoluble in EG; hence there are no r data for this solvent. For the amide model compounds and His₆-porin, each experiment was repeated at least twice; averages are reported; standard deviations were less than 22%. For the hydrophobic compounds, the data reported are from a single experiment.

Detergent / Solvent	r		His₆-porin	Y_{exp} (α)
	NAc-W-OEth + BOC-Y-NH₂	NAc-W-NH₂ + NAcY-NH₂		
EG	0.56	0.58		
8 M Urea	1.77	2.55	1.82	1.00
50 mM LDAO	0.10	2.64	0.82	0.23
10 mM DPC	0.50	2.91	0.85	0.25
3.5 mM SDS	1.51	2.24	1.39	0.77
50 mM SDS	1.08	1.71	1.45	0.70

Figure 2.7. SDUV absorption analysis. The 2:9 mixture of NAc-Trp-NH₂/NAc-Tyr-NH₂ was solubilized in **A**) 8 M urea (thick line), or EG (closed circles) or **B**) 3.5 mM SDS (open circles), 50 mM LDAO (filled squares), or 10 mM DPC (open squares). The second derivative plots of the UV absorbance spectra are presented. **C**) SDUV plots of the absorbance spectra of His₆-porin; the symbols are the same as those of panel B. For comparison, the tyrosine-derived minima in urea (filled circle) and ethylene glycol (filled triangle) are shown in panels B and C; they are highlighted by arrows.



interiors of these detergent micelles. Similarly, r is high (1.51) for BOC-Y-OMe in 3.5 mM SDS, supporting the fluorescence data that suggest this compound is not in the hydrophobic interior of the micelle. In contrast, r is low for the hydrophobic model compound in DPC (0.5). Together with the similarity between the fluorescence spectra of BOC-Y-OMe solubilized in DPC and methanol, this suggests partitioning of this model compound into the DPC micelles. The lowest r value results from solubilization of the hydrophobic model compounds in LDAO, suggesting that the extremely low intensity of BOC-Y-OMe fluorescence in LDAO results from quenching of molecules of the detergent micelle headgroups.

The SDUV plot of His₆-porin in urea (Fig. 2.7C) is similar to that of the amide model compounds, and r is 1.82, similar to that in urea. Thus, the aromatic residues are solvent-exposed in the denatured protein. In contrast, r values near 0.8 were calculated for His₆-porin solubilized in DPC and LDAO (Fig. 2.7C), indicative of conformations in which the tyrosine residues are exposed to less polar environments, presumably within detergent micelles. As described in Materials and Methods, the r values for the amide model compounds, the protein unfolded in urea, and for the “folded” protein can be used to estimate α , the Tyr exposure (Ragone *et al.* 1984). In DPC and LDAO, Tyr exposure is calculated to be about 0.25, indicating that on average two or three of the nine tyrosine residues in the protein are solvent exposed (Table 2.4). Given these results, the very low intensity Tyr fluorescence by DPC- or LDAO-solubilized His₆-porin is best explained by a high degree of quenching of fluorescence. In contrast, Tyr exposure was high in SDS (Fig. 2.7C), with an r value of 1.39, and α of 0.77, indicating that 7 of the 9 Tyr residues are exposed to solvent, where they would exhibit lower intensity fluorescence, and be accessible to quenching by detergent

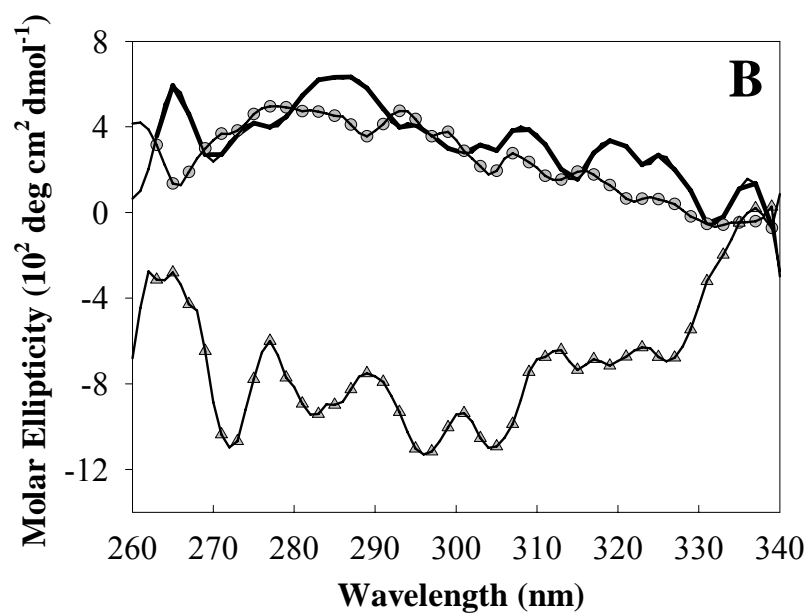
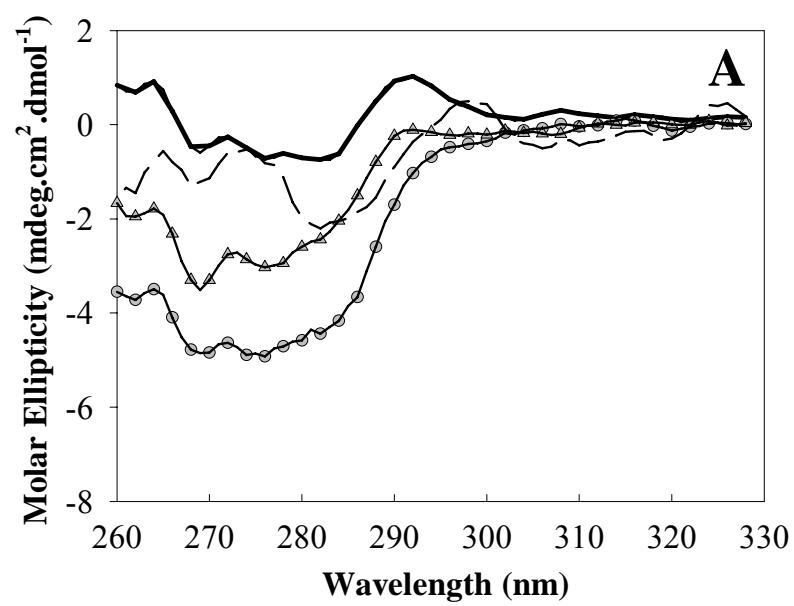
headgroups, or other exposed residues in the protein. These observations are compatible with the fluorescence data. Light scattering by liposomes prevented similar analyses of membrane-embedded His₆-porin.

2.4.12 Near-UV CD of His₆-porin in detergent and in liposomes

CD spectra obtained in the near-UV (260-330 nm) provide additional insight into the tertiary interactions in proteins. The 265-280 nm region is the most informative because both tryptophan (270-280 nm) and tyrosine residues (265-270 nm) absorb in this portion of the spectrum. His₆-porin could be solubilized at a concentration ($\geq 25 \mu\text{M}$) sufficient for this analysis in 8 M urea, 21 mM SDS, 300 mM LDAO and 100 mM DPC (Fig. 2.8A). In the region between 265 and 290 nm, the spectrum obtained in urea shows little indication of tertiary interactions, as noted for other proteins unfolded in urea (Reader *et al.* 2001, Masui *et al.* 1997). The negative ellipticity in the spectrum obtained in LDAO is of the same magnitude as in urea, suggesting an absence of tertiary structure in this detergent. The very weak ellipticity may reflect protein-protein interactions that occur in high concentration solutions. However, the ellipticity is at least an order of magnitude less than that observed during specific interactions between unfolded proteins, such as the self-association of partially-denatured bovine growth hormone (Havel *et al.* 1986).

In contrast to those in urea and LDAO, the near UV CD spectra of the protein dissolved in SDS and DPC show negative ellipticity suggesting that the protein is in a condensed state in which some of the aromatic residues exist in transiently stabilized tertiary interactions. The overall shape of the DPC and SDS spectra are similar, with a broad band

Figure 2.8. CD spectropolarimetry of His₆-porin in the near UV region. **A)** Spectra of 25-33 μ M His₆-porin solubilized in 100 mM DPC (circles), 8 M urea (solid line), 300 mM LDAO (dashed line) and 21 mM SDS (triangles) were obtained as described in Materials and Methods. **B)** Spectra of His₆-porin in SDS-liposomes generated by the freeze-thaw (solid line), sonication (triangles) and insertion (circles) methods. All spectra were corrected for protein concentration.



of negative ellipticity that spans both the tyrosine and tryptophan regions. The ellipticity is greater in DPC, suggesting stronger or more extensive interactions.

Near UV CD spectra of FT, SON and INS SDS-His₆-porin-liposomes were also examined (Fig. 2.8B). The spectrum of FT SDS-His₆-porin-liposomes had positive ellipticity in the 280-290 nm region. The near UV CD spectrum of INS SDS-His₆-porin-liposomes also demonstrated positive ellipticity near 276 nm. In contrast, the near UV CD spectrum of SON SDS-His₆-porin-liposomes had strong negative ellipticity in the 310-270 nm region (Fig. 2.8B), similar to that observed for DPC and SDS solubilized His₆-porin, suggesting a condensed state with stronger tertiary contacts than those promoted by single detergents only.

2.5 Discussion

2.5.1 Porin solubility

The denaturant urea and the detergent SDS are able to solubilize acetone-precipitated His₆-porin at the highest concentrations. This protein is also moderately soluble in the ionic detergents LDAO and DPC, but poorly soluble in neutral OG, Genapol X-080 and DDM. Taken with data obtained by other groups, these results emphasize the importance of the method of protein purification in determining the most suitable detergent for solubilization of the protein. A thorough study by De Pinto *et al.* (1989) revealed that the Tritons, dimethylamine oxides, and zwittergents were best for isolation of porin from bovine heart mitochondria, with LDAO optimal for maintaining the protein in a membrane-insertion competent state. OG was successfully used by Shao *et al.* (1996) to solubilize porin from *Neurospora* mitochondria. The protocols used by these groups differed from the method presented herein in several critical ways: they did not involve refolding of the porin, only

mild denaturation was needed to disrupt the membranes, and purification in LDAO recovers sterols as well (De Pinto *et al.* 1989).

Exchange of the urea, or guanidinium chloride, for detergent, to allow folding of the protein has been achieved previously by dialysis, and leads to high concentration of protein in LDAO (170 μ M) or OG (34 μ M; Koppel *et al.* 1998), but not in Genapol X-080 (DCB and DAC, unpublished results). However, routine preparation of highly concentrated porin in LDAO is prohibitively expensive using dialysis; instead, detergent exchange following acetone precipitation (Shao *et al.* 1996) of urea-solubilized His₆-porin was utilized in this study.

Several conclusions are apparent with respect to solubility of the acetone-precipitated His₆-porin in the various detergents tested. With the exception of OG, all of the detergents used have acyl chains of 12-13 residues. These lengths exceed the minimum chain lengths of 9-10 found by Kleinschmidt *et al.* (Kleinschmidt *et al.* 1999) to promote folding of the bacterial porin OmpA. Thus, the inability of octyl-glucoside to stably solubilize acetone-precipitated His₆-porin is likely due to the short length of the tail, rather than any characteristic of the headgroup. In this study, detergent concentrations greater than the CMC were required for optimal solubilization of the protein (data not shown), as also noted for OmpA (Kleinschmidt *et al.* 1999).

The highest levels of solubility were achieved with detergents with charged headgroups, the best being negatively-charged SDS, followed by the two zwittergents, LDAO and DPC. Since OG and DDM were unable to solubilize porin at useful concentrations, it appears that ionic charge, as in SDS and DPC, enhances the solubilization, presumably by disrupting inter-and intramolecular interactions in the precipitated protein and/or by

maintaining detergent-protein interactions required for solubility. Although the net charge on the headgroups of DPC and LDAO are both zero, the positively and negatively charged moieties in the head group of LDAO are in very close proximity, possibly limiting interactions with the precipitated protein and thereby reducing solubilization. In addition, the monomers of the uncharged detergents may be unable to effectively interact with the surface of the porin to create a stable protein-detergent micelle (Garavito and Ferguson-Miller 2001). A further hindrance to solubility in LDAO may be the increased β -strand content, because these structures have a preference for interacting with other segments of the protein to satisfy their hydrogen bonding potential, whereas individual α -helices can interact with lipid (Popot and Engelman 1990), or in this case, the hydrophobic portions of the detergent.

2.5.2 His₆-porin reconstituted into liposomes

Liposome swelling experiments involving His₆-porin solubilized by LDAO, DPC and SDS have demonstrated that, after FT in the presence of a SUV stock, each sample was capable of forming osmotically responsive pores in artificial membranes, as shown for porins isolated from mitochondria (Bathori *et al.* 1993, Shao *et al.* 1996). The spectroscopic features of His₆-porin in liposomes were similar to those observed for other β -barrel proteins – namely $\lambda_{\text{max}}\text{Trp}$ near 330 nm, and a conformation rich in β -strand (Linke *et al.* 2000, OEP16; Kleinschmidt and Tamm 2002, Pocanschi *et al.* 2006). The fact that His₆-porin solubilized in a variety of detergents formed channels is interesting since each detergent promotes a different secondary arrangement with different levels of tertiary interactions (Table 2.2, Fig. 2.8). However, the effectiveness of pore formation varied from highly reproducible channel formation by SDS-His₆-porin to variable results with LDAO-porin. The effectiveness of SDS may relate to the α -helical structure it promotes – the protein may be

less prone to aggregation upon dilution into the SUV solution, allowing a greater fraction to interact with the membrane (Surrey and Jahnig 1992). Alternatively, SDS may be most effective at disrupting membrane packing, a requirement for insertion of membrane proteins into preformed membranes (see Scotto and Zakim 1988 for discussion). The osmotic response of some preparations of LDAO-His₆-porin liposomes increased following heating, suggesting that a kinetic barrier to assembly may exist under these conditions.

In general, the freeze-thaw procedure was the only one to produce osmotically-responsive proteoliposomes that were resistant to heating at 65°C. Sonication of liposomes in the presence of porin was not successful, suggesting that conditions created during the freezing and/or thawing steps, in addition to membrane rupture, were required for pore formation by His₆-porin. The shape of the resulting vesicles or defects in membrane packing may explain this observation (Surrey and Jahnig 1992). Some aggregation of the protein in the membrane may be necessary for pore formation, as shown for short β -sheet peptides (xSxG)₆ that form voltage-gated channels upon aggregation in lipids bilayers (Thundimadathil *et al.* 2005, Thundimadathil *et al.* 2005).

Dilution of His₆-porin into a suspension of preformed liposomes also did not lead to osmotically responsive proteoliposomes, in contrast to the folding of OmpA that can be achieved under similar conditions (Surrey and Jahnig 1992, Kleinschmidt and Tamm 1999). The reaction did not occur at 30°C, and 42°C, temperatures which are sufficient for breaking the kinetic barriers to in vitro folding and membrane insertion of OmpA (reviewed in Kleinschmidt and Tamm 1996). As the goal of the reconstitution experiments was to obtain folded, channel forming porin, in-depth examination of folding and membrane insertion was beyond the scope of this study.

In contrast to their variable osmotic responsiveness, proteoliposomes prepared by all three methods contain protease-resistant porins (Fig. 2.3). This suggests that in all of these cases, His₆-porin is interacting strongly with the lipid and/or with other His₆-porin molecules. The latter possibility is suggested by the oligomers observed on western blots of all three types of proteoliposomes (Fig. 2.3). Oligomers were not detected in detergent-solubilized His₆-porin preparations, in contrast to experiments utilizing purified rat liver mitochondrial porin (Zalk *et al.* 2005). A possible explanation for this discrepancy is that isolation of His₆-porin in urea prevents the formation of contacts required for multimeric interactions.

Oligomers of His₆-porin were also not detected in detergent- and SEM-solubilized mitochondria. Although the urea included in the SDS-PAGE gels presented in this study might disrupt such interactions, oligomers are also undetectable in immunoblots of gels lacking urea (data not shown). Furthermore, although mitochondrial porin may be able to oligomerize under certain conditions, interactions with other proteins (Roman *et al.* 2006) and porin-associated sterols (De Pinto *et al.* 1989) may prevent the formation of oligomers in the mitochondrial outer membrane. Electron microscopic analysis of two-dimensional arrays of mitochondria outer membranes from *N. crassa* did not detect any oligomeric arrangements of mitochondrial porin (Mannella 1989, Thomas *et al.* 1991, Guo and Mannella 1993). In addition, chemical cross-linking was required for detection of the oligomers of rat liver mitochondrial porin. Finally, although VDAC1 is abundant in rat cells, there are at least three isoforms of porin in this organism (Pavlica *et al.* 1990), and it was not ruled out that the hetero-oligomers were formed in the more recent experiments (Zalk *et al.* 2005).

2.5.3 The folded states of His₆-porin reconstituted into liposomes

The conformation of His₆-porin following reconstitution into liposomes was examined by CD spectropolarimetry and fluorescence spectroscopy. SDS-His₆-porin incorporated into liposomes by all three procedures is β -strand rich, but only in FT SDS-His₆-porin liposomes was the β -strand content stably maintained upon heating (Fig. 2.4), suggesting different interactions with the membranes in each preparation. Similarly, intrinsic Trp fluorescence is most intense in SON and INS SDS-His₆-porin liposomes, but in FT liposomes, fluorescence intensity (at λ_{ex} 296 nm) is similar to that of the protein in SDS, and λ_{max} Trp is the least red-shifted in comparison to SDS-His₆-porin, suggesting that the tryptophans reside in quite different environments in the osmotically-responsive and non-responsive forms of the protein.

Analysis of near-UV CD spectra also reveals differences among the proteoliposomes formed via the three methods. These spectra are dominated by positive ellipticity for the FT and SON-type proteoliposomes, and negative ellipticity for the INS-type (Fig. 2.7). In all cases, these data imply that tertiary contacts or intermolecular interactions involving the aromatic amino acids in porin are occurring in the membrane, but their nature is determined by the method used for porin reconstitution. As there are no near-UV data for natively folded mitochondrial porins, comparisons can only be made with bacterial proteins. The spectrum of OmpA in SDS is negative, but upon folding by the addition of OG, it is dominated by a positive signal (Ohnishi and Kameyama 2001), suggesting that the tertiary contacts in SDS are different from those in the β -barrel structure. Similarly, near-UV CD spectra with strong positive ellipticity have been reported for native bacterial proteins including the PorB class 2 (Minetti *et al.* 1997) and class 3 (Minetti *et al.* 1998) porins of *Neisseria*. Further, changes

from positive to negative ellipticity in both the Tyr and Trp spectral regions have been observed during acid or thermal denaturation of several water-soluble β -rich proteins including the cardiotoxin analogue III, CTXIII, (Kumar *et al.* 1995, Sivaraman *et al.* 1997), CD40L (Matsuura *et al.* 2001) and TNF- α (Narhi *et al.* 1996). In all of these proteins, the aromatic amino acid residues reside in β -strands. However, this correlation is not absolute; for example, the near UV spectrum of the folded β -barrel of the src homology domain 3 of the growth factor receptor binding protein 2 displays strong negative ellipticity in the 280 nm region (Bousquet *et al.* 2000).

Although they do not form detectable pores in the membrane, it is possible that the forms of His₆-porin in the INS and SON liposomes resemble partially folded species of other β -barrel proteins. A detailed mechanism for folding and insertion of OmpA has been revealed by a series of elegant experiments using time resolved Trp fluorescence quenching (Kleinschmidt *et al.* 1999, Kleinschmidt, 1999 #462, see Fig. 1.5). The unfolded protein (U) becomes a hydrophobically collapsed water-soluble intermediate I_W upon dilution from urea into water. In the second stage this intermediate binds to the membrane (I_{M1}) and proceeds to intermediate (I_{M2}) where β -structure begins to develop at the membrane surface, but lacks tertiary contacts (“molten disk”). The β -hairpin loops translocate to the centre of the lipid bilayer lacking correct tertiary fold forming the final “molten globule” intermediate (I_{M3}) which then proceeds to the native state (N) (reviewed by Tamm *et al.* 2004). Trp fluorescence data suggest that porin in INS and SON-type proteoliposomes reside in a less hydrophobic environment than that in FT liposomes, which may indicate a partially inserted intermediate such as I_{M2} . However, it is not clear whether the weak tertiary contacts in His₆-porin detected by near-UV CD are compatible with the molten disk state as described for OmpA.

2.5.4 Detergent-promoted folded states

The secondary and tertiary structures of mitochondrial porin in urea, SDS, LDAO and DPC are unique, as demonstrated using a variety of spectroscopic techniques, most of which have not previously been applied to mitochondrial porins. As discussed by Nahri (Narhi *et al.* 1996), protein conformations are determined by both long and short range interactions established during folding of the protein, and each detergent was observed to promote a unique arrangement in terms of both secondary and tertiary structures.

Of the three detergents, DPC might be expected to promote correct folding of mitochondrial porins because 45% of the outer membrane is composed of the related lipid phosphatidylcholine (de Kroon *et al.* 1997). DPC does promote some β -strand structure (26-30%), but this amount is significantly lower than that obtained for porin isolated from mitochondria in OG (62-63%, Shao *et al.* 1996), and LDAO (45%, Koppel *et al.* 1998). Furthermore, the levels of unordered structure in DPC are high (>50%), suggesting that the DPC-solubilized porin is not in the same conformation as in mitochondria. In DPC, both Trp and most of the Tyr residues in His₆-porin were buried in the detergent/protein complex. Low tyrosine exposure has also been reported in *Neisserial* PorB porins folded in Zwittergent 3-14 (class 2 porin $\alpha = 0.09$ (Minetti *et al.* 1997) and class 3 porin $\alpha \sim 0$ (Minetti *et al.* 1998).

The DPC-promoted conformation is sensitive to heat denaturation, which is accompanied by a loss in α -helix, but not β -strand structure, suggesting that the α -helical structure plays an important role in maintenance of the protein in a soluble form. Reduction of this component at high temperature would then lead to protein precipitation, due to the constraints on maintaining β -strand rich protein in solution, as discussed above. In addition, fluorescence and near UV CD studies provide evidence for tertiary contacts in DPC-

solubilized porin; disruption of these contacts at high temperature may also contribute to precipitation of the protein.

Structural analysis of the protein in LDAO is particularly interesting, as this detergent is used for preparing porin for electrophysiological studies in artificial bilayers (Koppel *et al.* 1998). LDAO promoted high levels of β -strand content (32-39%), similar to the native protein in the same detergent (Koppel *et al.* 1998) but the absence of tertiary interactions suggests that the protein has not adopted its native conformation, but exists in a state that has been referred to as “molten globule” or “molten disk” (for example see Matsuura *et al.* 2001). This conformation requires tertiary mobility while maintaining interactions required for solubility of β -strands (Matsuura *et al.* 2001). Examples of β -strand rich molten globule proteins include CTXIII, Kumar *et al.* 1995, Sivaraman *et al.* 1997), which contains Tyr but no Trp residues, and Trp-containing proteins of the tumor necrosis factor family, CD40L (Matsuura *et al.* 2001) and TNF- α (Narhi *et al.* 1996). In the molten globule state, several arrangements are possible. One example is pockets of β -strand structure existing separately from large regions of unstructured protein. Alternatively, the protein may exist in a collapsed β -barrel, in which native β -strands form, but are maintained by interactions with the detergent rather than the adjacent β -strands as in a barrel structure.

Tyrosine exposure is very low under these conditions, suggesting that the C-terminal half of the protein, containing most of the Tyr residues (Fig. 2.1), is buried in the detergent/protein complex. The CD spectra obtained during thermal denaturation of LDAO-solubilized His₆-porin (Fig. 2.5D), resemble those of native porin in OG (Shao *et al.* 1996). However, unlike the OG-solubilized porin, His₆-porin in LDAO did not precipitate at high temperature (100°C), and partial refolding to a structure resembling that present at the 57°C

midpoint was observed upon cooling. The overall shape of the CD spectra at 65°C indicate similar changes in structure as reported by Shao *et al.* for porin in OG at 65°C (Shao *et al.* 1996). In contrast, thermal denaturation of β -strand in detergent-solubilized *Neisseria* PorB porins has a midpoint of 85-90°C (Minetti *et al.* 1998, Minetti, 1997 #260).

SDS-folded porin is predominantly α -helical, and contains the lowest levels of β -strand, and high levels of unordered structure (> 55%). α -helix formation is a common characteristic of many proteins in SDS (Visser and Blout 1971), including mitochondrial porin (Shao *et al.* 1996, Popp *et al.* 1997) and β -barrel bacterial porins (for example *E. coli* porin, Eisele and Rosenbusch 1990). Although the tryptophan residues are in a hydrophobic environment, most of the tyrosine residues are exposed, suggesting that the C-terminal half of the protein is folded very differently in SDS than in DPC and LDAO. This conformation is very stable during heating; only minor changes to secondary structure composition were observed, as reported for native porin in 35 mM SDS (Shao *et al.* 1996). These slight changes were completely reversible upon cooling (Fig. 2.2) and protein precipitation did not occur, in contrast to DPC-solubilized porin. Heating of the latter significantly reduced α -helical content from 20 to 11%, suggesting that maintenance of α -helix during heating is required to prevent precipitation. In spite of the non-native folded state, near UV CD spectra of SDS-solubilized porin indicates weak tertiary contacts in the protein, which in addition to detergent-protein interactions, may contribute to the overall stability of the protein in SDS.

Near UV CD spectra were obtained for DPC and SDS solubilized His₆-porin; in both cases, strong negative ellipticity in the 270-290 nm region was observed (Fig. 2.8). These spectra are unlike those of the protein in FT and INS SDS-His₆porin-liposomes. This

indicates that the weak tertiary contacts in SDS and DPC-solubilized His₆-porin are not characteristic of the membrane bound, osmotically-responsive conformation of His₆-porin.

2.5.5 Amino acid model compounds

Model compounds were critical for assessing the complex microenvironments provided by detergent systems. The N-acetyl-amide Trp and Tyr derivatives have been used extensively in fluorescence and UV absorption studies involving soluble proteins (for example, Nayar *et al.* 2002, Garcia-Borron *et al.* 1982, Cowgill 1967) or using organic solvents (for example, Nayar *et al.* 2002, Havel 1996, Guzow *et al.* 2005). Our work extends these studies to membrane proteins, by using the standard model compounds, and their hydrophobic alkylesters, and investigating their properties in detergent. Fluorescence and UV absorbance were used in combination to assess the interactions of the model compounds with detergent. In general, it should be noted that the useful concentrations for these studies are limited due to light scattering by detergent micelles, and that, in some cases, detergent solubility restricts the usable pH and temperature ranges.

There were two important observations from these model compound studies. First, detergent systems include multiple environments that prevent direct comparisons of detergent-solubilized protein with model compounds in simple solvents. Second, the commonly used hydrophilic model compounds NAc-Y-NH₂ and NAc-W-NH₂ are not suitable probes for the interior of detergent micelles, although they provide useful information about interactions between the detergent headgroups and amino acids exposed to the aqueous solution.

The multiple environments in detergent solutions are the hydrophobic core of the micelle, the micellar surface defined by the detergent headgroups, and the aqueous

environment surrounding the micelles. Like organic solvents, the hydrophobic environments provided by detergent micelles lead to blue-shifts in λ_{max} of Trp fluorescence (Table 2.3), and moieties in the detergent headgroups may quench this fluorescence. For example, LDAO almost completely quenches BOC-Y-OMe fluorescence, while SDS and DPC do not. This phenomenon is not observable with NAc-Y-NH₂ because it does not associate strongly enough with the micelle due to its relatively high polarity. Enhancements of Tyr fluorescence intensity were not observed in detergent, in spite of the predicted low dielectric in the micelle, suggesting that quenching is occurring. In contrast, in organic solvents, quantum yield increases with decreasing DEC (Lee and Ross 1998, Guzow *et al.* 2005). Therefore, the studies with model compounds revealed detergent-specific phenomena that provide context for future studies of detergent-solubilized membrane proteins.

There were striking differences between the interactions of the variants of the model compounds and each detergent, as seen in the fluorescence (Table 2.3) and UV absorbance data (Table 2.4, Fig. 2.7). NAc-W-OEtH was the most useful gauge of hydrophobic environments in fluorescence studies, because, compared to NAc-W-NH₂, its fluorescence spectrum had a larger blue-shift upon interaction with micelles of all of the detergents studied (Table 2.3). Fluorescence analysis of the Trp model compounds also revealed that partitioning of the model compound into the micelle may be more sensitive to detergent concentration than is protein solubilization, as shown for SDS (Table 2.3). Finally, it is noteworthy that the correlation between blue-shifted λ_{max} Trp and increased fluorescence intensity in LDAO and DPC, but not in SDS, suggests relatively high viscosity in the interior of the LDAO and DPC micelles.

Tyrosine fluorescence was somewhat less informative, as clear differences in λ_{max} Tyr could not be discerned, and low level fluorescence intensity could result from either exposure to a watery environment, or from quenching and resonance energy transfer. However, UV absorption analysis of mixtures of Trp and Tyr model compounds (Table 2.4) confirmed that the hydrophobic BOC-Y-OMe partitioned more effectively into the interior of the detergent micelle than the more hydrophilic NAc-Y-NH₂ compound.

Taken together, the results presented herein establish a framework for future structural studies of mitochondrial porins in part by presenting a set of model compound data useful for interpreting fluorescence data of detergent-solubilized membrane proteins. Characterization of membrane-bound and detergent-solubilized His₆-porin by fluorescence and near UV CD is also an important step in developing strategies for solubilization of high concentrations of correctly-folded porin needed for NMR studies. This work also demonstrates that detergents (Genapol-X80, LDAO, OG) that are successful for black lipid bilayer studies are not necessarily useful for preparing high concentration porin solutions for structural analysis. The LDAO results in particular emphasize that competence for insertion into artificial membranes is not indicative of native-type folding in detergent. In fact, this observation supports the intriguing hypothesis that incompletely folded β -strand protein, rather than the natively-folded form, is required for insertion into artificial membranes under the conditions of “black-lipid bilayer” experiments. The next chapter will focus on mixed detergent systems, which have been used for refolding bacterial porins (for example, Ohnishi and Kameyama 2001), to obtain high concentrations of stably-folded protein.

CHAPTER 3 Two-step folding of recombinant mitochondrial porin in detergent.

The material presented in chapter 3 was written with the intent to submit to the Journal of Bioenergetics and Biomembranes. I completed all of the experiments outlined in this chapter. The data were analyzed and the manuscript was written with guidance and feedback from my advisor and Dr. J. O'Neil, who are co-authors on the manuscript.

3.1 Abstract

Precise information regarding the transmembrane topology of mitochondrial porins is essential for understanding the mechanisms by which this protein forms a channel in the outer membrane, and interacts with small solutes and proteins to regulate mitochondrial function. The lack of a system for maintaining high levels of properly folded protein has hindered the acquisition of high resolution structural data. In the current studies, several mixed detergent systems were analyzed for their ability to fold porin. A mixture of sodium dodecyl sulfate and dodecyl- β -D-maltopyranoside in a 1:6 molar ratio supports a β -strand rich conformation. In this state, the two tryptophan residues in the protein reside in hydrophobic environments and about half of the nine tyrosines are solvent exposed. Most importantly, heat-labile tertiary contacts were detected by near-UV circular dichroism spectropolarimetry. The SDS/DDM folded porin adopts a high molecular weight conformation that is resistant to proteolysis as is the native protein. The tertiary contacts and protease resistance of the SDS/DDM solubilized porin are very similar to those of the protein following functional reconstitution into liposomes. Thus, a system has been identified with the potential to solubilize high levels of mitochondrial porin in a state that will be useful for structural studies.

3.2 Introduction

One of the most abundant proteins in the mitochondrial outer membrane is mitochondrial porin, otherwise known as the voltage-dependant anion selective channel (VDAC). Like their bacterial namesakes, these channels are presumed to exist in β -barrels composed of antiparallel transmembrane β -strands. Reconstitution of these proteins into artificial membranes generates channels that passively transport solutes and display voltage-dependent gating; the channels are “open” and anion-selective at low applied voltages and exist in partially-closed, cation-selective states upon application of high voltages (reviewed by Benz 1994). In artificial membranes systems, recombinant mitochondrial porins that bear N-terminal hexahistidiny-tags (His₆-porin) and were expressed in *Escherichia coli* are functionally indistinguishable from porins isolated from mitochondrial membranes (Popp *et al.* 1996, Koppel *et al.* 1998).

Mitochondrial porins have been shown to interact with small molecules and other proteins that participate in a variety of cellular processes. Examples of interaction partners include hexokinase (Arora *et al.* 1993) and creatine kinase (Brdiczka *et al.* 1994) involved in glucose metabolism. ATP (Rostovtseva and Colombini 1996, Rostovtseva and Colombini 1997), NADH (Zizi *et al.* 1994), and the inner membrane ATP/ADP carrier (reviewed in Crompton *et al.* 1999) also interact with porin and participate in processes involving oxidative phosphorylation. Furthermore, regulators of apoptosis, namely the Bcl-2 family of proteins (as reviewed by Shoshan-Barmatz *et al.* 2006) interact with VDAC in higher organisms, potentially controlling cytochrome *c* release and the induction of apoptosis. In many cases, these interactions modulate channel gating and reflect complex interactions of porin with its environment (reviewed by Blachly-Dyson and Forte 2001). The involvement of

mitochondrial porin in all of these cellular activities emphasizes the need for understanding the structural arrangement of this channel. However, in contrast to the wealth of information regarding bacterial porin structure, very little is known about the topology of mitochondrial porins.

Evidence supporting a β -barrel conformation has included structural predictions based on primary sequence on the properties of porin channels in artificial membranes and far-UV circular dichroism (CD) spectropolarimetry studies that revealed a β -strand rich secondary structure (40-70%) (Shao *et al.* 1996, Popp *et al.* 1997, Koppel *et al.* 1998, Runke *et al.* 2000). Electron microscopic analysis of two-dimensional and multi-lamellar arrays confirmed the barrel structure of porin, but the low resolution (nm) prevented the identification of membrane spanning segments (Mannella 1989, Thomas *et al.* 1991, Guo and Mannella 1993, Dolder *et al.* 1999). Other approaches to the determination mitochondrial porin structure have been hindered by the low yields of folded protein obtained from mitochondria, the low solubility of the recombinant protein in the detergents used for electrophysiological analysis, and the poor stability of mitochondrial porins in comparison to their bacterial counterparts (reviewed by Schulz 2000, Bay and Court 2002).

Isolation of native mitochondrial porin in quantities high enough for spectroscopic analysis (μ g amounts) requires a large quantity of cells and numerous purification steps involving initial solubilization in detergent, such as Triton X-100 (Colombini 1980, Roos *et al.* 1982, Freitag *et al.* 1982), Genapol X-080 (Troll *et al.* 1992) or lauryl dimethylamine oxide (LDAO; Aljamal *et al.* 1993). The low yields of protein restrict the techniques available for the characterization of the folded state. Furthermore, many of these detergents are not compatible with spectroscopic analyses.

Recombinant His₆-porin expressed in *E. coli* has facilitated the purification of higher concentrations of protein (mg), but at the cost of the native folded state, since these proteins must be isolated from inclusion bodies (Koppel *et al.* 1998, Chapter 2). Isolation and folding have involved denaturation and subsequent solubilization in detergent, using dialysis to remove the denaturant while encouraging folding that presumably reflects that of the native porin (Koppel *et al.* 1998). Unfortunately, depending on the detergent used, this approach can be prohibitively expensive where high concentrations of protein are concerned.

Our previous studies utilizing His-tagged *Neurospora crassa* mitochondrial porin involved the use of single detergents for protein solubilization and reconstitution into liposomes and permitted spectroscopic characterization of the protein (Chapter 2). His₆-porin was purified in 8 M urea, acetone precipitated, and the dried pellet dissolved directly in the detergent of choice. High concentrations of His₆-porin were attainable in LDAO, dodecyl phosphocholine (DPC) and sodium dodecyl sulfate (SDS), but high β -strand content was only exhibited by the protein in LDAO. The near-UV CD spectra of the LDAO-solubilized protein display almost no ellipticity, suggesting that the protein exists in a molten globule conformation. Therefore, single detergent solubilization of His₆-porin is not suitable for further structural characterization of the recombinant protein, but it is still an attractive means for the solubilization of high concentrations of porin.

In addition, SDS-, LDAO-, and DPC-solubilized His₆-porin can be reconstituted into liposomes by freeze-thawing and thereby produce osmotically-responsive proteoliposomes (Chapter 2). Only SDS-His₆-porin could be reconstituted into liposomes at protein concentrations sufficient for analysis by both CD spectropolarimetry and fluorescence spectrophotometry. The CD spectrum of freeze-thawed SDS-His₆-porin-liposomes in the far-

UV region was characteristic of β -strand rich proteins and demonstrated positive ellipticity in near-UV region, as shown for other bacterial β -barrel porins (Ohnishi and Kameyama 2001, Minetti *et al.* 1997, Minetti *et al.* 1998). Although His₆-porin reconstituted into liposomes is a more relevant system for studying mitochondrial porin architecture, the high concentrations of protein required for further analysis by other high resolution spectroscopic techniques such as NMR spectroscopy cannot be obtained. Hence, a detergent based system for recombinant mitochondrial porin refolding is preferable.

Alternative detergent systems for solubilizing other membrane proteins involve mixtures of anionic and non-denaturing, non-ionic detergents. For example, the *E. coli* integral outer membrane protein A (OmpA) has been folded in a mixture of SDS and octyl- β -D-glucopyranoside (OG) (Dornmair *et al.* 1990, Ohnishi *et al.* 1998, Ohnishi and Kameyama 2001). SDS and dodecyl- β -D-maltopyranoside (DDM) systems have been used for solubilization of other membrane proteins including DsbB (Otzen 2003), and the P5 outer membrane protein of *Haemophilus influenzae* (Webb and Cripps 1999). The focus of many of these studies was to characterize unfolding kinetics upon the addition of SDS to protein folded in a non-ionic detergent (Ohnishi *et al.* 1998, Lau and Bowie 1997). However, in the case of OmpA, folding into a β -rich conformation could be achieved by adding OG to SDS-solubilized protein at a particular molar ratio of the two detergents (Ohnishi and Kameyama 2001). Alternatively, peptides have been used to probe mixed detergent systems.

In this study, mixed detergent systems were used to solubilize recombinant His₆-tagged *Neurospora crassa* mitochondrial porin. SDS and DPC were chosen for primary solubilization of the protein, based on the high solubility of His₆-porin in these detergents (Chapter 2). Several non-ionic and zwitterionic detergents were added as the secondary

surfactants and varying molar ratios of the two detergents were examined. The folded states of the proteins in the resulting detergent mixtures were examined by CD spectropolarimetry in the far-UV and near-UV regions, fluorescence spectrophotometry, and UV absorption spectroscopy. To interpret the results obtained for His₆-porins in these binary systems, aromatic amino acid derivatives of varying hydrophobicity were also examined to probe the micellar environments experienced by the protein. Of the numerous mixed detergent systems examined, only SDS/DDM solubilized His₆-porin was suitable for reconstitution into liposomes and analysis by protease digestion.

3.3 Materials and Methods

3.3.1 Detergents and amino acid derivatives

DPC, DDM, and OG were purchased from Anatrace (Maumee, OH), and LDAO from Calbiochem (San Diego, CA). Sigma (St. Louis, MO) was the supplier of N-acetyl-tryptophan amide (NAc-W-NH₂), N-acetyl-tyrosine amide (NAc-Y-NH₂), SDS, urea and N-acetyl-tryptophan ethyl ester (N-Ac-W-OEth). N-tert-butoxycarbonyl-tyrosine methyl ester (BOC-Y-OMe), egg yolk L- α -phosphatidyl choline, and egg lecithin L- α -phosphatidic acid were purchased from FLUKA (Oakville, ON).

3.3.2 Expression and purification of His₆-porin

The construct encoding the N-terminal His₆-tagged version of *Neurospora crassa* has been described previously (Popp *et al.* 1996). Protein expression was carried in QIAexpress *Escherichia coli* M15 [pREP4] (Qiagen, Toronto, ON). His₆-porin was purified in 8 M urea, as described in (Chapter 2). Protein purity, as estimated by dodecyl sulfate-polyacrylamide

gel electrophoresis was at least 95%. Protein concentration was determined using the calculated extinction coefficient at 280 nm of $24,050 \text{ M}^{-1} \text{ cm}^{-1}$.

3.3.3 Detergent solubilization of His₆-porin

Following dialysis against 8 M urea, His₆-porin was acetone-precipitated and the dried pellets were resuspended either in SDS (3.5 or 21 mM) or DPC (20 or 100 mM), buffered in 50 mM sodium phosphate pH 7. Following mixing by repeated inversion overnight at room temperature (22°-25°C), samples were clarified by centrifugation at 10 000 *g* for 15 minutes. For mixed detergent systems, an appropriate amount of the second detergent, in powder form, was added and the samples mixed by inversion overnight. Insoluble aggregate was removed by centrifugation prior to analysis.

3.3.4 Liposome preparation and swelling assays

Modifications of the stock small unilamellar vesicles (SUV) preparation described by (Shao *et al.* 1996) were used for these studies. In brief, a 10:1 (^w/_w) mixture of egg yolk L- α -phosphatidyl choline and egg lecithin L- α -phosphatidic acid was dissolved in chloroform, evaporated at room temperature (22-25°C) and resuspended in 50 mM sodium phosphate buffer at pH 7. The milky suspension was diluted 1:1 with 50 mM sodium phosphate buffer pH 7 and sonicated on ice until the solution appeared clear yielding the stock SUV suspension (20 mg/ml).

Liposomes used for swelling assays were prepared with the stock SUV according to a modified procedure described by (Chapter 2) for type B (CD spectropolarimetry grade) liposomes described by (Shao *et al.* 1996). In short, the SUV suspension was diluted 1:1 with 1 μM (0.030 mg/ml) His₆-porin solubilized in 1.75 mM SDS/ 15 mM DDM. The resulting

suspension was frozen in liquid nitrogen for 1 min and thawed for 20 min at room temperature, and this cycle was repeated three times. After the final freeze-thaw cycle, the samples were diluted with 1.5 volumes of 50 mM sodium phosphate pH 7 resulting in a cloudy solution that contained a final concentration of 6.6 mg/ml total phospholipid, 0.6 mM SDS, 5 mM DDM, and 166 nM (0.012 mg/ml) His₆-porin. Negative controls were prepared with detergents mixtures only and lacked His₆-porin.

Liposome swelling assays were performed to assess the ability of 1.75 mM SDS/15 mM DDM-His₆-porin to insert into liposomes as described for *E. coli* OmpA (Surrey and Jahnig 1995). Liposomes used for insertion experiments were prepared as described above except that the 20 mg/ml stock SUV was diluted 1:1 with 50 mM sodium phosphate pH 7 buffer and subjected to three freeze-thaw cycles. After the third cycle 0.25 volumes of 1 μ M (0.03 mg/ml) His₆-porin solubilized in 1.75 mM SDS/15 mM DDM and 1.25 volumes of 50 mM sodium phosphate pH 7 buffer were added to the freeze-thawed SUV solution. To promote insertion, samples were incubated at room temperature, 30°C and 42°C overnight before measurement.

As described in (Chapter 2), liposome swelling was measured on an Ultrospec 3100 pro spectrophotometer as absorbance at 400 nm. Liposome swelling samples described above were diluted 1/100 into 50 mM sodium phosphate pH 7 buffer to a final volume of 0.5 ml and measured in a quartz cuvette. Liposomes were diluted with 40 μ l of the iso-osmotic 50 mM sodium phosphate buffer pH 7 at 300-400 seconds followed by an addition of 40 μ l of the hyperosmotic 1 M sucrose after 600-700 seconds. Liposome swelling in a sample is indicated by a gradual decrease in A_{400nm} over 1200 or 1800 seconds after sucrose addition.

3.3.5 Protease digestions of isolated mitochondria and His₆-porin reconstituted into liposomes or solubilized in mixed detergents

Mitochondria were isolated from *N. crassa* 97-20 *mus his⁻* (Ninomiya *et al.* 2004) according to the method described in (Chapter 2). Mitochondrial pellets were resuspended in SEM (250 mM sucrose, 1 mM EDTA, 9 mM MOPS pH 7.5), or in 3.5 mM SDS/30 mM DDM buffered at pH 7 with 50 mM sodium phosphate to a final concentration of 1 mg/ml mitochondrial protein as determined by a Bradford assay (Sigma). Mitochondrial digestions contained 0.5 mg/ml mitochondrial protein in 1.75 mM SDS and 15 mM DDM. All samples were digested with a final concentration of 0.15 mg/ml trypsin for 10 min or 30 min intervals at room temperature.

His₆-porin reconstituted into liposomes was prepared for spectroscopic examination as described by (Chapter 2). Briefly, His₆-porin at a concentration of 2.5 – 5 μ M in 3.5 mM SDS/ 30 mM DDM was diluted 1:4 into 50 mM sodium phosphate pH 7, which contained a final concentration of 2 mg/ml stock SUV. This liposome-detergent-His₆-porin mixture was subjected to one of three incorporation methods described by (Chapter 2): 1 cycle of freeze-thawing (FT), four 1 minute bursts of sonication (SON) on ice, or incubation with intact liposomes for direct porin insertion (INS). The resulting proteoliposomes were gently mixed overnight at room temperature (22-25°C) and centrifuged at 10 000 g for 10 min to remove precipitated material. Each proteoliposome sample was digested as described for mitochondria and contained 8-15 μ g/ml (0.25-0.5 μ M) His₆-porin, and 1 mg/ml phospholipid.

5 μ M His₆-porin in 3.5 mM SDS/ 30 mM DDM was digested with trypsin and chymotrypsin under the same conditions as for mitochondria. Final concentrations of samples were as follows: 0.075 mg/ml (2.5 μ M) His₆-porin and 1.75 mM SDS, and 15 mM DDM. All

protease digestions were stopped with phenylmethylsulfonylfluoride to a final concentration of 20 mM and 4:1 dilution into Laemmli buffer (Laemmli 1970) containing 8 M urea. All reaction mixtures were stored at -20°C until needed. As a control for protease activity in the SDS/DDM system, BSA (Sigma) was also digested and demonstrated susceptibility to trypsin (data not shown).

3.3.6 Western blots of liposomes and *N. crassa* mitochondria

All protease digested samples were loaded onto 0.1 % SDS- 3 M urea- 14% PAGE gels; the urea was necessary to aid migration of the protein into the gel in the presence of high concentrations of lipid. Electrophoresis was performed with the Mini-Protein® II system (Bio-Rad Laboratories, Hercules, CA). Gel loading was as follows: 5 µl 0.5 mg/ml mitochondria in SEM or detergent, 10 µl of 7.5- 15 µg/ml His₆-porin in 1 mg/ml phospholipids, and 1 µl 75 µg/ml His₆-porin in detergent. Gels were blotted with a Trans-Blot® Cell system (Bio-Rad) onto nitrocellulose 0.45 µm membranes (Bio-Rad) overnight at 4°C and stained with Ponceau S (Sigma) to visualise the Benchmark protein ladder (Invitrogen, Burlington, ON).

Immunoblotting was carried out at room temperature using rabbit antibodies directed against residues 7- 20 of *N. crassa* mitochondrial porin (α NcPor-N, generated by R. Lill, at Universität München) following the same procedure described in Chapter 2. Blots were detected using CDP- star (Roche Diagnostics, Indianapolis, IN) and exposed for 1- 2 hrs on X-Omat Blue XB-1 Scientific Imaging film (Kodak, Rochester, NY).

3.3.7 Fluorescence spectrophotometry

Fluorescence spectroscopic analyses of detergent-solubilized model compounds and

His₆-porin were performed using a Shimadzu RF-1501 fluorometer or a JASCO-810 (FMO-427S) spectropolarimeter/fluorometer, as described in Chapter 2. The relatively hydrophilic (NAc-W-NH₂ and NAc-Y-NH₂), and hydrophobic (BOC-Y-OMe and N-Ac-W-OEt) model compounds were used for comparison with fluorescence by His₆-porin. Samples of individual model compounds, and Trp:Tyr mixtures in the same molar ratio as in His₆-porin (2:9), were prepared at molar concentrations close to those of the individual residues in porin and all of the protein and model compound fluorescence spectra were normalized with reference to His₆-porin in urea. The sums of the spectra obtained from the individual components equalled those from the 2:9 mixtures, indicating a lack of interaction between the fluorophores.

When necessary, the fluorescence spectra were smoothed using a moving average over a window of 5 nm. To determine the maximum fluorescence emission of tyrosine (λ_{maxTyr}) and tryptophan (λ_{maxTrp}) in the porin or model compound spectra, the second derivatives of the averaged spectra were obtained with Jasco Spectra Analysis Software, Version 1.53.04, using data at 1-nm intervals and a window of 9-13 nm, depending on the noise in the spectrum (Table 3.2; Garcia-Borron *et al.* 1982).

3.3.8 UV absorption spectroscopy

UV absorption spectra were obtained on an Ultrospec 4000 spectrophotometer, as described in Chapter 2. Tyrosine exposure (α) was calculated using the method described in (Ragone *et al.* 1984, Chapter 2). Second derivative UV absorption spectra of proteoliposomes prepared for spectroscopic analysis could not be reliably measured due to high amounts of light scatter.

3.3.9 Circular dichroism spectropolarimetry

CD spectra were acquired on a JASCO J-810 spectropolarimeter-fluorometer calibrated with (+)-10-camphorsulfonic acid and purged with N₂ at 20 L/min (Manley and O'Neil 2003). CD spectra of 1.5 μ M or 5 μ M His₆-porin samples were measured in the far-UV region (195-250 nm) as described previously (Chapter 2). Following correction by baseline subtraction, CD spectra were converted to mean residue ellipticity (MRE) according to the formula: $[\theta]_M = M\theta / [(10)(l)(c)(n)]$ where $[\theta]_M$ is 10^{-3} deg cm² dmol⁻¹, M is the molecular weight of His₆-porin (31,402 g/mol), θ is the measured ellipticity in millidegrees, l is the path length of the cuvette in cm (0.1 cm), c is the protein concentration in g /L, and n is the number of amino acid residues in the protein (295). Spectra were deconvoluted with the CDSSTR algorithm (Compton and Johnson 1986, Manavalan and Johnson 1987, Sreerama *et al.* 2000) in the DichroWeb package (Whitmore and Wallace 2004).

Near-UV (245-330 nm) CD spectra of 33 μ M His₆-porin in mixed detergents were measured with a JASCO J-810 spectropolarimeter-fluorometer, as described in Chapter 2. Molar ellipticity was calculated from the baseline corrected spectra according to the formula: $[\theta] = M\theta / [(10)(l)(c)]$ where $[\theta]$ is the molar ellipticity in degrees cm² dmol⁻¹, θ is the measured ellipticity in millidegrees, l is 1 cm, and c is the protein concentration in g/L.

Temperature was controlled during thermal denaturation experiments using the Peltier device in the spectropolarimeter. Experiments were carried out with a 1°C / min ramp speed; θ (in mdeg) was monitored at 208 or 216 nm (far-UV) and at 268 nm (near-UV) at 1°C intervals, and full spectra were collected at 5°C intervals. High tension (HT) voltage (absorbance) measurements were monitored during single wavelength and full spectra collection experiments.

Far-UV CD spectra of FT proteoliposomes in the SDS/DDM system could not be collected below 200 nm due to light scatter and were not deconvoluted for secondary structure estimates. Due to reduced signal to noise ratios in both the far UV- and near-UV CD spectra of FT SDS/DDM-His₆-porin-liposomes, collected data were not shown for all mixed detergent His₆-porin reconstituted into liposomes.

3.4 Results

Addition of a non-ionic detergent to SDS-solubilized OmpA β -barrel was shown to convert the α -helical rich structure to one predominantly β -strand (Ohnishi and Kameyama 2001). To determine if a similar approach would yield well-folded mitochondrial porin, several detergent systems were examined. SDS and DPC were chosen initially to solubilize His₆-porin, based on the high solubility of the protein in these detergents (Chapter 2). Under these conditions, β -strand content is low, and ranges from 17-25%. The non-ionic detergents, DDM and OG, and the zwitterionic LDAO were used as the second detergents in the system. With the exception of LDAO, several molar ratios of the two detergents were examined. Phase separation occurred at several LDAO/SDS ratios, limiting the mixtures that could be tested. For simplicity, mixtures will be described by each detergent, with its concentration in mM, as a subscript. For example, SDS_{3.5}DDM_{7.5} is a mixture of 3.5 mM SDS and 7.5 mM DDM.

3.4.1 Characterization of mixed detergent-solubilized His₆-porin by far-UV circular dichroism spectropolarimetry

To determine the effects of secondary detergent addition on the folded states of the protein solubilized in DPC or SDS, far-UV CD was used (Fig. 3.1, Table 3.1). In 3.5 mM

SDS, the far-UV spectrum of His₆-porin is typical of an α -helical rich protein, in that it has a minimum at 208 nm and a shoulder at 220 nm. Upon addition of 7.5 mM DDM, a small shift in the spectrum is observed (Fig. 3.1A), but the overall α -helical character is retained and structural content, as revealed by deconvolution of this spectrum is identical to that in SDS (Table 3.1). However, in SDS_{3.5}DDM₁₅, the spectrum of the protein has a broad minimum in the 210-220 nm range, more typical of a β -strand rich protein. This observation is confirmed by deconvolution, which reveals a loss of α -helix concomitant with an increase in β -strand to 28%. As the DDM concentration was increased to generate SDS_{3.5}DDM₃₀ or SDS_{3.5}DDM₄₅, this trend continued, and β -strand content reached 35 and 38%, respectively (Table 3.1). Throughout the SDS/DDM series, the level of turns and unordered structure remained unchanged.

Similar trends of increasing β -strand and decreasing α -helix occur upon addition of OG (12.5 to 100 mM) to His₆-porin in SDS and maximum levels of β -strand were reached in SDS_{3.5}OG₅₀ (Fig. 3.1B). Secondary structural content in SDS_{3.5}LDAO₄₀ (Fig. 3.1C) resembled that in the SDS/DDM and SDS/OG mixtures; the SDS/LDAO and SDS/OG mixtures are not useful for further structural studies due to the low porin solubility under these conditions (~ 1.5 μ M, Table 3.1). Remarkably, the addition of either 10 or 100 mM DPC, which also promotes α -helix, increases the α -helical content of the protein to 52-58%, with a dramatic reduction in β -strand (7%). The very high α -helical content of SDS/DPC solubilized porin indicates that native folding has not been achieved.

SDS-solubilized His₆-porin is very stable during heating, and the limited unfolding that does occur is completely reversible (Chapter 2; Figs. 3.2A and 3.2B). Only the SDS/DDM system was capable of solubilizing porin at concentrations sufficient for this type

of analysis (Figs. 3.2C and 3.2D, Table 3.1). During heating of SDS_{3.5}DDM₃₀-solubilized porin to 45°C, there are only minor alterations to the secondary structural content. At 55°C, an increase in the (HT) voltage or absorbance of the sample, as monitored by the CD spectropolarimeter, indicated precipitation in the sample; absorbance measurements at the end of the experiment demonstrated that about 2/3 of the protein remained in solution. At 55°C, the far-UV CD spectra broadened, and developed minima characteristic of higher levels of α -helix. Deconvolution of these spectra confirms a steady loss in β -strand (35 to 28%) and constant α -helical content, with a significant increase in random structure (47 to 60%). Further large-scale changes did not occur at higher temperature. Unlike the situation in SDS (Fig. 3.2A), the thermal denaturation is not reversible and the structural content upon cooling to 20°C remains similar to that at 55°C and above (Table 3.1, Figs. 3.2C and 3.2D). When the protein was solubilized initially in DPC, the same trend in secondary structure content alterations upon addition of a second detergent were observed as for the SDS based systems. Addition of 30 mM DDM, 100 mM OG or 50 mM LDAO (Figs. 3.1D-3.1F) promoted structures with 33-38% β -strand, in contrast to the 25% present in the DPC-solubilized protein. Of all the DPC-based systems, only DPC/LDAO is capable of maintaining at least 5 μ M porin in solution.

3.4.2 Fluorescence of tryptophan model compounds in mixed-detergent systems

Model compounds were used to determine how the addition of a second detergent to SDS or DPC micelles affects the interactions of the aromatic amino acids, namely tyrosine and tryptophan, with the micelles. Two variants of each compound were used, the relatively hydrophobic O-alkyl-esters, BOC-Y-OMe and N-Ac-W-OEt, and the more hydrophilic amide variants, N-Ac-Y-NH₂ and N-Ac-W-NH₂. In previous studies, it was shown that the

Table 3.1. Analysis of His₆-porin solubilized in mixed detergent systems. Far UV region CD spectropolarimetry was performed on either 1.5 or 5 μ M porin samples as indicated; the resulting averaged spectra were deconvoluted with CDSSTR (Whitmore *et al.* 2004).

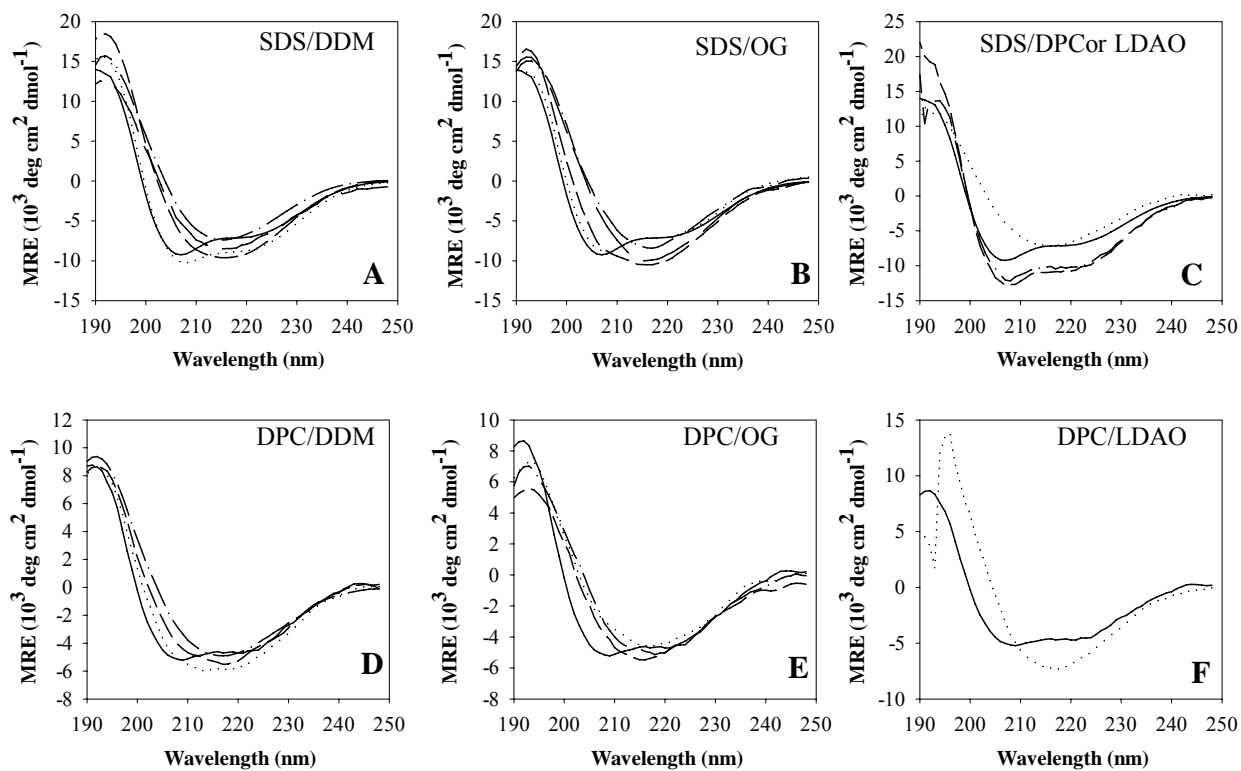
Solubilizing Detergent	Detergent added	Temp (°C)	α -helix (%)	β -strand (%)	turns & unordered	Maximum Concentration of soluble porin (μ M)
3.5 mM SDS		20	32	18	50	66
	7.5 mM DDM	20	33	17	50	5*
	15 mM DDM	20	23	28	49	5*
	30 mM DDM	20	18	35	47	5*
		35	14	36	50	5*
		45	14	33	52	5*
		55**	15	28	56	UD
		60	12	28	60	UD
		80	15	20	65	UD
		80→20	18	26	55	3.3*
	45 mM DM	20	13	38	49	5*
	12.5 mM OG	20	21	29	50	1.5
	25 mM OG	20	24	28	48	1.5
	50 mM OG	20	17	35	47	1.5
	100 mM OG	20	17	35	48	1.5
	40 mM LDAO	20	13	34	53	1.5
	10 mM DPC	20	58	7	36	5*
	100 mM DPC	20	52	7	41	5*
20 mM DPC		20	22	25	53	16
	7.5 mM DDM	20	14	33	54	1.5
	15 mM DDM	20	9	36	54	1.5
	30 mM DDM	20	9	38	53	1.5
	6.25 mM OG	20	13	29	58	1.5
	12.5 mM OG	20				1.5
	50 mM OG	20	7	35	57	1.5
	100 mM OG	20	6	38	56	1.5
	50 mM LDAO	20	16	33	51	5*

* Higher concentrations not tested.

** Precipitation of His₆-porin was detected by UV absorption at this temperature.

UD His₆-porin concentration in the sample was undetermined.

Figure 3.1. Far-UV CD analysis of 5 μ M His₆-porin in mixed detergent systems. Spectra were obtained as indicated in Materials and Methods. **A)** SDS/DDM systems. Far-UV spectra obtained for His₆-porin in the following SDS/DDM mixtures: SDS_{3.5} (solid line), SDS_{3.5}DDM_{7.5} (dotted line), SDS_{3.5}DDM₁₅ (short dashes), SDS_{3.5}DDM₃₀ (dash-dot-dash), and SDS_{3.5}DDM₄₅ (long dashes). **B)** Mixed SDS/OG systems. Far-UV spectra obtained for His₆-porin in the following SDS/OG mixtures: SDS_{3.5} (solid line), SDS_{3.5}OG_{12.5} (dotted line), SDS_{3.5}OG₂₅ (short dashes), SDS_{3.5}OG₅₀ (dash-dot-dash), SDS_{3.5}OG₁₀₀ (long dashes). **C)** SDS/DPC and SDS/LDAO systems. Far-UV spectra obtained for His₆-porin in the following mixtures are indicated as follows: SDS_{3.5} (solid line), SDS_{3.5}LDAO₄₀ (dotted line), SDS_{3.5}DPC₁₀ (short dashes), SDS_{3.5}DPC₁₀₀ (dash-dot-dash). **D)** DPC/DDM systems. Far-UV spectra obtained for His₆-porin in the following mixtures: 20 mM DPC (solid line), DPC₂₀DDM_{7.5} (dotted line) DPC₂₀DDM₁₅ (short dashes), DPC₂₀DDM₃₀ (dash-dot-dash). **E)** DPC/OG systems. Far-UV obtained for His₆-porin in the following mixtures are indicated as follows: 20 mM DPC (solid line), DPC₂₀OG_{12.5} (dotted line), DPC₂₀OG₂₅ (short dashes), DPC₂₀OG₅₀ (dash-dot-dash), and DPC₂₀OG₁₀₀ (long dashes). **F)** DPC and LDAO. Far-UV obtained for His₆-porin in the following mixtures are indicated as follows: 20 mM DPC (solid line), and DPC₂₀LDAO₄₀ (dotted line).



former compounds are better probes of the hydrophobic interiors of detergent micelles (Chapter 2). Trp fluorescence is described in relation to Burstein's classification system: Class S (λ_{max} Trp 316 nm), Class I (331 nm), Class II (342 nm) and Class III (347-351 nm). For these classes, increasing λ_{max} Trp is associated with increased solvent exposure of the Trp residues; Class III residues are completely exposed to the solvent (Burstein *et al.* 1973, Reshetnyak *et al.* 2001).

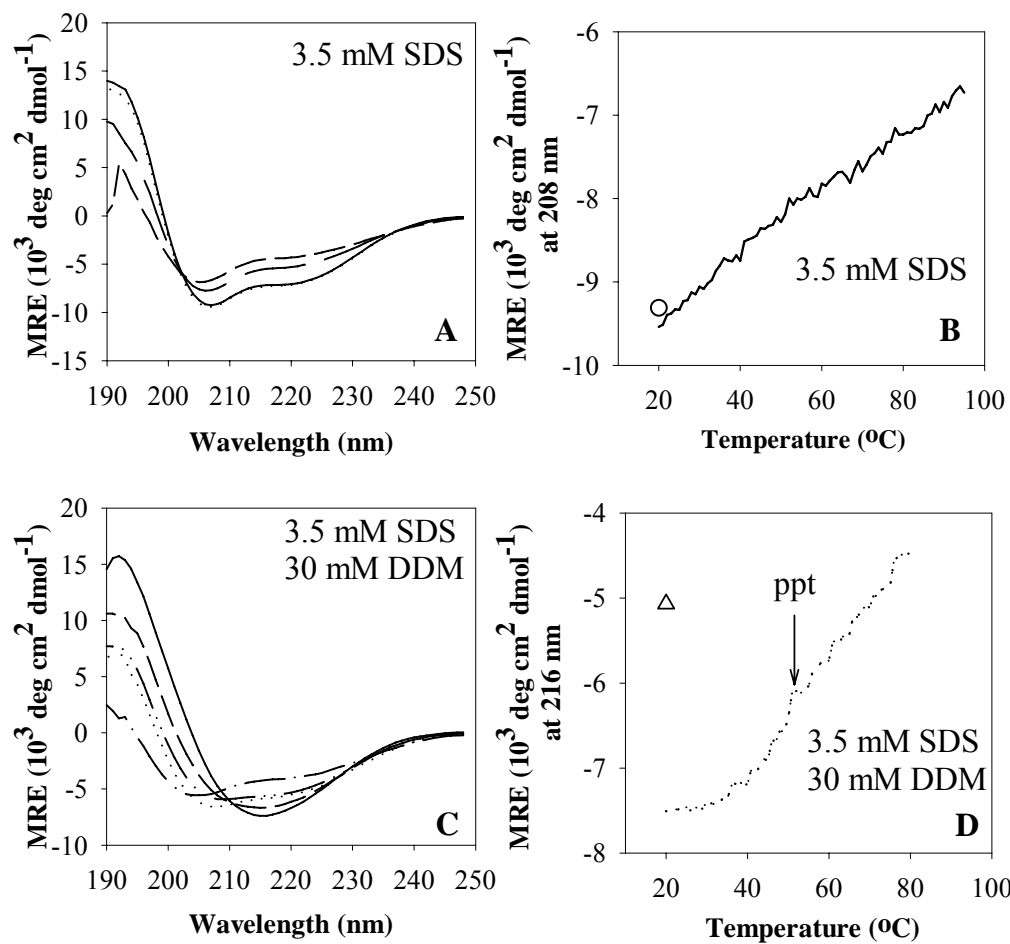
In 3.5 mM SDS, both model compounds display Class III fluorescence (Table 3.2), indicating that they are predominantly in the aqueous phase, although N-Ac-W-OEth interacts slightly more often with the micelle, as indicated by the blue shift in λ_{max} Trp (351 vs 347 nm), compared to that of N-Ac-W-NH₂. λ_{max} Trp of N-Ac-W-OEth blue-shifts to 341 (Class II) and 337 nm (Classes I/II) in SDS_{3.5}DDM_{7.5} and SDS_{3.5} DDM₁₅, respectively, indicating increased interactions between the micelles and the model compounds as the DDM concentration is increased. Relative to that in SDS_{3.5}DDM₁₅, a slight red-shift (343 nm (Class II)) occurs in SDS_{3.5}DDM₃₀, indicating that the interactions with micelles of higher DDM concentration are reduced. The fluorescence of N-Ac-W-NH₂ also blue-shifts upon addition of DDM to the SDS micelles; in this case, fluorescence shifts from Class III in SDS_{3.5} and SDS_{3.5}DDM_{7.5}, to Class II in higher relative DDM concentrations (340 nm in SDS_{3.5}DDM₃₀).

In SDS, quenching of model compound Trp fluorescence by the detergent headgroups occurs (Chapter 2). In parallel with the blue shift in λ_{max} Trp for N-Ac-W-OEth, fluorescence intensity increases in SDS_{3.5}DDM_{7.5} and SDS_{3.5}DDM₁₅ (Table 3.2), indicating that the quenching is reduced in the mixed micelles. However, the intensity in SDS_{3.5}DDM₃₀ is similar to that in SDS_{3.5}DDM_{7.5}. Thus, the changes in micellar environments do not parallel the relative detergent concentrations. In contrast, a steady increase in fluorescence intensity is

Figure 3.2. Thermal denaturation of His₆-porin as followed by far-UV CD

spectropolarimetry. The experiments were carried out as described in Materials and Methods.

A) 5 μ M His₆-porin in 3.5 mM SDS. Full spectra were obtained at the following temperatures: 20°C (solid line), 60°C (long dashes), 95°C (short dashes), and following cooling of the sample to 20°C (dotted line). **B)** Unfolding monitored by mean-residue ellipticity at 208 nm. Measurements were taken every 1°C in the experiment described in A). The open circle indicates the value following cooling to 20°C. **C)** Thermal denaturation of 5 μ M porin in SDS_{3.5}DDM₃₀. Spectra were obtained at the following temperatures: 20°C (solid line), 35°C (long dashes), 45°C (short dashes), 55°C (dotted line), 80°C (dash-dot-dash), and following cooling to 20°C (dash-dot-dot-dash). The arrow marked “ppt” indicates the point at which an increase in HT voltage indicates precipitate in the sample. **D)** 5 μ M porin in 3.5 mM SDS and 30 mM DDM thermal unfolding monitored at 216 nm: cooled 20°C (triangle), ppt temperature indicated by arrow. Unfolding monitored by mean-residue ellipticity at 208 nm. Measurements were taken every 1°C in the experiment described in C). The open triangle indicates the value following cooling to 20°C.



observed upon addition of DDM to the amide compound in SDS.

Addition of OG to the SDS-solubilized model compounds had a more modest effect on λ_{max} Trp for N-Ac-W-NH₂ (Table 3.2). A shift in λ_{max} Trp of N-Ac-W-OEth from Class III (347 nm) to Class II (342 nm) is observed only upon addition of high concentrations of OG (100 mM). In contrast, N-Ac-W-NH₂ remains mainly in the aqueous environment and only a small blue-shift, within the limits of Class III, is observed. In general, the fluorescence intensities for both compounds increase with the addition of 12.5 mM OG, but remain constant in the presence of up to 100 mM OG. Combinations of SDS and the two zwitterionic detergents, DPC and LDAO were also examined (Table 3.2). Only one DPC/SDS combination was used, because of the limitations of this system for porin studies (see above). Trp fluorescence of N-Ac-W-OEth is blue-shifted to Class II (337-338 nm) in both SDS_{3.5}/LDAO₄₀ and SDS_{3.5}/DPC₁₀, while that of the amide is shifted slightly less (to 344 nm). Thus, both compounds are interacting more often with these mixed micelles than with SDS alone. However, the fluorescence intensity is more similar to that in DPC or LDAO alone, than in SDS, indicating relative absence of quenching.

Both model compounds interact more with DPC than with SDS micelles (Table 3.2). For example, in DPC N-Ac-W-NH₂ displays Class II fluorescence, and that of N-Ac-W-OEth is intermediate between Classes I and II (Chapter 2). The addition of DDM or OG to DPC-solubilized model compounds does not alter λ_{max} Trp of N-Ac-W-Oeth (337-338 nm), and causes a slight blue-shift to that of N-Ac-W-NH₂ in DPC₂₀DDM₃₀, but its fluorescence remains near Class II (338-342 nm). In both DPC₂₀DDM mixtures, no change in intensity of N-Ac-W-OEth fluorescence is observed, suggesting that the interactions of this model compound with the DPC/DDM mixed micelles are similar to those in DPC alone. In

Table 3.2. Summary of fluorescence data collected at excitation wavelengths of 280 nm (Tyr) and 296 (Trp) nm. His₆-porin and amino model compounds were solubilized in various mixed detergents. Maximum intensity (Int_{max}) values were corrected for differences in concentration.

	His ₆ -porin											
	BOC-Y-OMe				N-Ac-Y-NH ₂				N-Ac-W-OEth + BOC-Y-OMe			
	Trp	Int _{max}	λ _{max}	Tyr	Trp	Int _{max}	λ _{max}	Tyr	Trp	Int _{max}	λ _{max}	Tyr*
Sample in 3.5 mM SDS with	λ _{max}	Int _{max}	λ _{max}	Int _{max}	λ _{max}	Int _{max}	λ _{max}	Int _{max}	λ _{max}	Int _{max}	λ _{max}	Int _{max}
	Trp	Int _{max}	λ _{max}	Tyr	Trp	Int _{max}	λ _{max}	Tyr	Trp	Int _{max}	λ _{max}	Tyr*
no addition	336	0.03	299	0.12	301	0.13	347	0.04	351	0.11	301	350
7.5 mM DDM	337	0.03	302	0.12	299	0.15	341	0.07	348	0.12	303	341
15 mM DDM	330	0.11	306	0.16	300	0.14	337	0.13	345	0.13	305	337
30 mM DDM	322	0.08	303	0.15	299	0.22	343	0.08	340	0.17	302	336
12.5 mM OG	339	0.05	304	0.14	298	0.17	347	0.09	349	0.15	304	347
25 mM OG	333	0.09	301	0.18	299	0.18	347	0.07	350	0.12	303	346
50 mM OG	330	0.08	301	0.21	302	0.19	345	0.10	352	0.13	302	344
100 mM OG	330	0.07	302	0.12	304	0.12	342	0.07	347	0.16	300	341
10 mM DPC	336	0.10	302	0.15	298	0.17	338	0.13	344	0.20	301	338
40 mM LDAO	332	0.14	302	0.04	303	0.12	337	0.15	344	0.25	300	338
Sample in 20 mM DPC with	λ _{max}	Int _{max}	λ _{max}	Int _{max}	λ _{max}	Int _{max}	λ _{max}	Int _{max}	λ _{max}	Int _{max}	λ _{max}	Int _{max}
	Trp	Int _{max}	λ _{max}	Tyr	Trp	Int _{max}	λ _{max}	Tyr	Trp	Int _{max}	λ _{max}	Tyr*
no addition	337	0.06	301	0.16	302	0.20	337	0.22	342	0.25	302	337
7.5 mM DDM	335	0.05	303	0.18	301	0.09	337	0.21	343	0.09	303	338
30 mM DDM	327	0.17	306	0.26	302	0.12	338	0.22	338	0.09	306	337
12.5 mM OG	333	0.09	302	0.13	300	0.15	338	0.11	342	0.11	301	340
50 mM OG	334	0.07	305	0.11	302	0.14	339	0.11	342	0.12	304	338
100 mM OG	334	0.07	302	0.10	302	0.06	338	0.09	342	0.11	301	335
50 mM LDAO	331	0.09	302	0.05	301	0.06	335	0.11	341	0.19	303	335

* Tyr fluorescence intensity could not be determined in mixtures of Trp and Tyr

contrast, fluorescence intensity of N-Ac-W-NH₂ in the DPC₂₀DDM mixtures was about half of that in DPC alone, indicating quenching in the mixed system. Similarly, both model compounds display decreased fluorescence in the DPC₂₀OG mixtures. Compared to that in DPC alone, the fluorescence intensity of N-Ac-W-OEt in DPC₂₀LDAO₅₀ is about half, and a smaller reduction is observed for the amide compound. These observations suggest quenching by the headgroups in the mixed micelles, which interestingly does not occur when either model compound is dissolved in the secondary detergent alone (Chapter 2, data not shown for OG and DDM).

3.4.3 Fluorescence of tyrosine model compounds in mixed-detergent systems

In terms of tyrosine fluorescence, intensity changes are more informative because only small shifts in $\lambda_{\text{max}}^{\text{Tyr}}$ occur, which are smaller than the +/- 3 nm sensitivity of the spectrofluorometer used. As seen in Table 3.2, $\lambda_{\text{max}}^{\text{Tyr}}$ ranges from 298-304 nm. The fluorescence intensity, however, provides clues about the degree of exposure of the model compounds to the aqueous environment. As shown previously (Chapter 2), in SDS both N-Ac-Y-NH₂ and BOC-Y-OMe have similar fluorescence characteristics, reflecting the fact that the neither compound interacts extensively with the interior of the micelle. These characteristics are unchanged for the BOC-Y-OMe in all of the mixed SDS/DDM micelles tested, and for N-Ac-Y-NH₂ in the lower concentrations of DDM. However, the intensity at $\lambda_{\text{max}}^{\text{Tyr}}$ of N-Ac-Y-NH₂ in SDS_{3.5}DDM₃₀ is twice that in SDS alone, suggesting that this compound spends slightly more time in the hydrophobic interior of the micelle.

For both compounds, intensity at $\lambda_{\text{max}}^{\text{Tyr}}$ is slightly higher (0.14-0.21 nm) in mixed SDS micelles formed in solutions containing up to 50 mM OG. However, these enhanced interactions are not detected in SDS_{3.5}OG₁₀₀, where the intensity is similar to that in SDS

alone (0.12). In SDS_{3.5}DPC₁₀ micelles, fluorescence of BOC-Y-OMe and NAc-Y-NH₂ (0.15-0.17) is increased slightly in comparison to SDS alone (0.12-0.13). In SDS_{3.5}LDAO₄₀, however, the intensity of BOC-Y-OMe fluorescence is about one-third of that in SDS alone, while that of the amide is similar in both SDS and SDS/LDAO. This suggests that BOC-Y-OMe is in a quenching environment.

In DPC alone, both BOC-Y-OMe and N-Ac-Y-NH₂ have similar fluorescence characteristics (Table 3.2). Addition of DPC₂₀DDM₃₀, but not DPC₂₀DDM_{7.5} increases fluorescence intensity of BOC-Y-OMe and decreases that of the N-Ac-Y-NH₂. Both model compounds display decreased fluorescence intensity in DPC/OG mixtures. Slight reductions of the fluorescence intensities of BOC-Y-OMe in all DPC/OG concentrations is seen, while a continued decrease in N-Ac-Y-NH₂ is observed as OG concentration increases. Very strong quenching is observed for N-Ac-Y-NH₂ in the DPC₂₀OG₁₀₀. Similar to BOC-Y-OMe in SDS_{3.5}LDAO₄₀, low fluorescence of both Tyr model compounds in DPC₂₀LDAO₅₀ occurs. Likely the LDAO headgroups are quenching BOC-Y-OMe fluorescence, as is observed in this detergent alone (Chapter 2).

3.4.4 Tryptophan fluorescence of His₆-porin in detergent

With the background information provided by the model compound studies, the Trp fluorescence of His₆-porin was investigated following excitation at 296 nm. In 3.5 mM SDS, His₆-porin fluorescence is intermediate between classes I and II, indicating that the Trp residues are partially exposed to the aqueous environment. The low intensity of the Trp fluorescence suggests quenching by the SDS headgroups as seen for hydrophobic model compounds (Chapter 2). These attributes are unchanged in SDS_{3.5}DDM_{7.5}. In SDS_{3.5}DDM₁₅, a dramatic blue-shift is observed (330 nm, Class I), indicating movement of the Trp residues

to more hydrophobic environments where they are hydrogen bonding in 2:1 exiplexes (Burstein *et al.* 1973). The blue-shift in $\lambda_{\text{max}}\text{Trp}$ is more dramatic in SDS_{3.5}DDM₃₀ (322 nm, intermediate between Class I and Class S fluorescence) and the Trp residues reside in an environment of increased hydrophobicity.

In terms of fluorescence intensity at $\lambda_{\text{max}}\text{Trp}$, no difference is observed between that of His₆-porin in SDS_{3.5} and in SDS_{3.5}DDM_{7.5}, in agreement with the consistency in $\lambda_{\text{max}}\text{Trp}$ and the secondary structure composition. However, the fluorescence intensity in SDS_{3.5}DDM₁₅ and SDS_{3.5}DDM₃₀, is two-to-three fold greater in intensity, compared to that in SDS alone. Combined with the corresponding alterations in secondary structure (Table 3.1), this observation suggests that the arrangement of the protein-detergent complex in these mixtures differs significantly from that in SDS alone, and that the Trp residues no longer encounter a quenching environment similar to that in SDS alone.

Generally, similar trends were observed in the SDS/OG system, but a higher mole fraction of OG was required to induce the conformational shift. $\lambda_{\text{max}}\text{Trp}$ blue-shifted from 339 nm (Class I/II) in SDS_{3.5}OG_{12.5} to 330 nm (Class I) in SDS_{3.5}OG₅₀ or SDS_{3.5}OG₁₀₀. Accompanying the blue shift is a three-fold increase in intensity in SDS_{3.5}OG₂₅, but the magnitude of the increase was less in the mixtures with higher OG concentrations. In agreement with the far-UV CD analysis (Table 3.1), the structures promoted by SDS_{3.5}OG₅₀ and SDS_{3.5}OG₁₀₀ are indistinguishable. Therefore, the consequences of the addition of the non-ionic detergents DDM and OG to SDS-solubilized His₆-porin are similar.

In contrast, addition of DPC to SDS-solubilized porin does not affect $\lambda_{\text{max}}\text{Trp}$; however, a three-fold increase in intensity is observed. Therefore, the very α -helix rich structure promoted by this detergent combination does not alter the overall hydrophobicity of

the Trp environments, but does remove the quenching effect of SDS. Quenching is even lower in the SDS_{3.5}LDAO₄₀ mixture, and in this case, the Trp residues are exposed to a slightly more hydrophobic environment than in SDS alone, but λ_{max} Trp remains intermediate between classes I and II.

Like SDS, DPC promotes a conformation of His₆-porin with significant α -helical content (Chapter 2). Addition of 7.5 mM DDM to porin in DPC₂₀ did not change Trp fluorescence significantly, but a blue-shift to 327 nm (Class I) and a three-fold increase in intensity was observed in DPC₂₀DDM₃₀. Given that quenching is not observed for porin in DPC alone (Chapter 2), these results suggest that the more hydrophobic environment inside the mixed micelles is responsible for the increase in fluorescence intensity. In contrast, in three DPC/OG mixtures, λ_{max} Trp of porin is only slightly blue-shifted to 333-334 nm (Class I), and there is little change in fluorescence intensity. Thus the increased levels of β -strand in porin dissolved in DPC₂₀/OG versus that in DPC₂₀ likely do not reflect differences in the folded state of the regions containing the Trp residues. Finally, there is a blue-shift in λ_{max} Trp in DPC₂₀LDAO₅₀ (331 nm, Class I); the accompanying increase in fluorescence intensity is small, indicating small changes in the phobicity of the Trp environment.

3.4.5 Tyrosine fluorescence of His₆-porin in detergent

As described for the model compounds, the intensity of Tyr fluorescence is the most informative factor. However, due to the large blue-shifts in Trp fluorescence in the SDS/DDM mixtures, it is difficult to precisely assign the intensity of Tyr fluorescence following excitation at 275 nm (Fig. 3.3). Nonetheless, several general trends can be noted. The spectrum of the protein in SDS_{3.5}DDM_{7.5} or in SDS_{3.5}OG_{12.5} broadens considerably, suggesting a significant contribution of Tyr fluorescence and that the addition of small

amounts of DDM or OG disrupts the protein/SDS micelle in such a way that at least some of the Tyr residues are exposed to more hydrophobic environments. At higher concentrations of DDM or OG, the overlap between Tyr fluorescence and the blue-shifted Trp fluorescence is too extensive to separate and properly analyze.

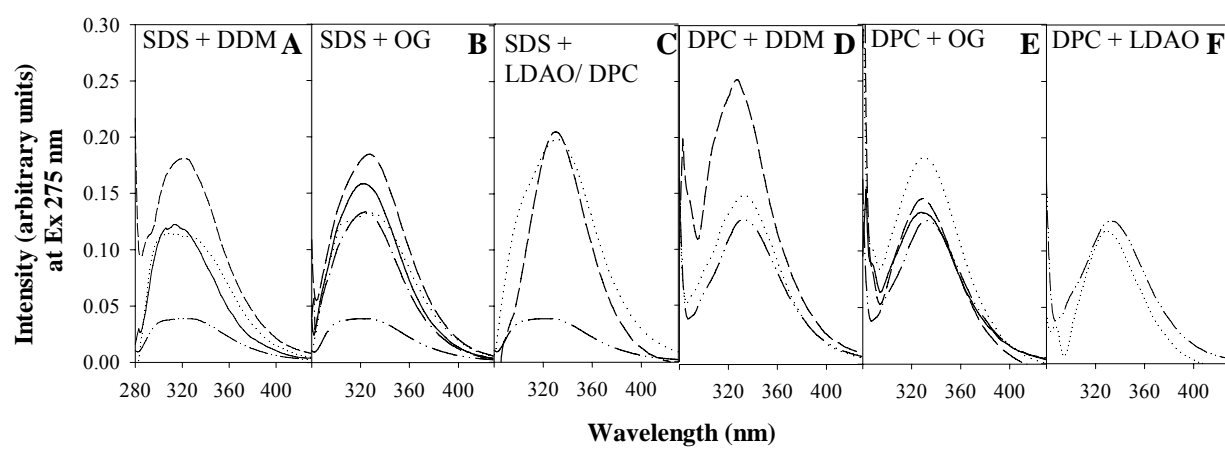
In SDS_{3.5}LDAO₄₀, Tyr fluorescence is quenched, as was observed for the model compounds in this mixture (Table 3.2). The clearly visible shoulder in the spectrum of SDS_{3.5}DPC₁₀-solubilized His₆-porin indicates a massive increase Tyr fluorescence compared to that in SDS alone; a difference of similar magnitude is not observed for the model compounds, indicating the folded state of the protein is responsible for the increased Tyr fluorescence in SDS/DPC micelles.

Blue-shifted Trp fluorescence also limits the analysis of His₆-porin in DPC/DDM and DPC/OG mixtures; in both systems the intensity near 300 nm is significantly higher than that in the SDS systems. In contrast, in DPC₂₀LDAO₅₀, quenching of the Tyr fluorescence of the protein is observed (Fig. 3.2F), and again likely reflects interactions with the LDAO headgroups.

3.4.6 SDUV analysis of tyrosine exposure in detergent-solubilized His₆-porin

Due to limited solubility, there were only three systems that were amenable to analysis by UV absorption: SDS/DDM, SDS/DPC and DPC/LDAO (Table 3.3). First, the model compounds were analyzed to examine interactions of the amino acids with the detergents. The second derivative plots of UV absorbance spectra were used to calculate r values; in general, high r values indicate exposure to solvent, while lower values are indicative of interactions with hydrophobic environments (Ragone *et al.* 1984). For

Figure 3.3. Fluorescence of His₆-porin in mixed detergent systems following excitation at 275 nm. Fluorescence of 0.42 μ M His₆-porin in detergent was measured as indicated in Materials and Methods. The protein was dissolved in the following detergent mixtures: **A)** 3.5 mM SDS (dash-dot-dot-dash), SDS_{3.5}DDM_{7.5} (dotted line), SDS_{3.5}DDM₁₅ (dashes), SDS_{3.5}DDM₃₀ (solid line). **B)** 3.5 mM SDS (dash-dot-dot-dash), SDS_{3.5}OG_{12.5} (dotted line), SDS_{3.5}OG₂₅ (dashed line), SDS_{3.5}OG₅₀ 50 mM OG (solid line), and SDS_{3.5}OG₁₀₀ 100 (dash-dot-dash) **C)** 3.5 mM SDS (dash-dot-dot-dash), SDS_{3.5}DPC₁₀ (dotted line), SDS_{3.5}LDAO₄₀ (dashed line) **D)** 20 mM DPC (dash-dot-dot-dash), DPC₂₀DDM_{7.5} (dotted line), DPC₂₀DDM₃₀ (dashed line) **E)** 20 mM DPC (dash-dot-dot-dash), DPC₂₀OG_{12.5} (dotted line), DPC₂₀OG₅₀ (dashed line), DPC₂₀OG₁₀₀ (solid line) **F)** 20 mM DPC (dash-dot-dot-dash), DPC₂₀LDAO₅₀ (dotted line).



example, in SDS, r calculated for the more hydrophobic Tyr compound, BOC-Y-OMe, is lower (1.51) than that of the amide compound, N-Ac-Y-NH₂ (2.24). In SDS_{3.5}/DDM_{7.5}, the r value calculated for BOC-Y-OMe (1.82) is slightly higher than that in SDS alone, but the values in mixtures with DDM concentrations of 15-20 mM are similar to that in SDS alone. In SDS_{3.5}DDM₃₀, Tyr exposure drops significantly, indicating that the interactions of the hydrophobic BOC-Y-OMe are more extensive with these DDM/SDS micelles than in SDS_{3.5}. As expected, solvent exposure of the hydrophilic NAc-Y-NH₂ compound is higher than for BOC-Y-OMe in SDS/DDM mixtures. Compared to those obtained for N-Ac-Y-NH₂ in SDS, lower r values are observed in SDS_{3.5}DDM₁₅ and SDS_{3.5}DDM₂₀, but not in SDS_{3.5}DDM₃₀ and SDS_{3.5}DDM₆₀. Finally, in SDS_{3.5}DPC₁₀, Tyr exposure is reduced for both compounds compared to SDS. The amide compound does not interact appreciably with DPC or DPC/LDAO micelles, as r values are high (2.5-2.7). In contrast, very low r values are calculated for BOC-Y-OMe and Tyr exposure is negligible in DPC₂₀LDAO₅₀. The striking differences between the SDS and DPC based systems likely reflect the strong ionic character of the SDS headgroups.

As noted previously, Tyr exposure is high (77%) in SDS-solubilized porin (Chapter 2). In comparison to that in SDS_{3.5}, there is a large difference between the environments seen by Tyr residues in porin solubilized in SDS_{3.5}DDM_{7.5}; on average only 22% (~2) of the Tyr residues are exposed to the aqueous environment in the latter system. This observation confirms the prediction that increased Tyr fluorescence intensity in the SDS/DDM system (Table 3.2) reflects a higher degree of interaction between the Tyr residues and the detergent micelles. At higher DDM concentrations (15-30 mM) in SDS, Tyr exposure is higher (50%),

Table 3.3. SDUV analysis of His₆-porin and model compounds. r and Y_{exp} values were calculated as described in Materials and Methods. For the amide model compounds and His₆-porin, each experiment was repeated at least twice; averages are reported; standard deviations were less than 22% for each listed value. For the hydrophobic compounds, the data reported are from a single experiment.

Detergents	<i>r</i>		His₆-porin	Y_{exp} (H)
	N-Ac-W-OEth + BOC-Y-OMe	N-Ac-W-NH₂ + N-AcY-NH₂		
3.5 mM SDS*	1.51	2.24	1.39	0.77
7.5 mM DDM + 3.5 mM SDS	1.82	2.48	0.85	0.22
15 mM DDM + 3.5 mM SDS	1.53	1.63	1.02	0.42
20 mM DDM + 3.5 mM SDS	1.59	1.80	1.16	0.55
30 mM DDM + 3.5 mM SDS	0.85	2.26	1.18	0.58
60 mM DDM + 3.5 mM SDS	1.17	2.36	1.40	0.79
10 mM DPC + 3.5 mM SDS	1.23	1.95	0.59	0.00
20 mM DPC	0.38	2.53	0.65	0.06
50 mM LDAO + 20 mM DPC	0.03	2.66	0.51	0.00

*Data taken from previous work (Chapter 2, Table 2.4)

in agreement with the apparent loss of Tyr fluorescence suggested by the narrowing of the spectrum following excitation at 275 nm (Fig. 3.3A).

In contrast, addition of DPC to SDS-solubilized porin essentially eliminated Tyr exposure, which suggests that the α -helical structure places these residues within the hydrophobic interior of the protein/detergent complex. Tyr exposure is also very low in DPC alone (0.06) and is nearly zero in the DPC₂₀LDAO₅₀ system, suggesting that there may be energy transfer to other groups in this particular folded state. Quenching by LDAO headgroups was not observed for the model compounds and therefore is unlikely to occur for the Tyr residues in LDAO-solubilized His₆-porin. Again these results confirm conclusions made based of Tyr fluorescence of porin.

3.4.7 Near-UV circular dichroism spectropolarimetry

To determine if alterations in tertiary interactions accompany the structural changes detected by the methods described above, near-UV CD spectropolarimetry was used. Only the SDS/DDM, DPC/LDAO and SDS/DPC systems held enough porin for these analyses; the latter system was not pursued as it promotes a high level of α -helix and is therefore not relevant for porin structural analysis. As shown previously, near-UV CD spectra of porin in SDS display strong negative ellipticity in the 260-290 nm range (Chapter 2), which includes signals from Trp (270-290 nm) and Tyr (265-270 nm). Higher concentrations of detergent were required for these studies, but the same molar ratios of the pairs of surfactants were used. For the SDS systems, the protein was first solubilized in 21 mM SDS, followed by addition of DDM to final concentrations of 45 to 270 mM. Increased negative ellipticity in the Tyr (268 nm) and the Trp (~275 nm) regions was observed in SDS₂₁DDM₄₅ (Fig. 3.4A), indicative of more extensive tertiary contacts involving these amino acids. In SDS₂₁DDM₉₀,

the overall shape of the spectrum is similar to that of the protein in urea (Chapter 2) or LDAO (Fig. 3.4B), but the negative intensity is intermediate between that in urea and in SDS₂₁DDM₄₅. Remarkably, the ellipticity is positive in SDS₂₁DDM₁₈₀ and SDS₂₁DDM₂₇₀, suggesting that the contacts surrounding the aromatic residues are significantly different in these micelles.

As in SDS, the near UV-spectra of His₆-porin in 100 mM DPC display negative ellipticity. A near-UV CD spectrum of similar overall shape is acquired from His₆-porin in DPC₁₀₀LDAO₃₀₀; neither spectrum resembles that of the molten-globule state of the protein in 300 mM LDAO alone (Fig. 3.4B and Chapter 2).

To assess the stability of the tertiary interactions involving aromatic residues, thermal denaturation was followed using near-UV CD. In SDS, the secondary structure composition of porin is not altered significantly by heating to 95°C (Chapter 2). However, heating alters the near-UV CD spectrum (Fig. 3.5A-B); above 40°C, the spectra resemble those of molten globules, with very little ellipticity. When the ellipticity at 268 nm is followed during heating to 90°C (Fig. 3.5B), a steady reduction in negative ellipticity is observed. Upon cooling of the heated sample to 20°C, some tertiary contacts are established, but the spectrum is not identical to that of the unheated sample.

During heating, the near-UV CD spectra of the protein in SDS₂₁DDM₁₈₀ show a steady decrease in ellipticity until 45°C is reached. At this point the spectrum resembles that of the protein in 8 M urea (Chapter 2). Protein precipitation is occurring at this temperature, as detected by an increase in HT voltage (Fig. 3.5D). Absorbance measurements taken after the completion of the experiment indicate that about one-third of the protein remained in solution. The near UV spectra of the protein at temperatures above 45°C therefore represent

Figure 3.4. Near-UV analysis of 33 μM His₆-porin in mixed systems. Spectra were obtained as described in Materials and Methods. **A)** SDS/DDM systems. Near-UV CD spectra of porin are as follows: SDS₂₁DDM₂₇₀ (filled circles), SDS₂₁DDM₁₈₀ (empty triangles), SDS₂₁DDM₉₀ (solid line), SDS₂₁DDM₄₅ (empty squares), and 21 mM SDS (filled triangles). **B)** DPC/LDAO systems. Near-UV spectra of His₆-porin in the following detergents are presented: 300 mM LDAO (solid line), DPC₁₀₀LDAO₃₀₀ (filled circles), and 100 mM DPC (open triangles).

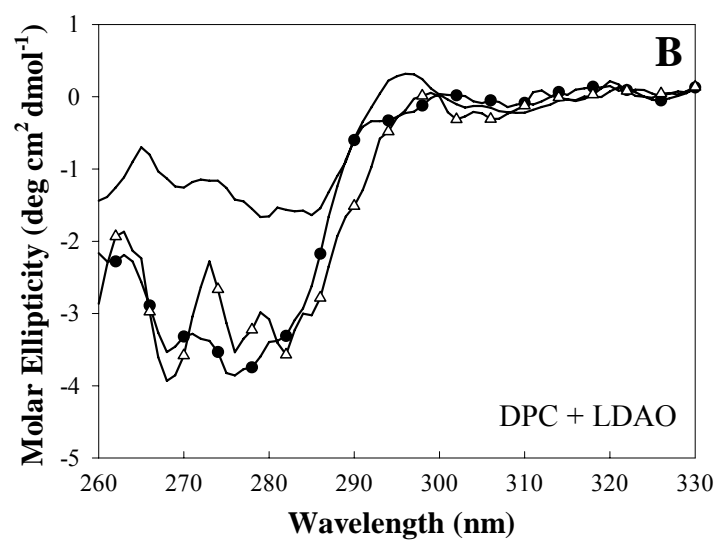
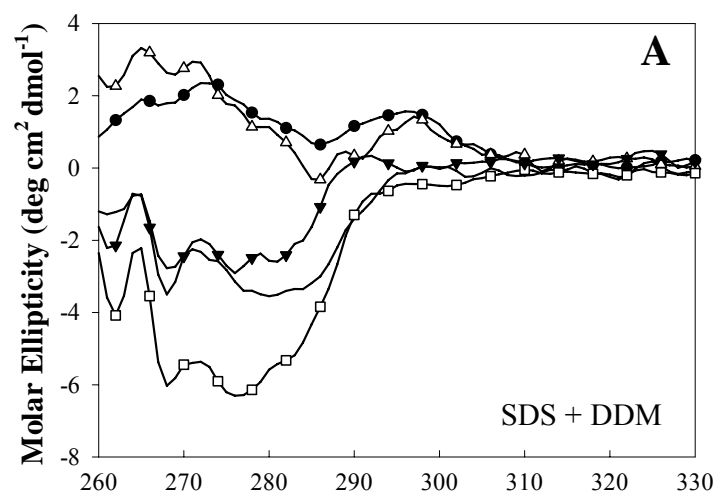
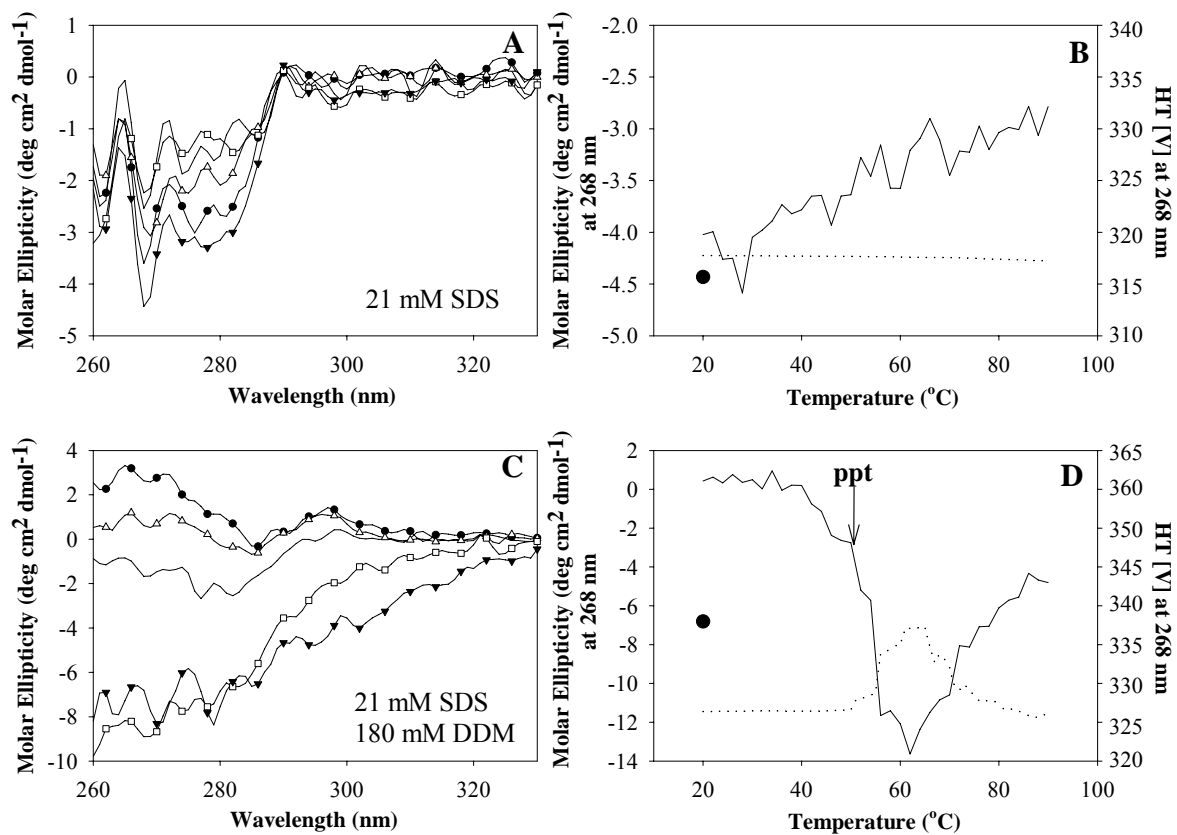


Figure 3.5. Thermal denaturation of His₆-porin in SDS and SDS_{3.5}DDM₁₈₀. Experiments were carried out as described in Materials and Methods. **A)** Near-UV CD spectra obtained following heating of 33 μ M His₆-porin dissolved in 21 mM SDS. Results obtained at 20°C (filled circles), 40°C (open triangles), 60°C (solid line), 90°C (open squares) are presented. The spectrum following cooling from 90°C to 20°C is indicated by filled triangles. **B)** Thermal denaturation during the experiment in **A)**, but monitored at 268 nm by near-UV CD at 1°C intervals. The filled circle indicates the molar ellipticity following cooling to 20°C. The dotted line indicates the HT values measured during the experiment. **C)** Near-UV CD spectra obtained following heating of 33 μ M His₆-porin dissolved in SDS₂₁DDM₁₈₀. Results obtained at 20°C (filled circles), 35°C (open triangles), 45°C (solid line), 55°C (open squares) and following cooling of the sample at 90°C to 20°C (filled triangles) are presented. **D)** Thermal denaturation during the experiment in **D)**, but monitored at 268 nm by near-UV CD at 1°C intervals. Symbols are the same as those in **B)**. The arrow labelled “ppt” shows the temperature at which an increase in HT indicates precipitation in the sample.



signals from a mixture of soluble and aggregated protein. In these cases, negative ellipticity was observed in both the Trp and Tyr regions (Fig. 3.5C).

3.4.8 Reconstitution of SDS/DDM-His₆-porin into liposomes

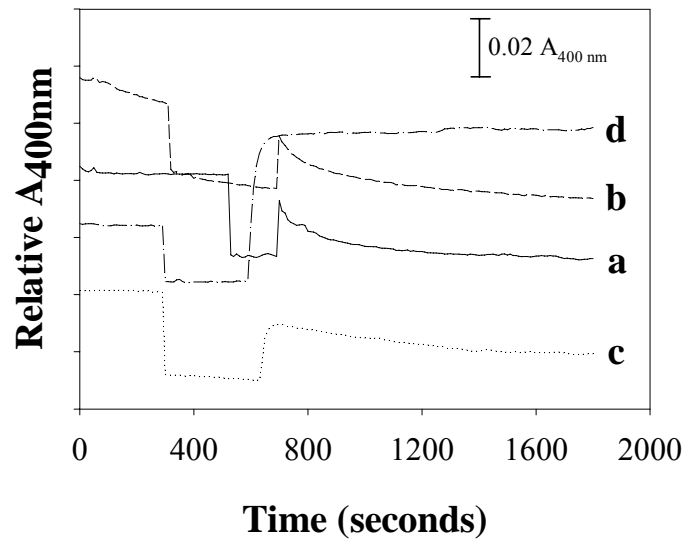
Since His₆-porin can be maintained at a high initial concentration in SDS_{3.5}/DDM₃₀, where it adopts a secondary structure with high β -strand content, this system was selected for further characterization in artificial membranes. Higher concentrations of DDM could not be used because the final DDM concentrations would have been in excess of its CMC. The SDS_{3.5}/DDM₃₀ system was also chosen for His₆-porin reconstitution into liposomes based on its ability to maintain high initial concentrations of protein in this solution necessary for membrane incorporation.

Liposome swelling assays performed for FT, SON, and INS SDS/DDM-His₆-porin-liposomes indicated that only FT proteoliposomes demonstrated swelling activity in response to sucrose (Fig. 3.6). Both INS and SON proteoliposomes had liposome swelling profiles that were almost identical to their respective control SDS/DDM-liposomes prepared in the absence of protein (data not shown).

3.4.9 Protease sensitivity of mitochondrial porin and SDS/DDM-solubilized His₆-porin reconstituted into liposomes

Protease resistance is often used as a criterion for refolding of bacterial porins, such as OmpG in detergent (Conlan and Bayley 2003) or OmpA following reconstitution into artificial membranes (Dornmair *et al.* 1990, Kleinschmidt and Tamm 1996). It was also used to confirm that *Neurospora* mitochondrial porin was assembled in the outer membrane

Figure 3.6. Liposome swelling assays. SDS/DDM-His₆-porin liposomes were prepared by the freeze-thaw (FT) method and swelling was measured directly (solid line; a) or following heating to 65°C (dashed lines; b) or 100°C (dotted lines; c) and liposomes lacking His₆-porin were measured as a control (line-dot-line; d). Relative A_{400 nm} values for each sample were plotted on the same scale, which permitted individual plots to be distinguishable from each other.



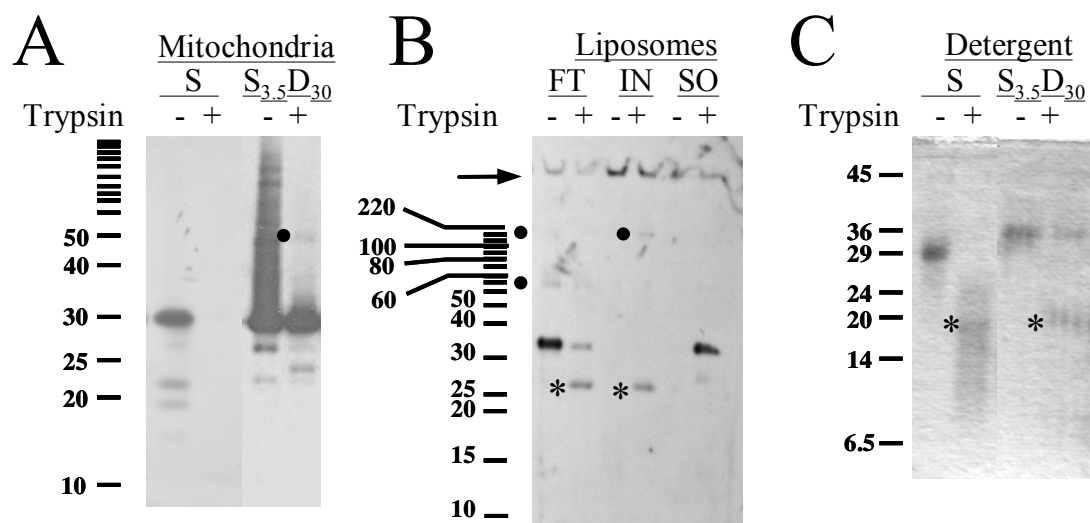
(Freitag *et al.* 1982). Protease sensitivity of native mitochondrial porin, and SDS or SDS_{3.5}/DDM₃₀-solubilized His₆-porin prior to and following reconstituting into liposomes was examined to determine the effects of mixed detergents on porin conformation. Immunoblotting was used to detect the low amounts of His₆-porin (< 2 µM) maintained in liposomes and porin in the isolated mitochondria. Trypsin (T) was also detected on the blots as 24 or 25-kDa bands due to sequence similarity between T and the porin peptide (residues 7-20) used to generate antibodies for this study.

Western blots of undigested *N. crassa* mitochondria in 3.5 mM SDS showed the intense 30-kDa porin band and minor 28 kDa, 21 kDa and 20 kDa proteolytic fragments resulting from activity of mitochondrially-associated proteases during isolation and/or the 30-min incubation at room temperature (Fig. 3.7A). All four species are in protease-sensitive conformations in this detergent, as they are not detected following T digestion. Blots of mitochondria in SDS_{3.5}/DDM₃₀ similarly have an intense band of intact porin at 30 kDa and minor proteolytic fragments (Fig. 3.7A). The full-length protein is highly resistant to digestion with T and very minor proteolytic fragments observed from the undigested sample lane are still detectable (Fig. 3.7A), as is the case for protease-digested *N. crassa* mitochondria in SEM (Chapter 2). Longer digestions did not reduce the intensity of the 30-kDa band (data not shown). A faint 55-kDa band can also be observed following T digestions of mitochondria in SDS_{3.5}/DDM₃₀, suggestive of a porin dimer.

His₆-porin migrates more slowly than mitochondrial porin (30 kDa) and has an apparent molecular mass of 32 kDa. Interestingly, undigested FT SDS/DDM-His₆porin-liposomes contained one additional faint 60-kDa species in the sample (Fig. 3.7B), suggesting dimers of the protein are present in the liposomes. Following digestion with

Figure 3.7. Protease susceptibility of porin in mitochondria, liposomes and detergent. **A)**

Western blot analysis of *N. crassa* mitochondria. Mitochondria (2.5 µg protein/well) were solubilized in 3.5 mM SDS (lanes 1 and 2) or 3.5 mM SDS/30 mM DDM (lanes 3 and 4) and analyzed following a 30-min digestion in the absence (lanes 1 and 3) or presence (lanes 2 and 4) of 0.75 µg T. **B)** Western blot analysis of FT, INS, and SON proteoliposomes formed in the presence of 0.9 mM SDS/7 mM DDM and containing 2.5 µg His₆-porin. Samples were undigested (lanes 1, 3 and 5) or digested with 0.075 µg T (lanes 2, 4, 6). **C)** Urea-SDS-PAGE analysis of 7.5 µg of His₆-porin solubilized in of 3.5 mM SDS (lanes 1 and 2), or 3.5 mM SDS/30 mM DDM (lanes 3 and 4). Samples were treated as described in B). An image of the Coomassie blue stained gel is presented. The molecular weights of markers in the Sigma low molecular weight ladder are indicated to the left of each panel. Filled circles indicate multimers of His₆-porin and cross-reacting trypsin is indicated by asterisks.



trypsin, the full-length His₆-porin band remained, but at less than half the intensity of the intact band in the undigested sample, and the 60-kDa species was no longer detectable.

Immunoblot analysis of INS and SON SDS/DDM-His₆porin-liposomes was much more difficult due to the high amount of protein retained in the wells of the gel (Fig. 3.7B). Only the lanes containing the SON SDS/DDM-His₆-porin-liposomes showed the 32-kDa His₆-porin band; additional bands at 65 and 90 kDa were not present (Fig. 3.7B).

This material was very sensitive to protease. In contrast, almost no His₆-porin was detected in the lanes containing the INS type proteoliposomes, possibly due to its inability to enter the gel.

Since His₆-porin could be maintained at high concentrations in SDS_{3.5}/DDM₃₀, the protease sensitivity of this form of the protein was examined directly on SDS-PAGE gels stained with Coomassie blue (Fig. 3.7C). Undigested SDS_{3.5}/DDM₃₀-His₆-porin contained a single porin species with an apparent molecular weight slightly larger than that of the native protein solubilized in 3.5 mM SDS (Fig. 3.7C). Bands of 65 kDa or greater were not observed on these gels or upon western blotting (data not shown). Digestion of SDS_{3.5}/DDM₃₀-His₆-porin with T resulted in reduced intensity of the 35-kDa His₆-porin band compared to the undigested protein band. This differs significantly from His₆-porin in 3.5 mM SDS which is completely digested by trypsin (Fig. 3.7C).

3.5 Discussion

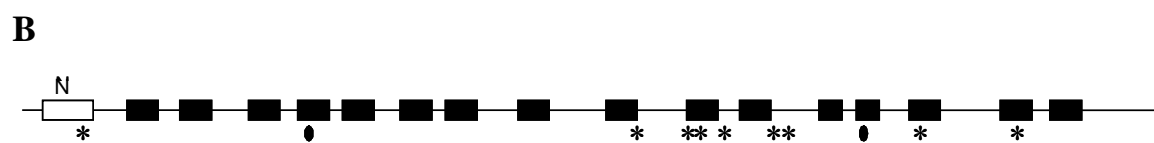
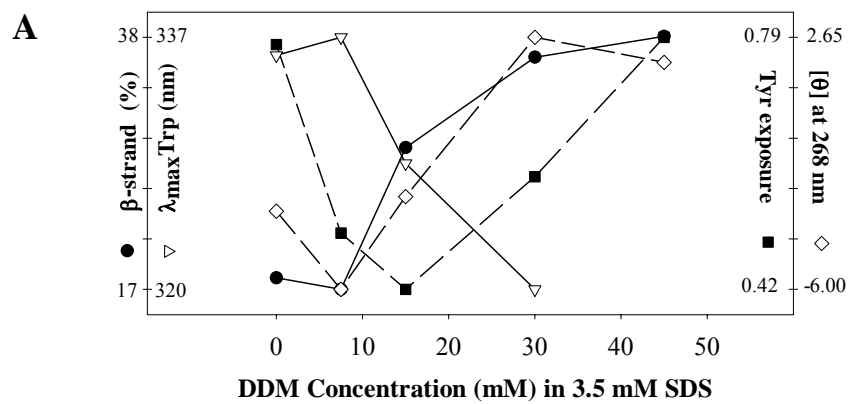
These studies revealed the usefulness of mixed detergent systems for two-step folding of recombinant mitochondrial porins, and of model compounds for interpreting the Tyr and Trp environments in the mixed micelles.

Overall, the SDS/DDM system was most suitable for maintaining high concentrations of His₆-porin in a β -strand rich state supported by tertiary contacts. The usefulness of the other systems examined, with the exception of the DPC/LDAO mixture, was limited by low solubility of the protein. Phase separation of mixed detergent systems containing LDAO, and the relatively high cost, compared to SDS based systems, limits the usefulness of the DPC/LDAO system, which also promoted high levels of β -strand in His₆-porin. Furthermore, addition of LDAO to DPC solubilized His₆-porin did not promote changes to the near-UV CD spectrum, suggesting that the environments surrounding the aromatic residues had not changed.

Addition of different molar ratios of DDM and SDS to porin promoted unique structural conformations, which are summarized in Fig. 3.8. At the low concentrations of DDM in SDS_{3.5}/DDM_{7.5} mixtures, the overall secondary structure content and $\lambda_{\text{max}}\text{Trp}$ are similar to those in SDS alone. However, rearrangements involving Tyr residues occur, as indicated by the large change in Tyr exposure. These changes are associated with increased negative ellipticity in the Tyr region of the near-UV CD spectrum. Since the α -helix and β -strand content are unchanged from those in SDS alone, these rearrangements are likely occurring within the turns or unordered regions of the protein. Seven of the nine Tyr are clustered in the C-terminal half of the protein (Fig. 3.8B), suggesting that this segment is unordered in the SDS-solubilized protein.

In SDS_{3.5}DDM₁₅, large-scale secondary structure changes occur, most notably the increase in β -strand at the expense of α -helical structure. This rearrangement involves placement of Trp residues in hydrophobic environments, as $\lambda_{\text{max}}\text{Trp}$ is blue-shifted. To date,

Figure 3.8. Summary of the folded state of His₆-porin in SDS/DDM systems. **A)** Composite figure showing the differences in β -strand content (filled circles), λ_{max} Trp (open triangles), Tyr exposure (filled squares) and molar ellipticity at 268 nm (open diamonds). All values were adjusted to the same arbitrary scale; the exact values of each parameter are listed on the x-axis in the same column as the descriptor for that parameter. **B)** One model for the secondary structure of mitochondrial porin. The model is that of (Runke *et al.* 2006), based on deletion analysis and the compilation of data from other experimental systems. Solid filled rectangles indicate predicted β -strands, and the lines joining them represent turns and loops. The N-terminus of the protein is shown on the left (diagonal line unfilled rectangle). Stars and filled ovals indicate the positions of the Tyr and Trp residues in the protein.



all models of mitochondrial porin structure (reviewed by Bay and Court 2002; Casadio *et al.* 2002) place the two Trp residues in predicted β -strand sequence (Fig. 3.8B). It is tempting to speculate that the regions of the protein flanking the two Trp residues are in α -helical structure in SDS and are arranged in β -strands in SDS_{3.5}DDM₁₅. Near-UV CD analysis suggests that the tertiary interactions involving Trp are less extensive in this conformation. Accompanying this change in secondary structure, Tyr exposure and negative ellipticity in the Tyr region of the near-UV CD spectrum are further reduced, suggesting significant changes to the folded state of large segments of the protein (Fig. 3.8B).

Higher DDM concentrations (SDS_{3.5}DDM₃₀), promote a higher level of β -strand (35%), with a concomitant decrease in α -helix. A large blue-shift in λ_{max} Trp is observed, indicating that the Trp residues are hydrogen-bonded in a very hydrophobic environment. Tyr exposure in SDS_{3.5}DDM₃₀ is intermediate between that in SDS alone and in SDS_{3.5}DDM₁₅. These observations suggest structural differences in several regions of the protein as less α -helix and more β -strand form. The fact that these are significant changes is supported by the observation that the near-UV CD spectrum displays positive ellipticity in both the Tyr and Trp regions. Strong positive ellipticity has been reported in the near-UV CD spectra of the native forms of the PorB class 2 (Minetti *et al.* 1997) and class 3 (Minetti *et al.* 1998) porins of *Neisseria*, and for the β -barrel segment of OmpA (Ohnishi and Kameyama 2001). Although the correlation is not absolute, a conversion from positive to negative ellipticity accompanies unfolding of other water-soluble β -strand proteins, such as cardiotoxin analogue III (CTXIII, Kumar *et al.* 1995, Sivaraman *et al.* 1997), CD40L (Matsuura *et al.* 2001) and TNF- α (Narhi *et al.* 1996). In His₆-porin, the positive ellipticity is lost upon heating to 45°C, and protein precipitation occurs, indicating that these interactions are required for stability in

SDS/DDM micelles and therefore they likely represent stable tertiary contacts within the protein. The negative ellipticity in the near-UV CD spectra of SDS-solubilized porin is lost upon heating, but, in contrast, precipitation does not occur, and the contacts can be restored upon cooling to 20°C. Thus, the positive ellipticity seen for porin in SDS-DDM is consistent with a β -barrel structure.

Protease digestions of His₆-porin at high DDM concentrations provide further support for well-folded His₆-porin in SDS/DDM systems. Both mitochondria and His₆-porin solubilized in SDS_{3.5}/DDM₃₀ demonstrate similar protease resistance to T, which suggests that the recombinant protein in this mixed system may share a similar conformation with mitochondrial porin.

In addition, SDS_{3.5}/DDM₃₀-His₆-porin could be readily reconstituted into liposomes by FT. Swelling assays of FT SDS/DDM-His₆-porin-liposomes demonstrated the most rapid osmotic response to sucrose, with a change of -0.02 A_{400 nm} over 20 min (Fig. 3.6). This response to sucrose is slightly better than the swelling measured for previous FT proteoliposomes prepared in single detergents (Chapter 2). These FT SDS/DDM-proteoliposomes also demonstrated far greater tolerance to heating than those formed in the presence of SDS, LDAO, or DPC (Chapter 2). This suggests that SDS/DDM-His₆-porin forms pores that are much more resilient to high temperatures than His₆-porin solubilized in single detergents.

If the conformation of His₆-porin in SDS_{3.5}/DDM₃₀ does represent a membrane bound arrangement of mitochondrial porin perhaps its reconstitution into liposomes by FT results in a much more stable pore. This stabilizing influence on pore formation in FT SDS/DDM-liposomes is likely due to the contribution of both ionic and non-ionic detergents within the

membrane. Studies focusing on the affects of mixed detergent-liposome interactions have indicated that SDS/ Triton X-100 (de la Maza and Parra 1996) and SDS/ nonylphenol ethylene oxide (NP(EO)10) mixed detergents (de la Maza and Parra 1996) cause increased solubilization and disruption of PC liposomes resulting in decreased liposome size and reduced individual CMC for each detergent. This behaviour of mixed detergent-liposomes must affect the incorporation of SDS/DDM-solubilized His₆-porin perhaps by facilitating the insertion of the protein into the phospholipid bilayers due to their disruptive abilities.

Taken together, these studies reveal that SDS/DDM promotes a His₆-porin conformation very similar to that for the protein reconstituted into artificial membranes (Chapter 2). The identification of a mixed detergent system for well-folded mitochondrial porin is an important first step toward high resolution structural studies using approaches such as NMR spectroscopy, which has recently been used to analyze the OmpA β -barrel and OmpX solubilized in detergent (Arora *et al.* 2001, Fernández *et al.* 2001 Fernández *et al.* 2001, Fernández *et al.* 2001, Fernández, 2004 #334}).

CHAPTER 4 The influence of sterols on the conformation of recombinant mitochondrial porin in detergents and liposomes

The material presented in chapter 4 was written with the intent to submit to the Journal of Bioenergetics and Biomembranes. I completed all of the experiments outlined in this chapter. The data were analyzed and the manuscript was written with guidance and feedback from my advisor and Dr. J. O'Neil, who are co-authors on the manuscript.

4.1 Abstract

Addition of sterols to detergent-solubilized mitochondrial porins is required for channel formation in artificial membranes. Although native mitochondrial porins co-purify with sterols, it is unclear what role sterols play with respect to mitochondrial porin folding *in vitro*. To investigate these interactions, detergent-solubilized recombinant *Neurospora crassa* His-tagged porin (His₆-porin) was incubated with various sterols (cholesterol, 4-cholesten-3-one, and ergosterol) and the resultant protein conformations were examined by fluorescence spectroscopy and CD spectropolarimetry. Sterols do not alter the secondary structure of porins dissolved in the detergents lauryl dimethylamine oxide (LDAO), dodecylphosphocholine (DPC), and mixtures of sodium dodecylsulfate (SDS) and dodecyl maltopyranoside (DDM). Near UV CD spectropolarimetry and fluorescence spectroscopy indicate that detergent-sterol solubilized porins possess slightly different tertiary interactions as compared to porin dissolved in detergent alone. His₆-porin reconstituted into liposomes in the presence of ergosterol by a freeze-thaw method generates altered osmotic responses to sucrose. Finally, His₆-porin was not capable of spontaneous insertion into ergosterol-liposomes. The subtle differences between the overall conformations in the presence and

absence of sterols suggests that the small changes in tertiary interactions are not sufficient for the formation of an insertion-competent structure and that the role of the sterol is to facilitate insertion into the artificial bilayers.

4.2 Introduction

Mitochondrial porin is the most abundant protein in the outer membrane and is responsible for the bi-directional transport of molecules across the lipid bilayer. *In vitro* analysis of this channel in artificial lipid bilayers has demonstrated pore-forming ability and voltage-dependence similar to those of bacterial porins (Benz 1994). Interactions of porin with many solutes and both soluble and membrane-bound proteins contribute to regulated channel activity that in turn controls mitochondrial metabolism. In particular, the participation of porin in the regulation of apoptosis, supports an important role for this protein in the global control of mitochondrial function in healthy and diseased cells (reviewed by Blachly-Dyson and Forte 2001, Lemasters and Holmuhamedov 2006).

Characterization of pore forming properties of native mitochondrial porin has largely been focused on reconstitution of detergent-solubilized porin into planar artificial membranes (Schein *et al.* 1976, Colombini 1980, Roos *et al.* 1982, Freitag *et al.* 1982, Pfaller *et al.* 1985, Aljamal *et al.* 1993, Troll *et al.* 1992) or liposomes (Colombini 1980, Colombini *et al.* 1987). In artificial planar lipid bilayer (or black lipid bilayer) experiments, mitochondrial porins form conductive channels under applied voltages, where the pores are anion-selective in their high conductance open state, but are converted to a slightly cation-selective partially-closed low conductance state with increasing voltage. These characteristics led to their alternative designation as voltage-dependent anion-selective channels (VDAC, Colombini 1980). In addition to revealing information regarding overall channel function, black lipid bilayer

experiments have been used in biotinylation assays to determine the relative positions of particular residues within the folded protein (Song *et al.* 1998, Song *et al.* 1998), to characterize channel ion selectivity (Blachly-Dyson *et al.* 1989, Blachly-Dyson *et al.* 1990), to examine the effects of amino acid deletions on pore formation and assembly (Runke *et al.* 2006), and to investigate auto-directed insertion (Zizi *et al.* 1995, Xu and Colombini 1996, Xu and Colombini 1997, Li and Colombini 2002). Liposomes have also been successfully used to examine porin function pertaining to diffusion of interacting molecules (Ca²⁺ Bathori *et al.* 2006, Gincel *et al.* 2001; Koenig's polyanion Colombini *et al.* 1987; reactive oxygen species Madesh and Hajnoczky 2001), or interacting proteins (Bcl-2 family Shimizu *et al.* 1999, Shimizu *et al.* 2000, Shimizu and Tsujimoto 2000; Plasminogen kringle 5 Gonzalez-Gronow *et al.* 2003).

In many of these artificial membrane experiments, in particular those using black lipid bilayers, sterols are required in the artificial membrane or with the solubilizing detergent, suggesting that sterols may influence mitochondrial porin channel formation *in vitro*. An *in vivo* role is suggested by the observations that ergosterol copurifies with *Neurospora crassa* porin (Freitag *et al.* 1982) and five molecules of cholesterol are associated with the rat heart and bovine mitochondrial porins (De Pinto *et al.* 1989). The requirement for sterols during mitochondrial porin insertion into artificial membranes was first demonstrated in black lipid bilayer experiments involving *N. crassa* mitochondrial porin (Pfaller *et al.* 1985). In this study, the protein was converted to a water-soluble form by treatment at high pH to remove any carry-over lipids. It formed conductive voltage-dependent channels only in artificial membranes containing one of several sterols. Similarly, detergent solubilized or water-soluble mitochondrial porins from *Dictyostelium discoideum*, *Paramecium tetraurelia*, and

rat liver only display strong channel forming activity and ion selectivity when pre-incubated with sterols or in membranes containing sterol (Popp *et al.* 1995). Sterols are also required for wild-type channel formation by recombinant mitochondrial (Popp *et al.* 1996, Koppel *et al.* 1998) or plastidal (Popp *et al.* 1997) porins expressed in *E. coli*, and bearing N-terminal hexahistidiny-tags (His₆-porin). Far UV CD analysis of detergent-solubilized native and recombinant pea root plastid porins indicated similar high levels of β -strand content both in the presence or absence of sterol (Popp *et al.* 1997).

In contrast to experiments involving pre-formed membranes, detergent-solubilized *N. crassa* His₆porin can be reconstituted into phospholiposomes lacking sterols by the freeze-thaw (FT) method (Chapters 2 and 3). Following reconstitution, His₆-porin has high β -strand content and displays positive ellipticity in the near UV CD region, similar to that observed for folded bacterial porins. His₆-porin did not directly insert into liposomes without FT treatment, but structural examination by CD analysis and fluorescence spectroscopy strongly suggested that the protein was interacting with liposomes. Therefore, a sterol may be necessary for either insertion into preformed artificial membranes or for proper folding therein.

With the establishment of fluorescence and near UV CD as tools for investigating mitochondrial porins (Chapters 2 and 3), we are able to further investigate the role sterols play on the folded state of *N. crassa* mitochondrial porin in detergents and artificial membranes. His₆-porin was solubilized in a collection of detergents, SDS/DDM, LDAO, and DPC in the presence of three different sterols: ergosterol, the native sterol found in *N. crassa* mitochondrial outer membranes (de Kroon *et al.* 1997), cholesterol, a major sterol common to mammalian mitochondrial outer membranes (Asworth and Green 1966), and 4-cholesten-3-

one, an oxidized form of cholesterol, to examine the effects of each sterol on the conformation of the protein in solution. Channel forming activity of His₆-porin reconstituted into liposomes containing ergosterol was examined and CD spectropolarimetry, fluorescence spectroscopy and protease digestion were used to determine the effect of sterols on porin structural arrangements.

4.3 Materials and Methods

4.3.1 Lipids, sterols, detergents, and amino acid derivatives

Egg yolk L- α -phosphatidyl choline, egg lecithin L- α -phosphatidic acid, SDS, urea, cholesterol, 4-cholesten-3-one (cholestenone), and ergosterol were obtained from Sigma (St. Louis, MO). DPC, DDM, and LDAO were purchased from Anatrace (Maumee, OH).

4.3.2 Expression and purification of His₆-porin

The cloning of the cDNA for *N. crassa* mitochondrial porin into the pQE-9 vector (Qiagen, Toronto, ON), which encodes an N-terminal His₆-tag has been described previously (Popp *et al.* 1996). Protein expression was carried out using the QIAexpress *E. coli* M15 [pREP4] strain from Qiagen.

The recombinant His₆-porin used in this study was expressed in *E. coli* and purified by immobilized nickel nitrotriacetic acid (Ni-NTA) in 8 M urea, using the procedure described in (Chapter 2). The yield of His₆-porin was 2-5 mg/L and the protein concentration was determined using the calculated extinction coefficient at 280 nm of 24,050 M⁻¹ cm⁻¹. Protein purity was monitored by sodium dodecyl sulfate-polyacrylamide gel electrophoresis and was estimated to be at least 95%.

4.3.3 Sterol-detergent solubilization of His₆-porin.

Dialyzed His₆-porin was acetone-precipitated and the dried pellets were resuspended in aqueous detergent-sterol solutions, buffered in 50 mM sodium phosphate pH 7. Detergent-sterol solutions were prepared in microfuge tubes by evaporation of 0.10 mg sterol (ergosterol, cholesterol, or cholestenone) in 1 ml of chloroform overnight in a fumehood at room temperature (22°-25°C). Each 0.10 mg aliquot of dried sterol was resuspended in 1 ml of a high concentration of detergent (21 mM SDS, 300 mM LDAO, and 100 mM DPC). These samples were vortexed for 10 minutes and inverted overnight at room temperature. The detergent-sterol solutions were centrifuged at 10,000 g for 15 minutes to remove any insoluble material; pellets were not visible after centrifugation. One ml from each high concentration detergent- (0.1 mg/ml) sterol supernatant was added directly to acetone-precipitated His₆-porin at high concentrations (0.90-1.80 mg/ml) to prepare near-UV CD samples. For far-UV CD analysis, detergent-sterol supernatants were diluted 1/5 into 50 mM sodium phosphate buffer pH 7 and used to solubilize acetone-precipitated His₆-porin at lower initial concentrations (0.15-0.30 mg/ ml). For SDS/ DDM-sterol samples, powdered DDM was added to His₆-porin solubilized in 21 mM SDS, 0.1 mg/ml sterol to a final concentration of 180 mM DDM. The detergent-sterol- His₆-porin samples were mixed by repeated inversion overnight (14-16 hrs) at room temperature, centrifuged at 10,000 g for 15 minutes, and the optically-cleared supernatants were collected. Samples lacking His₆-porin were prepared as described above and used as baselines for spectroscopic analysis or as negative controls for swelling assays.

4.3.4 Liposome stock preparation

His₆-porin was reconstituted into small unilamellar vesicles in the presence of ergosterol using modifications of the procedure described in (Chapter 2). Briefly, a 10:1:0.8 (w/w/w) mixture of egg yolk L- α -phosphatidyl choline, egg lecithin L- α -phosphatidic acid, and ergosterol was dissolved in chloroform and evaporated in a fumehood at room temperature overnight. Dried lipids and sterols were resuspended in 50 mM sodium phosphate buffer at pH 7 or stored at -20°C in a dessicator until needed. The resulting milky suspension was diluted 1:1 with phosphate buffer pH 7 and sonicated on ice until the microtip (Fisher Scientific Sonifier Model 300) could clearly be observed to yield the stock SUV-ergosterol suspension (20 mg phospholipid/ml). Stock SUV suspensions lacking ergosterol were prepared by the same method as described above.

4.3.5 Liposome swelling assays

Liposome swelling assays were based on the methods described by (Chapter 2); all samples were buffered with 50 mM sodium phosphate pH 7. To determine if the inclusion of ergosterol in the detergent (type D) or in the artificial membranes (type L) affects liposome swelling, proteoliposomes were prepared by freeze-thaw (FT) or insertion (INS) methods. Type D experiments were set up by mixing equal volumes of stock SUV lacking ergosterol and 0.5- 2.5 μ M His₆-porin solubilized in detergents containing 0.01 mg/ml ergosterol. Following mixing, detergent concentrations were 1.25 mM SDS, 1.25 mM SDS/15 mM DDM, 3.75 mM LDAO, and 1 mM DPC. These samples were then subjected to either FT or INS protocols as described in (Chapters 2 and 3). Briefly, freeze-thaw (FT) samples were subjected to three cycles of 1 min in liquid nitrogen followed by thawing at room temperature. The insertion (INS) method was based on that of Surrey *et al.* (Surrey and

Jahnig 1995), and involved incubation of His₆-porin/detergent complexes with preformed liposomes at room temperature. Following either treatment, the proteoliposomes were placed on a rotating mixer overnight at room temperature. Following liposome swelling analysis, samples were centrifuged at 10,000 g for 10 min and the pelleted material was resuspended in 8 M urea for measurement by UV absorption spectroscopy at 280 nm. This allowed determination of the concentration of insoluble protein in the pellet, which was then used to calculate the concentration of soluble His₆-porin. Final concentrations of each component were as follows: 6.6 mg/ml phospholipid, 0.002 mg/ml ergosterol, 0.2-0.8 μ M His₆-porin, and for each detergent examined 0.6 mM SDS, 0.6 mM SDS/ 5 mM DDM, 1.3 mM LDAO, or 0.3 mM DPC.

Type L (ergosterol-containing) proteoliposomes were prepared by first diluting stock SUV 1:2 (high ergosterol) or 1:20 (low ergosterol) with stock SUV lacking the sterol. Both high and low ergosterol-liposomes were mixed 1:1 with detergent-solubilized His₆-porin at the same concentrations as described for type D proteoliposomes. These samples were subjected to either FT or INS treatments as described for type D proteoliposomes (above). The only exception in these treatments was for type L INS samples, which were briefly sonicated on ice to ensure homogenous ergosterol-liposomes formation before incubation with detergent- His₆-porin. The lower ergosterol concentration (0.01 mg/ml) in the type L samples was identical to that in type D; the higher ergosterol concentration was 10-fold as high. The concentrations of all other components were identical in the types D and L experiments.

Liposome swelling was measured on an Ultrospec 3100 pro spectrophotometer at an absorbance of 400 nm. Both type D and L proteoliposome samples prepared as described

above were diluted 1/100 into 50 mM sodium phosphate pH 7 buffer to a final volume of 0.5 ml and measured in a 1 cm quartz cuvette. After 300-400 seconds, liposomes were diluted with 40 μ l of iso-osmotic phosphate buffer pH 7, followed by an addition of 40 μ l of hyperosmotic 1 M sucrose after 600-700 seconds. Liposome re-swelling, as indicated by a gradual decrease in $A_{400\text{ nm}}$ was followed for 1200 or 1800 seconds after sucrose addition.

4.3.6 Reconstitution of SDS-solubilized His₆-porin in ergosterol-containing liposomes for spectroscopic analysis

His₆-porin was resuspended in 3.5 mM SDS to 10-35 μ M; subsequent dilutions of 1:3 or 1:4 in phosphate buffer resulted in final detergent concentrations near the CMC (0.9-1.0 mM SDS). Ergosterol was examined in these studies since it is the predominant sterol in *N. crassa* mitochondrial outer membranes. Other detergents were not pursued due to low initial concentrations ($\leq 5\text{ }\mu\text{M}$) of His₆-porin maintained in solution. The SDS-solubilized protein was diluted 1:4 into type L liposomes (2 mg phospholipid/ml) containing 0.02 mg/ml ergosterol, buffered in 50 mM sodium phosphate pH 7. Liposome-ergosterol-detergent-His₆-porin mixtures were then subjected to one cycle of freeze-thaw (FT) or the INS method described above. Type D SDS- His₆-porin-ergosterol-liposomes were not examined spectroscopically since liposome swelling profiles were similar to samples lacking ergosterol (see results section 4.4).

4.3.7 Fluorescence spectrophotometry

Fluorescence spectroscopic analyses of detergent-sterol-solubilized His₆-porin were performed using a JASCO-810 (FMO-427S) spectropolarimeter/fluorometer. All emission spectra were measured in a 1-cm path length quartz cuvette after excitation at 280 nm or 296

nm. Detergent-sterol-solubilized His₆-porin samples were measured at A₂₈₀ of 0.01, which corresponds to a protein concentration of 0.42 μM. All His₆-porin-liposome samples were diluted 1:10 in 50 mM sodium phosphate buffer pH 7 to a final lipid concentration of 0.2 mg/ml, 0.002 mg/ml ergosterol, and 1.0-0.2 μM His₆-porin. His₆-porin-ergosterol-liposome spectra were normalized to a concentration of 0.42 μM with reference to His₆-porin in urea (Chapter 2).

4.3.8 Circular dichroism (CD) spectropolarimetry

CD spectra were acquired on a JASCO J-810 spectropolarimeter-fluorometer calibrated with (+)-10-camphorsulfonic acid and purged with N₂ at 20 L/min (Manley and O'Neil 2003). CD spectra of 1.5 μM sterol-detergent-solubilized His₆-porin samples and His₆-porin-ergosterol-liposome samples (Type L) containing 0.5-2.0 μM His₆-porin were measured in the far UV region (190-250 nm) using 0.05-0.10-cm path length quartz cuvettes at 22°C, a scan rate of 10 nm/min and a response time of 8 s. High initial concentrations of His₆-porin in SDS were necessary to maintain 1-2 μM of protein in the SUV samples after centrifugation. CD spectra were corrected by baseline subtraction and were converted to mean residue ellipticity (MRE) according to the formula: $[\theta]_M = M\theta / \{(10)(l)(c)(n)\}$ where $[\theta]_M$ is 10⁻³ deg cm² dmol⁻¹, M is the molecular weight of His₆-porin (31 402 g/mol), θ is the measured ellipticity in millidegrees, l is the path length of the cuvette in cm (0.1 cm), c is the protein concentration in g /L, and n is the number of amino acid residues in the protein (295). Detergent-sterol-solubilized His₆-porin spectra were deconvoluted with the CONTINLL algorithm (Provencher and Glockner 1981, van Stokkum *et al.* 1990) in the DichroWeb package (Whitmore and Wallace 2004). Light scattering by the ergosterol-liposome samples

prevented reliable acquisition of spectra below 200 nm and prohibited deconvolution with secondary structure prediction algorithms.

Temperature was controlled during thermal denaturation experiments of His₆-porin-ergosterol-liposomes using the Peltier device in the spectropolarimeter. These experiments were carried out in the far UV region (200-250 nm), with a 1°C / min ramp speed; θ (in mdeg) was monitored at 217 nm at 1°C intervals, and full spectra were collected at 10°C intervals.

Near-UV (245-330 nm) CD spectra of 33 μ M His₆-porin in 0.02 mg/ml sterol-detergent were measured with a JASCO J-810 spectropolarimeter-fluorometer in a 1-cm path length jacketed quartz cuvette at room temperature, with a scan rate of 2 nm/min, and a response time of 8 s. CD spectra of His₆-porin reconstituted into Type L ergosterol-liposomes were measured in a 5-cm path length jacketed quartz cuvette at room temperature with a scan rate of 10 nm/ min, a response time of 8 seconds. Scans were measured in triplicate for averaging to reduce noise. Molar ellipticity of His₆-porin in detergent-sterol or sterol-containing liposomes was calculated from the baseline corrected spectra according to the formula: $[\theta] = M\theta / \{(10)(l)(c)\}$ where $[\theta]$ is the molar ellipticity in degrees cm² dmol⁻¹, θ is the measured ellipticity in millidegrees, l is 1 cm for detergent-sterol-His₆-porin or 5 cm for His₆-porin-sterol-liposomes, and c is the protein concentration in g/ L.

4.3.9 Protease digestions of His₆-porin reconstituted into ergosterol-liposomes

His₆-porin in liposomes was digested with protease after spectroscopic examination. Each liposome sample was digested with 0.15 mg/ml trypsin (T) or chymotrypsin (CT) for 30 minutes at room temperature and contained 0.0075- 0.015 mg/ml (0.25- 0.5 μ M) His₆-porin, 0.01 mg/ml ergosterol, and 1 mg/ml phospholipid. All protease digestions were arrested by

adding 20 mM PMSF (f.c.) and 3:1 dilution to Laemmli (Laemmli 1970) buffer containing 8 M urea. All reactions were stored at -20°C until loaded onto SDS-PAGE gels.

4.3.10 Western blots of His₆-porin-ergosterol-liposomes

All protease digested samples were loaded onto 0.1 % SDS- 3 M urea- 14% PAGE gels and electrophoresis was performed with the Mini-Protean[®] II system (Bio-Rad Laboratories, Hercules, CA). 10 µl of 7.5- 15 µg/ ml His₆-porin in 1 mg/ml phospholipids with or without 0.02 mg/ml ergosterol were loaded into each well. Gels were blotted with a Trans-Blot[®] Cell system (Bio-Rad) onto 0.45 µM nitrocellulose membranes (Bio-Rad) overnight at 4°C and stained with Ponceau S (Sigma) to visualise the Benchmark protein ladder (Invitrogen, Burlington, ON).

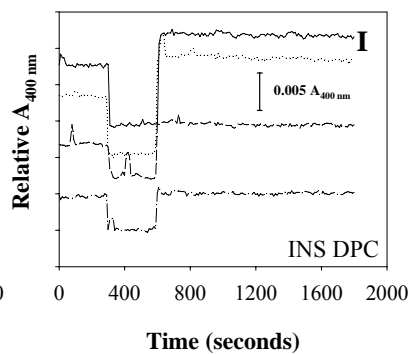
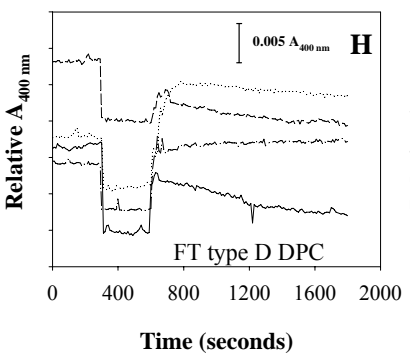
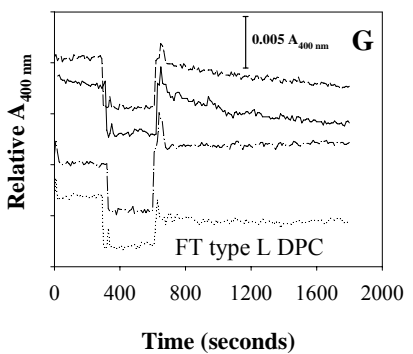
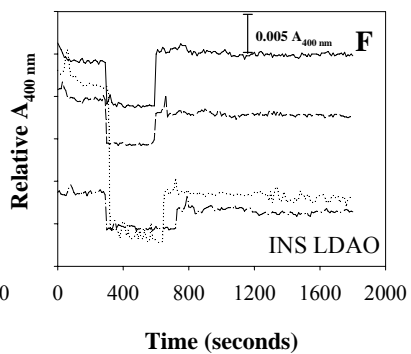
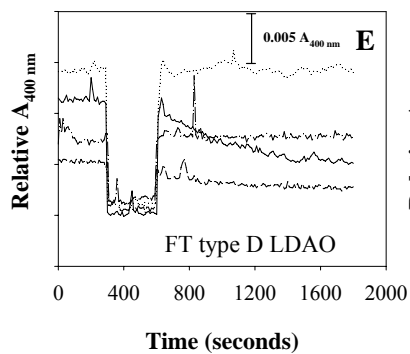
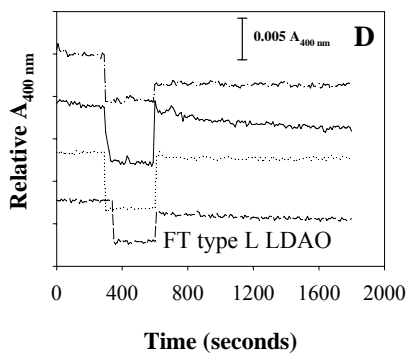
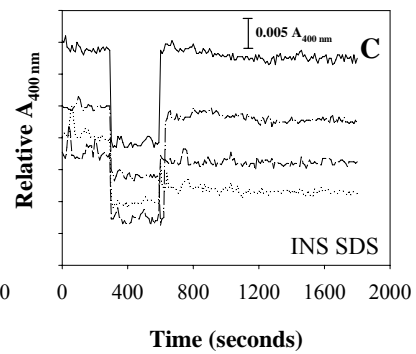
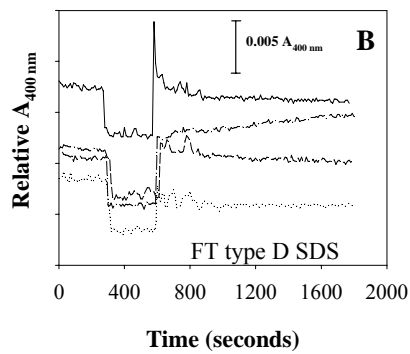
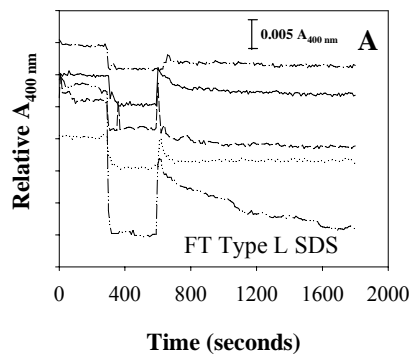
Immunoblotting was carried out at room temperature using rabbit antibodies directed against residues 7- 20 of *N. crassa* mitochondrial porin (αNcPor-N, generated by R. Lill, at Universität München). Membranes were immunoblotted according to the procedure described by (Chapter 2). Membranes were detected by CDP- star (Roche Diagnostics, Indianapolis, IN) and exposed for 1- 2 hrs on X-Omat Blue XB-1 Scientific Imaging film (Kodak, Rochester, NY) before image development.

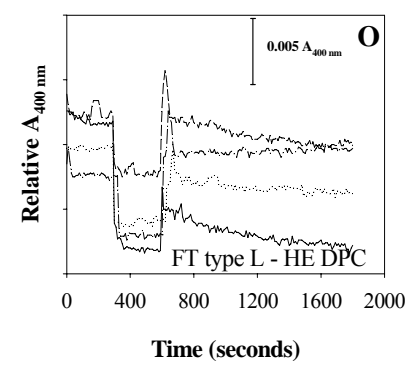
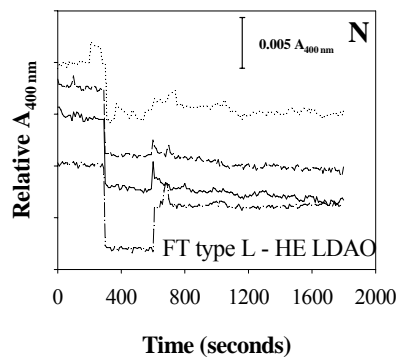
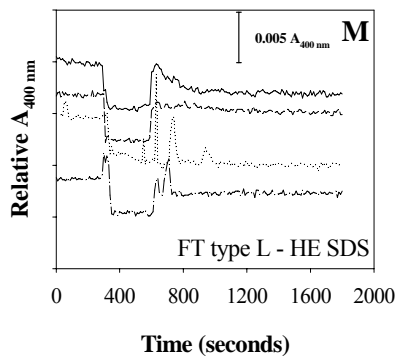
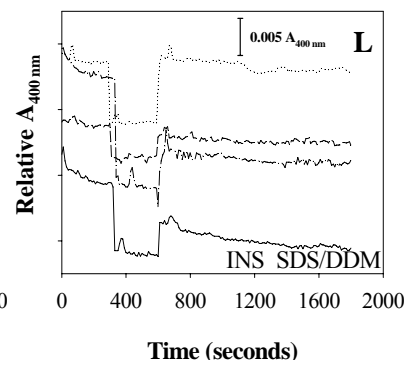
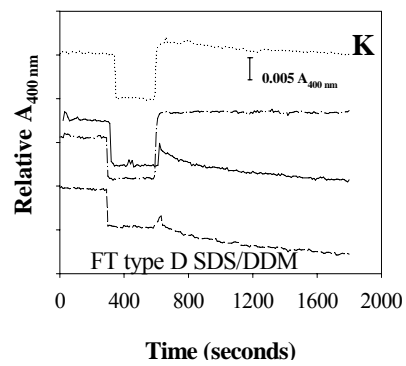
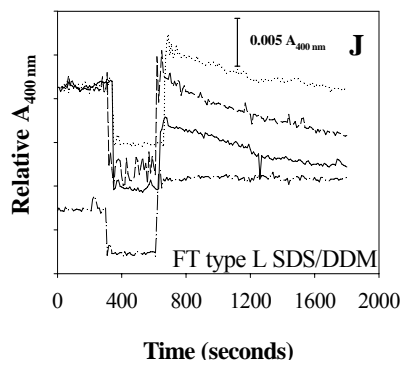
4.4 Results

4.4.1 Liposome swelling assays of His₆-porin in the presence of ergosterol

Osmotic swelling assays were performed on His₆-porin reconstituted into liposomes in the presence of ergosterol added in detergent (Type D) or incorporated into the stock SUV (Type L) to determine the effects of sterol on porin channel formation. Type L liposome solutions were formed in the presence of either 20 µg/ml (Fig. 4.1A, D, G, and J) or 200

Figure 4.1. Liposome swelling assays. Detergent-solubilized-His₆-porin-liposomes with ergosterol included either in the liposomes or in the detergent were prepared by the freeze-thaw (FT) method (**A,B, D, E, G,H, J, K, M, N, O**) or the insertion (INS) method (**C, F, I, L**). In all FT proteoliposomes, swelling was measured directly (solid line) or following heating to 65°C (dashed lines) or 100°C (dotted lines) and liposomes lacking His₆-porin were measured as a control (line-dot-line). In panel A only, a proteoliposome sample lacking ergosterol is shown (line-dot-dot-line). Panels M, N, O display liposome swelling assays for type L liposomes prepared with 10-fold greater ergosterol concentrations (high ergosterol – HE) than in all remaining experiments. For INS proteoliposomes (**C, F, I**) prepared with ergosterol added to the lipid (solid (RT) and dashed lines (30°C)) or to the detergent (dotted (RT) and line-dot-lines (30°C)), swelling was monitored directly (RT) or after overnight incubation at 30°C. For SDS/DDM INS proteoliposomes, swelling of INS proteoliposomes lacking sterol (dot-dash) and FT SDS/DDM proteoliposomes (dotted line) are also shown along with INS type L (solid line) and INS type D liposomes (dashed line). Relative $A_{400\text{ nm}}$ values collected over time for each sample were adjusted and plotted on the same scale which permitted individual plots to be distinguishable from each other.





$\mu\text{g/ml}$ ergosterol (Fig. 4.1M, N and O; Table 4.1). Due to the poor solubility of ergosterol in the low detergent concentrations necessary for type D experiments, these solutions were prepared in the presence of 20 $\mu\text{g/ml}$ ergosterol only (Fig. 4.1B, E, H and K; Table 4.1). Osmotic responses were detected as a gradual decrease in $A_{400\text{ nm}}$ following the addition of sucrose to the liposome solution at 600 seconds (Shao *et al.* 1996).

Following FT, in all detergents tested, both types of D and L proteoliposomes demonstrated an osmotic response to sucrose (Fig. 4.1, Table 4.1). The presence of ergosterol increased the noise in the spectra (see Fig. 4.1A) and many of the traces from sterol-containing liposomes displayed a sharp drop in $A_{400\text{ nm}}$ at the beginning of the swelling phase, followed in some cases by a more gradual decline in $A_{400\text{ nm}}$. With the exception of DPC-containing type D liposomes, the rapid drop was not observed in the absence of porin, suggesting that it reflects movement of solution through porin, rather than resulting from altered membrane structure *per se*. The reason then for two-phase reswelling is not clear – it could represent either two populations of liposomes, with different porin content or activity. The slow phase is characteristic of wild-type pore activity (Shao *et al.* 1996, Bathori *et al.* 1993). For these reasons, only the slow reswelling phase will be considered in the following discussion.

The magnitude of the osmotic response to sucrose in FT, ergosterol-containing liposomes was generally less than that in the corresponding sterol-free systems. For example, the associated $A_{400\text{ nm}}$ changes ranged from -0.004 to -0.008 in type D proteoliposomes, and from -0.002 to -0.006 in both high and low ergosterol Type L systems. In contrast, a gradual change of -0.01 A_{400} units was observed for SDS-His₆-porin liposomes lacking ergosterol (Fig. 4.1A, see Chapter 2).

Table 4.1. Summary of proteoliposome swelling data. Relative liposome swelling activity was determined for each preparation of detergent-solubilized His₆-porin reconstituted into type L or D containing liposomes, or those without sterol. Assays were carried out as described in Materials and Methods.

Detergent for Porin Solubilization	Ergosterol Content *	Proteoliposome Type †	Temperature (°C)	Rapid Reswelling Phase ‡	Slow Reswelling Phase ‡
SDS	none§	none	RT**	+	+++
			65	++	++
			100	-	-
	high	L	RT	+	+
			65	-	-
			100	nd††	nd
	low	L	RT	++	-
			65	++	-
			100	+	-
	low	D	RT	+++	-
			65	-	-
			100	-	-
DPC	none	none	RT	-	+++
			65	+	+++
			100	-	+
	high	L	RT	+	+
			65	++	+
			100	+	-
	low	L	RT	+	++
			65	+	+
			100	+	-
	low	D	RT	-	++
			65	-	+
			100	-	-
LDAO	none	none	RT	-	+++
			65	+++	+++
			100	-	+
	high	L	RT	+	-
			65	-	-
			100	-	-
	low	L	RT	-	+
			65	-	-
			100	-	-
	low	D	RT	+	++
			65	-	-
			100	-	-

continued on following page

SDS/DDM	none	none	RT	++++	++++
			65	+++	++++
			100	-	+++
	high	L	RT	is§§	is
			65	is	is
			100	is	is
	low	L	RT	-	++
			65	+	+++
			100	+	++
	low	D	RT	+	++
			65	+	++
			100	-	+

Table 4.1, footnotes

* high, (0.1 mg/ml); low (0.01 mg/ml)

† L, sterol added in liposomes; D, sterol added in detergent

‡ rapid swelling phase, 100 seconds after sucrose addition; slow swelling phase 100-1800 seconds after addition change in A_{400} <0.0020 (-) ; 0.0020-0.0030 (+), 0.0030-0.0060 (++) , > 0.0060 (+++)

§ Data for proteoliposomes lacking sterol are taken from Chapters 1 and 2.

** RT, room temperature (22-25°C)

†† nd, not determined, reproducibly high levels of noise in sample

§§ is, insufficient solubility, high concentrations of ergosterol not soluble in SDS/DDM

Maintenance of swelling activity following incubation at increased temperatures (65°C or 100°C) varied, depending on how the sterol was included in the sample, and on the detergent used (Table 4.1). In SDS alone, gradual reswelling was observed at room temperature. This response was partially or completely lost following incubation at 65°C and 100°C, respectively. In contrast, the slow swelling phase was not observed in the presence of sterols, but a much more rapid temperature-sensitive response was seen. Types D or L LDAO-His₆-porin liposomes demonstrated the lowest osmotic response to sucrose among all of the detergents tested (Fig. 4.1D and 4.1E). For L-type proteoliposomes, gradual reswelling was weak or not observed at room temperature, and a relatively small shrinkage phase was observed in high ergosterol Type L liposomes (Fig. 4.1N). However, D type LDAO-proteoliposomes maintained slow reswelling behaviour that was temperature sensitive.

The osmotic response of proteoliposomes formed with DPC-solubilized His₆-porin was unchanged upon addition of sterol to the detergent, but was strongly diminished when the sterol was initially incorporated into the liposomes (Table 4.1). The slow phase was absent in the Type L samples with high ergosterol concentrations (Fig. 4.1M, N, O), and reduced at lower concentrations (Fig. 4.1A, D, G, J). Responses seen at room temperature remained after 65°C treatment, but were lost at 100°C. Finally, SDS/DDM could only be used for generating Type L and low-ergosterol Type D liposomes, due to solubility issues at high concentrations of ergosterol. Remarkably, enhanced liposome swelling was observed for Type L SDS/DDM proteoliposomes, and this response was partially resistant to heating at 100°C (Fig. 4.1J). Incorporation of sterol to the stock SUVs did not alter osmotic responsiveness in this system (Fig. 4.1C, F, I, L).

Bacteriorhodopsin can insert into preformed liposomes containing cholesterol, but requires freeze-thaw treatment for integration in the absence of the sterol (Scotto and Zakim 1988). To determine if the same trend exists for mitochondrial porin, swelling assays were performed to determine if detergent-solubilized His₆-porin possesses the capacity to insert into preformed liposomes in the presence of ergosterol either added to the porin in detergent (type D) or incorporated into phospholipids (type L). All type D and L His₆-porin insertion experiments did not produce liposomes with significant osmotic responses, following incubation overnight at either 30°C or 40°C (Fig. 4.1C and D). Higher temperatures were also not effective, as brief heating (10 minutes) of INS ergosterol-proteoliposomes to 65°C or 100°C before swelling assay collection also did not generate osmotically responsive liposomes (Figs. 4.1C and D). Hence, the addition of ergosterol did not influence the inability of His₆-porin to insert into liposomes.

4.4.2 Protease digestion of His₆-porin in ergosterol-liposomes

Resistance to protease treatment has been used frequently to confirm bacterial porin refolding in detergent (OmpG; Conlan and Bayley 2003) or following reconstitution into artificial membranes (OmpA; Dornmair *et al.* 1990, Kleinschmidt and Tamm 1996). *Neurospora* His₆-porin reconstituted into liposomes has similar resistance to high levels of protease as observed for *N. crassa* mitochondrial porin in protease-treated mitochondria (Freitag *et al.* 1982, Chapter 2). To determine if SDS-solubilized His₆-porin reconstituted into ergosterol-laden liposomes by FT or INS acquires protease resistance, western blots of trypsin (T) and chymotrypsin (C) treated samples were performed. As observed on previous immunoblots, T and C were also detected as 24 or 25-kDa bands on the western blots due to

sequence similarity between T and C and the porin peptide (residues 7-20) used to generate antibodies for this study (Chapter 2).

Three porin species with apparent molecular masses of 32, 65, and 90 kDa were detected in undigested FT SDS- His₆-porin-ergosterol-liposomes (Type L); they were identical to those observed in FT SDS-His₆-porin-liposomes (Fig. 4.2). The 32 kDa band corresponds to intact His₆-porin and the two additional bands with molecular masses of approximately 90 and 65 kDa are suggestive of trimers and dimers. Following digestion with both T and C, full-length protein was still detectable in each lane but the putative oligomeric bands were not observed (Fig. 4.2). Accumulation of protein in the wells during electrophoresis prevented quantitation of intact His₆-porin bands but nonetheless confirmed that FT SDS-solubilized His₆-porin reconstituted into liposomes prepared with ergosterol acquired protease resistance.

Western blot analysis of undigested INS SDS-His₆-porin-ergosterol-liposomes did not reveal species with molecular masses of 90 and 65 kDa. Small amounts of the 32-kDa His₆-porin remained following digestion with either T or C (Fig. 4.2). Therefore, some of the protein in INS SDS-His₆-porin-ergosterol-liposomes acquired protease-resistance similar to INS SDS- His₆-porin-liposomes lacking ergosterol.

4.4.3 Characterization of detergent-sterol-solubilized His₆-porin and His₆-porin-ergosterol-liposomes by far-UV circular dichroism spectropolarimetry

CD spectropolarimetry in the far UV region (190-250 nm) was used to determine the secondary structures of His₆-porin in detergents and liposomes containing sterols (Figs. 4.3 and 4.4). To determine if sterols alter secondary structural arrangements of His₆-porin solubilized in 3.5 mM SDS, 3.5 mM SDS/30 mM DDM, 50-75 mM LDAO, and 10-20 mM

Figure 4.2. Protease sensitivity of His₆-porin reconstituted into ergosterol containing liposomes. His₆-porin was solubilized in SDS and incorporated into liposome in the presence or absence of 0.02 mg/ml ergosterol by the freeze-thaw (FT) or insertion (INS) methods as described in Materials and Methods. In total 0.15 µg His₆-porin, 0.05 µg ergosterol and 0.01 mg lipid were digested for 30 minutes at room temperature in the absence (uncut) or presence (+) of 0.15 µg trypsin (T) or 0.15 µg chymotrypsin (C) and analyzed by urea-SDS-PAGE. Urea-SDS-PAGE gels were immunoblotted and probed with anti-NcPor-N antibodies. The BenchmarkTM protein ladder (Invitrogen) positions are indicated to the left of the panel. Position of wells (arrow), multimers of His₆-porin (filled circles), minor degradation products (open circles), and cross reacting trypsin (asterisk) are indicated on the blot.

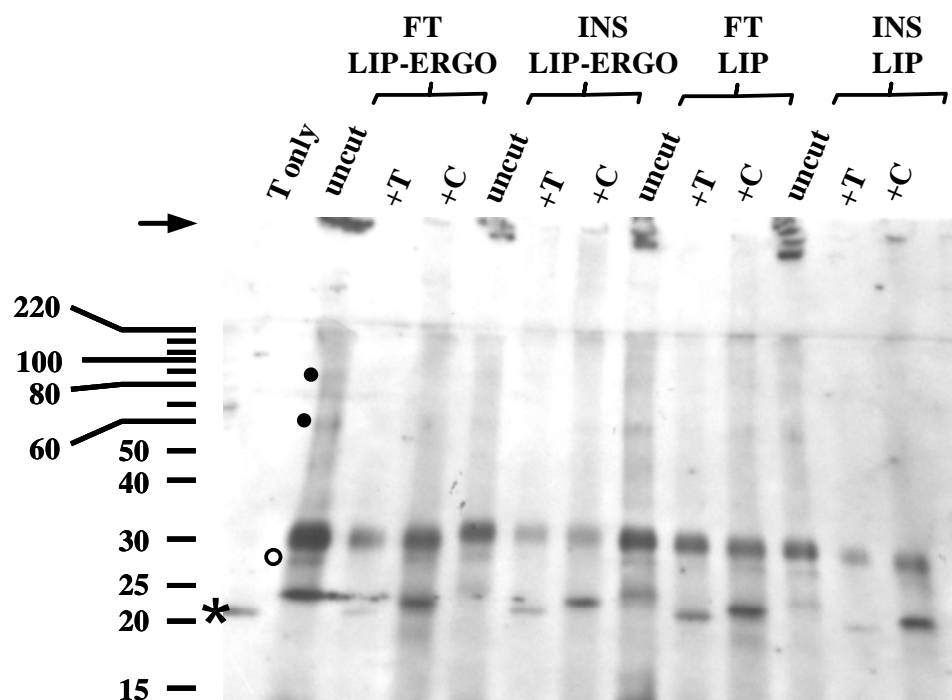
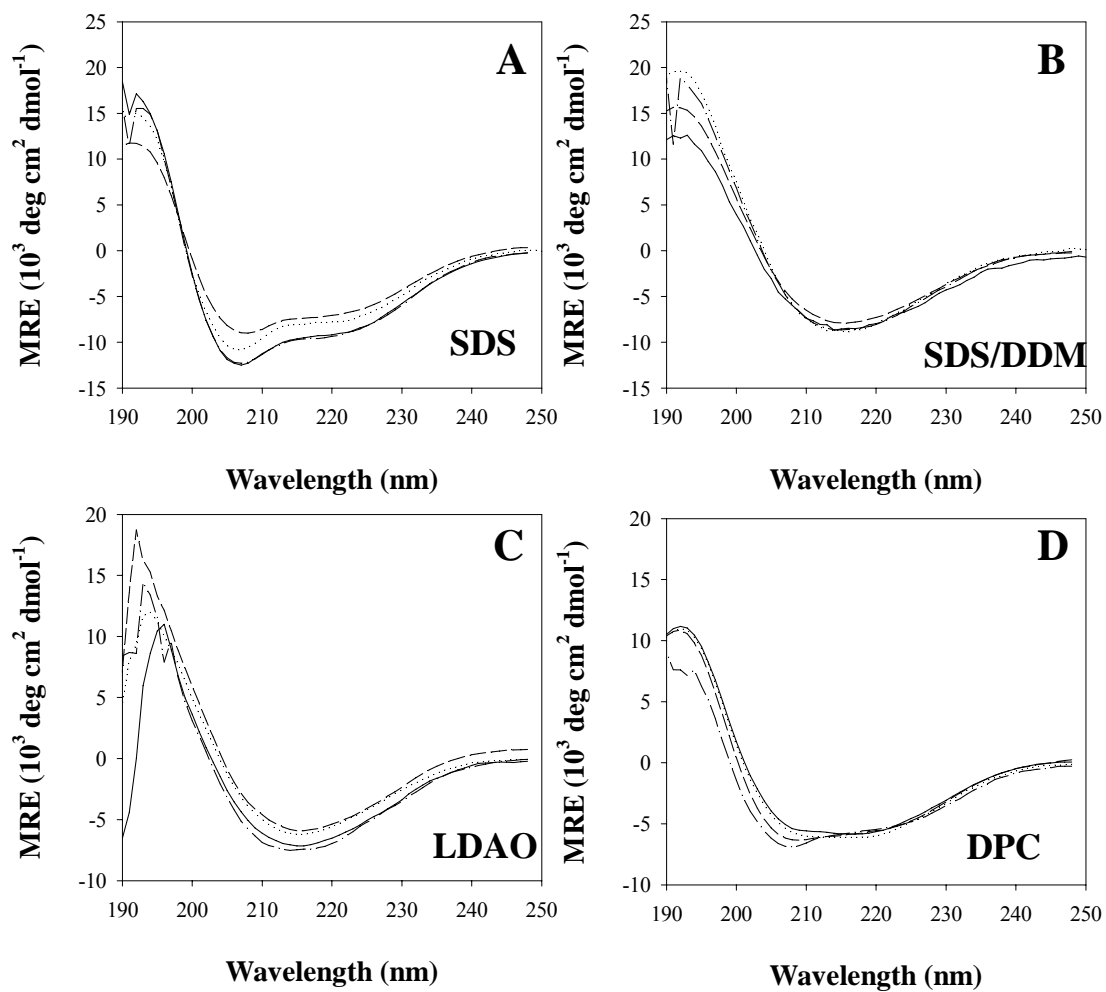


Table 4.2. Analysis of His₆-porin solubilized in detergents with sterol. Far- UV CD spectropolarimetry was performed on 1.5 μ M porin samples; the resulting spectra were deconvoluted with CONTINLL (Whitmore *et al.* 2004).

Detergent	Sterol	α -helix (%)	β -strand (%)	turn & unordered (%)
50 mM LDAO		16	32	52
50 mM LDAO	cholesterol	17	35	48
75 mM LDAO		19	39	42
75 mM LDAO	ergosterol	9	34	57
75 mM LDAO	cholestenone	16	30	54
10 mM DPC		16	30	54
10 mM DPC	cholesterol	16	28	56
20 mM DPC		20	29	51
20 mM DPC	ergosterol	18	30	52
20 mM DPC	cholestenone	16	31	53
3.5 mM SDS		24	20	56
3.5 mM SDS	ergosterol	23	23	54
3.5 mM SDS	cholesterol	31	17	52
3.5 mM SDS	cholestenone	29	23	48
3.5 mM SDS, 30 mM DDM		18	35	47
3.5 mM SDS, 30 mM DDM	ergosterol	16	34	50
3.5 mM SDS, 30 mM DDM	cholesterol	18	32	50
3.5 mM SDS, 30 mM DDM	cholestenone	17	35	48

Figure 4.3. Far-UV CD spectra of detergent-solubilized His₆-porin in the presence of sterols. In each panel CD spectra of 1.5 μ M His₆-porin (solid line) were collected in the presence of ergosterol (dashed line), cholesterol (dot line), and cholestenone (dotted line) and all CD spectra were collected at room temperature. **A)** 3.5 mM SDS. **B)** 3.5 mM SDS, 30 mM DDM. **C)** 50 mM LDAO (line dot lines) and 75 mM LDAO. **D)** 10 mM DPC (solid and line dot lines) and 20 mM DPC (dashed and dotted lines).



DPC, ergosterol, cholesterol, and cholestenone, were included in each system at a concentration of 0.02 mg/ml. The CD spectrum of His₆-porin solubilized in each detergent in the presence of each sterol is presented in Figure 4.3 and the results obtained by deconvolution with CONTINLL (Whitmore and Wallace 2004) are shown in Table 4.2. The CD spectrum of 3.5 mM SDS-solubilized His₆-porin exhibits the characteristic minimum at 208 nm and shoulder region centred at 220 nm typical for an α -helix rich protein. Far-UV CD spectra of His₆-porin solubilized in SDS containing each of the three sterols were not significantly different, but spectrum flattening was observed in samples containing ergosterol and cholestenone (Fig. 4.3A). Deconvolution of the SDS-His₆-porin-sterol CD spectra revealed that cholesterol and cholestenone containing samples had slight increases in α -helix content (29-31%) whereas samples with or without ergosterol had similar secondary structure (23-24%; Table 4.2).

The addition of 30 mM DDM to 3.5 mM SDS- solubilized His₆-porin results in a CD spectrum with a single sharp λ_{\min} of 216 nm, which was present in CD spectra collected in the presence of each sterol (Fig. 4.3B). Differences among the CD spectra of SDS/DDM His₆-porin with and without added sterols occur below 200 nm where increased ellipticity is observed. When spectra of sterol containing SDS/DDM-His₆-porin were deconvoluted, secondary structure content was largely unaltered in comparison to His₆-porin lacking sterol, although differences in the shapes of the spectra suggest perturbation of the system.

The CD spectrum of His₆-porin in 50 or 75 mM LDAO displays a strong minimum centred at 215-216 nm and is characteristic of proteins possessing high β -strand content. The CD spectra of LDAO-His₆-porin in each sterol have similar λ_{\min} to the spectrum of LDAO-His₆-porin in the absence of sterol, but at 195 nm, where spectra of His₆-porin in the presence

of sterol have increased ellipticity (Fig. 4.3C). Deconvolution showed that β -strand content is slightly reduced in ergosterol and cholestenone containing samples in comparison to those lacking sterol (Table 4.2). The greatest difference in secondary structure for LDAO-His₆-porin is the reduction of α -helix content of LDAO-ergosterol-His₆-porin (16% to 9 % α -helix), suggesting either contacts with the protein or slight variations in LDAO micelles encompassing the protein.

CD spectra of individual preparations of His₆-porin solubilized in 10 or 20 mM DPC varied from those with a flat broad λ_{\min} centred around 214-216 nm to spectra with a λ_{\min} of 208 nm characteristic of α -helix rich proteins; this phenomenon is discussed in (Chapter 2). The presence of sterols does not significantly alter the shapes of the CD spectra of DPC-His₆-porin (Fig. 4.3D, Table 4.2). Due to the variability in secondary structure content in DPC-His₆-porin alone, any sterol interactions with the protein may not be measurable in this detergent system.

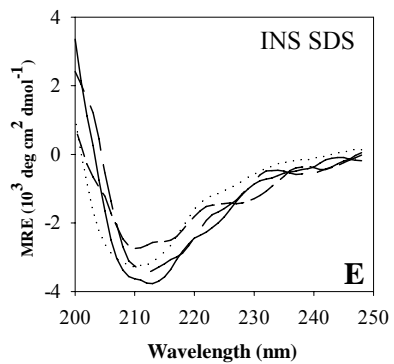
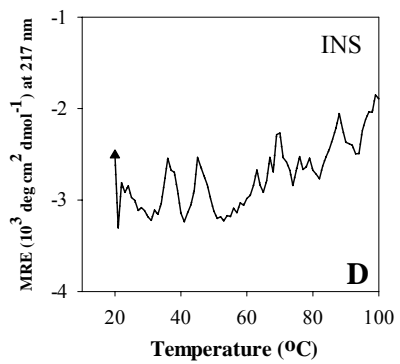
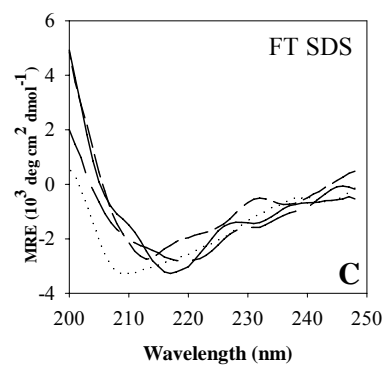
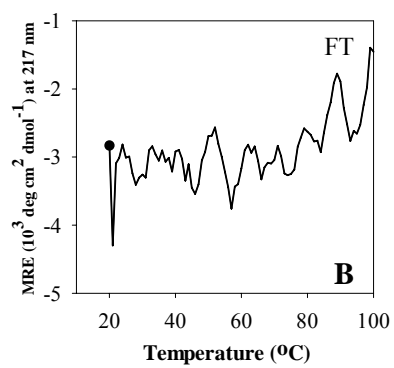
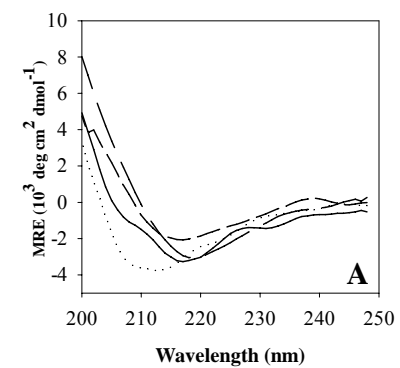
SDS-solubilized His₆-porin reconstituted into liposomes containing ergosterol (type L) by freeze-thaw and insertion methods were also examined by far UV CD; these liposomes demonstrated swelling activity at increased temperatures and maintained sufficient protein concentrations for spectroscopy. As in previous experiments (Chapter 2 and 3), light scattering by the liposomes prohibited collection at wavelengths below 200 nm and therefore deconvolution of CD spectra for secondary structure estimations.

A direct comparison of SDS-solubilized His₆-porin reconstituted into liposomes in the presence and absence of ergosterol demonstrates slightly elevated amounts of noise in the CD spectra of samples possessing sterol in the liposomes (Fig. 4.4A). This increase is likely contributed by the presence of the moderately absorbing ergosterol, which has sufficient π -

bonding to absorb in this region (Arthington-Skaggs *et al.* 1999). The CD spectra of both FT and INS His₆-porin-ergosterol-liposomes λ_{\min} (FT; 216 nm, INS; 212 nm) indicate slight differences in the secondary structure content in samples lacking sterols (Fig. 4.4A). Differences between λ_{\min} of FT proteoliposome spectra collected in the presence and absence of ergosterol are quite small (with ergosterol; 216 nm, no ergosterol; 217 nm) and the minima are sharp, characteristic of protein with high β -strand content, suggesting that ergosterol is not significantly altering the conformation of the protein in the membrane. However, differences are observed when comparing CD spectra of INS proteoliposomes in the presence or absence of ergosterol. INS proteoliposomes prepared with sterols resulted in a CD spectrum with λ_{\min} of 211 nm in contrast to that lacking sterols (λ_{\min} of 217 nm) (Fig. 4.4A). Based on shape of the CD spectrum and location of the λ_{\min} for INS SDS-His₆-porin-ergosterol-liposomes, His₆-porin is likely richer in α -helix than the β -strand rich conformation observed in INS SDS-His₆-porin-liposomes (Chapter 2).

Thermal unfolding experiments of FT SDS-His₆-porin-ergosterol-liposomes monitored mean residue ellipticity (MRE) at λ 217 nm, and showed a constant MRE centred around -3×10^3 until temperatures exceed 70°C, after which ellipticity steadily increased to -1.5×10^3 (Fig. 4.4B). Upon cooling to 20°C an MRE close to that at 20-30°C was observed. Examination of CD spectra (200-250 nm) collected at 10°C intervals demonstrates a progressive broadening and increase in λ_{\min} during heating from 20°C (λ_{\min} 216 nm) to 60°C (λ_{\min} 220 nm) (Fig. 4.4C). CD spectra collected from 60°C to 80°C have similar shapes with spectral broadening at λ_{\min} 220 nm indicating that the conformation of protein at these temperatures is not undergoing significant changes. At temperatures of 90°C to 100°C, λ_{\min} is 212 nm, suggesting increased α -helix content in His₆-porin. Upon cooling the samples to

Figure 4.4. Far-UV CD spectra of His₆-porin in ergosterol-liposomes. **A)** His₆-porin reconstituted into liposomes prepared with (solid and dotted lines) or without ergosterol (short and long dashed lines) by freeze-thawing (FT) (solid and long dashed lines) or by direct insertion (INS) (dotted and short dashed lines). Panels **B)** and **D)** correspond to the thermal denaturation profiles of FT (**B)** and INS (**D)** SDS-His₆-porin reconstituted into ergosterol-containing liposomes monitored at 217 nm from 20-100°C and 20°C cooled endpoint (circle and triangle). Panels **C)** and **E)** correspond to full length (200-250 nm) CD spectra of FT (**C)** and INS (**E)** SDS-His₆-porin reconstituted into ergosterol-liposomes at 20°C (solid line), 60°C (long dashed lines), 100°C (short dashed lines), and 100-20°C cooled (dotted lines).



20°C, the resulting CD spectrum has λ_{\min} of 209 nm, indicating retention of high α -helix content (Fig. 4.4C). These results are in stark contrast to thermal unfolding CD spectra collected for FT SDS-His₆-porin-liposomes which maintain a constant λ_{\min} of 217 nm during heating from 20-100°C and subsequent cooling to 20°C (Chapter 2). Clearly, the presence of ergosterol in the phospholipid membrane allows significant structural alterations of the protein at elevated temperatures; however, these altered His₆-porin conformations maintain some channel forming ability at 100°C (Fig. 4.1A).

The thermal denaturation profile of INS SDS-His₆-porin-ergosterol-liposomes show MRE values at 217 nm that remain unchanged at around -3×10^3 until temperatures reached 60°C (Fig. 4.4D). Heating the protein above 60°C resulted in a small gradual increase in MRE to -2×10^3 and a shift in λ_{\min} to 210 nm above 70°C, suggesting that the protein has higher α -helix content than at lower temperatures (Fig. 4.4E). Cooling these liposomes to 20°C resulted in an MRE value of -2.5, and a CD spectrum resembling that at 100°C, suggesting that the protein has adopted a conformation similar to one observed above 60°C. The heating profile of INS SDS-His₆-porin-ergosterol-liposomes differs dramatically from INS SDS-His₆-porin-liposomes where CD spectra demonstrate a progressive broadening of λ_{\min} at 217 nm that shifts to a λ_{\min} of 209 nm above 70°C (Chapter 2). Although INS proteoliposomes in the presence and absence of ergosterol have very different initial conformations, both INS proteoliposomes undergo thermally induced changes above 70°C, leading to spectra with λ_{\min} at 210 nm. Both INS SDS-His₆-porin-liposomes in the presence and absence of ergosterol are incapable of swelling

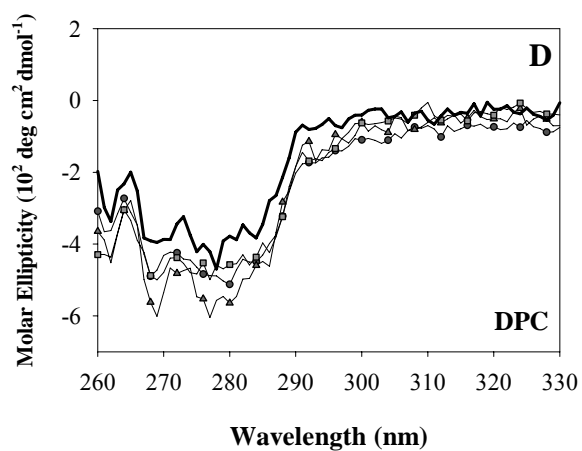
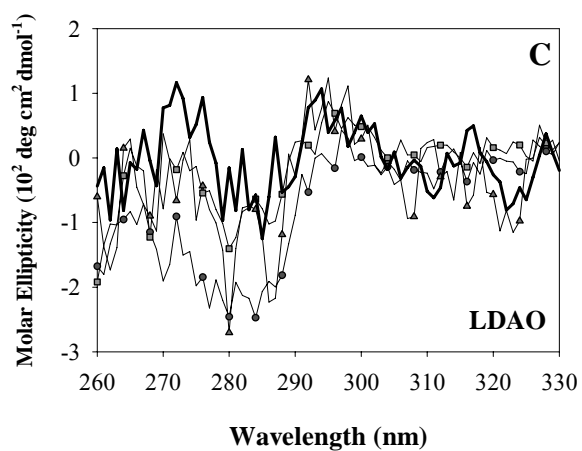
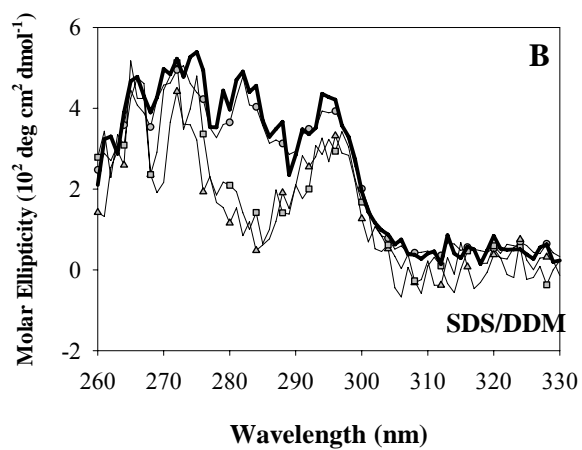
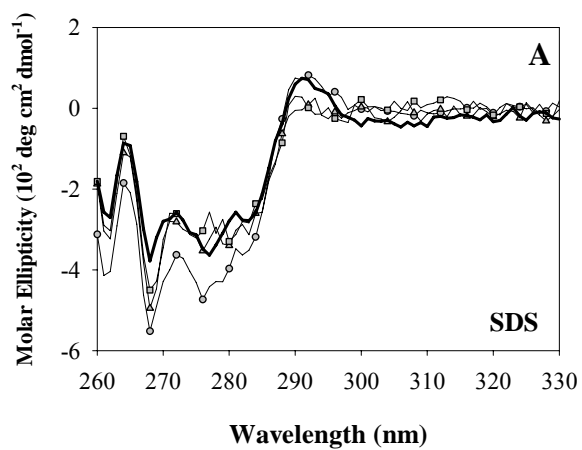
4.4.4 Near-UV circular dichroism spectropolarimetry of detergent-sterol-solubilized His₆-porin

Near-UV region (260-330 nm) CD spectropolarimetry was used to examine tertiary interactions in His₆-porin. In general, this region provides information on the tertiary arrangements of aromatic residues based on the absorption of tryptophan (270-280 nm) and tyrosine (265-270 nm) residues. Near-UV CD spectra of FT and INS SDS-His₆-porin-liposomes could be collected, but spectra of His₆-porin in sterol-containing liposomes showed no measurable ellipticity (data not shown). This may in part be due the absorption of ergosterol from 240-400 nm (Arthington-Skaggs *et al.* 1999) and light scattering by the liposomes, reducing the signal to noise ratio in spectra of His₆-porin in sterol-containing liposomes.

Increasing detergent concentrations five-fold (21 mM SDS, 21 mM SDS/180 mM DDM, 300 mM LDAO and 100 mM DPC) permitted the solubilization of high concentrations of sterols (0.1 mg/ml) and His₆-porin ($\geq 25 \mu\text{M}$) for near-UV CD analysis, while maintaining all components at the ratio used for far-UV CD analysis. In general, the addition of sterol to the solubilizing detergents used for His₆-porin resuspension did not result in dramatic changes in the near-UV CD spectra, but small to moderate changes could be observed in some detergent systems (Fig. 4.5).

The CD spectrum of His₆-porin solubilized in 21 mM SDS demonstrates a broad negative ellipticity spanning 265-285 nm, marked by smaller peaks, including one constant peak with λ_{min} of 268 nm. The addition of any sterol to the solubilizing detergent does not appear to significantly alter peak positions in the His₆-porin CD spectrum, but does increase intensity at λ_{min} 268 nm (Fig. 4.5A). Interestingly, this effect is strongest in the 265-

Figure 4.5. Near-UV CD spectra of detergent-solubilized His₆-porin in the presence of sterols. In each panel near-UV region (260-330 nm) CD spectra of 25-33 μ M His₆-porin (thick solid line) were collected in the presence of 0.1 mg/ml sterol, specifically: ergosterol (circles), cholesterol (triangles), and cholestenone (squares). All CD spectra were collected at room temperature. **A)** 21 mM SDS. **B)** 21 mM SDS, 180 mM DDM. **C)** 300 mM LDAO. **D)** 100 mM DPC.



285 region of negative ellipticity in the presence of ergosterol, suggesting that this sterol has some influence on the arrangements of Tyr and Trp residues in the protein.

The near-UV CD spectrum of His₆-porin solubilized in 21 mM SDS/180 mM DDM (Fig. 4.5B) has positive ellipticity at λ_{max} of 275 nm. Positive ellipticity has also been observed for His₆-porin reconstituted into liposomes and suggests that the protein conformation in SDS/DDM is close to that in liposomes (Chapters 2 and 3). The CD spectrum of His₆-porin in SDS/DDM changes very little in the presence of ergosterol. However, a major positive peak near 283 nm in His₆-porin with or without ergosterol is absent from the CD spectra of His₆-porin collected in the presence of cholesterol or cholestenone (Fig. 4.5B). Thus, the presence of the latter sterols appears to alter Trp residue arrangements within His₆-porin.

The CD spectrum of His₆-porin solubilized in 300 mM LDAO closely resembles the spectrum of His₆-porin in 8 M urea (Chapter 2); both near-UV CD spectra fluctuate around zero (Fig. 4.5C). Although LDAO promotes high β -strand content in His₆-porin, tertiary contacts involving aromatic residues are not present and suggest His₆-porin in LDAO is a β -strand rich “molten globule” (Surrey and Jahnig 1995, Kumar *et al.* 1995, Sivaraman *et al.* 1997, Matsuura *et al.* 2001). Of the sterols tested, only ergosterol appears to have some affect on His₆-porin conformation in LDAO, as evidenced by the slight increase in negative ellipticity resulting in a minimum near 280 nm (Fig. 4.5C).

The CD spectrum of His₆-porin solubilized in 100 mM DPC demonstrates broad negative ellipticity that spans 265-285 nm, similar to the CD spectrum of His₆-porin dissolved in 21 mM SDS. As seen for SDS-His₆-porin, the addition of any sterol to the solubilizing detergent does not appear to significantly alter peak positions in the His₆-porin

CD spectrum, but does result in a slight increase in intensity and suggests that each sterol has only slight influences on the arrangements of Tyr and Trp residues in the protein.

Overall, sterols appear to have more influence on the tertiary structure of His₆-porin, as measured by near-UV CD, when the protein has high β -strand content, as in SDS/DDM and LDAO. Ergosterol has less of an effect on His₆-porin structure in SDS/DDM than in SDS, DPC, or LDAO detergent systems.

4.4.5 Tryptophan fluorescence of His₆-porin in detergent-sterol and sterol-liposomes

Fluorescence spectrophotometry is a useful technique to probe the environments surrounding aromatic residues Trp and Tyr in His₆-porin. Due to high amounts of light scattering in sterol-containing solutions at low wavelengths (≤ 310 nm) Tyr fluorescence could not be reliably determined. However, Trp fluorescence could be examined following excitation at 280 or 296 nm in detergent-sterol and ergosterol-liposome systems. In most mitochondrial porin structural models, both Trp residues are located within β -strand spanning regions of the protein (reviewed by Bay and Court 2002, Runke *et al.* 2006), where hydrophobic interactions with the surrounding lipids as well as with adjacent β -strands are expected. In the current studies, there is the added complexity of possible protein-sterol interactions.

First, the effects of sterols on Trp environments in detergent-solubilized porin were examined. Emission spectra of His₆-porin solubilized in SDS or DPC in the presence of either cholesterol or cholestenone are similar and slightly blue-shifted λ_{max} (2-3 nm) from those of the corresponding samples lacking sterols, while the addition of ergosterol led to a larger blue shift (~ 6 nm) (Figs. 4.6A and 4.6B, Table 4.3). Cholesterol and cholestenone were associated with slightly decreased fluorescence intensity at λ_{max} (Int_{max}), while Int_{max} was unchanged in

Figure 4.6. Fluorescence analysis of His₆-porin in detergent-sterol systems. Fluorescence spectra were collected following excitation at 280 nm (and 296 nm) of 0.4 μ M His₆-porin in one of four detergents containing - 0.01-0.02 mg/ml sterol. In each panel (**A-D**) His₆-porin (solid) alone or in the presence of ergosterol (dashed lines), cholesterol (line-dot-lines), or cholestenone (dotted lines) is shown. **A)** 3.5 mM SDS. **B)** 10 mM DPC (dotted and line-dot-lines) and 20 mM DPC (solid and dashed lines) **C)** 50 mM LDAO. **D)** 3.5 mM SDS/ 30 mM DDM.

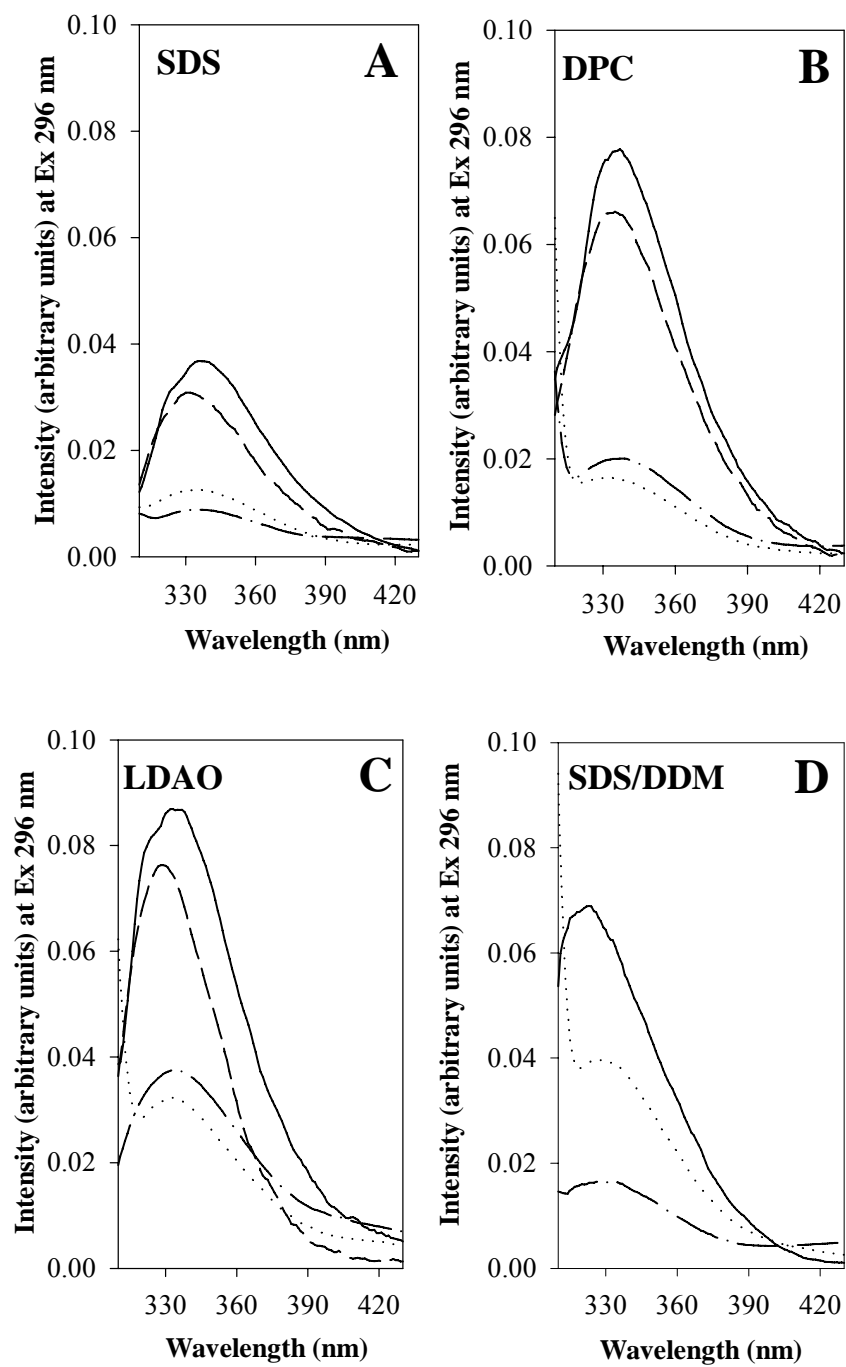


Table 4.3. Summary of normalized fluorescence emission maxima collected at excitation wavelength of 296 nm of His₆-porin and solubilized in various detergents in the presence or absence of sterol. Intensity values were corrected for differences in concentration. Note that the intensity of Trp fluorescence could not be determined in His₆-porin (nd).

Detergent/ Liposome	Sterol	Fluorescence Trp (Ex 296 nm)	
		λ_{max}	Intensity _{max}
3.5 mM SDS		336	0.04
	0.02 mg/ml ergosterol	327	0.03
	0.01 mg/ml cholesterol	334	0.02
	0.01 mg/ml cholestenone	334	0.01
3.5 mM SDS, 30 mM DDM		322	0.08
	0.02 mg/ml ergosterol	nd*	nd*
	0.01 mg/ml cholesterol	335	0.02
	0.01 mg/ml cholestenone	335	0.04
50 mM LDAO		333	0.09
	0.02 mg/ml ergosterol	328	0.08
	0.01 mg/ml cholesterol	335	0.04
	0.01 mg/ml cholestenone	335	0.03
20 mM DPC		337	0.08
	0.02 mg/ml ergosterol	335	0.07
10 mM DPC		339	0.08
	0.01 mg/ml cholesterol	334	0.02
	0.01 mg/ml cholestenone	333	0.02
FT 0.2 mg/ml liposomes		329	0.04
	0.02 μ g/ml ergosterol	330	0.03
INS 0.2 mg/ml liposomes		335	0.09
	0.02 μ g/ml ergosterol	328	0.03

* Scattering below 320 nm prohibited reliable data acquisition.

nd, not determined

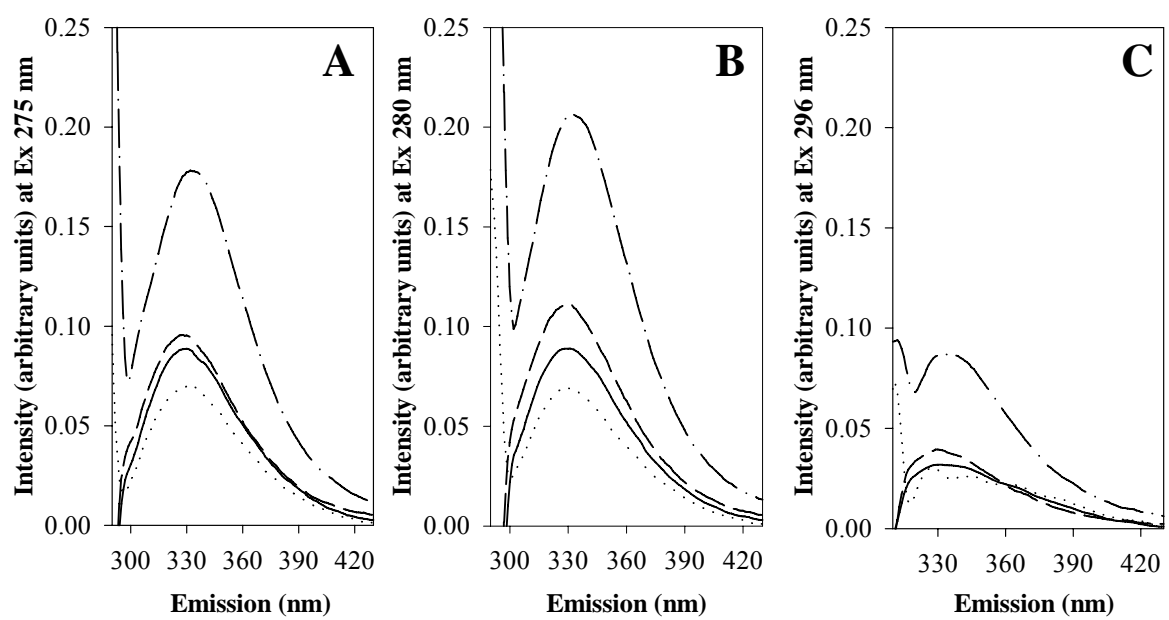
the presence of ergosterol. Thus, the two types of sterol promote different conformations of the protein; in the presence of the former two sterols one or both Trp residues may be placed close to quenching moieties in environments less hydrophobic than those formed in the presence of ergosterol.

The emission spectra of His₆-porin-LDAO and His₆-porin-SDS/DDM, in the presence of either cholesterol or cholestenone, following excitation at 296 nm have slightly (2 nm) or highly red shifted λ_{max} (13 nm), in comparison to those of the protein in each detergent alone (Figs. 4.6C and 4.6D, Table 4.3). Fluorescence intensity is also reduced, as expected if the Trp residues are located in a region of decreased hydrophobicity, perhaps in the vicinity of quenching moieties. The presence of ergosterol did not influence fluorescence properties of LDAO-His₆-porin. Light scattering was too intense to allow analysis of the effects of this sterol on SDS/DDM-His₆-porin.

Next, the effects of sterols on liposome-embedded His₆-porin were examined. Emission spectra were collected for FT SDS-His₆-porin-ergosterol-liposomes only, as this system is the most efficient at incorporating His₆-porin into liposomes, and ergosterol is the native sterol in fungal mitochondria. Similar trends were observed following excitation at 280 nm (data not shown) or 296 nm (Fig. 4.7A). In contrast to the detergent-based systems, ergosterol has little effect on λ_{max} and leads to only a slight reduction in Int_{max} of spectra of His₆-porin reconstituted into liposomes by the FT method (Fig. 4.7A and Table 4.3). This suggests that ergosterol has less influence on the Trp residue environment in the protein when SDS-His₆-porin is FT into ergosterol-liposomes.

In contrast, the presence of ergosterol in liposomes led to significant changes in the intensity of Trp fluorescence of His₆-porin treated by the INS method. Following excitation at

Figure 4.7. Fluorescence spectra of His₆-porin reconstituted into ergosterol-liposomes. Fluorescence spectra were collected following excitation (Ex) at 275 nm, 280 nm, and 296 nm of 0.1-0.2 μ M His₆-porin reconstituted into 0.2 mg/ml liposomes in the presence or absence of 0.02 μ g/ml ergosterol prepared by freeze-thawing (FT) or insertion (INS) methods. In each panel (**A-C**) FT proteoliposomes in the presence (solid line) or absence (dashed line) of ergosterol and INS proteoliposomes in the presence (dotted line) or absence (line-dot-line) of ergosterol are presented. **A)** Ex 275 nm. **B)** Ex 280 nm. **C)** Ex 296 nm.



280 nm, the λ_{max} of INS proteoliposomes with and without ergosterol remained similar (~329 nm) but Int_{max} was reduced to about $\frac{3}{8}$ of the intensity of INS SDS-His₆-porin-liposomes (Fig. 4.7B). The reduced fluorescence intensity of INS ergosterol-proteoliposomes suggests that the environment of the Trp residues is far more quenched than in liposomes lacking sterol and that these residues could be interacting with adjacent charged residues in the protein or associating with SDS detergent/ phospholipid head groups or the sterol. When taken together with the results of far- UV CD analysis, this may suggest that the protein is loosely associated with liposomes, where ergosterol encourages α -helix rich His₆-porin arrangements and Trp quenching in the liposomes.

4.5 Discussion

4.5.1 The influence of sterols on His₆-porin conformation in detergents

Each detergent system, SDS, SDS/DDM, LDAO, and DPC, examined in this study promotes a unique combination of secondary structure and arrangement of Trp and Tyr residues (Chapters 2 and 3). Although only His₆-porin in SDS/DDM has secondary structure and aromatic residue arrangements that are consistent with a folded β -barrel protein (Ohnishi and Kameyama 2001, Chapter 3), the other systems promoted protein arrangements compatible with incorporation into liposomes, making all of these detergents valuable tools to study the influence of sterols on the conformation of His₆-porin.

Previous examination of the influence of sterols on eukaryotic porin folding involved far-UV CD analysis of recombinant N-terminally His-tagged pea root plastid porin solubilized in Genapol-X080 (Popp *et al.* 1997). Neither of the plant sterols stigmasterol or β -sitosterol significantly altered secondary structure in detergent. The data presented herein

are similar: far-UV CD analysis of recombinant *N. crassa* mitochondrial porin (His₆-porin) in various detergent-sterol mixtures did not demonstrate any significant changes in the estimated protein secondary structure content. However, the use of other techniques, namely near-UV CD spectropolarimetry and fluorescence spectrophotometry revealed changes in the environments surrounding the aromatic residues within these systems and thereby indicating that sterols do have detergent-specific effects on the conformation of His₆-porin.

In SDS, fluorescence revealed that the Trp residues in His₆-porin are exposed to increasingly hydrophobic environments in the presence of sterols. Both cholesterol and cholestenone also led to quenching of Trp fluorescence, possibly due to promoting interactions between Trp and charged side-chains or detergent head groups, or directly quenching fluorescence. The largest difference between the near-UV CD spectra obtained in SDS in the presence and absence of these sterols, is the intensification of the peak near 268 nm, supporting a change in the Tyr environment(s). Ergosterol has a different influence on His₆-porin conformation in SDS, as evidenced by blue-shifted but unquenched Trp fluorescence, and increased intensity of Trp (276 nm), Tyr (268 nm) and Phe (263 nm) derived peaks in the near-UV spectrum. Therefore, all of the sterols examined in this study influence the folded arrangement of SDS-solubilized His₆-porin. These conformational changes promoted by the sterol may also influence channel formation based on previous black lipid bilayer (BLB) experiments of native mitochondrial porin isolated in SDS which only demonstrated channel forming ability in the presence of sterol (Popp *et al.* 1995). Therefore, these small structural changes in sterol-SDS-His₆-porin have some influence on protein conformation in SDS but are more significant for porin channel forming ability in BLB.

Sterols appear to have little influence on secondary structure arrangements or aromatic residue interactions within the protein in DPC (Figs. 4.3, 4.5, 4.6). The addition of sterol does lead to more hydrophobic environments surrounding Trp; significant quenching of fluorescence was not observed. Although both SDS and DPC promote α -helix rich conformations, these results suggest that the interactions between the sterols and the detergent-protein micelles are different in each case and that the overall conformation of His₆-porin in DPC is far less influenced by the addition of any native or non-native sterols than is the conformation in SDS. These observations also confirm previous reports that DPC promotes a His₆-porin conformation that is far less influenced by the addition of a secondary detergent (Chapter 3) or by increasing temperature (Chapter 2) than the SDS system. Taken together, these findings support a unique conformation of His₆-porin in DPC, that promotes much more hydrophobic Trp residue environments in the presence of a sterol; Trp residues are likely buried deeper within the acyl chain core of DPC micelles or reside closer to the sterol(s).

The near-UV spectra of LDAO-His₆-porin in the presence or absence of cholestenone or cholesterol were very similar to that of His₆-porin in 8 M urea (Chapter 2) indicating that these sterols do not promote tertiary contacts involving the aromatic residues of His₆-porin (Fig. 4.5C). Some quenching of Trp fluorescence is observed. In contrast, in the presence of ergosterol, the near-UV CD spectrum showed negative ellipticity similar to that in the spectra of SDS or DPC solubilized His₆-porin, and Trp fluorescence that was blue-shifted and moderately reduced in intensity. These observations suggest that this sterol promotes stable, albeit weak, interactions involving aromatic residues interactions. It is noteworthy that

LDAO promotes a β -rich structure, and only interacts with the native fungal sterol – ergosterol.

Previous BLB experiments involving LDAO-solubilized His-tagged yeast and *N. crassa* recombinant mitochondrial porins have demonstrated channel formation in the presence of ergosterol only (Koppel *et al.* 1998). However, it is uncertain if cholesterol and cholestenone would be capable of promoting LDAO-His₆-porin channel formation in BLB experiments. Channel formation by *D. discoideum*, *P. tetraurelia*, and rat water-soluble mitochondrial porins occurs in the presence of cholesterol, but each is enhanced when a native sterol was used (Popp *et al.* 1995). Therefore, it is very likely that both cholesterol and cholestenone could promote channel formation of LDAO-His₆-porin in BLB experiments but enhanced channel forming ability would require ergosterol.

The SDS/DDM system was of greatest interest because it promotes a conformation of His₆-porin most similar to that of the membrane inserted form of the protein (see Chapter 3). Very similar near-UV CD spectra were generated for SDS/DDM-His₆-porin in the presence and absence of ergosterol; unfortunately reliable Trp fluorescence could not be obtained for this system. In contrast, both cholesterol and cholestenone led to marked changes in the Trp-derived peaks in the near-UV spectrum of the protein, and blue-shifted Trp fluorescence of greatly reduced intensity was observed. Interestingly, these may represent non-native protein-sterol interactions, since these sterols are not found in *N. crassa*.

Therefore, sterols influence the conformation of His₆-porin in a detergent-dependent manner. Further interpretation of these results is precluded by the absence of information regarding the specific sites of sterol association with mitochondrial porins. Nonetheless, these

differences can be examined with respect to the ability of the protein to incorporate into liposomes, and the resulting stability of the membrane-associated forms.

4.5.2 His₆-porin reconstituted into liposomes in the presence of ergosterol

The freeze-thaw method reconstitutes native and recombinant mitochondrial porins into liposomes to generate osmotically responsive pores (for examples see Chapter 2, Shimizu *et al.* 1999 or Bathori *et al.* 1993) in the absence of sterols, a process that was first described for α -helical membrane proteins such as bacteriorhodopsin (Scotto and Zakim 1988). Given that native mitochondrial porin inserts into the sterol-containing outer membrane, we wanted to test the effects of sterol on His₆-porin incorporation into liposomes, with particular attention to the effects in different detergents. With the exception of type D LDAO-His₆-porin liposomes, a swelling response was observed in all FT detergent-His₆-porin-liposomes prepared in the presence of ergosterol, whether it was added to the detergent (type D) or to the SUV stock (type L) (Fig. 4.1). Generally, the osmotic response was of a lower magnitude, but much more rapid than that in sterol-free systems (Chapter 2 and see Fig. 4.1A). This may suggest that a relatively small number of very responsive pores occur within these ergosterol-containing liposomes or more likely, the incorporation of sterol into the liposomes may have reduced the capacity for swelling by promoting altered membrane organization (see below). Notably, the effects differed depending on whether the sterol was added to the detergent, or incorporated into the SUV stock. For LDAO and SDS, the response was of greater magnitude when the sterol was in the stock SUV; in fact, swelling was often not observed for LDAO-ergosterol solubilized His₆-porin. These observations fit with the lack of significant changes to LDAO-His₆-porin arrangement detected by the various spectroscopic methods. Although the addition of sterol to LDAO-solubilized protein does not

promote an insertion-competent state of His₆-porin, the sterol enhances either the channels' ability to incorporate into the membrane, or the state of the channel therein. In contrast, in SDS/DDM, the swelling response was greater if the sterol was added to the protein-detergent solution, which is intriguing given that the significant changes were not observed in the far and near UV CD spectra obtained in this system. It is conceivable that ergosterol stabilizes the tertiary contacts detected in SDS/DDM-His₆-porin – and perhaps these contacts survive dilution during proteoliposome formation, where the detergent concentrations are at or below the CMC.

Differences between type D and low ergosterol type L FT proteoliposome swelling profiles were observed after heat treatment at 65°C and 100°C; the associated structural changes were followed for the low ergosterol type L SDS system. As shown previously (Chapter 2), heating of both SDS- and SDS-ergosterol-proteoliposomes to 65°C does not alter the overall β -strand character of the CD spectra, but does reduce swelling significantly at 65°C (see Table 4.1). This general trend in reduced swelling at 65°C was also observed if ergosterol was present in the SDS-protein solution (Type D). In striking contrast, low ergosterol type L FT detergent-His₆-porin-liposomes retained swelling activity following heating to 65°C or 100°C. Above 70°C, far UV CD spectra of type L FT SDS-ergo-proteoliposomes has transitions from β -strand to α -helix character and upon cooling from 100°C, the CD spectrum resembles α -helix character unlike SDS-proteoliposomes which retain overall β -strand character from 70-100°C heating and cooling (Chapter 2). This suggests that the sterol in the membrane does not act effectively as a chaperone, but perhaps allows folding of at least a subpopulation of the protein into conformations that create osmotically responsive liposomes. Caution must be taken in interpreting the refolding data

however, as the CD spectra were collected over a total of 210 min of heating, while the samples for swelling were only heated for 10 min – it remains possible that irreversible changes to folding occurred during long-term heating.

Incorporation of sterol into liposomes reduced the osmotic responses of proteoliposomes formed with SDS-, DPC- and LDAO-solubilized porin. In contrast, the swelling activity of SDS/DDM-His₆-porin liposomes was increased in the presence of sterol. These observations may reflect the membrane rigidifying effects of sterols on lipid bilayers. Increasing the concentration of cholesterol has been shown to result in more densely packed, ordered phospholipid membranes, in comparison to the more fluid membranes at lower sterol concentrations (Kakorin *et al.* 2005). Comparative molecular dynamics modeling experiments performed for lipid bilayers containing cholesterol or ergosterol at 25 mol % of sterol indicated that ergosterol resulted in higher rigidification of phospholipid bilayers than cholesterol (Czub and Baginski 2006). In this study, 2 mol % sterol was used for low ergosterol type L and type D proteoliposomes; this concentration was sufficient for a large impact on osmotic responsiveness. The high ergosterol type L proteoliposomes (20 mol%) were closer to those used by Czub *et al.* 2006 and Kakorin *et al.* 2005. Hence, increased membrane rigidity in high ergosterol FT proteoliposomes may explain the enhanced loss of swelling after 100°C treatment of SDS- and DPC-His₆-porin-liposomes in the presence of high, but not low ergosterol concentrations. *In vivo* sterols occur within membranes at 30-50 mol % (Simons and Ikonen 2000), therefore the behaviour of high ergosterol FT proteoliposomes at high temperatures may have more relevance to porin channel activity *in vivo*.

Finally, addition of sterol to either the detergent-solubilized protein or the stock SUV does not encourage or facilitate direct insertion (INS) of His₆-porin into liposomes. Even at elevated temperatures of 30°C or 40°C, His₆-porin insertion into type D or L liposomes did not lead to proteoliposomes with swelling activity. However, different interactions with the liposomes were established, as higher α -helical content was demonstrated in His₆-porin following interaction with ergosterol-containing liposomes (Fig. 4.4). The α -helical nature of the protein was retained during heating to 100°C, indicating that increased temperature did not drive insertion into the membrane.

In DPC, LDAO and SDS/DDM systems, swelling of type D proteoliposomes was similar to that in the absence of sterols (Table 4.1). One possible explanation for this observation may be found in studies of detergent-solubilized sterol incorporation into lipid vesicles (Proulx *et al.* 1984). These experiments have primarily focused on the use of bile salts to deliver sterols to the necessary membranes. Both ionic and non-ionic detergents have demonstrated a limited ability to incorporate sterols into phospholipid containing membranes by partially disruptive mechanisms (Proulx *et al.* 1984). This suggests that sterols added to the solubilizing detergent can incorporate sterol into phospholipid membranes, but that this process results in very low overall sterol concentrations within vesicles. Based on these experiments, it is likely that type D proteoliposomes contained very little sterol, and were therefore less rigid than low ergosterol type L proteoliposomes.

The lack of insertion into liposomes is in contrast to the direct insertion of OmpA into liposomes at 30°C (Surrey and Jahnig 1995), and the insertion of α -helical proteins such as bacteriorhodopsin and UDP glucuronosyltransferase into sterol-containing liposomes in the absence of freeze-thaw treatment (Scotto and Zakim 1988). The most likely explanations

involve the energetic requirements for mitochondrial porin insertion into artificial membranes and the membrane curvature of the target membranes. In black lipid bilayer experiments recombinant and native mitochondrial porin insertion occurs only at low applied voltages in the presence of sterol. Under these conditions, the actual mechanism of initial porin insertion into the membrane is unknown, but likely involves a specific conformation of porin inserting into the artificial membrane at a site where the energy barrier of insertion can be overcome under transmembrane potential (Zizi *et al.* 1995, Xu and Colombini 1996, Xu and Colombini 1997; Li and Colombini 2002). For mitochondrial porins, these initial porin insertion sites may be focused in or around sterols (Popp *et al.* 1995, Popp *et al.* 1997), as has been suggested for other β -barrel forming integral membrane proteins such as members of the cholesterol binding pore forming toxin (CBT) family (reviewed by Gilbert 2002) and the α -helix rich integral membrane proteins (Scotto and Zakim 1988). However, as is the case for CBT family proteins, porin insertion into artificial membranes can occur in the absence of sterol (Popp *et al.* 1995).

The second major difference between the SUV experiments described herein and the planar bilayer studies is the curvature of the respective membranes. Planar artificial membranes during black lipid bilayer experiments are in stark contrast to the highly curved lipid bilayers of SUVs and LUVs. Membrane curvature and thickness as well as membrane elasticity influence the insertion of OmpA into LUVs and SUVs and the kinetics of the process (Kleinschmidt and Tamm 2002, Pocanschi *et al.* 2006, Marsh *et al.* 2006). High insertion rates of OmpA were observed in liposomes with thicker membranes (C₁₄-C₁₈ chains) and high membrane curvature (SUVs), although insertion into C₁₂ LUVs was also achieved (Kleinschmidt and Tamm 2002). The addition of sterols, such as cholesterol or

ergosterol, to phosphatidyl choline bilayer membranes alone also increases membrane rigidity, resulting in thicker and more densely packed phospholipids (Kakorin *et al.* 2005, Czub and Baginski 2006). In our experiments, His₆-porin incubated with SUVs prepared with phosphatidyl choline with C₁₂ acyl chains in the presence or absence of ergosterol was incapable of producing pores responsive to sucrose (Chapters 2 and 3). Therefore, ergosterol alone cannot promote His₆-porin insertion directly into liposomes and conversely, may hinder His₆-porin insertion into liposomes due to the membrane rigidifying effects on the ergosterol-containing membranes.

The relevance of these discussions toward understanding the *in vivo* assembly of mitochondrial porin is complicated by the uncertainty regarding the presence of a transmembrane potential across the mitochondrial outer membrane (Lemeshko and Lemeshko 2000, Lemeshko and Lemeshko 2004, Lemeshko and Lemeshko 2004) and by the fact that native pathway for insertion of porin into the mitochondrial outer membrane involves two transmembrane complexes, the translocase of the mitochondrial outer membrane (TOM), and the topogenesis of outer membrane β -barrel protein (TOB) complex, as well as soluble intermembrane space components (reviewed in Paschen *et al.* 2005). It has been argued that the voltage applied in black lipid bilayer studies represents the transmembrane potential that would be present across the mitochondrial outer membrane *in vivo* (as reviewed by Benz 1994, Mannella 1998), Lemeshko and Lemeshko 2004; Lemeshko and Lemeshko 2004). *In vivo*, the energetic constraints are effected by protein-protein interactions, as well as those between protein and lipid/sterol.

Clearly, sterols have some influence on His₆-porin conformations both in detergent and in artificial membranes. In detergents, sterols have a greater influence on tertiary

arrangements of aromatic residues, primarily Trp, than on the secondary structure of His₆-porin. Their presence is not sufficient for insertion into lipids, suggesting that future studies of the assembly of porin into mitochondrial membranes should focus on *in organello* systems.

5.1 Conclusions

In summary, ten major conclusions can be drawn from the experiments described in this thesis and they are as follows:

- i. Single detergent systems do not fold His₆-porin into a β -barrel structure reminiscent of bacterial porins.
- ii. His₆-porin solubilized in single detergents produces osmotically responsive channels when reconstituted into liposomes by freeze-thaw
- iii. Reconstitution of detergent-solubilized His₆-porin into liposomes by freeze-thaw results in tertiary arrangements similar to those observed for bacterial porins, supporting a β -barrel conformation.
- iv. His₆-porin solubilized in detergents or in urea cannot insert into pre-formed phosphatidyl choline based liposomes as described for OmpA (Surrey and Jahnig 1995).
- v. Mixed detergent systems, in particular SDS/DDM, can solubilize high concentrations of His₆-porin and promote secondary and tertiary structure arrangements similar to those in liposomes.
- vi. SDS/DDM-solubilized His₆-porin can be reconstituted into liposomes to form osmotically responsive channels.
- vii. His₆-porin solubilized in both mixed and single detergent systems that promote high β -strand content share similar protease resistance profiles with native mitochondrial porin.

- viii. Porin in proteoliposomes prepared by freeze-thaw, insertion or sonication all possess some protease resistance, but spectroscopic analysis indicates that each of these protease-resistant forms has a unique structural arrangement
- ix. The presence of sterol in detergents does not drastically alter the secondary structure content of His₆-porin, but has some minor effects on tertiary arrangements.
- x. Sterol-containing FT proteoliposomes possess reduced swelling activity relative to sterol-free systems, indicating that sterols did not enhance pore forming activity.

In summary these studies determined that:

- i) The folded state of His₆-porin in several single detergent systems was not a β -barrel conformation based their tertiary interactions (Fig. 5.1A-C).
- ii) The mixed detergent system SDS/ DDM at a 1:9 ratio was capable of promoting a β -rich folded state of His₆-porin with similar tertiary arrangements as His₆-porin reconstituted into liposomes (Fig. 5.1D-G).
- iii) Sterols alter tertiary interactions within His₆-porin in both detergent and lipid-based systems and do not promote direct insertion of the protein into liposomes (Fig. 5.1H).

Furthermore, these studies were essential to further the current understanding of mitochondrial porin structure *in vitro* by examining porin arrangements in a variety of membrane mimetic systems. Although the spectroscopic characterization of His₆-porin is not itself novel, the focus on porin tertiary arrangement by a combination of spectroscopic techniques has permitted a much more detailed examination of the folded states of porin that extends beyond existing secondary structure analysis. In addition, a large set of aromatic

amino acid compounds were examined in both single and mixed detergent systems by UV absorbance spectroscopy and fluorescence spectrophotometry and will serve as an extremely useful reference set for future *in vitro* spectroscopic analysis of porin, as well as other membrane proteins.

Therefore, these studies represent the first thorough characterization of mitochondrial porin folding states in detergents and in artificial membranes. These experiments on detergent solubilized His₆-porin indicate that only particular mixed detergent systems enable denatured porin to re-fold into a tertiary conformation similar to porin within artificial membranes. They also revealed that sterols are not essential for promoting porin channel formation in liposomes, but do alter some tertiary interactions in detergent-solubilized protein. The major achievement of this work is the first identification of a system capable of solubilizing high concentrations of well folded protein essential for the development of a high resolution structure.

5.2 Future Directions

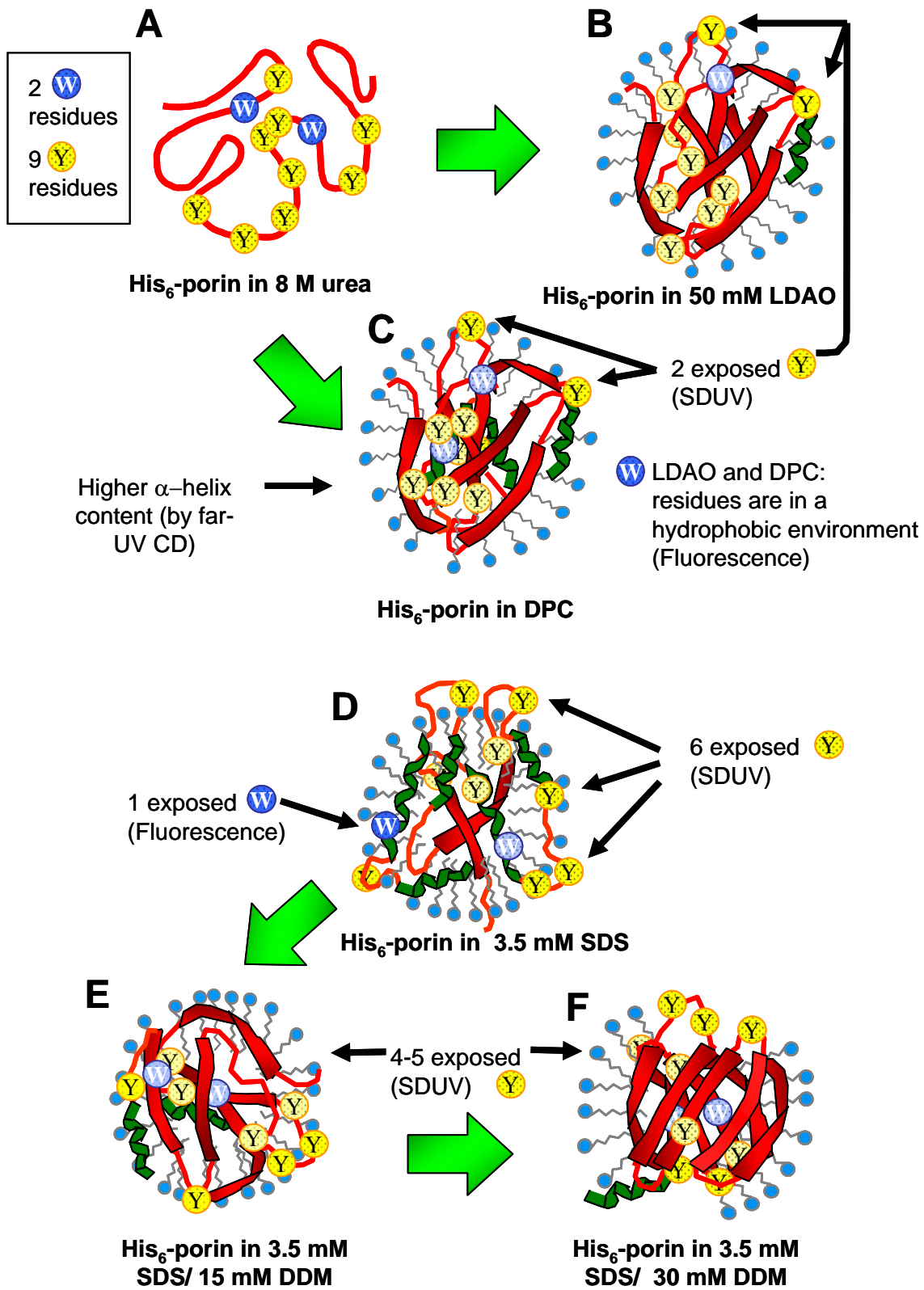
Logically, the next step toward the *in vitro* characterization of mitochondrial porin structure would be to further analyze the structure of His₆-porin in the SDS/DDM system. Examination of His₆-porin structure by transverse relaxation optimized spectroscopy (TROSY) NMR, used successfully to determine the structural arrangements of other bacterial porins (Arora *et al.* 2001, Fernández *et al.* 2001, Fernández *et al.* 2004), could enable the acquisition of a high resolution porin structural data essential for refining transmembrane models. This detergent system may also serve as a useful starting point for crystallization trials, with the hopes of obtaining crystals of sufficient quality for resolution the conformation of porin by X-ray diffraction.

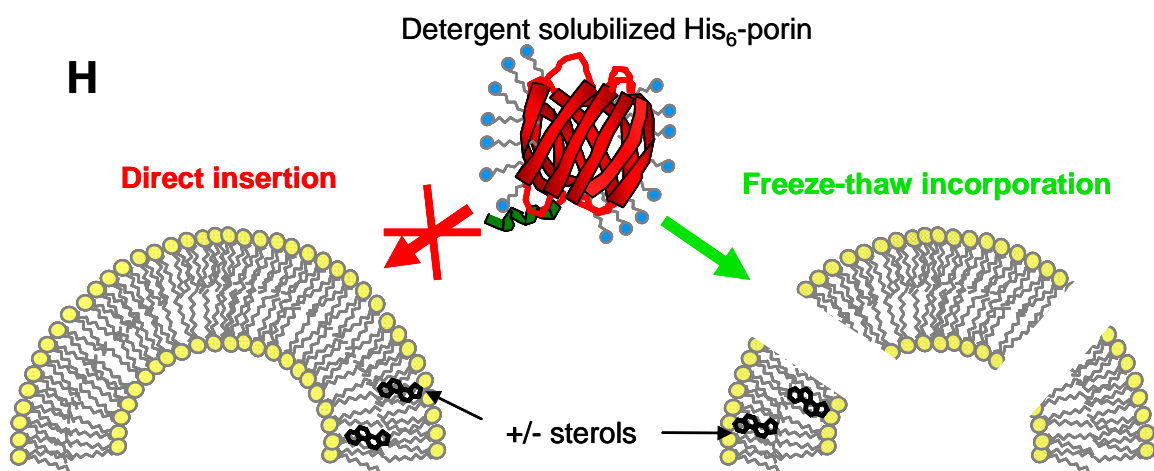
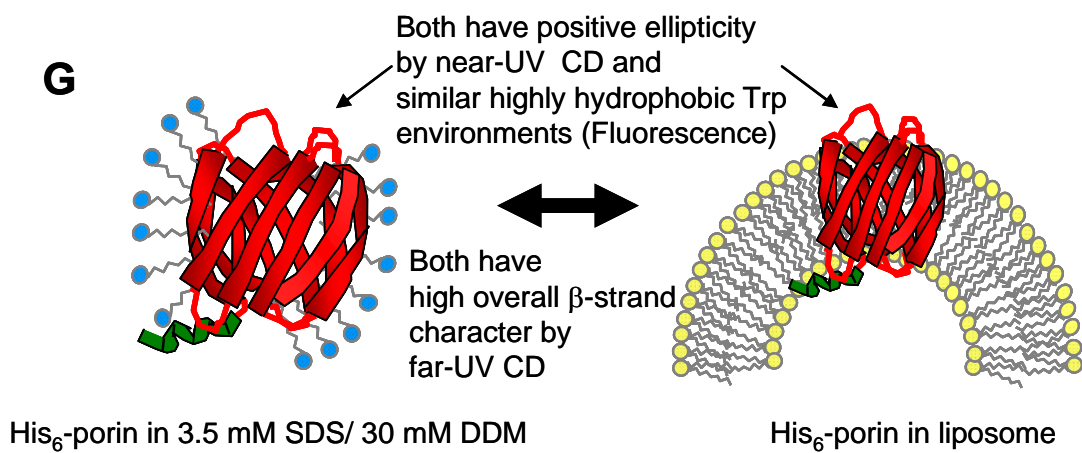
Future experiments regarding the arrangement of porin across the outer membrane, and its oligomer state could involve fluorescently labelled or green fluorescent protein (GFP) tagged mitochondrial porin both *in vivo* and *in vitro*. A technique referred to as fluorescence resonance energy transfer (FRET) used previously by (Zalk *et al.* 2005) to examine VDAC oligomerization *in vitro*, would be useful for these studies. For example, FRET could be used to determine the orientation of porin inserted within artificial membranes, to identify the location of the N-terminus relative to the barrel or to the membrane (using fluorescently labelled lipids), and to resolve the oligomeric status of the channel in both the outer membrane and in artificial membranes.

These studies have only begun to explore *in vitro* the folding and insertion of mitochondrial porins. Based on the experiments described herein, the folding of mitochondrial porins may differ from the folding and insertion pathway of bacterial OmpA (refer to section 1.8 and reviews by Kleinschmidt 2003, Tamm *et al.* 2004, Kleinschmidt 2006). To expand His₆-porin-liposome studies, time-resolved fluorescence quenching (TDFQ) techniques developed by L. Tamm and J. Kleinschmidt may be useful. Also combining TDFQ experiments with the techniques used to examine synthetic peptide insertion into liposomes as described in (Thundimadathil *et al.* 2005, Thundimadathil *et al.* 2006, Thundimadathil *et al.* 2006, Thundimadathil *et al.* 2005) could be used to study porin insertion and possibly develop a model for the folding mechanism of mitochondrial porin.

In the end, only a three-dimensional structure will set the stage for directed *in vitro* and *in vivo* studies into the mechanism of VDAC gating and into its interactions with proteins in the outer membrane, cytosol, and intermembrane space.

Figure 5.1 Cartoon diagram summarizing the various conformational states of His₆-porin in detergents and liposomes. In panels A to H, detergent solubilized His₆-porin structure represented by green α -helices and red rectangular β -strand secondary ribbon structures that are separated by red interconnecting lines (loops and β -turns) and are shown within a detergent micelle represented by a circular arrangement of blue filled circles (polar head group) attached to a zig zagging line (hydrocarbon tail). Aromatic amino acids Trp (a blue filled circle labelled with a white “W”) and Tyr (a yellow filled circle labelled with a black “Y”) are indicated on the His₆-porin ribbon diagram that suggests a the possible aromatic tertiary arrangement within the protein in the indicated detergent. The phospholipid bilayers of a liposome are represented by yellow filled circles (polar head group) attached to two zig-zagged lines (hydrocarbon tails) arranged in a half circle on panels G and H. Sterols in panel H are indicated as black 4 hexameric rings within the phospholipid bilayer. Denatured His₆-porin (red line) in 8 M urea is shown on panel A. In panels B and C, the conformation of His₆-porin in single detergent systems LDAO (B) and DPC (C) is indicated. Panels D to F, represent the conformational changes to SDS solubilized His₆-porin (D) upon addition of DDM to 5 DDM: 1 SDS molar ratio (E) and to a 9 DDM: 1 SDS molar ratio (F). The cartoon diagram in panel G compares His₆-porin conformation in the mixed 1 SDS: 9 DDM detergent system to the conformation of His₆-porin reconstituted into liposomes. In panel H, the ability of all detergent solubilized His₆-porin preparations to form osmotically responsive pores within liposomes by direct insertion or freeze-thaw is summarized. A crossed red arrow indicates a lack of pore formation while an uncrossed green arrow represents osmotic swelling activity of the proteoliposome.





6. APPENDIX Protein and gene structures of mitochondrial porins

Some of the material presented in this appendix has been recently submitted to BioMed Central Evolutionary Biology. My major contributions are presented as Sections 6.1 to 6.3, Table 6.1, and Figures 6.2 and 6.3 that were taken, with permission from the coauthors, from the manuscript: The Evolutionary History of Mitochondrial Porins, by Young, M. J., Bay, D. C., Hausner, G. and D. A. Court.

6.1 Introduction

The understanding of mitochondrial porin function has been complicated over the last ten years by the identification of multiple porin isoforms in many cell types. The first porin isoforms isolated were extracted from potato mitochondria (POM34 and POM36), and both formed pores in black lipid bilayers (Heins *et al.* 1994). In *Saccharomyces*, a genetic screen revealed a second isoform that, in high copy number, complemented a strain in which the known VDAC gene, *POR1* was disrupted (Blachly-Dyson *et al.* 1997). Since then, advances in molecular techniques, and the accumulation of large amounts of sequence data from genome sequence projects and expressed sequence tag (EST) libraries, have led to an abundance of information regarding porin isoforms (see Table 6.1 and references therein). The number of porin variants can range from a single isoform in fungi such as *Neurospora*, to five potential isoforms in *Lotus japonicus* (Wandrey *et al.* 2004). In some cases, as in *L. japonicus*, gene sequences obtained from a cDNA library are the only evidence of the presence of isoforms, but these sequences could also represent different alleles at the same locus. Generally, the genes encoding porin isoforms are located on different chromosomes (for example, in mice Sampson *et al.* 1997; see Fig. 6.2), with the exception of *Drosophila* spp. where they are arranged in tandem repeats (Graham and Craigen 2005).

Unfortunately, there are only a few cases where electrophysiological analyses have been performed for the various porin isoforms (for more detailed explanations of electrophysiological analyses refer to Chapter 1). For example, in BLB experiments in addition to complementation experiments using the yeast *ΔPOR1* strain (Table 6.1), revealed that organisms, such as *Drosophila melanogaster*, express at least one porin isoform with the characteristics of the originally described VDAC (Blachly-Dyson *et al.* 1997). This functional conservation is even more striking given the relatively low levels of primary sequence conservation (Fig. 6.1). In contrast, some porin variants were not capable of forming characteristic channels. This may be due to specialization of porin function for developmental regulation or for tissue-specific differential expression which has been suggested for human (Rahmani *et al.* 1998), mouse (Buettner *et al.* 2000) and plant (Elkeles *et al.* 1995, Al Bitar *et al.* 2002, Al Bitar *et al.* 2003) porin isoforms. Further evidence that supports isoform specialization comes from cell lines and knock-out mice lacking porin isoforms singly or in combination (Xu *et al.* 1999). For mammals in particular, VDAC1 has been reported to have NADH-ferricyanide activity within both the plasma membrane and the outer mitochondrial membrane (Baker *et al.* 2004) and VDAC2 has demonstrated pro-apoptotic BAK protein inactivation (Cheng *et al.* 2003). VDAC3 has a variety of spliceoforms that are expressed within specific tissues (Anflous *et al.* 1998, Sampson *et al.* 1998, Decker and Craigen 2000) and in mice the loss of VDAC3 is associated with infertility and sperm immotility (Sampson *et al.* 2001).

Table 6.1. Characteristics of mitochondrial porin isoforms.

Organism	Porin isoform	Pore size (nS) ^{a,b}	Ion selectivity ^c	Gating	Complements <i>Δpor1</i> yeast	Reference
<i>Saccharomyces cerevisiae</i>	Por1p or VDAC1 (NP_014343)	4.1	anion	yes	n/a ^h	Ryerse <i>et al.</i> 1997; Ludwig <i>et al.</i> 1988
	Por2p or YVDAC2 (NP_012152)	none	n/d	n/d	yes – at high copy	Blachly-Dyson <i>et al.</i> 1997
	DVDAC or porin (AAL47980.1)	4.1 ^d 4.5 ^e	anion ^{d,e}	yes ^{d,e}	yes	Komarov <i>et al.</i> 2004
<i>Drosophila melanogaster</i>	CG17137 or Porin2-PA (NP_609462)	(variable) 0.5-8 ^d 4.5 ^e	variable ^d	variable ^d	yes	Komarov <i>et al.</i> 2004 ^d , Aiello <i>et al.</i> 2004 ^e
	CG17140 (AAF53019)	1.38	anion	required 110 mV ^f	no	Komarov <i>et al.</i> 2004
	CG17139 (NP_609462)	none	n/d ^g	n/d	no	Komarov <i>et al.</i> 2004
	VDAC1 (Q60932)	4.3	anion	yes	yes	Xu <i>et al.</i> 1999
	VDAC2 (NP_03582)	3.8	anion	yes	yes	Xu <i>et al.</i> 1999
<i>Mus musculus</i>	VDAC3 (NP_35826)	highly variable	n/d	n/d	partial	Xu <i>et al.</i> 1999
	VDAC1 (NP_003365)	4.1	anion	yes	yes ⁱ	Blachly-Dyson <i>et al.</i> 1993
	VDAC2 (NP_003366)	4	anion	yes	yes	Blachly-Dyson <i>et al.</i> 1993
<i>Homo sapiens</i>	VDAC3 (NP_005653)	n/d	n/d	n/d	n/d	Blachly-Dyson <i>et al.</i> 1993
	VDAC1 (P46274)	3.8 ^d - 4.1	anion	yes	yes	Elkeles <i>et al.</i> 1997 or Blumenthal <i>et al.</i> 1993
	VDAC2 (S59546)	4.0 ^d	anion	yes	yes	Elkeles <i>et al.</i> 1997
<i>Triticum aestivum</i>	VDAC3 (S59547)	4.0 ^d	anion	yes	partial	Elkeles <i>et al.</i> 1997
	VDAC1.1 (AAQ87019)	n/d	n/d	n/d	yes	Wandrey <i>et al.</i> 2004
	VDAC1.2 (AAQ87020)	n/d	n/d	n/d	yes	Wandrey <i>et al.</i> 2004
<i>Lotus japonicus</i>	VDAC2.1 (AAQ87022)	n/d	n/d	n/d	yes	Wandrey <i>et al.</i> 2004
	VDAC3.1 (AAQ87023)	n/d	n/d	n/d	yes	Wandrey <i>et al.</i> 2004
	VDAC1.3 (AAQ87021)	n/d	n/d	n/d	no	Wandrey <i>et al.</i> 2004

see footnotes on following page

Table 6.1, footnotes

^a unless otherwise stated, prepared from mitochondrial membranes

^b in 1 M KCl or 1 M NaCl

^c pAnion/pCation = 1.5-1.8

^d isolated following heterologous expression in *Saccharomyces*

^e recombinant *D. melanogaster* VDAC2, expressed in *E. coli* and refolded in 1% Genapol X-080 in the presence of 0.5% (w/v) cholesterol

^f the midpoint for gating is usually around 50 mV

^g n/d, not determined

^h n/a, not applicable

ⁱ Complementation was performed with chimeric constructs in which the HVDAC1 and HVDAC2 genes were fused to the 11th and 22nd codons, respectively, of the yeast *POR1* gene (Blachly-Dyson *et al.* 1993).

The purpose of this appendix is to briefly highlight some of my work on the structural similarities and dissimilarities of mitochondrial porins and their genes, from different organisms as well as within families of isoforms. To accomplish this, mitochondrial porin protein sequences retrieved primarily from National Cell Biology Institute (NCBI) GenBank and The Institute for Genomic Research (TIGR), were aligned using the web server PRALINE. From these alignments, conserved residues and porin motif distribution within mitochondrial porins from fungi, plants, and animals were identified. These alignments also permitted potential TM β -strand comparisons using the prediction algorithm SSPRO available from PRALINE. Finally, the genetic organization of mitochondrial porins was also examined using genetic data collected from the NCBI genome map viewer. To determine if porin secondary structure is conserved in parallel to gene organization, the gene structures of representatives, including isoforms, from the animals, plants and fungi have been compared.

6.2. Materials and Methods

6.2.1 Database searches for porin protein and gene sequences

A variety of databases were searched in order to obtain VDAC sequences. GenBank was searched via blastp and tblastx against previously published VDAC sequences from related organisms. Porin sequences were also extracted from the genome sites that included: Stramenopiles: [*Phytophthora* sp., *Thalassiosira pseudonana* (Diatom)]: http://genome.jgi-psf.org/euk_curl.html; this site also provided access to the following genomes *Fugo*, *Chlamydomonas*, *Ciona*, *Populus*; and for fungi: <http://www.fgsc.net/outlink.html>; <http://genome.jgi-psf.org/whiterot1/whiterot1.home.html> (*Phanerochaete chrysosporium*); <http://mips.gsf.de/projects/fungi>; <http://www.broad.mit.edu/annotation/fungi/fgi/>

Additional fungal, plants, protozoan, animals genomes were accessed via the TIGR sites: <http://www.tigr.org/db.shtml> and <http://www.tigr.org/plantProjects.shtml>. Overall, over 280 potential/putative VDAC homologs were recovered from various databases; however, the final data set comprised a total of 244 sequences.

Additionally, gene sequences used to prepare Fig. 6.3 were collected from the NCBI genome map viewer web server [<http://www.ncbi.nlm.nih.gov/mapview/>]. VDAC sequences were retrieved based on gene annotation and/or GenBank accession numbers obtained from the initial protein sequence blastp searches.

6.2.2. PRALINE Alignment of porin sequences

The retrieved mitochondrial porin sequences were aligned with the online PRALINE multiple sequence alignment program [<http://ibivu.cs.vu.nl/programs/pralinewww>, (Simossis and Heringa 2003, Simossis and Heringa 2005)] and this program was utilized for its secondary structure prediction capabilities (Heringa 2000, Heringa 2002, Simossis and Heringa 2005). This multiple sequence alignment program was chosen based on its ability perform global progressive alignments, optimal for proteins with high to medium sequence similarity, coupled with a choice of seven different secondary structure prediction methods.

Predictions were performed using Version 2 of SSPRO (Pollastri *et al.* 2002) following multiple alignment. Similar results (data not shown) were obtained with YASPIN (Lin *et al.* 2005); some predicted β -strands were one or two residues longer in the YASPIN predictions, but otherwise their locations were the same. SSPRO predicts protein secondary structure in three structural classes (α -helix, β -strand and unordered/ turns) using a bidirectional recurrent neural network (Pollastri *et al.* 2002) where as YASPIN predicts secondary structure into 7 structural elements using hidden neural networks. Based on

analysis by EVA [<http://cubic.bioc.columbia.edu/eva/>], the SSPRO algorithm results in a lower level of “confused” α and β -strand predictions than does YASPIN (BAD 3.0 vs 6.3), while the latter program generates higher percentages of correctly predicted strands compared to observed strands (72% for YASPIN vs 61% for SSPRO).

The conservation of amino acid sequence motifs was assessed on the aligned sequences using the column composition function associated with PRALINE. The following groups of amino acids were considered chemically similar: (S,T), (I,LV), (C,M), (K,R), (D,E), (F,Y,W), and (A,G).

6.3 Results and Discussion

6.3.1 VDAC alignments using PRALINE and secondary structure predictions

Although the precise transmembrane topology of mitochondrial porin is not known, secondary structural predictions are useful in determining whether there have been constraints on porin sequence features and structures during their evolution. To this end, SSPRO was used to predict the secondary structure porin sequences aligned by PRALINE (see Materials and Methods). In general, these predictions revealed remarkably similar patterns for all of the retrieved porin sequences. This similarity extends to the overall secondary structure position and lengths within the annotated isoforms of each of the three crown groups (plants animals and fungi) (Fig. 6.1).

Figure 6.1. PRALINE alignment and secondary structure predictions of eukaryotic porin sequences using SSPPRO. Amino acid sequences from **A)** fungi, **B)** animals, and **C)** plants were aligned using PRALINE, as described in Materials and Methods. Amino acids predicted to reside in α -helices (red) or β -strands (green) by SSPPRO are indicated. Chemically-similar residues in all four representative sequences are shown in bold. The GLK motif (for example residues 87-89 of Osat1) and the existing eukaryotic porin motif (PS00558, for example residues 216-238 of Osat1) are indicated on each of the three panels by blue boxes.

A				10	20	30	40	50															
																		
	<i>Aspergillus nidulans</i>	MAAPAA	FSDI	AKAANDLLNK	DFYHGS	AASL	EVKSA	APNGV	TFNVKG	KSAH													
	<i>Aspergillus fumigatus</i>	MSAPAA	FSDI	AKAANDLLNK	DFYHT	AGIL	EVKSA	APNGV	TFNVKG	KSAH													
	<i>Neurospora crassa</i>	MAVP	-AFSDI	AKSANDLLNK	DFYHLA	AGTI	EVKSN	TPNNV	AFKVT	GKSTH													
	<i>Magnaporthe grisea</i>	MSIP	-NFEDI	TKSANDLLTR	EFYHLA	AGTL	EVKST	TPNNV	DFKVK	GKSTH													
	<i>Gibberella zeae</i>	MSVP	-AFSDI	AKPANDLLNK	DFYHLS	ATTF	EFKDT	APNGV	AFKVT	GKSSH													
	<i>Yarrowia lipolytica</i>	MAPL	-AFSDI	AKASNDLLNK	DYYHLA	RASL	EIKT	APNGV	AFVAKG	KSSQ													
	<i>Coccidioides posadasii</i>	MAAPAA	GFDI	AKTVNDLLNK	DFYHTS	AASL	EVKSA	APNGV	TFNVKG	KSAH													
	<i>Mycosphaerella graminicola</i>	LLPI	PAFGDL	GKAANDLLNK	DFYHAA	AGTL	DVKL	APNGT	CLNVKG	KQGF													
	<i>Candida albicans</i>	MAPA	-AYSDL	SKASNDLLNK	DFYHLS	TAAV	DVKTV	APNGV	TFTVK	GKTTK													
	<i>Clavispora lusitanae</i>	MAPI	-AFSDI	QKSSNDLLNK	DFHLS	SAAV	DVKST	APNGV	AFTVK	GTA													
	<i>Debaryomyces hansenii</i>	MAPP	-AFSDI	QKSSNDLLNK	DFHLS	TAAV	DVKST	APNGV	GFTVK	GTA													
	<i>Pichia guilliermondii</i>	MAPP	-AFSDI	QKSSNDLLTR	DFHLS	TAAP	DVKTV	APNGV	GFTVK	GTA													
	<i>Phanerochaete chrysosporium</i>	-DLG	-----	-KSSNDLLGR	DFY	-FAGTSL	EVKT	TPSNV	AFKVS	GKQDD													
<i>Cryptococcus neoformans</i> var. <i>neoformans</i>	QAVPPS	WRDL	GKSSD	LLLK	DYP	-I	QGTSL	EVKLT	TPSNV	AFKVA	GTKDA												
<i>Antrodia cinnamomea</i>	QPVPPS	WKDL	GKSSND	LLGK	DYP	-I	NGITL	EVKLT	TPSNV	SFKVG	GTRDT												
<i>Ustilago maydis</i>	QPVPPS	WKDL	GKAAGD	LLSK	DYP	-I	HGNSL	EVKLT	TPNGV	TFRVL	GTRDS												
<i>Schizosaccharomyces pombe</i>	MAPP	-AYAAI	NKLCND	LLQR	DYP	-VGATLL	SVRT	APNGV	VFNVS	GNQDA													
<i>Saccharomyces cerevisiae</i> POR1	-MSP	PVYSDI	SRNI	NDLLNK	DFYHAT	PAAF	DVQTT	TANGI	KFSL	LKAPQV													
<i>Saccharomyces paradoxus</i> POR1	TMSP	PVYSDI	SRNI	NDLLNK	DFYHAT	PAAF	DVQTT	TANGI	KFSL	LKAPQV													
<i>Saccharomyces mikatae</i> POR1	-MSP	PLYSDI	SRNI	NDLLNK	DFYHAT	PAAF	DVQTT	TANGI	KFSL	LKAPQV													
<i>Saccharomyces kudriavzevi</i> POR1	-MSP	PVYSDI	SRNI	NDLLNK	DFYHAT	PAAF	DVQTT	TANGI	KFSL	LKAPQV													
<i>Saccharomyces bayanus</i> POR1	-MSP	PVYSDI	SRNI	NDLLNK	DFYHAT	PAAF	DVQTT	TANGI	KFSL	LKAPQV													
<i>Saccharomyces castellii</i> POR1	-MSP	PFNDI	SKDI	NGLLNR	DFYHNT	PAAV	VVNTV	TNGV	KFTVN	ARQV													
<i>Candida glabrata</i> POR1	-MAP	PFSDI	FKSV	NDLLNK	DFYHS	TAAP	DLESV	AKNGV	KFNVS	KQLV													
<i>Eremothecium gossypii</i>	I	MAPPF	SDI	AKDI	NGLLNR	DFYHST	PAAL	DVKTS	APNGV	GFTVK	GKTSP												
<i>Kluyveromyces lactis</i>	-MAP	PFSDI	SKDI	NGLLNR	EFFHA	TPASV	DVKTT	APNGV	AFTVK	GKTSP													
<i>Saccharomyces paradoxus</i> POR2	-MVL	PFNDI	SRDI	NGLLNR	DFHHTN	PLSL	NI	STTTENG	NFTL	LKAGQV													
<i>Saccharomyces bayanus</i> POR2	-MAL	RFNDI	SRDV	NGLLNR	DFHHTN	PLSL	NI	STTTENG	NFTL	LKAGQV													
<i>Saccharomyces cerevisiae</i> POR2	-MVQ	PFNDI	SRDI	NGLLNR	DFHHS	PLAL	NVST	TTENG	SFSL	LKAGQV													
<i>Candida glabrata</i> POR2	TMAP	PFHDI	SRDI	NGLLNR	DFHHTS	PLSL	NVST	TQNGA	NFTL	LKAGQV													
<i>Ajellomyces capsulatus</i>	-MI	PVEGEI	SRNA	QGVLR	DFHGT	GGVI	QVST	-SSDDF	RFNS	SRGKFS-													
<i>Botryotinia fuckeliana</i>	-----	-----	-----	-----	-----	-----	-----	-----	-----	-----													
<i>Saccharomyces kudriavzevi</i> POR2	QSCL	-----	-----	-----	-----	-----	-----	-----	-----	-----													
<i>Blastocladiella emersonii</i>	TMAP	PFHDI	PRDI	NGLLNR	DFHHTS	PLSL	SVST	TQNGV	NFTL	LKAGQV													
<i>Metarhizium anisopliae</i>	I	V	-----	FSDI	GKAASD	LLGK	DFP	-VGSIKL	EAKTT	ASNGV													
<i>Coprinopsis cinerea</i>	-----	-----	-----	-----	-----	-----	-----	-----	-----	-----													
<i>Hebeloma cylindrosporum</i>	-----	-----	-----	-----	-----	-----	-----	-----	-----	-----													
				60	70	80	90	100															
																		
	<i>Aspergillus nidulans</i>	-EG	PI	AGSLE	AKY	V	DAPTGL	TLTQAW	TTAN	AL	DTKLELDN	NI	AKGL	KAEL									
	<i>Aspergillus fumigatus</i>	-EG	PI	AGSLE	AKY	V	DLPTGL	TLTQAW	TTAN	AL	DTKLELDN	NI	AKGL	KAEL									
	<i>Neurospora crassa</i>	-DK	VT	SGALE	GKFT	DKP	NGL	TVTQT	WNTAN	AL	ETKVE	MAD	NL	AKGL	KAEG								
	<i>Magnaporthe grisea</i>	-EG	AT	SGSLE	GKF	ADK	SLGL	TLTQSW	WNTAN	AL	ESKLELDN	TL	AKGL	KLEG									
	<i>Gibberella zeae</i>	-EK	AT	SAAL	E	GKY	T	DKPTGL	TLTQT	WNTAN	AL	DTKIE	VD	SL	AKGL	KLEG							
	<i>Yarrowia lipolytica</i>	KDG	S	I	AGNLE	AKY	ADKANGV	TVTQGW	TTAN	VLD	SKI	EI	DE	AL	ACGL	KGEL							
	<i>Coccidioides posadasii</i>	-EG	PI	AGSLE	AKY	V	DPPTGL	TLTQT	WTTGN	AL	DTKLELDN	NI	AKGL	KAEL									
	<i>Mycosphaerella graminicola</i>	-DG	VT	SGSVE	GKH	V	LKPQGI	TITOAW	STAS	LL	DSKVELND	VV	ADGV	KVDL									
	<i>Candida albicans</i>	-DD	T	SA	SVD	AKY	L	DKATGL	TLTQGW	NNAN	AL	NTKIELSE	LL	T	PGL	KGEL							
	<i>Clavispora lusitanae</i>	-DN	S	IA	SVD	AKY	ADKATGL	TLTQGW	NNAN	V	NTKIELSE	LL	T	PGL	KGEL								
	<i>Debaryomyces hansenii</i>	-DN	S	IA	SVE	AKY	ADKPSGL	TLTQAW	NNAN	SL	DTKIELSE	LL	T	PGL	KGEL								
	<i>Pichia guilliermondii</i>	-AN	A	IA	SVE	AKY	ADKSTGL	TLTQAW	NNAN	AL	DTKIELSE	LL	T	PGL	KGEL								
	<i>Phanerochaete chrysosporium</i>	KTH	L	V	SGELE	AKY	T	NKAHGL	VFTQAW	TTTN	F	RTQVE	AEN	HL	ACGL	KFDL							
<i>Cryptococcus neoformans</i> var. <i>neoformans</i>	KTD	A	SGDI	E	GKY	V	DFKNGL	TFTQGW	TTTN	V	LTQLE	LEN	QI	AKGL	KFDL								
<i>Antrodia cinnamomea</i>	KST	L	ITGDL	E	GKY	V	DKKHGV	VFTQGW	TTTN	TL	RTQLE	LEN	QI	AKGL	KFDL								
<i>Ustilago maydis</i>	KSQ	A	I	NGDLE	AKW	E	DRKNGV	TFTQAW	STAN	V	LRNHI	ELEN	HI	AKGL	KLEL								
<i>Schizosaccharomyces pombe</i>	-KG	V	I	SGKLE	T	SF	N	DKANGL	T	I	SGQW	TTAN	V	ESKVG	LS	E	QF	APGL	HLNV				
<i>Saccharomyces cerevisiae</i> POR1	KDGP	L	STNVE	AKL	N	DKQ	TGL	GLTQGW	SNTN	N	KT	KLEF	-A	N	L	T	PGL	KNEL					
<i>Saccharomyces paradoxus</i> POR1	KDGP	L	STNVE	AKL	N	DKQ	TGL	GLTQGW	SNTN	N	KT	KLEF	-A	N	L	T	PGL	KNEL					
<i>Saccharomyces mikatae</i> POR1	KDGP	L	STNVE	AKL	N	DKQ	TGL	GLTQGW	SNTN	N	KT	KLEF	-A	N	L	T	PGL	KNEL					
<i>Saccharomyces kudriavzevi</i> POR1	KDGP	L	STNVE	AKL	N	DKQ	TGL	GLTQGW	SNTN	N	KT	KLEF	-A	N	L	T	PGL	KNEL					
<i>Saccharomyces bayanus</i> POR1	KDGP	L	STNVE	AKL	N	DKQ	TGL	GLTQGW	SNTN	N	KT	KLEL	-A	D	L	T	PGL	KNEL					
<i>Saccharomyces castellii</i> POR1	KEG	P	L	QANVE	SKF	S	E	KTTGL	TLTQGW	S	NQN	R	N	T	KI	E	L	A	PGL	KSEF			
<i>Candida glabrata</i> POR1	KEG	P	L	QANVE	SKF	S	E	KTTGL	TLTQGW	S	NQN	R	N	T	KI	E	L	A	PGL	KSEF			
<i>Eremothecium gossypii</i>	KDG	S	IA	ANVE	ARV	ADKATGL	TLTQGW	SSAN	V	NTKIEL	-N	N	I	T	PGL	KTEL							
<i>Kluyveromyces lactis</i>	KDG	S	IA	ANVE	VKAS	DKSTGL	TFTQGW	NNAN	T	DTKIEL	-A	E	L	T	PGL	KTEL							
<i>Saccharomyces paradoxus</i> POR2	TEGP	I	Q	SVE	GRF	N	DRKEGV	SLSQGW	S	NQN	R	N	T	R	I	E	F	-S	KI	A	PGL	KDGV	
<i>Saccharomyces bayanus</i> POR2	TEGP	I	Q	SVE	GRF	N	DRKEGV	SLSQGW	S	NQN	R	N	T	R	I	E	F	-S	KI	A	PGL	KDGV	
<i>Saccharomyces cerevisiae</i> POR2	TEGP	I	Q	SVE	GRF	N	DRKEGV	SLSQGW	S	NQN	R	N	T	R	I	E	F	-S	KI	A	PGL	KDGV	
<i>Candida glabrata</i> POR2	KEG	P	L	QANVE	SKF	S	E	KTTGL	TLTQGW	S	NQN	R	N	T	R	I	E	F	-S	KI	A	PGL	KDGV
<i>Ajellomyces capsulatus</i>	-DG	N	F	GANLS	GRH	A	T	KGTGI	AVSQSL	DNKN	Q	F	STKFEY	-	-	N	N	S	R	S	DV		
<i>Botryotinia fuckeliana</i>	-EG	PI	NGALE	AKY	V	DAPTGL	TLTQT	WNTAN	AL	DTKLELDN	KI	M	TGL	KAEL									
<i>Saccharomyces kudriavzevi</i> POR2	-NT	P	NNVAFK	VTG	K	STHDNA	TSGL	L	E	AKFT	DK	P	TGL	LT	Q	TWNT	L	N	ALDT				
<i>Blastocladiella emersonii</i>	KDGP	L	STNVE	AKL	N	DKQ	TGL	GLTQGW	S	NRS	KL	N	T	R	I	E	F	-S	KI	A	PGL	KDGV	
<i>Metarhizium anisopliae</i>	KTG	G	I	AGDLK	TKY	ADKSK	EL	TLTET	WTTSN	V	L	SAE	VELAD	AL	T	KGL	KLNL						
<i>Coprinopsis cinerea</i>	-----	-----	-----	-----	-----	-----	-----	-----	-----	-----	-----	-----	-----	-----	-----	-----	-----	-----	-----	-----	-----		
<i>Hebeloma cylindrosporum</i>	-----	-----	-----	-----	-----	-----	-----	-----	-----	-----	-----	-----	-----	-----	-----	-----	-----	-----	-----	-----	-----		

		110	120	130	140	150				
<i>Aspergillus nidulans</i>	ITQY	LPAKQS	K-G	AKLNLHF	KQPNL	HARAF	FDL--LNGP-	SANFDAVLG-		
<i>Aspergillus fumigatus</i>	LTQY	LPSKQS	K-G	AKLNLHF	KQPNL	HARAF	FDL--LNGP-	SANFDAVLG-		
<i>Neurospora crassa</i>	IFSF	LPAATNA	R-G	AKFNLHF	KQSN	FHGRAF	FDL--LKGP-	TANI DAIVG-		
<i>Magnaporthe grisea</i>	LFGL	LPAATSA	T-A	AKLNLHF	KQSN	VHGRAF	FDL--LKGP-	TANVDAVIG-		
<i>Gibberella zeae</i>	LFNF	LPAATA	K-G	AKFNLHF	KQPGF	HGRAF	FDL--LKGP-	VANVDAVVG-		
<i>Yarrowia lipolytica</i>	ATSE	VPSSGA	K-N	AKLSLFF	KQPSF	QARAF	FDL--LKGP-	TVTSDATLG-		
<i>Coccidioides posadasii</i>	LTQY	LPYSNS	K-G	AKLNLHF	KQPNL	HARAF	FDL--LKGP-	TANFDAVLG-		
<i>Mycosphaerella graminicola</i>	QNLW	NPSKAG	S-A	AKLNLAF	KNPNV	HSRAF	LNYGTAKGNI	DAVVDVTAG-		
<i>Candida albicans</i>	DTSV	VPNGAR	N--	AKLNFFY	QSAVN	NARLF	FDL--LKGP-	IATADLVVA-		
<i>Clavispora lusitanae</i>	DTSV	VPNGAK	N--	AKLNFFY	QSAVN	NARLF	FDL--LKGP-	IATADLTVA-		
<i>Debaryomyces hansenii</i>	VTSL	VPNGPR	N--	AKLNFFY	QQNAV	NARLF	FDL--LKGP-	IADADLVG-		
<i>Pichia guilliermondii</i>	VTSL	VPNGAR	N--	AKLNFFY	QQNVN	NARLF	FDL--LKGP-	IATADLVA-		
<i>Phanerochaete chrysosporium</i>	NTSL	AANGSG	K-S	ALITTTY	KQPLH	HTRAF	LDL--FKGP-	TFTADTVIG-		
<i>Cryptococcus neoformans</i> var. <i>neoformans</i>	ATTL	NPAKAS	K-S	ALTAIY	KQPSL	HTRAT	VDL--FKGP-	TFTADTVVG-		
<i>Antrodia cinnamomea</i>	NTAL	TPDSGA	K-T	ALLTSIY	KQPG	LHSRAF	LDL--FKGP-	TFTADTVLG-		
<i>Ustilago maydis</i>	VSTL	VPEKQT	K-N	ALFASTY	KQPLH	HTROH	LDL--FKGP-	TFTADAVLG-		
<i>Schizosaccharomyces pombe</i>	NTTF	SPATAA	K-T	AILNLEH	QHPL	HTHAS	VNA--LERK-	-FLGDFTVG-		
<i>Saccharomyces cerevisiae</i> POR1	ITSL	TPGVAK	S--	AVLNTTF	TQPF	FTARGA	FDL-CLKSP-	TFVGDLTMA-		
<i>Saccharomyces paradoxus</i> POR1	ITSL	TPGVAK	S--	AVLNTTF	TQPF	FTARGA	FDL-CLKSP-	TFVGDLTMA-		
<i>Saccharomyces mikatae</i> POR1	ITSL	TPGVAK	S--	AVLNTTF	TQPF	FTARGA	FDL-CLKSP-	TFVGDLTMA-		
<i>Saccharomyces kudriavzevi</i> POR1	ITSL	TPGVAK	S--	AVLNTTF	AQPF	FTARGA	FDL-CLKSP-	TFVGDLTMA-		
<i>Saccharomyces bayanus</i> POR1	ITSL	TPGVAK	S--	AVLNTTF	VQPF	FTARGS	FDL-CLKSP-	TFVGDLTMA-		
<i>Saccharomyces castellii</i> POR1	VTSL	VPNGAK	T--	AQLNLSF	VQPF	FAAGV	FDL--FKTP-	SFVGNLTLA-		
<i>Candida glabrata</i> POR1	MTSE	VPNISK	V--	AKNLSF	VQPF	FTARGA	FDL--LKGP-	GFVGDMLAH		
<i>Eremothecium gossypii</i>	VTSC	VPGTSN	A--	AKNLSF	VQPA	FTARGF	FDL--IKGP-	SFVGDLTLA-		
<i>Kluyveromyces lactis</i>	ITSG	VPGVSK	A--	AKLVNLF	VQPL	FAARGF	FDL--LKGP-	SFVGDLTLA-		
<i>Saccharomyces paradoxus</i> POR2	NASL	TPQSIK	N--	AKFNLSY	AKKS	LTARSS	IDV--LQPK-	DFVGSVTLG-		
<i>Saccharomyces bayanus</i> POR2	NASL	TPQSIK	N--	AKFNLSY	AKKS	FAARTS	IDV--LQPK-	DFVGSVTLG-		
<i>Saccharomyces cerevisiae</i> POR2	NASL	TPQAIK	N--	AKFNLSY	AKKS	FTTRSS	VDI--LQPK-	DFVGSVTLG-		
<i>Candida glabrata</i> POR2	NACM	TPQAIK	N--	AKVNLSF	AQEF	FTTRAS	VDL--LHTK-	DFVGNVTLA-		
<i>Ajellomyces capsulatus</i>	TTNW	VPGTVN	IKS	SRLGFNY	FNAL	MNSKMS	VDL--FNPT-	KVVGSMTMG-		
<i>Botryotinia fuckeliana</i>	LTQY	LPNSQS	K-G	VKLNLHF	KQPS	FHARAF	FDL--LKGP-	SASFDAVLG-		
<i>Saccharomyces kudriavzevi</i> POR2	KIEI	NDISIAK	G--	LKAEILS	EAPT	LQKKGA	KVN--LHFK-	QPNFHGRAF-		
<i>Blastocladiella emersonii</i>	NACL	TPQAIK	N--	AKFNLSY	AQQS	FSARSS	MDI--LQLK-	DFVGSISLG-		
<i>Metarhizium anisopliae</i>	LGSL	LPHIQK	K-N	AKFSAEY	KQDA	VATRSS	IDL--FKGP-	IATADIAFN-		
<i>Coprinopsis cinerea</i>	TSAA	IEGKYT	D--	KPSGLTL	TQTWNT	ANAL	DTK--LEVND	TLAKGKLKLE-		
<i>Hebeloma cylindrosporum</i>	ITGD	LEAKYT	T--	KAHGLTV	TQAWT	TSNVL	RNQ--VELEN	QLAKGKLKLD-		
	IHGD	IEXKWT	D--	KVHGLTL	TQTWT	TSNVL	RNQ--VELDN	LMAKGKLKLD-		
		160	170	180	190	200				
<i>Aspergillus nidulans</i>	HEGF	LVGAEG	GYD	VQKAAI	TKYS	AAVGY	S-VPO	YSAAIQ	AANNLT	VFSA
<i>Aspergillus fumigatus</i>	HEGF	LVGAEG	GYD	VQKAAI	TKYS	AAVGY	S-VPO	YTAAT	AGNNLT	VFSA
<i>Neurospora crassa</i>	HEGF	LAGASA	GYD	VQKAAI	IGYS	AAVGYH	A-APT	YSAAI	TADNLS	VFSA
<i>Magnaporthe grisea</i>	HEGF	LAGLSG	GYN	VQKAAI	TTYS	AAVGY	S-APQ	YTAAVT	ATDNAS	VFAA
<i>Gibberella zeae</i>	HEGF	LAGASA	GYD	ANKAAI	TAYS	AAVGYA	A-APQ	YSAAI	ASDNLS	VFAA
<i>Yarrowia lipolytica</i>	HDGF	IAGAEV	GYD	VSDAKV	TKYS	AAVGYT	A-APV	YSTSI	ATNLS	VFSA
<i>Coccidioides posadasii</i>	HEGF	LVGAEG	GYD	VQKAAI	TKYS	AAVAYS	S-LPE	YSAAI	ATNNLT	LFSA
<i>Mycosphaerella graminicola</i>	SDGF	LVGGEA	GYD	VQKAAI	TRYSL	LGLGYQ	T-PNY	TASI	VTQNL	SIAA
<i>Candida albicans</i>	HDGF	TAGAEI	GYD	ISAAKV	NKYS	VGVGYA	A-NLN	YGLAAT	ATNLS	VFSA
<i>Clavispora lusitanae</i>	HDGF	TAGAEI	GYD	ISAAKL	NKYS	VGVGYA	A-NPL	YTVGVT	STNLS	VFTA
<i>Debaryomyces hansenii</i>	HDGF	TAGAEI	GYD	ISAAKV	NKYS	LGVGYA	A-KPL	YTVAA	ATNLS	VFTA
<i>Pichia guilliermondii</i>	HDGF	TAGAEI	GYD	INDATV	NKYS	VGVGYA	A-HPL	YNVAAT	ATNLS	VFTA
<i>Phanerochaete chrysosporium</i>	RDGF	LLGAEA	SYN	VTEGKV	TRYAA	AVGFS	A-APE	YAVTLG	GLNNLS	LFSA
<i>Cryptococcus neoformans</i> var. <i>neoformans</i>	RDGF	LVGAEA	SYD	VLSGAL	TRYAG	AVGFS	A-APE	YAVTLH	GLGNLS	TFAA
<i>Antrodia cinnamomea</i>	RDGF	LVGAEA	SYN	VTEGKI	TRYA	AVGFS	A-APE	YAVTLH	GLGNMS	TFAA
<i>Ustilago maydis</i>	RDGF	LAGAEA	SYD	VKAGKL	SRYNL	GAGFH	A-APD	YAVTFH	GLGNLS	TYSA
<i>Schizosaccharomyces pombe</i>	HEGF	VGGAEF	GYD	ISAGSI	SRYA	MAISYF	A-AKD	YSLGAT	LNNE	QITTV
<i>Saccharomyces cerevisiae</i> POR1	HEGF	VGGAEF	GYD	ISAGSI	SRYA	MAISYF	A-AKD	YSLGAT	LNNE	QITTV
<i>Saccharomyces paradoxus</i> POR1	HEGF	VGGAEF	GYD	ISAGSI	SRYA	MAISYF	A-AKD	YSLGAT	LNNE	QITTV
<i>Saccharomyces mikatae</i> POR1	HEGF	VGGAEF	GYD	ISAGSI	SRYA	MAISYF	A-AKD	YSLGAT	LNND	QITTV
<i>Saccharomyces kudriavzevi</i> POR1	HEGF	VGGAEF	GYD	ISAGSI	SRYA	MAISYF	A-AKD	YSLGAT	LNND	QITTV
<i>Saccharomyces bayanus</i> POR1	HEGF	VGGAEF	GYD	ISAGSI	SRYA	MAISYF	A-AKD	YSLGAT	LNND	QITTV
<i>Saccharomyces castellii</i> POR1	HEGF	VGGAEF	GYD	ITGGTI	SRYA	LALGYS	A-ARD	YTLGSI	INEA	QITSA
<i>Candida glabrata</i> POR1	ESGV	VAGAQF	GYD	IAAGSL	SKYAI	ALGYA	A-AQD	YHLGLN	INNND	QVTTA
<i>Ajellomyces capsulatus</i>	HKGF	VGGAEV	GYD	IAAATV	SRYA	VALGYR	T-TGL	YSVALG	VNNA	QITTA
<i>Eremothecium gossypii</i>	HEGF	VGGAEV	GYD	ISAGAV	SRYA	LALGYN	A-ASG	YSVGLS	VNNA	QITTA
<i>Kluyveromyces lactis</i>	HRGF	VGGTEI	AYD	IAAGGL	ARYAM	SLGYL	A-SRD	YSFILS	TNNR	QCAT
<i>Saccharomyces paradoxus</i> POR2	HRGF	VGGTDI	AYD	TAGALC	ARYAM	SI GYL	A-ARE	YSFILS	TNNR	QCAT
<i>Saccharomyces bayanus</i> POR2	HRGF	VGGSEV	AYD	LLGRSL	ARYAM	SI GYL	A-SRD	YSFVLS	TNNR	QCAIA
<i>Saccharomyces cerevisiae</i> POR2	HDGF	VGGTEI	AYD	IPGQAL	ARYA	VALGYL	A-ASD	YSFVLS	TNNK	QFTSA
<i>Candida glabrata</i> POR2	YGKM	VGGSEV	TCO	I AQNK	TRYAL	SMGIY	A-AGK	RNLTFI	INDA	HVMTL
<i>Botryotinia fuckeliana</i>	HEGF	LVGAEG	GYD	VQKAAI	TKYS	AAIAYC	S-VPE	YSAAVT	AQNNLS	LFSA
<i>Saccharomyces kudriavzevi</i> POR2	FDLL	KGPTAT	VDA	VI QDGF	FLAGA	TAGYD	A-VQK	AAI TSY	SAAVGY	TAPT
<i>Blastocladiella emersonii</i>	RDGF	VGGTEI	AYD	IPSGSL	ARYAM	SLGYL	A-ARD	YSFVLS	TNNR	QCAT
<i>Metarhizium anisopliae</i>	HDGF	LAGAAT	AYD	LATGHV	SKYN	VAFGYA	A-TRE	YSVALT	GANKFD	TFAG
<i>Coprinopsis cinerea</i>	GLFN	FLPATA	GKG	AKFNLF	KQPGF	HGRAF	FDDL	KGPVAN	GDVAV	-VVG
<i>Hebeloma cylindrosporum</i>	LTTS	SLAPEKG	AKT	AVLGGVF	KQSG	LHTRAV	L	DLFK	GPTFT	TDAV--VGRD
	LAT	SLTPDKG	SKS	AILNAA	YKQSG	LHTRAA	L	DFVK	GPTFT	AXTV--LGRD

		210	220	230	240	250
<i>Aspergillus nidulans</i>	SYHHRVNA	QVEAGAKATW	NSKTGNSV	G LEVASKYRL	D PSSFAK	W
<i>Aspergillus fumigatus</i>	SYHHRVNA	QVEAGAKATW	NSKAGNSV	G LEVASKYRL	D PSSFAKSA	
<i>Neurospora crassa</i>	SYHHRVNS	QVEAGSKATW	NSKTGNTV	G LEVATKYRI	D PVSFVK	G
<i>Magnaporthe grisea</i>	SYHHRVNS	LVKAGAKASW	NSKI GNSV	G LEVATKYRI	D PLSFVK	G
<i>Gibberella zeae</i>	SYHHRVNS	QVEAGAKATW	NSKTGNV	G LEVASKYRI	D PVSFVK	W
<i>Yarrowia lipolytica</i>	AYFHRVNP	ATEVGAKATW	NSKAAAAP	G LEI GAKHTL	D ANSFVK	A
<i>Coccidioides posadasii</i>	SYHHRVNS	QVEAGAKATW	NSKAGNTV	G LEVASKYRL	D PSSFAK	A
<i>Mycosphaerella graminicola</i>	SYHHRVNT	SVEFGAKAGY	DVNA-QKA	G LEI ASKYKL	D PLSFVK	A
<i>Candida albicans</i>	AYFHRVNP	LQVGAKATW	NSI KSSNV	N VEFATKYAL	D NTSFVK	A
<i>Clavispora lusitanae</i>	AYHHRVNP	LVEAGAKATW	NSVKSSAV	N VEFATKYKL	D ATTFVK	A
<i>Debaryomyces hansenii</i>	AYHHRVNP	LVEAGAKATW	NSVKSSNV	N VEFATKYKL	D STAFVK	A
<i>Pichia guilliermondii</i>	SYHHRVNP	LVEAGAKATW	NSVKSSAV	N VEFATKYKL	D STAFVK	A
<i>Phanerochaete chrysosporium</i>	SYHHRVNP	DVEAGAKATY	DTKGTQNVH	LEVGAKEYL	D NAASFVK	A
<i>Cryptococcus neoformans</i> var. <i>neoformans</i>	SYHHRVNS	DVEAGAKAVY	DTKSTAGNV	LEVGAKEYL	D NAASFVK	A
<i>Antrodia cinnamomea</i>	SYHHRVNP	DVEAGAKAIY	DTKATTAGVS	LEVGAKEYL	D TAAAFVK	A
<i>Ustilago maydis</i>	SYHHRVNA	DTEAGARATY	DSKSPNSNVN	LEVGTKEYL	D NAASFVK	A
<i>Schizosaccharomyces pombe</i>	SYHHRVNS	DVEAGGNVTW	DAASTANA	T LELASKYAL	D KDTFVK	G
<i>Saccharomyces cerevisiae</i> POR1	DFQNVNA	FLQVGAKATM	NCKLPNSNVN	IEFATRYLP	D ASSQVK	A
<i>Saccharomyces paradoxus</i> POR1	DFQNVNA	FLQVGAKATM	NCKLPNSNVN	IEFATRYLP	D ASSQVK	A
<i>Saccharomyces mikatae</i> POR1	DFQNVNA	FLQVGAKATM	NCKLPNSNVN	IEFATRYLP	D ASSQVK	A
<i>Saccharomyces kudriavzevi</i> POR1	DFQNVNA	FLQVGAKATM	NCKLPNSNVN	IEFATRYLP	D ASSQVK	A
<i>Saccharomyces bayanus</i> POR1	DFQNVNA	FLQVGAKATM	NCKLPNSNVN	IEFATRYLP	D ASSQVK	A
<i>Saccharomyces castellii</i> POR1	SFYQSIK	I LQVGAKATL	N-PKKGSNV	N IEFATRYLP	D ATSQVK	A
<i>Candida glabrata</i> POR1	TFQNVNP	QLQI GSRATL	NPRQTVSNV	N IEFATRYLP	D PISQVK	A
<i>Eremothecium gossypii</i>	SFFQRVNP	ALEVGAKAAL	N-PAAGSKVN	N IEFATRYAL	D LTAQVK	A
<i>Kluyveromyces lactis</i>	SFFQKVP	I LQVGAKAAL	N-PQAGSNV	N IEFASKYAL	D AVSQVK	A
<i>Saccharomyces paradoxus</i> POR2	TFQNVNR	FLQVGATKATL	Q-SKENPN	N IEFVTRYVP	D PISQVK	A
<i>Saccharomyces bayanus</i> POR2	SFFQNVNR	YLVGATKATL	Q-SKTSNM	N IEFVTRYVP	D SISQVK	A
<i>Saccharomyces cerevisiae</i> POR2	SFFQNI	DR-CLQVGARATL	Q-SKTSNM	N IEFVTRYAP	D PTSSQVK	A
<i>Candida glabrata</i> POR2	SFFQNVN	R-HLVGAKATV	Q-SKATPSM	N IEFVTRYLP	D STSQVK	A
<i>Ajellomyces capsulatus</i>	TLYQKLS	P-QFEAAAKTTT	R-FNESNKT	S-VEVATAYR	H-NSAQYK	L
<i>Botryotinia fuckeliana</i>	SYHHRVNP	QVEACAKATW	NSKAGNSV	G LEVGSKYRL	D PSSFAK	W
<i>Saccharomyces kudriavzevi</i> POR2	YSAAITAA	DNLVSFSASY	YHKVNTQV	E-AGAKATWDS	K-NTNSVG	L
<i>Blastocladiella emersonii</i>	SFFQNI	NR-YLVGAKATV	--QSKTRI	-----	P-PQW	
<i>Metarhizium anisopliae</i>	SYHHRVNP	D-NSKTRI	-----	P-PQW		
<i>Coprinopsis cinerea</i>	GFLAGASAGY	DVNKAATAY	SAAVGYAAPQ	YSAAVTATDN	LSVFASYYH	
<i>Hebeloma cylindrosporum</i>	GFLAGAEASY	NVTEGKVT	RY-AAALGYNAPE	YAVTLHGLNN	LSTFTASYYH	
	GFLVGAEAAAY	NVTGGNI	TRY-AAAVGYNAPE	YAVTLHGLNN	FKTFASYYH	
		260	270	280	290	300
<i>Aspergillus nidulans</i>	KIN--DRG	AALAYNVLLR	PGVTLGLGAS	F--DTQNLNQ	-----	
<i>Aspergillus fumigatus</i>	KIN--DRG	AALAYNVLLR	PGVTLGLGAS	F--DTQNLNQ	-----	
<i>Neurospora crassa</i>	KIN--DRG	AAIAYNVLLR	EGVTLGVGAS	F--DTQKLDQ	-----	
<i>Magnaporthe grisea</i>	KIN--DRG	AAVAYTLLR	PGVTFGLGAS	F--DTQKLDQ	-----	
<i>Gibberella zeae</i>	KIN--DRG	AALAYNVLLR	EGVTLGLGGS	F--DTQKLDQ	-----	
<i>Yarrowia lipolytica</i>	KIN--NQG	AALAYSVGLK	PGVRVGVGAS	I--DTQRLQ	-----	
<i>Coccidioides posadasii</i>	KIN--DRG	AALAYNVLLR	PGVTLGLGAS	V--DTQNLNQ	-----	
<i>Mycosphaerella graminicola</i>	KIN--DRG	AALAYSTKLN	AGTTLGLGLS	L--DTNKLNE	-----	
<i>Candida albicans</i>	KIA--DSGL	TALSYQELR	PGVKLGLGAS	F--DALKLAE	-----	
<i>Clavispora lusitanae</i>	KIA--DSGL	TAVSYQELR	PGVRLGLGAS	F--DALKLAE	-----	
<i>Debaryomyces hansenii</i>	KIA--DSGL	TALSYQELR	PGVRLGLGAS	F--DALKLAE	-----	
<i>Pichia guilliermondii</i>	KIA--DSGL	AALSYQELR	PGVTLGLGAS	F--DALKLAE	-----	
<i>Phanerochaete chrysosporium</i>	KIN--NAG	LGLGYTOALR	PGVKASFLA	L--DTQRLNE	--VG--	
<i>Cryptococcus neoformans</i> var. <i>neoformans</i>	KIN--NAG	LSLGYTOALR	PGVKASAGVS	V--DTTRLNE	--PQ--	
<i>Antrodia cinnamomea</i>	KIN--NSG	LALGYTOSL	PGVRASFGVA	L--DTQRLND	VTPS-G--	
<i>Ustilago maydis</i>	KIN--NAG	LCLGYTOALR	PGVKASFLA	L--DTFKLS	D--SA--	
<i>Schizosaccharomyces pombe</i>	KIN--SAG	ATLSYFOTVR	PGVTVGLGLQ	L--DTQRLGQ	-----	
<i>Saccharomyces cerevisiae</i> POR1	KVS--DSG	VTLAYKOLLR	PGVTLGVGSS	F--DALKLSE	-----	
<i>Saccharomyces paradoxus</i> POR1	KVS--DSG	VTLAYKOLLR	PGVTLGVGSS	F--DALKLSE	-----	
<i>Saccharomyces mikatae</i> POR1	KVS--DSG	VTLAYKOLLR	PGVTLGVGSS	F--DALKLSE	-----	
<i>Saccharomyces kudriavzevi</i> POR1	KVS--DSG	VTLAYKOLLR	PGVTLGVGSS	F--DALKLSE	-----	
<i>Saccharomyces bayanus</i> POR1	KVS--DSG	VTLAYKOLLR	PGVTLGVGSS	F--DALKLSE	-----	
<i>Saccharomyces castellii</i> POR1	KIT--DAG	MTLSYKODLK	PGITLGVGTS	L--DALKLNE	-----	
<i>Candida glabrata</i> POR1	KIS--DAG	VALSYKQALR	PGVTLGVGTS	F--DALKLSE	-----	
<i>Eremothecium gossypii</i>	KIA--DSGL	VALSYKQALR	PGVELGVGAS	F--DALKLAE	-----	
<i>Kluyveromyces lactis</i>	KIA--DSGL	VALSYQELR	PGVTLGLGAS	F--DALKLAE	-----	
<i>Saccharomyces paradoxus</i> POR2	KIA--DSGL	TTLSYKRNLN	KDISLGVGMS	F--NALQLTE	-----	
<i>Saccharomyces bayanus</i> POR2	KIA--DSGL	TTLSYKRNLN	KDISLGVGMS	F--NALQLTE	-----	
<i>Saccharomyces cerevisiae</i> POR2	KIT--DSG	ATLSYKQNLK	KDISLGMGMS	F--NALELAD	-----	
<i>Candida glabrata</i> POR2	KLN--DAG	ACLSYKVPFQ	KNISLGLGIS	M--DVCNPT	-----	
<i>Ajellomyces capsulatus</i>	KVN--DRG	AALAYNVLLR	PGVTLGLGAS	M--DTQKLSQ	-----	
<i>Botryotinia fuckeliana</i>	EVA--SKYR	LDPLSFAKVK	I NDRGVAAYA	Y--NVVLRPG	ATLG-LGASF	
<i>Saccharomyces kudriavzevi</i> POR2	--R--DS	-----	I-S	-----		
<i>Blastocladiella emersonii</i>						
<i>Metarhizium anisopliae</i>	KVNSQVEAGA	KATWNSK-TG	NAVGLEVASK	YRIDPVSF	FAK-VXI	NDRGI-AA
<i>Coprinopsis cinerea</i>	RI NRDVQAGA	KAVYDPKATH	GGVALEVGS	K-VYLDAAAF	VK-AKI	NNSGVIA
<i>Hebeloma cylindrosporum</i>	RVS RDVEAGA	KAIYDSKSTH	G-----			

 310 320
<i>Aspergillus nidulans</i>	----- AAH KVG A-- SFTF EA-----	
<i>Aspergillus fumigatus</i>	----- AAH KVG A-- SFTF EA-----	
<i>Neurospora crassa</i>	----- ATH KVG T-- SFTF ES-----	
<i>Magnaporthe grisea</i>	----- ATH KVG T-- SFTF ES-----	
<i>Gibberella zeae</i>	----- ATH KLGA-- SFTF EG-----	
<i>Yarrowia lipolytica</i>	----- SAH NLGV-- SFTF EG-----	
<i>Coccidioides posadasii</i>	----- AAH KVG A-- SFTF EG-----	
<i>Mycosphaerella graminicola</i>	----- AGH KIG T-- SLTF EG-----	
<i>Candida albicans</i>	----- PVH KLGF-- SLSF AA-----	
<i>Clavispora lusitanae</i>	----- PVH KLGV-- SLSF SA-----	
<i>Debaryomyces hansenii</i>	----- PVH KLGF-- SLSF SA-----	
<i>Pichia guilliermondii</i>	----- PVH KLGF-- SLSF SS-----	
<i>Phanerochaete chrysosporium</i>	----- PAH KIG A-- HFVF EG-----	
<i>Cryptococcus neoformans</i> var. <i>neoformans</i>	----- AAH KVG A-- SIVF NA-----	
<i>Antrodia cinnamomea</i>	----- PAH KVG A-- SFTF-----	
<i>Ustilago maydis</i>	----- NAH KLGA-- SVTF EA-----	
<i>Schizosaccharomyces pombe</i>	----- PAH KAG L-- SLAF SA-----	
<i>Saccharomyces cerevisiae</i> POR1	----- PVH KLGV-- SLSF DA-----	
<i>Saccharomyces paradoxus</i> POR1	----- PVH KLGV-- SLSF DA-----	
<i>Saccharomyces mikatae</i> POR1	----- PVH KLGV-- SLSF DA-----	
<i>Saccharomyces kudriavzevi</i> POR1	----- PVH KLGV-- SLSF DA-----	
<i>Saccharomyces bayanus</i> POR1	----- PVH KLGV-- SLSF DA-----	
<i>Saccharomyces castellii</i> POR1	----- PVH KIG W-- SLSF DA-----	
<i>Candida glabrata</i> POR1	----- PVH KLGV-- SLSF SA-----	
<i>Eremothecium gossypii</i>	----- PVH KLGV-- SLSF AA-----	
<i>Kluyveromyces lactis</i>	----- PVH KFGW-- SLSF SV-----	
<i>Saccharomyces paradoxus</i> POR2	----- PVH KFGW-- SLSF SP-----	
<i>Saccharomyces bayanus</i> POR2	----- PVH KLGV-- SLSF SA-----	
<i>Saccharomyces cerevisiae</i> POR2	----- PVH KFGW-- SLSF SA-----	
<i>Candida glabrata</i> POR2	----- VK KFGW-- SLNF Q-----	
<i>Ajellomyces capsulatus</i>	----- TAH KVG A-- S----- FT-----	
<i>Botryotinia fuckeliana</i>	DTQKLDD AT H KI GT-- SFTF ES-----	
<i>Saccharomyces kudriavzevi</i> POR2	-----	
<i>Blastocladiella emersonii</i>	-----	
<i>Metarhizium anisopliae</i>	LATSS-----	
<i>Coprinopsis cinerea</i>	LG Y T Q G P P S W R Q G F L S G L R X S K T Q K X N E P	
<i>Hebeloma cylindrosporum</i>	-----	

B

 10 20 30 40 50
<i>Ancylostoma caninum</i>	----- MAPPTF	ADLGKSAKDL	FNKGYNFG	FL KI	OSTTR-- -AGDN- KEVE
<i>Caenorhabditis elegans</i> VDAC2	----- MAPPTF	ADLGKSAKDL	FNKGYNFG	FL KI	OSTTR-- -AGDN- KEVE
<i>Caenorhabditis elegans</i>	----- MAPPTF	ADLGKSAKDL	FNKGYNFG	FL KI	OSTTR-- -AGDN- KEVE
<i>Ascaris suum</i>	----- MSPPAY	VDLGKDAKDL	FTSEYNHG	FL KV	ETTTT-- -AGEK- EEVE
<i>Haemonchus contortus</i>	----- FCQ-----	TRKSAKDL	FNKGYNHG	FI KV	OTTTT-- -AGEN- KEVE
<i>Monodelphis domestica</i> VDAC2	----- MCIPPAY	ADLGKSAARDI	FNKGF GFG	LV KL	OVKTK-- -SCSG- VE
<i>Macaca mulatta</i> VDAC2	----- MCIPPSY	ADLGKSAARDI	FNKGF GFG	LV KL	OVKTK-- -SCSG- VE
<i>Bos taurus</i> VDAC2	----- MCIPPSY	ADLGKSAARDI	FNKGF GFG	LV KL	OVKTK-- -SCSG- VE
<i>Rattus norvegicus</i> VDAC2	----- MCIPPSY	ADLGKSAARDI	FNKGF GFG	LV KL	OVKTK-- -SCSG- VE
<i>Mus musculus</i> VDAC2	----- MCIPPSY	ADLGKSAARDI	FNKGF GFG	LV KL	OVKTK-- -SCSG- VE
<i>Homo sapiens</i> VDAC2	----- MCIPPSY	ADLGKSAARDI	FNKGF GFG	LV KL	OVKTK-- -SCSG- VE
<i>Homo sapiens</i> VDAC2	----- MCIPPSY	ADLGKSAARDI	FNKGF GFG	LV KL	OVKTK-- -SCSG- VE
<i>Homo sapiens</i> VDAC2	----- MCIPPSY	ADLGKSAARDI	FNKGF GFG	LV KL	OVKTK-- -SCSG- VE
<i>Gallus gallus</i> VDAC2	----- MAIPPSY	ADLGKSAARDI	FNKGY GFG	LV KL	OVKTK-- -SASG- VE
<i>Meleagris gallopavo</i> VDAC2	----- AIPPSY	ADLGKSAARDI	FNKGY GFG	LV KL	OVKTK-- -SASG- VE
<i>Pan troglodytes</i> VDAC2	----- MCIPPSY	ADLGKSAARDI	FNKGF DI T	S GCS	VVMLV I P ATQEA-- -E- E
<i>Gasterosteus aculeatus</i>	----- MAVPPCY	ADLGKSAKDI	FNKGY GFG	LV KL	OVKTK-- -SASG- VE
<i>Fugu rubripes</i>	PVT MAVPPCY	ADLGKSAKDI	FNKGY GFG	TV KL	OVKTK-- -SASG- VE
<i>Fugu rubripes</i>	----- MAVPPCY	ADLGKSAKDI	FNKGY GFG	TV KL	OVKTK-- -SASG- VE
<i>Tetraodon nigroviridis</i>	----- MAVPPCY	ADLGKSAKDI	FNKGY GFG	TV KL	OVKTK-- -SASG- VE
<i>Ictalurus punctatus</i>	----- MAVPPCY	ADLGKSAKDI	FNKGY GFG	LV KL	OVKTK-- -SASG- VE
<i>Oncorhynchus mykiss</i>	----- MAVPPSY	GD LGKSAKDI	FSKGY GFG	LV KL	OVKTK-- -SGSG- VE
<i>Oryzias latipes</i> VDAC2	----- MAVPPAY	ADLGKSAKDI	FDKGY GFG	VV KL	OVKTK-- -SASG- VE
<i>Danio rerio</i>	----- MAVPPAY	ADLGKSAKDI	FNKGY GFG	MV KL	OVKTK-- -SASG- VE
<i>Xenopus laevis</i> VDAC2	----- AVPPSY	ADLGKSAKDI	FNKGY GFG	LV KL	OVKTK-- -SATG- VE
<i>Fugu rubripes</i>	----- MAVPPAY	VDLGKSAKDI	FNKGY GFG	LV KL	OVKTK-- -SSSG- VE
<i>Fugu rubripes</i>	----- MAVPPGF	SDLGKSAKDI	FNKGF GFG	VL KL	OVKTK-- -SSSG- VE
<i>Squalus acanthias</i>	----- MSVPFSY	ADLGKSAARDL	FNKGY GFG	LV KL	ELKTK-- -SSSG- VE
<i>Danio rerio</i>	----- MAVPPAY	ADLGKSAKDI	FSKGY GFG	TV KL	DLKTK-- -SQSG- VE
<i>Salmo salar</i>	----- MAVPPAY	SDLGKSAARDI	FGKGY GFG	IV KL	DLKTK-- -AQSG- VE
<i>Monodelphis domestica</i> VDAC1	----- MAVPPTY	ADLGKSAARDV	FTKGY GFG	LI KL	DLKTK-- -SENG- LE
<i>Gallus gallus</i> VDAC1	----- MAVPPAY	ADLGKSAARDV	FTKGY GFG	LI KL	DLKTK-- -SENG- LE
<i>Rattus norvegicus</i> VDAC1	----- MAVPPTY	ADLGKSAARDV	FTKGY GFG	LI KL	DLKTK-- -SENG- LE
<i>Bos taurus</i> VDAC1	----- MAVPPTY	ADLGKSAARDV	FTKGY GFG	LI KL	DLKTK-- -SENG- LE
<i>Sus scrofa</i> VDAC1	----- MAVPPTY	ADLGKSAARDV	FTKGY GFG	LI KL	DLKTK-- -SENG- LE

		10	20	30	40	50
<i>Homo sapiens</i> VDAC1	--MAVPPT	YADLGKSARDV	FTKGYGFG	LI KL DLKTK	--SENG--	E
<i>Mus musculus</i> VDAC1	--MAVPPT	YADLGKSARDV	FTKGYGFG	LI KL DLKTK	--SENG--	E
<i>Rattus norvegicus</i> VDAC1	--MAVPT	YDLAKSARDV	FTKDYGFG	LI KL DLKTK	--SENR--	E
<i>Xenopus laevis</i> VDAC1	--MAIPPA	YVDLGKSARDI	FTKGYGFG	LI KL DLKTK	--SENG--	E
<i>Xenopus tropicalis</i>	--MAIPPA	YADLGKSARDI	FTKGYGFG	LI KL DLKTK	--SENG--	E
<i>Fundulus heteroclitus</i> VDAC1	--LGRAPS	YVDLGKSARDV	FTKGYGFG	LI KL DLKTK	--SDNG--	E
<i>Oryzias latipes</i> VDAC1	--MAVPPT	YADLGKSARDV	FTKGYGFG	LI KL DLKTK	--SENG--	E
<i>Danio rerio</i> VDAC1	--MAVPPT	YVDLGKSARDI	FTKGYGFG	LI KL DLKTR	--SENG--	E
<i>Petromyzon marinus</i>	--MAVPPT	FVDLGKSARDV	FSKGYGFG	LV KL DLKTK	--TSSG--	E
<i>Tetraodon nigroviridis</i>	--MTVPPA	YADLGKSARDI	FNKGYGFG	LV KL DVKTK	--SSTG--	E
<i>Oryctolagus cuniculus</i> VDAC3	--MCNTPT	YCDLGKAAKDV	FNKGYGFG	MV KI DLRTK	--SCSG--	E
<i>Sus scrofa</i> VDAC3	--MCNTPT	YCDLGKAAKDV	FNKGYGFG	MV KI DLRTK	--SCSG--	E
<i>Bos taurus</i> VDAC3	--MCNTPT	YCDLGKAAKDV	FNKGYGFG	MV KI DLRTK	--SCSG--	E
<i>Mus musculus</i> VDAC3	--MCNTPT	YCDLGKAAKDV	FNKGYGFG	MV KI DLKTK	--SCSG--	E
<i>Homo sapiens</i> VDAC3	--MCNTPT	YCDLGKAAKDV	FNKGYGFG	MV KI DLKTK	--SCSG--	E
<i>Rattus norvegicus</i> VDAC3	--MCSTPT	YCDLGKAAKDV	FNKGYGFG	MV KI DLKTK	--SCSG--	E
<i>Pongo pygmaeus</i> VDAC3	--MCNTPT	YCDLGKAAKDV	FNKGYGFG	MV KI DLKTK	--SCSG--	E
<i>Gallus gallus</i> VDAC3	--MAVPPS	YSDLGKAARDV	FNKGYGFG	MV KL ELKTK	--SSSG--	E
<i>Pimephales promelas</i>	--MAVPPA	YADLGKAAKDV	FNKGYGFG	MV KL DVKTK	--SANG--	E
<i>Argopecten irradians</i>	--MAPPSY	YSDLGKAAKDL	SDKGYNFG	LY KL ECKTK	--SSSG--	E
<i>Spisula solidissima</i>	--MAPPAY	YGDLGKAAARDL	FSKGFNYG	SH KL EVKSK	--TDSG--	E
<i>Daphnia magna</i>	--MAPPVY	YADLGKSSRDV	FGKGYHFS	LL KL ECKTK	--TSNG--	E
<i>Apis mellifera</i>	--APPSY	YNDLGKSARDL	FSKGYHFG	LI KL DVKTK	--TKSG--	E
<i>Homalodisca coagulata</i>	--MAPPTY	YGDLGKSAARDV	FGKGYHFG	LV KL DVKTK	--TSSG--	E
<i>Anopheles gambiae</i>	--MAPPSY	YSDLGKQARDV	FNKGYHFG	LV KL DVKTK	--TNSG--	E
<i>Drosophila melanogaster</i>	--MAPPSY	YSDLGKQARDI	FSKGYNFG	LV KL DLKTK	--TSSG--	E
<i>Drosophila pseudoobscura</i> PORB	--MAPPSY	YSDLGKQARDI	FSKGYNFG	LV KL DLKTK	--TPSG--	E
<i>Aedes aegypti</i>	--MAPPAY	YADLGKQARDV	FNKGYHFG	LV KL DVKTK	--TNSG--	E
<i>Rhipicephalus appendiculatus</i>	--MAPPCY	YADLGKQARDL	FNKGYHFG	LV KL DCKST	--TQTG--	E
<i>Ciona intestinalis</i>	--MPVPPQ	YTDLGKSAKDL	FEKGFYGF	FA KV DLKTK	--TSTG--	E
<i>Strongylocentrotus purpuratus</i>	--SY	YSDLGKAARDI	FGKGFYGF	FV KL DAKTT	--TSNN--	E
<i>Drosophila pseudoobscura</i> PORA	--MAPPSY	YDGLGKLARDL	FRRGYHPG	VW QL DCKSM	--SSPG--	E
<i>Drosophila melanogaster</i>	--AAKTPT	YDGLGKLARDL	FRRGYHPG	VW QL DCKTL	--TNSG--	E
<i>Monodelphis domestica</i> VDAC3	--MCTTPT	YCDLGKAAKDV	FNKGYG--	--EF--	--TSGH--	E
<i>Molgula tectiformis</i>	--KS	YARDL	FDKGYNYG	SN KV DVKSK	--SIDG--	E
<i>Macaca mulatta</i> VDAC1	--MAVPPK	FADLGKSARDV	FTKGYGFG	LI EL DLKTK	--EKNK--	E
<i>Hydra magnipapillata</i>	--TRPD	YI	YQKNFHF	GV KL EAKTK	--AKNG--	E
<i>Schistosoma japonicum</i>	--MVPPS	FSDLGKDARDL	LFKKFYFG	VY NI HCET	--KKNN--	E
<i>Drosophila melanogaster</i> Porin B	--EGEMPT	YFHVGLAKKDC	LINGFKI	GAW QM HCSTR	--TDND--	E
<i>Drosophila pseudoobscura</i>	--EGEMPT	YFHVGLAKKDC	LIRGYKFG	VW HL RCSSK	--MDNG--	E
<i>Drosophila melanogaster</i> Porin A	--EGEMPS	YFHVGLAKKMC	LI HGYTI	GAW KL DCTSK	--TEKD--	E
<i>Fugu rubripes</i>	--	--	--EF--	--	--TSTG--	E
<i>Fugu rubripes</i>	--	--	--EF--	--	--ATSG--	E
<i>Xenopus tropicalis</i> VDAC1	--MAVPPS	YADLGKSARDI	FNKGYGFG	LV KL DVKTK	--SATG--	E
<i>Xenopus tropicalis</i>	--MAVPPS	YADLGKSARDI	FNKGYGFG	LV KL DVKTK	--SATG--	E
<i>Amblyomma variegatum</i>	--MAPPCY	YADLGKQARDL	FNKGYHFG	VV KL DCKST	--TQTG--	E
<i>Branchiostoma floridae</i>	--	--	--	--	--	E
<i>Pratylenchus penetrans</i>	--LG	YKAAREL	FTKGYNFG	SM RV DACSR	--SGENH--	E
<i>Meloidogyne incognita</i>	--MAPPO	FYDFGKSTKDL	FTKGYTHG	LL KL DVKSK	--SGPN--	E
<i>Lymnaea stagnalis</i>	--LSPPS	FSDLGKSARDV	FSKGFNWG	FF KL DANKT	--TQNN--	E
<i>Necator americanus</i>	--	--	--	--	--	E
<i>Ancylostoma ceylanicum</i>	--MAPPT	FADLGKSARDL	FNKGYNHG	FL KV DSTTK	--AGDS--	E
<i>Nippostrongylus brasiliensis</i>	--MAPPT	FADLGKSARDL	FNKGYTHG	FL KV DATTR	--AGDN--	E
<i>Parastrongyloides trichosuri</i>	--RTVFN	--	--KGYFPG	LY KV ETTSN	--SGDN--	E
<i>Tribolium castaneum</i>	--MAPPP	--	--YSDLGK	AK AK DVFG	--KGYH--	E
<i>Ambystoma tigrinum</i>	--MAIPPT	--	--YVDLGKA	AR DVFA	--KGYG--	E
<i>Spermophilus lateralis</i>	--	--	--YADLGK	AS AR DVFT	--KGYG--	E
<i>Ixodes scapularis</i>	--	--	--	--	--	E
		60	70	80	90	100
<i>Ancylostoma caninum</i>	--SH--	YNLG	YSGKL	YGGNLDV	YKYI	YPAYGLT
<i>Caenorhabditis elegans</i> VDAC2	FKSAASHNI	GSGKL	YGGNLDV	YKYI	YPQYG	T LTEKWNTENQ
<i>Caenorhabditis briggsae</i>	FKSNASHNL	GSGKL	YGGNLDV	YKYI	YPQYG	T LTEKWNTENQ
<i>Caenorhabditis elegans</i>	FKSAASHNI	GSGKL	YGGNLDV	YKYI	YPQYG	T LTEKWNTENQ
<i>Ascaris suum</i>	FKTGAHV	TIASGR	YMAGNLDV	YKYI	PSYG	T LTEKWNTDNM
<i>Haemonchus contortus</i>	FKTSAAHNL	GSGKL	YGGNLDV	YKYI	PSYG	T LTEKWNTENQ
<i>Monodelphis domestica</i> VDAC2	FSSSGSSNTD	TGKVS	GTLET	YKWKCEY	GLT	FTEKWNTDNT
<i>Macaca mulatta</i> VDAC2	FSTSGSSNTD	TGKVT	GTLET	YKWKCEY	GLT	FTEKWNTDNT
<i>Bos taurus</i> VDAC2	FSTSGSSNTD	TGKVT	GTLET	YKWKCEY	GLT	FTEKWNTDNT
<i>Rattus norvegicus</i> VDAC2	FSTSGSSNTD	TGKVS	GTLET	YKWKCEY	GLT	FTEKWNTDNT
<i>Mus musculus</i> VDAC2	FSTSGSSNTD	TGKVS	GTLET	YKWKCEY	GLT	FTEKWNTDNT
<i>Homo sapiens</i> VDAC2	FSTSGSSNTD	TGKVT	GTLET	YKWKCEY	GLT	FTEKWNTDNT
<i>Sus scrofa</i> VDAC2	FSTSGSSNTD	TGKVT	GTLET	YKWKCEY	GLT	FTEKWNTDNT
<i>Homo sapiens</i> VDAC2	FSTSGSSNTD	TGKVT	GTLET	YKWKCEY	GLT	FTEKWNTDNT
<i>Gallus gallus</i> VDAC2	FTTSGSSNTD	TGKVN	GSLET	YKWA	EYGLT	FTEKWNTDNT
<i>Meleagris gallopavo</i> VDAC2	FTTSGSSNTD	TGKVN	GSLET	YKWA	EYGLT	FTEKWNTDNT
<i>Pan troglodytes</i> VDAC2	FSTSGSSNTD	TGKVT	GTLET	YKWKCEY	GLT	FTEKWNTDNT

		60		70		80		90		100																																								
<i>Gasterosteus aculeatus</i>	F	K	T	T	G	S	S	N	T	D	T	S	K	V	A	G	N	L	E	T	K	R	A	E	Y	G	L	T	F	T	E	K	W	N	T	D	N	T	L	G	-	T	E	I	T	V	E	D		
<i>Fugu rubripes</i>	F	K	T	S	G	S	S	N	T	D	T	S	K	V	A	G	S	L	E	T	K	Y	K	R	P	E	Y	G	L	T	F	T	E	K	W	N	T	D	N	T	L	G	-	T	E	I	T	V	E	D
<i>Fugu rubripes</i>	F	K	T	S	G	S	S	N	T	D	T	S	K	V	A	G	S	L	E	T	K	Y	K	R	P	E	Y	G	L	T	F	T	E	K	W	N	T	D	N	T	L	G	-	T	E	I	T	V	E	D
<i>Tetraodon nigroviridis</i>	F	K	T	S	G	S	S	N	T	D	T	S	K	V	A	G	S	L	E	T	K	Y	K	R	P	E	Y	G	L	T	F	T	E	K	W	N	T	D	N	T	L	G	-	T	E	I	T	V	E	D
<i>Ictalurus punctatus</i>	F	K	T	S	G	S	S	N	T	D	T	S	K	V	V	G	S	L	E	T	K	Y	K	R	S	E	Y	G	L	T	F	T	E	K	W	N	T	D	N	T	L	G	-	T	E	I	T	V	E	D
<i>Oncorhynchus mykiss</i>	F	K	T	A	G	S	T	N	T	D	T	S	K	V	A	G	S	L	E	T	K	Y	K	R	S	E	Y	G	L	T	F	T	E	K	W	N	T	D	N	T	L	G	-	T	E	I	T	V	E	D
<i>Oryzias latipes</i> VDAC2	F	K	T	S	G	S	S	N	T	D	T	S	K	V	S	G	T	L	E	T	K	Y	K	R	A	E	Y	G	L	T	F	T	E	K	W	N	T	D	N	T	L	G	-	T	E	I	T	V	E	D
<i>Danio rerio</i>	F	K	T	S	G	S	S	N	T	D	T	S	K	V	V	G	S	L	E	T	K	Y	K	R	S	E	Y	G	L	T	F	T	E	K	W	N	T	D	N	T	L	G	-	T	E	I	N	I	E	D
<i>Xenopus laevis</i> VDAC2	F	T	T	S	G	T	S	N	T	D	S	G	K	V	N	G	S	L	E	T	K	Y	K	W	G	E	Y	G	L	T	F	T	E	K	W	N	T	D	N	T	L	G	-	T	E	I	A	I	E	D
<i>Fugu rubripes</i>	F	K	T	S	G	S	S	N	I	D	N	S	K	V	T	G	T	L	E	T	K	Y	K	W	A	E	Y	G	L	T	F	T	E	K	W	S	T	E	N	T	L	G	-	T	E	V	C	V	E	D
<i>Fugu rubripes</i>	F	A	T	S	G	S	S	N	T	D	T	G	K	S	G	G	H	L	E	T	K	Y	K	M	K	E	L	G	L	N	F	S	Q	K	W	N	T	N	N	T	L	T	-	T	E	V	T	M	E	D
<i>Squalus acanthias</i>	F	T	T	S	G	S	S	N	T	D	T	G	K	A	T	G	S	L	E	T	K	Y	K	L	K	E	Y	G	L	T	F	T	E	K	W	N	T	D	N	N	L	A	-	T	E	I	T	V	E	D
<i>Danio rerio</i>	F	T	T	G	S	S	S	N	T	D	T	G	K	A	A	G	N	L	E	T	K	Y	K	V	K	E	L	G	L	S	L	N	Q	K	W	N	T	D	N	V	L	T	-	T	E	V	T	L	E	D
<i>Salmo salar</i>	F	A	T	S	G	S	S	N	T	D	T	G	K	A	A	G	N	L	E	T	K	Y	K	V	K	E	L	G	L	S	F	T	Q	K	W	N	T	D	N	T	L	T	-	T	E	V	S	M	E	D
<i>Monodelphis domestica</i> VDAC1	F	T	S	S	G	S	A	N	T	E	T	S	K	V	S	G	S	L	E	T	K	Y	K	W	S	E	Y	G	L	T	F	I	E	K	W	N	T	D	N	T	L	G	-	T	E	I	T	V	E	D
<i>Gallus gallus</i> VDAC1	F	T	S	S	G	S	A	N	S	E	T	S	K	V	S	G	S	L	E	T	K	Y	R	W	V	E	Y	G	L	M	F	T	E	K	W	N	T	D	N	T	L	G	-	T	E	I	T	L	E	D
<i>Rattus norvegicus</i> VDAC1	F	T	S	S	G	S	A	N	T	E	T	T	K	V	T	G	S	L	E	T	K	Y	R	W	T	E	Y	G	L	T	F	T	E	K	W	N	T	D	N	T	L	G	-	T	E	I	T	V	E	D
<i>Bos taurus</i> VDAC1	F	T	S	S	G	S	A	N	T	E	T	T	K	V	T	G	S	L	E	T	K	Y	R	W	T	E	Y	G	L	T	F	T	E	K	W	N	T	D	N	T	L	G	-	T	E	I	T	V	E	D
<i>Sus scrofa</i> VDAC1	F	T	S	S	G	S	A	N	T	E	T	T	K	V	T	G	S	L	E	T	K	Y	R	W	T	E	Y	G	L	T	F	T	E	K	W	N	T	D	N	T	L	G	-	T	E	I	T	V	E	D
<i>Homo sapiens</i> VDAC1	F	T	S	S	G	S	A	N	T	E	T	T	K	V	T	G	S	L	E	T	K	Y	R	W	T	E	Y	G	L	T	F	T	E	K	W	N	T	D	N	T	L	G	-	T	E	I	T	V	E	D
<i>Mus musculus</i> VDAC1	F	T	S	S	G	S	A	N	T	E	T	T	K	V	N	G	S	L	E	T	K	Y	R	W	T	E	Y	G	L	T	F	T	E	K	W	N	T	D	N	T	L	G	-	T	E	I	T	V	E	D
<i>Rattus norvegicus</i> VDAC1	F	T	S	S	V	S	A	N	T	E	T	T	K	V	N	C	S	L	E	T	K	Y	R	W	T	E	Y	G	V	T	F	T	E	K	W	N	T	D	N	T	L	G	-	T	E	T	T	V	E	D
<i>Xenopus laevis</i> VDAC1	F	T	S	S	G	S	A	N	A	E	T	S	K	V	S	G	N	L	E	T	K	Y	K	W	A	E	Y	G	L	T	F	T	E	K	W	N	T	D	N	T	L	G	-	T	E	I	T	V	E	D
<i>Xenopus tropicalis</i>	F	T	S	S	G	S	A	N	A	E	T	N	K	V	A	G	S	L	E	T	K	Y	K	W	A	E	Y	G	L	T	F	T	E	K	W	N	T	D	N	T	L	G	-	T	E	I	T	V	E	D
<i>Fundulus heteroclitus</i> VDAC1	F	T	S	T	C	S	G	N	T	E	T	S	K	V	A	G	S	L	E	T	K	Y	K	W	A	E	H	G	L	T	F	T	E	K	W	N	T	D	N	T	L	G	-	T	E	I	T	V	E	D
<i>Oryzias latipes</i> VDAC1	F	T	S	T	G	S	A	N	T	E	T	S	K	V	A	G	S	L	E	T	K	Y	K	W	A	E	H	G	L	T	F	T	E	K	W	N	T	D	N	T	L	G	-	T	E	I	T	V	E	D
<i>Danio rerio</i> VDAC1	F	K	S	S	G	S	A	N	T	E	T	S	K	V	A	G	T	L	E	T	K	Y	K	W	A	E	H	G	L	T	F	T	E	K	W	N	T	D	N	T	L	G	-	T	E	I	T	L	E	D
<i>Petromyzon marinus</i>	F	S	T	S	G	S	S	N	S	E	T	G	K	V	N	A	S	L	E	T	K	Y	K	W	A	D	Y	G	L	N	L	T	E	K	W	S	T	O	N	T	L	A	-	T	E	I	S	V	E	D
<i>Tetraodon nigroviridis</i>	F	K	T	S	G	S	S	N	I	D	N	S	K	V	T	G	N	L	E	T	K	Y	K	W	A	E	Y	G	L	T	F	T	E	K	W	S	T	E	N	T	L	G	-	T	E	V	C	F	E	D
<i>Oryctolagus cuniculus</i> VDAC3	F	S	T	S	G	H	A	Y	T	D	T	G	K	A	S	G	N	L	E	T	K	Y	K	V	C	N	Y	G	L	T	F	T	Q	K	W	N	T	D	N	T	L	G	-	T	E	I	S	L	E	N
<i>Sus scrofa</i> VDAC3	F	S	T	S	G	H	A	Y	T	D	T	G	K	A	S	G	N	L	E	T	K	Y	K	I	C	D	H	G	L	T	F	T	Q	K	W	N	T	D	N	T	L	G	-	T	E	I	S	L	E	N
<i>Bos taurus</i> VDAC3	F	S	T	S	G	H	A	Y	T	D	T	G	K	A	S	G	N	L	E	T	K	Y	K	I	C	N	Y	G	L	T	F	T	Q	K	W	N	T	D	N	T	L	G	-	T	E	I	S	L	E	N
<i>Mus musculus</i> VDAC3	F	S	T	S	G	H	A	Y	T	D	T	G	K	A	S	G	N	L	E	T	K	Y	K	V	C	N	Y	G	L	T	F	T	Q	K	W	N	T	D	N	T	L	G	-	T	E	I	S	L	E	N
<i>Homo sapiens</i> VDAC3	F	S	T	S	G	H	A	Y	T	D	T	G	K	A	S	G	N	L	E	T	K	Y	K	V	C	N	Y	G	L	T	F	T	Q	K	W	N	T	D	N	T	L	G	-	T	E	I	S	L	E	N
<i>Rattus norvegicus</i> VDAC3	F	S	T	S	G	H	A	Y	T	D	T	G	K	A	S	G	N	L	E	T	K	Y	K	V	C	N	Y	G	L	T	F	T	Q	K	W	N	T	D	N	T	L	G	-	T	E	I	S	L	E	N
<i>Pongo pygmaeus</i> VDAC3	F	S	T	S	G	H	A	Y	T	D	T	G	K	A	S	G	N	L	E	T	K	Y	K	V	R	N	Y	G	L	T	F	T	Q	K	W	N	T	D	N	T	L	G	-	T	E	I	S	L	E	N
<i>Gallus gallus</i> VDAC3	F	T	A	T	G	S	S	N	T	D	T	G	K	A	L	G	N	L	E	T	K	Y	K	I	K	D	Y	G	L	T	F	I	Q	K	W	N	T	D	N	T	L	G	-	T	E	V	S	M	E	D
<i>Pimephales promelas</i>	F	K	T	C	G	T	S	N	M	D	N	S	K	V	S	G	N	L	E	T	K	Y	K	W	A	E	Y	G	L	T	F	T	E	K	W	N	T	D	N	T	L	G	-	T	E	I	T	V	E	D
<i>Argopecten irradians</i>	F	T	T	K	G	S	S	S	H	D	S	G	K	V	S	G	S	L	E	T	K	Y	K	L	P	E	H	G	L	T	F	V	E	K	W	N	T	D	N	V	L	A	-	T	E	I	T	L	E	D
<i>Spisula solidissima</i>	F	T	T	K	G	S	H	N	T	D	T	G	R	V	S	G	E	L	T	E	K	C	S	D	Y	G	T	T	F	K	E	T	W	N	T	D	N	V	L	S	-	T	E	F	T	L	E	D		
<i>Daphnia magna</i>	F	T	T	G	G	S	S	N	L	D	S	G	K	V	V	G	N	L	E	T	K	Y	K	V	P	E	Y	G	L	T	F	T	E	K	W	N	T	D	N	T	L	G	-	T	E	I	A	I	E	D
<i>Apis mellifera</i>	F	S	S	G	G	V	S	N	Q	D	T	G	K	V	F	G	S	L	E	T	K	Y	N	I	D	D	Y	G	L	K	F	S	E	K	W	N	T	D	N	T	L	A	-	T	D	I	T	F	A	D
<i>Homalodiscus coagulata</i>	F	S	T	G	G	V	S	N	Q	E	T	G	K	V	F	G	T	L	E	T	K	Y	K	L	K	D	Y	G	V	T	F	T	E	K	W	N	T	D	N	V	L	V	-	T	E	V	S	-	A	Q
<i>Anopheles gambiae</i>	F	S	T	S	G	H	S	N	Q	D	T	G	K	V	F	G	S	L	E	T	K	Y	K	V	K	E	Y	G	L	N	F	S	E	K	W	N	T	D	N	T	L	T	-	S	E	V	S	V	E	N
<i>Drosophila melanogaster</i>	F	N	T	A	G	H	S	N	Q	E	T	G	K	V	F	G	S	L	E	T	K	Y	K	V	K	D	Y	G	L	T	L	E	K	W	N															

		110	120	130	140	150
<i>Ancylostoma caninum</i>	QFGRGL	KLT	FDSLY	APHAG	KR----	TGKL KADWSLQ TAR--TAEVGLT
<i>Caenorhabditis elegans</i> VDAC2	QFGRGL	KVT	LDSLY	APHAG	KR----	SGKV KLDWA--LPT ARVTADVGV
<i>Caenorhabditis briggsae</i>	QFGRGV	KVT	LDSLY	APHAG	KR----	SGKV KLDWA--LPT ARI TADVGV
<i>Caenorhabditis elegans</i>	QFGRGV	KVT	LDSLY	APHAG	KR----	SGKV KLDWA--LPT ARI TADVGV
<i>Ascaris suum</i>	QFARGL	KLT	LDSSY	APQVG	KR----	TGKV KAEWA--AES AKVTCDLGLD
<i>Haemonchus contortus</i>	QFGRGL	KLT	FDSLY	APHAG	KR----	TGKL KADWS--LNT ARI TGEVGI T
<i>Monodelphis domestica</i> VDAC2	QICQGL	KLT	FDTTF	SPNTG	KK----	SGKI KSAYKRECI N LGCDI DFDFA
<i>Macaca mulatta</i> VDAC2	QICQGL	KLT	FDTTF	SPNTG	KK----	SGKI KSAYKRECI N LGCDVDFDFA
<i>Bos taurus</i> VDAC2	QICQGL	KLT	FDTTF	SPNTG	KK----	SGKI KSAYKRECI N LGCDVDFDFA
<i>Rattus norvegicus</i> VDAC2	QICQGL	KLT	FDTTF	SPNTG	KK----	SGKI KSAYKRECI N LGCDVDFDFA
<i>Mus musculus</i> VDAC2	QICQGL	KLT	FDTTF	SPNTG	KK----	SGKI KSAYKRECI N LGCDVDFDFA
<i>Homo sapiens</i> VDAC2	QICQGL	KLT	FDTTF	SPNTG	KK----	SGKI KSAYKRECI N LGCDVDFDFA
<i>Sus scrofa</i> VDAC2	QICQGL	KLT	FDTTF	SPNTG	KK----	SGKI KSAYKRECI N LGCDVDFDFA
<i>Homo sapiens</i> VDAC2	QICQGL	KLT	FDTTF	SPNTG	KK----	SGKI KSAYKRECI N LGCDVDFDFA
<i>Gallus gallus</i> VDAC2	QIAKGL	KLT	FDTTF	SPNTG	KK----	SGKI KSAYKRECI N LGCDVDFDFA
<i>Meleagris gallopavo</i> VDAC2	QIAKGL	KLT	FDTTF	SPNTG	KK----	SGKI KSAYKRECI N LGCDVDFDFA
<i>Pan troglodytes</i> VDAC2	QICQGL	KLT	FDTTF	SPNTG	KK----	SGKI KSAYKRECI N LGCDVDFDFA
<i>Gasterosteus aculeatus</i>	QIAKGL	KLT	FDTTF	SPNTG	KK----	SGKV KTAYKREYVN VGCDVDFDFA
<i>Fugu rubripes</i>	QIAKGL	KLT	FDTTF	SPNTG	KK----	SGKV KTAYKREYVN LGCDVDFDFA
<i>Fugu rubripes</i>	QIAKGL	KLT	FDTTF	SPNTG	KK----	SGKV KTAYKREYVN LGCDVDFDFA
<i>Tetraodon nigroviridis</i>	QIAKGL	KLT	FDTTF	SPNTG	KK----	SGKV KTAYKREYVN LGCDVDFDFA
<i>Ictalurus punctatus</i>	QIAKGL	KLT	FDTTF	SPNTG	KK----	SGKV KTAYKREYVN LGCDVDFDFA
<i>Oncorhynchus mykiss</i>	QIVKGL	KLT	FDTTF	SPNTG	KK----	SGKV KTAYKREYVN LGCDVDFDFA
<i>Oryzias latipes</i> VDAC2	QIAKGL	KLT	FDTTF	SPNTG	KK----	SGKV KAAYKREYVN LGCDVDFDFA
<i>Danio rerio</i>	QIAKGL	KLT	FDTTF	SPNTG	KK----	SGKV KTAYKREYVN LGCDVDFDFA
<i>Xenopus laevis</i> VDAC2	QIAKGL	KLT	FDTTF	SPNTG	KK----	SGKV KAAYKREYVN LGCDVDFDFA
<i>Fugu rubripes</i>	QITKGL	KLN	FETTF	SPNTG	KK----	SGKI KTAYKREYVN AGLDVDFDFA
<i>Fugu rubripes</i>	QLAKGL	KLK	LDTSF	VPNTG	KK----	SAKL KTSYKRDYVN VGCDLDFDMA
<i>Squalus acanthias</i>	QLAKGL	KLT	FDTTF	VPNTG	KK----	SAKL KTAYKRDYVN LGCDI DFDFA
<i>Danio rerio</i>	QLAKGL	KLK	LDTSF	VPNTG	KK----	SAKL KTGYKREYMN VGCDLDFDLA
<i>Salmo salar</i>	QLAKGL	KLK	LDTSF	VPNTG	KK----	SAKL KTGYKRDYFN LGCDLDFDMA
<i>Monodelphis domestica</i> VDAC1	QLARGL	KLT	FDSSF	SPNTG	KK----	NAKI KSGYKREHI N LGCDMDFDIS
<i>Gallus gallus</i> VDAC1	QLARGL	KLT	FDSSF	SPNTG	KK----	NAKI KTGYKREHI N MGCDMDFDIA
<i>Rattus norvegicus</i> VDAC1	QLARGL	KLT	FDSSF	SPNTG	KK----	NAKI KTGYKREHI N LGCDMDFDIA
<i>Bos taurus</i> VDAC1	QLARGL	KLT	FDSSF	SPNTG	KK----	NAKI KTGYKREHI N LGCDVDFDIA
<i>Sus scrofa</i> VDAC1	QLARGL	KLT	FDSSF	SPNTG	KK----	NAKI KTGYKREHI N LGCDVDFDIA
<i>Homo sapiens</i> VDAC1	QLARGL	KLT	FDSSF	SPNTG	KK----	NAKI KTGYKREHI N LGCDMDFDIA
<i>Mus musculus</i> VDAC1	QLARGL	KLT	FDSSF	SPNTG	KK----	NAKI KTGYKREHI N LGCDVDFDIA
<i>Rattus norvegicus</i> VDAC1	QLARGL	KLT	FDSSF	SPNTG	EK----	NAKI KTGYKREHI N LGCDVDFDIT
<i>Xenopus laevis</i> VDAC1	QLAKGL	KLT	FDSSF	SPNTG	KK----	NAKV KSAYKREHLN VGCDMDFDIA
<i>Xenopus tropicalis</i>	QLAKGL	KLT	FDSSF	SPNTG	KK----	NAKV KTAYKREHLN IGCDVDFDIA
<i>Fundulus heteroclitus</i> VDAC1	QLLKGL	KLT	LDSSF	SPNTG	KK----	GGKI KTAYKCDHIN LGCDVNYDIN
<i>Oryzias latipes</i> VDAC1	QLAKGL	KLT	LDSSF	SPNTG	KK----	GGKV KTAYKCDHVN VGCDVNYDIN
<i>Danio rerio</i> VDAC1	QLTKGL	KLT	FDSSF	SPNTG	KK----	SGKI KSAYKREHI N LGCDVDFDIN
<i>Petromyzon marinus</i>	QLAKGL	KLT	LDTTF	APNTG	KK----	SGKL KSTYKREYLN VGCDVDFDFA
<i>Tetraodon nigroviridis</i>	QITKGL	KLN	FETTF	SPNTG	KK----	SGKI KTAYKREYLN AGLDVDFDFA
<i>Oryctolagus cuniculus</i> VDAC3	KLAEGL	KLT	LDTF	FVPNTG	KK----	SGKL KASYKRDYFN LGSNVDIDFS
<i>Sus scrofa</i> VDAC3	KLAEGL	KLT	LDTF	FVPNTG	KK----	SGKL KASYKRDYFN LGSNVDIDFA
<i>Bos taurus</i> VDAC3	KLAEGL	KLT	LDTF	FVPNTG	KK----	SGKL KASYKRDYFN LGSNVDIDFS
<i>Mus musculus</i> VDAC3	KLAEGL	KLT	LDTF	FVPNTG	KK----	SGKL KASYKRDYFN LGSNVDIDFS
<i>Homo sapiens</i> VDAC3	KLAEGL	KLT	LDTF	FVPNTG	KK----	SGKL KASYKRDYFN VGSNVDIDFS
<i>Rattus norvegicus</i> VDAC3	KLAEGL	KLT	LDTF	FVPNTG	KK----	SGKL KASYKRDYFN VGSNVDIDFS
<i>Pongo pygmaeus</i> VDAC3	KLAEGL	KLT	LDTF	FVPNTG	KK----	SGKL KASYKRDYFN VGSNVDIDFS
<i>Gallus gallus</i> VDAC3	QLAEGL	KVA	LDTF	FVPNTG	KK----	SGKL KTSYKRDYVN LGCDVDFDLS
<i>Pimephales promelas</i>	QITKGL	KLT	FDTTF	SPNTG	KK----	SGKV KSAYKREYLN VGCDVDFDFA
<i>Argopecten irradians</i>	QLCKGL	KLK	FESSF	APQTG	KK----	NGKI KTAYKMDYLN ASCDVDFDFA
<i>Spisula solidissima</i>	QLAQGL	KLK	FDTSF	APQTG	KK----	SGKV KTGYKNDYVN MNCVDFDFA
<i>Daphnia magna</i>	KIAQGL	KLT	FDSTF	APQTG	KK----	TGVV KAEFKHDT AT LNADVD--LN
<i>Apis mellifera</i>	KLLKGL	TLG	YGCTF	SPQTG	TK----	TGKL KTAYKHONVS AAADFDSLS
<i>Homalodisca coagulata</i>	DFMKGV	KVS	LDTSF	KPQTG	DK----	SKA KTEFRNQT VS VNCDLDFKA
<i>Anopheles gambiae</i>	QLVKGL	KVS	FDGMF	APHTG	SK----	TGRF KTAYSHDR VR VDADFNVDS
<i>Drosophila melanogaster</i>	QLLEGL	KLS	LEGNF	APQSG	NK----	NGKF KVAYGHENVK ADSDVNI DLK
<i>Drosophila pseudoobscura</i> PORB	QLLEGL	KLS	LEGNF	APQSG	NK----	NGKF KVGFGEHYVK ADSDVNI DLK
<i>Aedes aegypti</i>	QLVKGL	KLS	FDGSF	APQTG	SK----	TGRF KTAYSHDKVR VDADFNVDLA
<i>Rhipicephalus appendiculatus</i>	KLARGL	KVA	FNANF	APQTG	KK----	SGAL KAAYKLENVH LGCDVDFLGPP
<i>Ciona intestinalis</i>	QIATGM	KLT	LCTSF	APNTG	KK----	SGAL KTAYKRDYFN CNLDLDFNFA
<i>Strongylocentrotus purpuratus</i>	QIAQGV	KLT	LDTSF	SPQTG	KK----	SGKI KTAYKRDYFN ITDLDVDFDFA
<i>Drosophila pseudoobscura</i> PORA	KLAQGL	MLG	LEGRF	QPS--	E----	DGKF KLGYY--EDH FNF LDMGSL
<i>Drosophila melanogaster</i>	KLAQGL	MLA	VEAKF	QPSGN	EA----	DGKF KMGYA--QDN FNF LADI GLN
<i>Monodelphis domestica</i> VDAC3	KLADGL	KLT	LDTF	FVPNTG	KK----	SGKL KASYKRDYFN LGSNVDIDFS
<i>Molgula tectiformis</i>	QLCNGS	KVT	LCSAF	SPDTG	KK----	SGAL KTEYKRDYFN LNLDLDFDFA
<i>Macaca mulatta</i> VDAC1	QLSHEL	KVT	FNSSF	SPNTG	EK----	MLKS RQGT--RST LTWAE TWILT
<i>Hydra magnipapillata</i>	KIAQGV	KVD	FDTTF	APVTG	KK----	SAKV KSAYAHENLH ATT D DFDFA
<i>Schistosoma japonicum</i>	KLVDGL	KQT	FQI	SRDPFKK	CK----	NANL INSFNRDHN VN SNVEMFFKSA
<i>Drosophila melanogaster</i> Porin B	MNFGSRLY	GL	LKSTI	GTKDE	VSF--	QTKL KCGLE--RDP VKVELVDFLY
<i>Drosophila pseudoobscura</i>	LVAGGI	HSI	LRSALSMTDE	HQFSI	GS	SLL KAGFM--RSP ENIEIVVPIV
<i>Drosophila melanogaster</i> Porin A	DGLGGTW	STV	LKSMV	SYPEG	RKF--	QCKL KCGFD--RNP GKVMYFIPIY

		160	170	180	190	200
<i>Bos taurus</i> VDAC1	--GP-SI--	R GALVVG-YEG	WLAGYQMNFE	TAKSRVT	QSN	FAVGYKTDF
<i>Sus scrofa</i> VDAC1	--GP-SI--	R GALVVG-YEG	WLAGYQMNFE	TAKSRVT	QSN	FAVGYKTDF
<i>Homo sapiens</i> VDAC1	--GP-SI--	R GALVVG-YEG	WLAGYQMNFE	TAKSRVT	QSN	FAVGYKTDF
<i>Mus musculus</i> VDAC1	--GP-SI--	R GALVVG-YEG	WLAGYQMNFE	TSKSRVT	QSN	FAVGYKTDF
<i>Rattus norvegicus</i> VDAC1	--GP-SI--	R GSLVVG-YEG	WLAGYQMNFE	TSKSRVT	QSN	FAVGYKTDF
<i>Xenopus laevis</i> VDAC1	--GP-SV--	R GAVVVG-YEG	WLAGYQMTFE	SSKSRVS	QSN	FAVGYKTDF
<i>Xenopus tropicalis</i>	--GP-SV--	R GAVVVG-YEG	WLAGYQMTFE	SSKSRVS	QSN	FAVGYKTDF
<i>Fundulus heteroclitus</i> VDAC1	--GT-AV--	H GAAVVG-FEG	WLAGYQMTFE	AAGTRSP	RAI	FAVGYKTDF
<i>Oryzias latipes</i> VDAC1	--GT-AI--	H GAAVVG-YEG	WLAGYQMTFE	AGRNKVT	QSN	FAVGYKTDF
<i>Danio rerio</i> VDAC1	--GT-AV--	H GALVVG-LDG	WLAGYQMTFE	AGRNRI	TQSN	FAVGYKTDF
<i>Petromyzon marinus</i>	--GP-TV--	N GAAVVG-YEG	WLAGYQLAFD	TAKSKL	TRSN	FAIGYKTADF
<i>Tetraodon nigroviridis</i>	--GP-TI--	H GAAVAG-YEG	WLAGYQMTID	SAKSKL	MAHSN	FAIGYKTGDF
<i>Oryctolagus cuniculus</i> VDAC3	--GP-TI--	Y GWAVLA-FEG	WLAGYQMSFD	TAKSKL	SQNN	FALGYKAADF
<i>Sus scrofa</i> VDAC3	--GP-TI--	Y GWAVLA-FEG	WLAGYQMSFD	TAKSKL	SQNN	FALGYKAADF
<i>Bos taurus</i> VDAC3	--GP-TI--	Y GWAVLA-FEG	WLAGYQMSFD	TAKSKL	SQNN	FALGYKAADF
<i>Mus musculus</i> VDAC3	--GP-TI--	Y GWAVLA-FEG	WLAGYQMSFD	TAKSKL	SQNN	FALGYKAADF
<i>Homo sapiens</i> VDAC3	--GP-TI--	Y GWAVLA-FEG	WLAGYQMSFD	TAKSKL	QNN	FALGYKAADF
<i>Rattus norvegicus</i> VDAC3	--GP-TI--	Y GWAVLA-FEG	WLAGYQMSFD	TAKSKL	QNN	FALGYKAADF
<i>Pongo pygmaeus</i> VDAC3	--GP-TI--	Y GWAVLA-FEG	WLAGYQMSFD	TAKSKL	QNN	FALGYKAADF
<i>Gallus gallus</i> VDAC3	--GP-TI--	Y GWAVLG-YEG	WLAGYQMAFD	TAKSKL	SQNN	FALGYKAGDF
<i>Pimephales promelas</i>	--GP-AV--	H GAAVLA-FEG	WLAGYQMTFD	TAKSKM	TRSN	FAIGYKTGDF
<i>Argopecten irradians</i>	--GP-TV--	H GAAVVG-YN	FLAGYQMSFD	TSKSKL	SKNN	FAFGYSSDDM
<i>Spisula solidissima</i>	--GP-TV--	N GAAVLG-YN	FLAGYQMAFD	TSKSKL	TNN	ISGGYDAGDF
<i>Daphnia magna</i>	--GGP-TV--	N GAAVCG-YMG	WLAGYQMSFD	MSKSKL	TRNN	FSIAYAAKDF
<i>Apis mellifera</i>	-TGP-LV--	N ASTVVG-YQG	WLAGYQACFD	TQRNKL	TKNN	FALGYTASDF
<i>Homalodisca coagulata</i>	-GAP-LV--	N AAVALG-YN	WLAGYSTKFD	SQKSKL	TGNN	FALGYAAGDL
<i>Anopheles gambiae</i>	--GP-LV--	N ASGVAA-YQG	WLAGYQVAFD	SQKSKL	TANN	FALGYAGDF
<i>Drosophila melanogaster</i>	--GP-LI--	N ASAVLG-YQG	WLAGYQTAFD	TQSKL	LTNN	FALGYTTKDF
<i>Drosophila pseudoobscura</i> PORB	--GP-LI--	N ASAVLG-YN	WLAGYQAADF	TQSKL	LTNN	FALGYTTKDF
<i>Aedes aegypti</i>	--GP-LV--	N ASGVFN-YQG	WLAGYQVAFD	SQKSKV	TANN	FALGYTGDF
<i>Rhipicephalus appendiculatus</i>	--GP-LV--	H GAVALH-YQG	WLAGAQVAFD	TQSKL	LTNN	FALGYTGDF
<i>Ciona intestinalis</i>	--GP-TL--	Q GACVFG-YEG	WLAGYQVAFD	TNKSALT	KNN	VAVGYNGADF
<i>Strongylocentrotus purpuratus</i>	--GP-TV--	H STGVVG-YE	GLAGFQVSFD	TAESKL	KKSN	FALGYKTADF
<i>Drosophila pseudoobscura</i> PORA	--SSP-IM--	N CSLVLG-HKE	FLGGLGCTFD	LGDTSL	SSWK	VALGWSNDKA
<i>Drosophila melanogaster</i>	--SEP-IL--	N CSLVLG-HKE	FLGGVGTDF	VGNTL	LKWK	VALGWTNETA
<i>Monodelphis domestica</i> VDAC3	--GP-TI--	Y GWAVLA-YEG	WLAGYQMSFD	TAKSKL	QNN	FALGYKAGDF
<i>Molgula tectiformis</i>	--GP-TL--	Q GAVALG-YEG	WLAGYQVAFD	TSCSALT	KNN	LALGYNGSDF
<i>Macaca mulatta</i> VDAC1	LLGPQSR--	V LWCWVT-RAG	WPATRI LRMQ	SPEPRAT	V-Q	LATRLMNSSF
<i>Hydra magnipapillata</i>	--GP-TV--	H GSAVFA-YKG	FHAGYQASFN	SANSKLT	SN	VCLAYKNGDL
<i>Schistosoma japonicum</i>	--I-P-DL--	S PSLVFG-YQG	YLVGADVCLD	CTNQI	LKAN	FAVGYTKQDF
<i>Drosophila melanogaster</i> Porin B	--NEP-LF--	L GYVLVAPVEN	WVLGYRTEYN	FDEKGF	KHA	LCLGYNNGRT
<i>Drosophila pseudoobscura</i>	--KEP-TL--	M GYVLAAPEN	WVLGYRTVYS	VAEKADF	KHA	FCLGYNNGST
<i>Drosophila melanogaster</i> Porin A	--KEP-TL--	M GYI MMQPVKN	YLLGYRTVFN	VEDRDFN	MHA	FCGGYNDVT
<i>Fugu rubripes</i>	--GT-AI--	H GAAVVG-YEG	WLAGYQMTFE	AGRNRI	YTQSN	FAVGYKTDF
<i>Fugu rubripes</i>	--GP-TI--	Q AAVALG-YEG	WLAGYQLAFD	TAKSTLT	QNN	FAFGYRAGDF
<i>Xenopus tropicalis</i> VDAC1	--AGP-AI--	H GSAVVG-YEG	WLAGYQMTFD	SAKSKLT	KNN	FAVGYKTGDF
<i>Xenopus tropicalis</i>	--AGP-AI--	H GSAVVG-YEG	WLAGYQMTFD	SAKSKLT	KNN	FAVGYKTGDF
<i>Amblyomma variegatum</i>	PPGP-IA--	H GAVALH-YQG	WLAGGQVSFD	TTKNRLS	RTN	FAVGQYAGDF
<i>Branchiostoma floridae</i>	--GP-TI--	H GAVALG-YEG	WLAGYQMSFD	TAKSKL	TRSN	FALGYKTGDF
<i>Pratylenchus penetrans</i>	--TGP-QI--	N FSGVT-GLHG	WLLGAQSAFD	VSSSQLK	AI	SFGRI GTDY
<i>Meloidogyne incognita</i>	-GAP-VL--	E VFGVSKYK	WMAGAKAKYD	LQANELK	ATS	LAF LHQTSDY
<i>Lymnaea stagnalis</i>	--GP-TV--	H GAVALG-YEG	WLAGYQLSFD	TSKSKLT	RSN	FGFGYAGGDF
<i>Necator americanus</i>	--SAP-VV--	N AAGVFS-REG	WLFGAAASFD	TATNKLAS	STS	LAFGHQTSNY
<i>Ancylostoma ceylanicum</i>	--SAP-VI--	N AAGVFS-REG	WLFGAAASFD	TATNKLAS	STS	LAFGHQTSNY
<i>Nippostrongylus brasiliensis</i>	--ASP-VI--	N AAGVFS-REG	WLFGAAATFD	TSTNKVA	STS	LAFGHQHSY
<i>Parastrongyloides trichosuri</i>	--STP-VV--	N AAGVFS-REG	WLFGAAASFD	TASNKLA	SSQ	LAFGHQTADY
<i>Tribolium castaneum</i>	-----	K GLKLS--SDL	TFSPQTGSKS	ARVKTA	FTND	RVALNCDVDL
<i>Ambystoma tigrinum</i>	-----	K GLKLT--FDS	SFSPNTGKKN	AKI KSA	YKRE	HINLGCDMDF
<i>Spermophilus lateralis</i>	-----	R GLKLT--FDS	SFSPNTGKKN	AKI KTG	YKRE	HINLGCDVDF
<i>Ixodes scapularis</i>	-----	R GLKLA--FNA	HFAPQTGKKS	GALKTA	YKVD	NIHVNSDVDL
		210	220	230	240	250
<i>Ancylostoma caninum</i>	TLHSFVN-S	TDFGASLFHK	VAHNVEI GTI	LGW-KV	GGSG	-A-DFGVATK
<i>Caenorhabditis elegans</i> VDAC2	TLHSFVN-S	TDFGASLYHK	VASNVEVGTQ	LGW-KV	GGNG	-A-DYALATK
<i>Caenorhabditis briggsae</i>	TLHSFVN-S	NDFGASLYHK	VASNVEI GTQ	VGW-KV	GSNG	-A-DYALATK
<i>Caenorhabditis elegans</i>	TLHSFVN-S	NDFGASLYHK	VAPNVEI GTQ	LGW-KV	GGNG	-A-DYALATK
<i>Ascaris suum</i>	TLHSFVND-G	QDFGASLYHR	AAHNVEVGAQ	LGW-TV	GDQG	-A-RFALAAK
<i>Haemonchus contortus</i>	TLHSFVNV-S	TDFGASLFHR	VSPNVELGTM	LGW-KV	GGNG	-A-DFAVAANK
<i>Monodelphis domestica</i> VDAC2	QLHTNVND-G	TEFGGSI YQK	VCEDLDTSVN	LAW-T	SGTNC	-T-RFGIAAK
<i>Macaca mulatta</i> VDAC2	QLHTNVND-G	TEFGGSI YQK	VCEDLDTSVN	LAW-T	SGTNC	-T-RFGIAAK
<i>Bos taurus</i> VDAC2	QLHTNVND-G	TEFGGSI YQK	VCEDLDTSVN	LAW-T	SGTNC	-T-RFGIAAK
<i>Rattus norvegicus</i> VDAC2	QLHTNVNN-G	TEFGGSI YQK	VCEDFDTSVN	LAW-T	SGTNC	-T-RFGIAAK
<i>Mus musculus</i> VDAC2	QLHTNVNN-G	TEFGGSI YQK	VCEDFDTSVN	LAW-T	SGTNC	-T-RFGIAAK
<i>Homo sapiens</i> VDAC2	QLHTNVND-G	TEFGGSI YQK	VCEDLDTSVN	LAW-T	SGTNC	-T-RFGIAAK
<i>Sus scrofa</i> VDAC2	QLHTNVND-G	TEFGGSI YQK	VCEDLDTSVN	LAW-T	SGTNC	-T-RFGIAAK
<i>Homo sapiens</i> VDAC2	QLHTNVND-G	TEFGGSI YQK	VCEDLDTSVN	LAW-T	SGTNC	-T-RFGIAAK

	210	220	230	240	250
<i>Gallus gallus</i> VDAC2	QLHTNVND-G	SEFGGSIYQK	VSDNLETAVN	LAWTAGSNS	-T-RFGIAAK
<i>Meleagris gallopavo</i> VDAC2	QLHTNVND-G	SEFGGSIYQK	VSDNLETAVN	LAWTAGSNS	-T-RFGIAAK
<i>Pan troglodytes</i> VDAC2	QLHTNVND-G	TEFGGSIYQK	VCEDLDTSVN	LAWTSGTNC	-T-RFGIAAK
<i>Gasterosteus aculeatus</i>	QLHTNVND-G	AEFGGSIYQK	VSDQLETAVN	LAWTAGSNS	-T-RFGIAAK
<i>Fugu rubripes</i>	QLHTNVND-G	AEFGGSIYQK	VSDKLETAVN	LAWTAGSNS	-T-RFGIAAK
<i>Fugu rubripes</i>	QLHTNVND-G	AEFGGSIYQK	VSDKLETAVN	LAWTAGSNS	-T-RFGIAAK
<i>Tetraodon nigroviridis</i>	QLHTNVND-G	AEFGGSIYQK	VSDKLETAVN	LAWTAGSNS	-T-RFGIAAK
<i>Ictalurus punctatus</i>	QLHTNVND-G	AEFGGSIYQK	VSDNLETAVN	LAWTAGSNS	-T-RFGIAAK
<i>Oncorhynchus mykiss</i>	QLHTNVND-G	VQFGGSIYQK	VSPALETAVN	LAWTAGSNS	-T-RFGIAAK
<i>Oryzias latipes</i> VDAC2	QLHTNVND-G	SEFGGSIYQK	VSDKLETAVS	LAWTAGSNS	-T-RFGIAAK
<i>Danio rerio</i>	QLHTNVND-G	SEFGGSIYQK	VSDKLETAVN	LAWTAGSNS	-T-RFGIAAK
<i>Xenopus laevis</i> VDAC2	QLHTNVND-G	SEFAGSIYQK	VSDKLETAVN	LAWTSGNNS	-T-RFGIAAK
<i>Fugu rubripes</i>	QLHTNVND-G	SEFGGSIYQK	VNDKLETAVN	LAWTAGSNG	-T-RFGIAAK
<i>Fugu rubripes</i>	QLHTSVND-G	TEFGGSVYQK	VNSNLETAVT	LAWTAGSNN	-T-RFGVGA
<i>Squalus acanthias</i>	QLHTNVND-G	AEFGGSIYQK	VNDKLETAVN	LAWTAGSNN	-T-RFGIAAK
<i>Danio rerio</i>	QLHTNVND-G	TEFGGSIYQK	VNGQLETAVN	LAWTAGSNN	-T-RFGIAAK
<i>Salmo salar</i>	QLHTNVND-G	TEFGGSIYQK	VNCHLETAVN	LAWTAGSNN	-T-RFGIAAK
<i>Monodelphis domestica</i> VDAC1	QLHTNVND-G	TEFGGSIYQK	VNKKLETAVN	LAWTAGSNN	-T-RFGIAAK
<i>Gallus gallus</i> VDAC1	QLHTNVND-G	TEFGGSIYQK	VNEKLETAVN	LAWTAGSNN	-T-RFGIAAK
<i>Rattus norvegicus</i> VDAC1	QLHTNVND-G	TEFGGSIYQK	VNKKLETAVN	LAWTAGSNN	-T-RFGIAAK
<i>Bos taurus</i> VDAC1	QLHTNVND-G	TEFGGSIYQK	VNKKLETAVN	LAWTAGSNN	-T-RFGIAAK
<i>Sus scrofa</i> VDAC1	QLHTNVND-G	TEFGGSIYQK	VNKKLETAVN	LAWTAGSNN	-T-RFGIAAK
<i>Homo sapiens</i> VDAC1	QLHTNVND-G	TEFGGSIYQK	VNKKLETAVN	LAWTAGSNN	-T-RFGIAAK
<i>Mus musculus</i> VDAC1	QLHTNVND-G	TEFGGSIYQK	VNKKLETAVN	LAWTAGSNN	-T-RFGIAAK
<i>Rattus norvegicus</i> VDAC1	QLHTNVND-G	TEFGGSIYQK	VNKKLETAVN	LAWTAGSNN	-T-RFGIAAK
<i>Xenopus laevis</i> VDAC1	QLHTNVND-G	TEFGGSVYQK	VNDKLETAVN	LAWTAGSNN	-T-RFGIAAK
<i>Xenopus tropicalis</i>	QLHTNVND-G	TEFGGSVYQK	VNDKLETAVN	LAWTAGSNN	-T-RFGIAAK
<i>Fundulus heteroclitus</i> VDAC1	QLHTNVND-G	TEFGGSIYQK	VNDKLETAVN	LAWTAGSNN	-T-RFGIAAK
<i>Oryzias latipes</i> VDAC1	QLHTNVND-G	TEFGGSIYQK	VNEQLETAVN	LAWTAGSNN	-T-RFGIAAK
<i>Danio rerio</i> VDAC1	QLHTNVND-G	TEFGGSIYQK	VNDNLETAVN	LAWTAGSNN	-T-RFGIAAK
<i>Petromyzon marinus</i>	QLHTNVND-G	TEFGGSIYQK	VNDKLETAVD	LAWTAGSNT	-T-RFGIAAK
<i>Tetraodon nigroviridis</i>	QLHTNVND-G	AEFGGSIYQK	VSDKLETAVN	LAWTAGSNN	-T-RFGIAAK
<i>Oryctolagus cuniculus</i> VDAC3	QLHTNVND-G	TEFGGSIYQK	VNEKLETAVN	LAWTAGSNN	-T-RFGIAAK
<i>Sus scrofa</i> VDAC3	QLHTNVND-G	TEFGGSIYQK	VNEKLETAVN	LAWTAGSNN	-T-RFGIAAK
<i>Bos taurus</i> VDAC3	QLHTNVND-G	TEFGGSIYQK	VNEKLETAVN	LAWTAGSNN	-T-RFGIAAK
<i>Mus musculus</i> VDAC3	QLHTNVND-G	TEFGGSIYQK	VNERLETAVN	LAWTAGSNN	-T-RFGIAAK
<i>Homo sapiens</i> VDAC3	QLHTNVND-G	TEFGGSIYQK	VNEKLETAVN	LAWTAGSNN	-T-RFGIAAK
<i>Rattus norvegicus</i> VDAC3	QLHTNVND-G	TEFGGSIYQK	VNEKLETAVN	LAWTAGSNN	-T-RFGIAAK
<i>Pongo pygmaeus</i> VDAC3	QLHTNVND-G	TEFGGSIYQK	VNEKLETAVN	LAWTAGSNN	-T-RFGIAAK
<i>Gallus gallus</i> VDAC3	QLHTNVND-G	TEFGGSIYQK	VNKKLETAVN	LAWTAGSNN	-T-RFGIAAK
<i>Pimephales promelas</i>	QLHTNVND-G	TEFGGSIYQK	VNDKLETAVN	LAWTAGSNN	-T-RFGIAAK
<i>Argopecten irradians</i>	TLHCNND-G	AEFGGSVYQK	VNSKLETAVN	LAWTAGSNN	-T-RFGIAAK
<i>Spisula solidissima</i>	TLNTSVND-F	TEFGGSVYQK	VNKNLETAVN	LAWTAGSNN	-T-RFGIAAK
<i>Daphnia magna</i>	ALHTNVND-G	QEFGGALFQK	VNPNLETAVN	LAWTAGSNN	-T-RFGIAAK
<i>Apis mellifera</i>	TLHAAVND-G	CDFSGLIYHK	VKPELETAVN	LAWTAGSNN	-T-RFGIAAK
<i>Homalodisca coagulata</i>	VFHTSVND-G	QEFGGSIYQK	VNPNLETAVN	LAWTAGSNN	-T-RFGIAAK
<i>Anopheles gambiae</i>	VLHTNVND-G	REFGGSIYQK	CNDRLETAVN	LAWTAGSNN	-T-RFGIAAK
<i>Drosophila melanogaster</i>	VLHTNVND-G	QEFSGSIYQK	TSDKLETAVN	LAWTAGSNN	-T-RFGIAAK
<i>Drosophila pseudoobscura</i> PORB	VLHTNVND-G	QEFSGSIYQK	TSDKLETAVN	LAWTAGSNN	-T-RFGIAAK
<i>Aedes aegypti</i>	VLHTNVND-G	REFGGSIYQK	CNDRLETAVN	LAWTAGSNN	-T-RFGIAAK
<i>Rhipicephalus appendiculatus</i>	VLHTNVND-G	QEFAGSVYQK	VSPQLETAVN	LAWTAGSNN	-T-RFGIAAK
<i>Ciona intestinalis</i>	QLTTMND-A	SEFGGSIYQK	VNKNLETAVN	LAWTAGSNN	-T-RFGIAAK
<i>Strongylocentrotus purpuratus</i>	QLHTNVND-G	SDFGGSIYQK	VNDSLETAVN	LAWTAGSNN	-T-RFGIAAK
<i>Drosophila pseudoobscura</i> PORA	TLHGELND-G	DSWLASLFYK	LNDQDAAVE	LAWTAGSNN	-T-RFGIAAK
<i>Drosophila melanogaster</i>	TLHGELND-G	DLWLASLFYK	ASEKDAVE	LAWTAGSNN	-T-RFGIAAK
<i>Monodelphis domestica</i> VDAC3	QLHTNVND-G	TEFGGSIYQK	VSEKLETAVN	LAWTAGSNN	-T-RFGIAAK
<i>Molgula tectiformis</i>	QLTTMND-G	TEFGGSIYQK	VNKNLETAVN	LAWTAGSNN	-T-RFGIAAK
<i>Macaca mulatta</i> VDAC1	TL-----	KM-I	GQFGGSIYQK	VN-K	LETTINLTW
<i>Hydra magnipapillata</i>	VIHSGVAD-A	SKFVGSVHHQ	INEQLAAAL	LAWTAGSNN	-T-RFGIAAK
<i>Schistosoma japonicum</i>	AFHGLITNWG	KQFSANMFQR	ITDR	LAWTAGSNN	-T-RFGIAAK
<i>Drosophila melanogaster</i> Porin B	EVGLKLEN-F	EDLRGSIYQK	IGEA	LAWTAGSNN	-T-RFGIAAK
<i>Drosophila pseudoobscura</i>	EMGLKAEN-F	KDLRGSIYQK	IGES	LAWTAGSNN	-T-RFGIAAK
<i>Drosophila melanogaster</i> Porin A	EVGLKLEN-F	KALRGSIYQK	IGEK	LAWTAGSNN	-T-RFGIAAK
<i>Fugu rubripes</i>	QLHTNVND-G	TEFGGSIYQK	VNEQLETAVN	LAWTAGSNN	-T-RFGIAAK
<i>Fugu rubripes</i>	QLHTSVND-G	TEFGGSVYQK	VNSNLETAVT	LAWTAGSNN	-T-RFGIAAK
<i>Xenopus tropicalis</i> VDAC1	QLHTNVND-G	SEFAGSIYQK	VSDKLETAVN	LAWTAGSNN	-T-RFGIAAK
<i>Xenopus tropicalis</i>	QLHTNVND-G	SEFAGSIYQK	VSDKLETAVN	LAWTAGSNN	-T-RFGIAAK
<i>Amblyomma variegatum</i>	AVHTNVND-G	QEVAGSVYQK	VNPQLETAVN	LAWTAGSNN	-T-RFGIAAK
<i>Branchiostoma floridae</i>	QLHTNVND-G	TEFGGSIYQK	VNKNLETAVN	LAWTAGSNN	-T-RFGIAAK
<i>Pratylenchus penetrans</i>	VLHTNVND-G	REFGGSIYQK	VNKNLETAVN	LAWTAGSNN	-T-RFGIAAK
<i>Meloidogyne incognita</i>	SLHTYVND-A	NEFGGSIYQK	VHKNLETAVN	LAWTAGSNN	-T-RFGIAAK
<i>Lymnaea stagnalis</i>	SFTTFVND-G	QEFVGSVYQK	VSDNLETAVN	LAWTAGSNN	-T-RFGIAAK
<i>Necator americanus</i>	TLHSFVND-G	TEFGGSIYQK	VNKNLETAVN	LAWTAGSNN	-T-RFGIAAK
<i>Ancylostoma ceylanicum</i>	TLHSFVND-G	TEFGGSIYQK	VNKNLETAVN	LAWTAGSNN	-T-RFGIAAK
<i>Nippostrongylus brasiliensis</i>	TLHSFVND-G	TEFGGSIYQK	VNKNLETAVN	LAWTAGSNN	-T-RFGIAAK
<i>Parastrongylus trichosuri</i>	TLHSFVND-G	TEFGGSIYQK	VNKNLETAVN	LAWTAGSNN	-T-RFGIAAK
<i>Tribolium castaneum</i>	DSSGPLIQA-A	AAVVGHGWL	AGYQTAFTDQ	KSKLTKNFA	LGFSTGDFIL
<i>Ambystoma tigrinum</i>	DIAGPSVR-G	AAVVGHGWL	AGYQTAFTDQ	KSKLTKNFA	LGFSTGDFIL
<i>Spermophilus lateralis</i>	DIAGPSVR-G	AAVVGHGWL	AGYQTAFTDQ	KSKLTKNFA	LGFSTGDFIL
<i>Ixodes scapularis</i>	GI GGPIAH-A	GAVLHYQGWL	AGAQLSYDAN	KSRSLKTNFA	VGYGGGDFVL

	260	270	280	290	300
<i>Ancylostoma caninum</i>					Y S P S R D
<i>Caenorhabditis elegans</i> VDAC2					Y A P S R D
<i>Caenorhabditis briggsae</i>					Y S P S R D
<i>Caenorhabditis elegans</i>					Y S P S R D
<i>Ascaris suum</i>					Y C P A K D
<i>Haemonchus contortus</i>					Y S P T R D
<i>Monodelphis domestica</i> VDAC2					Y Q L D S T
<i>Macaca mulatta</i> VDAC2					Y Q L D P T
<i>Bos taurus</i> VDAC2					Y Q L D P T
<i>Rattus norvegicus</i> VDAC2					Y Q L D P T
<i>Mus musculus</i> VDAC2					Y Q L D P T
<i>Homo sapiens</i> VDAC2					Y Q L D P T
<i>Sus scrofa</i> VDAC2					Y Q L D P T
<i>Homo sapiens</i> VDAC2					Y Q L D P T
<i>Gallus gallus</i> VDAC2					Y K L D S T
<i>Meleagris gallopavo</i> VDAC2					Y K L D S T
<i>Pan troglodytes</i> VDAC2					Y Q L D P T
<i>Gasterosteus aculeatus</i>					Y Q L D K D
<i>Fugu rubripes</i>					Y Q L D K D
<i>Fugu rubripes</i>					Y Q L D K D
<i>Tetraodon nigroviridis</i>					Y Q L D K D
<i>Ictalurus punctatus</i>					Y Q L D K D
<i>Oncorhynchus mykiss</i>					Y Q L D K S
<i>Oryzias latipes</i> VDAC2					Y Q L D K D
<i>Danio rerio</i>					Y Q L D K D
<i>Xenopus laevis</i> VDAC2					Y Q L D S H
<i>Fugu rubripes</i>					Y Q L D S S
<i>Fugu rubripes</i>					Y Q L D K N
<i>Squalus acanthias</i>					Y Q I D S D
<i>Danio rerio</i>					Y Q L D K D
<i>Salmo salar</i>					Y Q L D K D
<i>Monodelphis domestica</i> VDAC1					Y Q I D P E
<i>Gallus gallus</i> VDAC1					Y Q I D P D
<i>Rattus norvegicus</i> VDAC1					Y Q V D P D
<i>Bos taurus</i> VDAC1					Y Q I D P D
<i>Sus scrofa</i> VDAC1					Y Q I D P D
<i>Homo sapiens</i> VDAC1					Y Q I D P D
<i>Mus musculus</i> VDAC1					Y Q V D P D
<i>Rattus norvegicus</i> VDAC1					Y Q V D P D
<i>Xenopus laevis</i> VDAC1					Y Q I D S D
<i>Xenopus tropicalis</i>					Y Q I D S D
<i>Fundulus heteroclitus</i> VDAC1					Y Q I D S D
<i>Oryzias latipes</i> VDAC1					Y Q I D P D
<i>Danio rerio</i> VDAC1					Y Q I D S D
<i>Petromyzon marinus</i>					Y Q L D S N
<i>Tetraodon nigroviridis</i>					Y Q I D S S
<i>Oryctolagus cuniculus</i> VDAC3					Y K L D C R
<i>Sus scrofa</i> VDAC3					Y K L D C R
<i>Bos taurus</i> VDAC3					Y K L D C R
<i>Mus musculus</i> VDAC3					Y K L D C R
<i>Homo sapiens</i> VDAC3					Y M L D C R
<i>Rattus norvegicus</i> VDAC3					Y R L D C R
<i>Pongo pygmaeus</i> VDAC3					Y M L D C R
<i>Gallus gallus</i> VDAC3					Y Q L D E K
<i>Pimephales promelas</i>					Y M L D S S
<i>Argopecten irradians</i>					Y T L D K N
<i>Spisula solidissima</i>					Y I L D K N
<i>Daphnia magna</i>					Y Q L D K D
<i>Apis mellifera</i>					Y N L D N D
<i>Homalodisca coagulata</i>					Y N L D H D
<i>Anopheles gambiae</i>					Y D L D K D
<i>Drosophila melanogaster</i>					Y Q L D D D
<i>Drosophila pseudoobscura</i> PORB					Y Q L G D D
<i>Aedes aegypti</i>					Y D L D K D
<i>Rhipicephalus appendiculatus</i>					Y D L D M E
<i>Ciona intestinalis</i>					Y N I D A D
<i>Strongylocentrotus purpuratus</i>					Y V L D S E
<i>Drosophila pseudoobscura</i> PORA					Y R L E G D
<i>Drosophila melanogaster</i>					Y H L E E D
<i>Monodelphis domestica</i> VDAC3					Y K L D H K
<i>Molgula tectiformis</i>					Y A M D N N
<i>Macaca mulatta</i> VDAC1					Y Q I D P D
<i>Hydra magnipapillata</i>					Y D I D K D
<i>Schistosoma japonicum</i>					Y I L D N Q
<i>Drosophila melanogaster</i> Porin B					Y D F Q N G

	260	270	280	290	300
<i>Drosophila pseudoobscura</i>					YQLGDG
<i>Drosophila melanogaster</i> Porin A					YEWEPG
<i>Fugu rubripes</i>					YQIDPD
<i>Fugu rubripes</i>					YQLDKN
<i>Xenopus tropicalis</i> VDAC1					YQLDSH
<i>Xenopus tropicalis</i>					YQLDSH
<i>Amblyomma variegatum</i>					YEMDQD
<i>Branchiostoma floridae</i>					YTI DSK
<i>Pratylenchus penetrans</i>					YCPTKD
<i>Meloidogyne incognita</i>					YQV NPD
<i>Lymnaea stagnalis</i>					
<i>Necator americanus</i>					YAPSRD
<i>Ancylostoma ceylanicum</i>					
<i>Nippostrongylus brasiliensis</i>					
<i>Parastrongyloides trichosuri</i>					
<i>Tribolium castaneum</i>	HTNVDDGQEF	GGSIYQKLSP	KLETGIQLAW	SAGSNNTKFG	IXAKYDLDQD
<i>Ambystoma tigrinum</i>	HTNVNDGTDF	GGSIYQKVND	KLETAVNLAW	TAGNSNTRFX	IAAKYQLDSD
<i>Spermophilus lateralis</i>	HTNVNDGTDF	GGSIYQKVND	KLETAVNLAW	TAGNSNTRFG	IAAKYQIDPD
<i>Ixodes scapularis</i>	HTNVNDGQEF	AGSIYQVRND	CLETGVQLSW	TAGTNATRFG	LGCVYQLDRE

	310	320	330	340	350
<i>Ancylostoma caninum</i>	LVLRA-KYNN	SSHI ALAATH	SLSPDLTMTL	STRINLTSYD	H--HKFGMVL EYEP S
<i>Caenorhabditis elegans</i> VDAC2	LTVRA-KYNS	SSQVAVAATH	SLSPALKLTL	STQFNLAAND	A--HKFGLGL EFD P-
<i>Caenorhabditis briggsae</i>	LALRA-KYNS	SSQVAVAATH	SLSPALKLTL	STQFNLAAND	A--HKFGLGL EFD P-
<i>Caenorhabditis elegans</i>	LALRA-KYNS	SSQVAVAATH	SLSPALKLTL	STQFNLSAND	A--SQ--G--SGL-
<i>Ascaris suum</i>	LELKA-KYON	QSKVAFAATH	HLTNQLKLIL	STQFGLNTLN	EGGHKFGGLGL VY--
<i>Haemonchus contortus</i>	LTLRG-KYNN	SSQVALAVTH	SLSPDLKATL	SSQFN--	
<i>Monodelphis domestica</i> VDAC2	ASISA-KYNN	SSLIGVGYTQ	TLRPGVKLTL	SALVDGKSI N	AGGHK LGLAL ELEA-
<i>Macaca mulatta</i> VDAC2	ASISA-KYNN	SSLIGVGYTQ	TLRPGVKLTL	SALVDGKSI N	AGGHK LGLAL ELEA-
<i>Bos taurus</i> VDAC2	ASISA-KYNN	SSLIGVGYTQ	TLRPGVKLTL	SALVDGKSI N	AGGHK LGLAL ELEA-
<i>Rattus norvegicus</i> VDAC2	ASISA-KYNN	SSLIGVGYTQ	TLRPGVKLTL	SALVDGKSF N	AGGHK LGLAL ELEA-
<i>Mus musculus</i> VDAC2	ASISA-KYNN	SSLIGVGYTQ	TLRPGVKLTL	SALVDGKSF N	AGGHK LGLAL ELEA-
<i>Homo sapiens</i> VDAC2	ASISA-KYNN	SSLIGVGYTQ	TLRPGVKLTL	SALVDGKSI N	AGGHK LGLAL ELEA-
<i>Sus scrofa</i> VDAC2	ASISA-KYNN	SSLIGVGYTQ	TLRPGVKLTL	SALVDGKSI N	AGGHK LGLAL ELEA-
<i>Homo sapiens</i> VDAC2	ASISA-KYNN	SSLIGVGYTQ	TLRPGVKLTL	SALVDGKSI N	AGGHK LGLAL ELEA-
<i>Gallus gallus</i> VDAC2	ASISA-KYNN	SSLVGVGYTQ	TLRPGVKLTL	SALVDGKSI N	AGGHK LGLAL ELEA-
<i>Meleagris gallopavo</i> VDAC2	ASISA-KYNN	SSLVGVGYTQ	TLRPGVKLTL	SALVDGKSI N	AGGHK LGLAL ELEA-
<i>Pan troglodytes</i> VDAC2	ASISA-KYNN	SSLVGVGYTQ	TLRPGVKLTL	SALVDGKSI N	AGGHK LGLAL ELEA-
<i>Gasterosteus aculeatus</i>	ASVSA-KYNN	NSLVGVGYTQ	TLRPGVKLTL	SALFDGKNI N	SGGHK LGLAL ELEA-
<i>Fugu rubripes</i>	ASVSA-KYNN	NSLVGVGYTQ	TLRPGVKLTL	SGLVDGKNI N	AGGHK LGLAL ELEA-
<i>Fugu rubripes</i>	ASVSA-KYNN	NSLVGVGYTQ	TLRPGVKLTL	SGLVDGKNI N	AGGHK LGLAL ELEA-
<i>Tetraodon nigroviridis</i>	ASVSA-KYNN	SSLVGVGYTQ	TLRPGVKLTL	SGLVDGKNI N	AGGHK LGLAL ELEA-
<i>Ictalurus punctatus</i>	ASISA-KYNN	SSLVGVGYTQ	TLRPGVKLTL	SALVDGKSI N	SGGHK LGLAL ELEA-
<i>Oncorhynchus mykiss</i>	ASISA-KYNN	SSLVGVGYTQ	TLRPGVKLTL	SALVDGKSI N	TGGHK LGLAL ELEA-
<i>Oryzias latipes</i> VDAC2	ASISA-KYNN	NSLVGVGYTQ	TLRPGVKLTL	AGLVDGKSI N	AGGHK LGLAL ELEA-
<i>Danio rerio</i>	ASISA-KYNN	SSLVGVGYTQ	TLRPGVKLTL	SALVDGKSI N	SGGHK LGLAL ELEA-
<i>Xenopus laevis</i> VDAC2	ASISA-KYNN	SSLVGVGYTQ	TLRPGVKLTL	SALVDGKNI N	AGGHK LGLAL ELEA-
<i>Fugu rubripes</i>	ASISA-KYNN	ASLVGIGYTQ	TLRPGMKVTL	SALVDGKNI N	AGGHK LGLAL ELEA-
<i>Fugu rubripes</i>	SSLST-KYON	GCLVGLGYTQ	TLRPGVKLTL	SGLIDGKNVN	GGGHK VGLGF ELEA-
<i>Squalus acanthias</i>	AYVSA-KYNN	SSLIGVGYTQ	TLRPGVKLTL	SGLIDGKNF H	AGGHK VGMGF ELEA-
<i>Danio rerio</i>	SVVSA-KYNN	ASLVGVGYTQ	TLRPGVKLTL	SALIDAKNF N	AGGHK VGMGF ELEA-
<i>Salmo salar</i>	ASLSA-KYNN	ASLVGVGYTQ	ALRPGVKLTL	SALIDAKNF N	AGGHK VGMGF ELEA-
<i>Monodelphis domestica</i> VDAC1	ASFSA-KYNN	SSLIGLGYTQ	TLKPGIKLTL	SALLDGKNVN	AGGHK LGLAL EFQA-
<i>Gallus gallus</i> VDAC1	ASFSA-KYNN	SSLIGLGYTQ	TLKPGIKLTL	SALLDGKNVN	AGGHK LGLAL EFQA-
<i>Rattus norvegicus</i> VDAC1	ACFSA-KYNN	SSLIGLGYTQ	TLKPGIKLTL	SALLDGKNVN	AGGHK LGLAL EFQA-
<i>Bos taurus</i> VDAC1	ACFSA-KYNN	SSLIGLGYTQ	TLKPGIKLTL	SALLDGKNVN	AGGHK LGLAL EFQA-
<i>Sus scrofa</i> VDAC1	ACFSA-KYNN	SSLIGLGYTQ	TLKPGIKLTL	SALLDGKNVN	AGGHK LGLAL EFQA-
<i>Homo sapiens</i> VDAC1	ACFSA-KYNN	SSLIGLGYTQ	TLKPGIKLTL	SALLDGKNVN	AGGHK LGLAL EFQA-
<i>Mus musculus</i> VDAC1	ACFSA-KYNN	SSLIGLGYTQ	TLKPGIKLTL	SALLDGKNVN	AGGHK LGLAL EFQA-
<i>Rattus norvegicus</i> VDAC1	ACFLA-KYNN	SSLIGLGYTQ	TLKPGIKLTL	SALLDGKNVN	AGSHK LGLAL EFQA-
<i>Xenopus laevis</i> VDAC1	AFSSA-KYNN	SSLIGLGYTQ	TLKPGIKLTL	STLVDGKNI N	AGGHK LGLAL EFQA-
<i>Xenopus tropicalis</i>	AFSSA-KYNN	SSLIGLGYTQ	TLKPGIKLTL	STLVDGKNI N	AGGHK LGLAL EFQA-
<i>Fundulus heteroclitus</i> VDAC1	AFSSA-KYNN	SSLVGLGYTQ	TLKPGIKLTL	AALLDGKNI N	SGGHK LGLAL EFQA-
<i>Oryzias latipes</i> VDAC1	AFSSA-KYNN	SSLVGLGYTQ	TLKPGIKLTL	SALLDGKNI N	AGGHK LGLAL EFQA-
<i>Danio rerio</i> VDAC1	AFSSA-KYNN	SSLVGLGYTQ	TLKPGIKLTL	SALLDGKNI N	AGGHK LGLAL EFQA-
<i>Petromyzon marinus</i>	TTINA-KYNN	SSLVGLGYTQ	TLRPGVKLSL	SALLDGKNI N	AGGHK LGLAL ELEA-
<i>Tetraodon nigroviridis</i>	ASLSA-KYNN	ASLVGIGYTQ	ALRPGMKVTL	SALVDGKNI N	AGGHK LGLAL ELEA-
<i>Oryctolagus cuniculus</i> VDAC3	TSLSA-KYNN	ASLIGLGYTQ	TLRPGVKLTL	SALIDGKNF N	AGGHK VGLGF ELEA-
<i>Sus scrofa</i> VDAC3	TSLSA-KYNN	ASLIGLGYTQ	TLRPGVKLTL	SALIDGKNF S	AGGHK VGLGF ELEA-
<i>Bos taurus</i> VDAC3	TSLSA-KYNN	ASLIGLGYTQ	TLRPGVKLTL	SALIDGKNF N	AGGHK VGLGF ELEA-
<i>Mus musculus</i> VDAC3	TSLSA-KYNN	ASLIGLGYTQ	TLRPGVKLTL	SALIDGKNF N	AGGHK VGLGF ELEA-
<i>Homo sapiens</i> VDAC3	TSLSA-KYNN	ASLIGLGYTQ	TLRPGVKLTL	SALIDGKNF S	AGGHK VGLGF ELEA-
<i>Rattus norvegicus</i> VDAC3	TSLSA-KYNN	ASLIGLGYTQ	TLRPGVKLTL	SALVDGKNF N	AGGHK VGLGF ELEA-

				310		320		330		340		350	
<i>Pongo pygmaeus</i> VDAC3	TLSA	KVNN	AS	LIGLGY	TQ	TLRPG	VKLT	SALI	DGKNFS	AGGHK	VGLGF	ELEA	--
<i>Gallus gallus</i> VDAC3	TSIGA	KVNN	AS	LIGIGYT	TL	ALRPG	VKLT	SGLI	DGKNFS	AGGHK	VGLGF	ELEA	--
<i>Pimephales promelas</i>	SSISA	KVNN	SS	MVGIGYT	TQ	TLRPG	VKLT	SALV	DGKSI	AGGHK	LG	--	--LG
<i>Argopecten irradians</i>	SYVNM	KVNN	AF	QIGMGYT	Q	NLRDG	VKLT	SSLI	EGKNFN	QGGH	KVGMGL	EFD	--
<i>Spisula solidissima</i>	SSINA	KVNN	NG	QVGIGYSQ	NVRNG	VKLT	SSMI	EAKNIN	AGGHK	VGLGL	EFD	--	--
<i>Daphnia magna</i>	SAVRA	KINN	AS	QLGLGY	QK	LRQGV	VTITL	SSMV	DLKNFN	QGGHK	GMAL	ELEA	--
<i>Apis mellifera</i>	ASIRA	KVNS	NL	QVGLGY	QK	LRDGI	VTITL	STNI	DGKNFG	SGGHK	GLAL	DLQA	--
<i>Homalodisca coagulata</i>	TAVRA	KVNN	AS	QIGLSYSQ	KLREG	VTISL	STLI	DGKNFN	EGGHK	VGFSL	ELEA	--	--
<i>Anopheles gambiae</i>	ACVRA	KVNN	QS	QIGLGY	QK	LRDGI	TLTL	STLV	DGKNFN	AGGHK	I	GVAL	ELEA
<i>Drosophila melanogaster</i>	ASVRA	KVNN	AS	QVGLGY	QK	LRDGI	VTITL	STLV	DGKNFN	AGGHK	I	GVGL	ELEA
<i>Drosophila pseudoobscura</i> PORB	ASVRA	KVNN	AS	QVGLGY	QK	LRDGI	VTITL	STLV	DGKNFN	DGGHK	I	GVGL	ELEA
<i>Aedes aegypti</i>	ACVRA	KVNN	QS	QIGLGY	QK	LRDGI	VTITL	STMI	DGKSFN	TGGHK	I	GVAL	ELEA
<i>Rhipicephalus appendiculatus</i>	TSVRA	KVNN	SG	QIGLGFTH	RLRPG	ISLTL	STML	DGKNFN	QGGHK	KLGLGL	DL	SA	--
<i>Ciona intestinalis</i>	AALNA	KVNN	VG	QVGFYSH	QLRKG	VKLT	SSLV	DAKNLN	GGGHK	KLGLGV	EFEV	--	--
<i>Strongylocentrotus purpuratus</i>	ASLNA	KVSN	TS	QVGIGYT	TQ	TLRPG	MKITL	STLI	DGKSLN	PGGHK	KLGLGL	NLE	--
<i>Drosophila pseudoobscura</i> PORA	ALIRA	KINS	KA	ELGLGYEQ	KVREG	TASI	SAVLD	GRNIS	DGNH	KFGVGL	ALE	CC	--
<i>Drosophila melanogaster</i>	ALVRA	KVNN	LV	ELGLGYEQ	KLRDGI	TASI	SAVLD	CNNFK	DGNH	RFGVGL	AL	CC	--
<i>Monodelphis domestica</i> VDAC3	TSLS	KVNN	AS	LIGLGY	TQ	TLRAG	VKLT	SALI	DGKNFN	AGGHK	VGLGF	ELEA	--
<i>Molgula tectiformis</i>	TTINA	KISN	DG	QLGIAHT	ALRS	VKLT	SSLI	DVHNLN	GGGH	--	KMG	--	--TGV
<i>Macaca mulatta</i> VDAC1	ACFSA	KVNN	SS	LRGLGY	TQ	TLKPG	VKLT	SALL	DGKNVN	AGGHK	LG	GL	EFQA
<i>Hydra magnipapillata</i>	TFLKT	KINN	DL	HLGLSYVQ	KLRPG	VQLTL	SSLI	NAKSE	F	GGH	--	KL	GL
<i>Schistosoma japonicum</i>	NKHSK	CRLDH	LN	QISLAF	TH	YLSKG	LQTL	SGVF	NGPDI	A	--	--	KMG
<i>Drosophila melanogaster</i> Porin B	TMVKA	KLRE	DS	RMGFVYQS	KIGEN	LDVG	HLAF	DGVDPI	GAH	RIGVSW	GF	HC	--
<i>Drosophila pseudoobscura</i>	SLLKA	KVRD	DG	NVGVVFQT	KIGEN	VDVTY	HVGC	DGKDP	I	SGEH	KIGASW	FN	CC
<i>Drosophila melanogaster</i> Porin A	SMLKA	KVRG	DS	RIGLIFQK	KLRED	IEVLF	HVGF	EGSDPI	I	NGKH	KFGSSW	YF	NM
<i>Fugu rubripes</i>	ASFSA	KVNN	SS	LVGLGY	TQ	TLKPG	VKLT	SALL	DGKNIN	AGGHK	I	GL	GL
<i>Fugu rubripes</i>	SSLST	KVDN	GC	LVGLGY	TQ	TLRPG	VKLT	SGLI	DGKNVN	GGGHK	VGLGF	ELEA	--
<i>Xenopus tropicalis</i> VDAC1													
<i>Xenopus tropicalis</i>													
<i>Amblyomma variegatum</i>	TSVR		--	AK									
<i>Branchiostoma floridae</i>	SSFRA	KVNN	SS	QIGLGY	TQ	ELVRP	VKVT	STLLD	GKNFN	QGGH	KLGLGL	DL	EA
<i>Pratylenchus penetrans</i>	L-E		--	LK									
<i>Meloidogyne incognita</i>	LCL		--	RA									
<i>Lymnaea stagnalis</i>													
<i>Necator americanus</i>	LLRA	KINN	SS	QIALA	ATH	SL	SPDL	KMT					
<i>Ancylostoma ceylanicum</i>													
<i>Nippostrongylus brasiliensis</i>													
<i>Parastrongyloides trichosuri</i>													
<i>Tribolium castaneum</i>	AAIRA	KVHN	SS	QI									
<i>Ambystoma tigrinum</i>	ASFSA	KVNN	SS	PSWVG	YTQ	TLKPG	LSALL	EEKNVHAG	--	G	--	--	--
<i>Spermophilus lateralis</i>	ACFSA	KVNN	SS	LI	GLGY	TQ	TLKPG	IXLTL	SALLDGKN	--			
<i>Ixodes scapularis</i>	TSVRA	KVNN	SG	QVGLGF	TH	RLRPG	ISLTL	STML	DGKNFN	QGGHK	KLGLGL	DL	--

C

C																																																																																																																																																																																																																																																																																																																																																																																																																																																																																																																																																																																																																																																																																																																																																																																																																																																																																																																																																																																																																																																																																																																																																																																																																																																																																																																																																																																																																																																																																																																																																																																																																																																																																
---	--	--	--	--	--	--	--	--	--	--	--	--	--	--	--	--	--	--	--	--	--	--	--	--	--	--	--	--	--	--	--	--	--	--	--	--	--	--	--	--	--	--	--	--	--	--	--	--	--	--	--	--	--	--	--	--	--	--	--	--	--	--	--	--	--	--	--	--	--	--	--	--	--	--	--	--	--	--	--	--	--	--	--	--	--	--	--	--	--	--	--	--	--	--	--	--	--	--	--	--	--	--	--	--	--	--	--	--	--	--	--	--	--	--	--	--	--	--	--	--	--	--	--	--	--	--	--	--	--	--	--	--	--	--	--	--	--	--	--	--	--	--	--	--	--	--	--	--	--	--	--	--	--	--	--	--	--	--	--	--	--	--	--	--	--	--	--	--	--	--	--	--	--	--	--	--	--	--	--	--	--	--	--	--	--	--	--	--	--	--	--	--	--	--	--	--	--	--	--	--	--	--	--	--	--	--	--	--	--	--	--	--	--	--	--	--	--	--	--	--	--	--	--	--	--	--	--	--	--	--	--	--	--	--	--	--	--	--	--	--	--	--	--	--	--	--	--	--	--	--	--	--	--	--	--	--	--	--	--	--	--	--	--	--	--	--	--	--	--	--	--	--	--	--	--	--	--	--	--	--	--	--	--	--	--	--	--	--	--	--	--	--	--	--	--	--	--	--	--	--	--	--	--	--	--	--	--	--	--	--	--	--	--	--	--	--	--	--	--	--	--	--	--	--	--	--	--	--	--	--	--	--	--	--	--	--	--	--	--	--	--	--	--	--	--	--	--	--	--	--	--	--	--	--	--	--	--	--	--	--	--	--	--	--	--	--	--	--	--	--	--	--	--	--	--	--	--	--	--	--	--	--	--	--	--	--	--	--	--	--	--	--	--	--	--	--	--	--	--	--	--	--	--	--	--	--	--	--	--	--	--	--	--	--	--	--	--	--	--	--	--	--	--	--	--	--	--	--	--	--	--	--	--	--	--	--	--	--	--	--	--	--	--	--	--	--	--	--	--	--	--	--	--	--	--	--	--	--	--	--	--	--	--	--	--	--	--	--	--	--	--	--	--	--	--	--	--	--	--	--	--	--	--	--	--	--	--	--	--	--	--	--	--	--	--	--	--	--	--	--	--	--	--	--	--	--	--	--	--	--	--	--	--	--	--	--	--	--	--	--	--	--	--	--	--	--	--	--	--	--	--	--	--	--	--	--	--	--	--	--	--	--	--	--	--	--	--	--	--	--	--	--	--	--	--	--	--	--	--	--	--	--	--	--	--	--	--	--	--	--	--	--	--	--	--	--	--	--	--	--	--	--	--	--	--	--	--	--	--	--	--	--	--	--	--	--	--	--	--	--	--	--	--	--	--	--	--	--	--	--	--	--	--	--	--	--	--	--	--	--	--	--	--	--	--	--	--	--	--	--	--	--	--	--	--	--	--	--	--	--	--	--	--	--	--	--	--	--	--	--	--	--	--	--	--	--	--	--	--	--	--	--	--	--	--	--	--	--	--	--	--	--	--	--	--	--	--	--	--	--	--	--	--	--	--	--	--	--	--	--	--	--	--	--	--	--	--	--	--	--	--	--	--	--	--	--	--	--	--	--	--	--	--	--	--	--	--	--	--	--	--	--	--	--	--	--	--	--	--	--	--	--	--	--	--	--	--	--	--	--	--	--	--	--	--	--	--	--	--	--	--	--	--	--	--	--	--	--	--	--	--	--	--	--	--	--	--	--	--	--	--	--	--	--	--	--	--	--	--	--	--	--	--	--	--	--	--	--	--	--	--	--	--	--	--	--	--	--	--	--	--	--	--	--	--	--	--	--	--	--	--	--	--	--	--	--	--	--	--	--	--	--	--	--	--	--	--	--	--	--	--	--	--	--	--	--	--	--	--	--	--	--	--	--	--	--	--	--	--	--	--	--	--	--	--	--	--	--	--	--	--	--	--	--	--	--	--	--	--	--	--	--	--	--	--	--	--	--	--	--	--	--	--	--	--	--	--	--	--	--	--	--	--	--	--	--	--	--	--	--	--	--	--	--	--	--	--	--	--	--	--	--	--	--	--	--	--	--	--	--	--	--	--	--	--	--	--	--	--	--	--	--	--	--	--	--	--	--	--	--	--	--	--	--	--	--	--	--	--	--	--	--	--	--	--	--	--	--	--	--	--	--	--	--	--	--	--	--	--	--	--	--	--	--	--	--	--	--	--	--	--	--	--	--	--	--	--	--	--	--	--	--	--	--	--	--	--	--	--	--	--	--	--	--	--	--	--	--	--	--	--	--	--	--	--	--	--	--	--	--	--	--	--	--	--	--	--	--	--	--	--	--	--	--	--	--	--	--	--	--	--	--	--	--	--	--	--	--	--	--	--	--	--	--	--	--	--	--	--	--	--	--	--	--	--	--	--	--	--	--	--	--	--	--	--	--	--	--	--	--	--	--	--	--	--	--	--	--	--	--	--	--	--	--	--	--	--	--	--	--	--	--	--	--	--	--	--	--	--	--	--	--	--	--	--	--	--	--	--	--	--	--	--	--	--	--	--	--	--	--	--	--	--	--	--	--	--	--	--	--	--	--	--	--	--	--	--	--	--	--	--	--	--	--	--	--	--	--	--	--	--	--	--	--	--	--	--	--	--	--	--	--	--	--	--	--	--	--	--	--	--	--	--	--	--	--	--	--	--	--	--	--	--	--	--	--	--	--	--	--	--	--	--	--	--	--	--	--	--	--	--	--	--	--	--	--	--	--	--	--	--	--	--	--	--	--	--	--	--	--	--	--	--	--	--	--	--	--	--	--	--	--	--	--	--	--	--	--	--	--	--	--	--	--	--	--	--	--	--	--	--	--	--	--	--	--	--	--	--	--	--	--	--	--	--	--	--	--	--	--	--	--	--	--	--	--	--	--	--	--	--	--	--	--	--	--	--	--	--	--	--	--	--	--	--	--	--	--	--	--	--	--	--	--	--	--	--	--	--	--	--	--	--	--	--	--	--	--	--	--	--	--	--	--	--	--	--	--	--	--	--	--	--	--	--	--	--	--	--	--	--	--	--	--	--	--	--	--	--	--	--	--	--	--	--	--	--	--	--	--	--	--	--	--	--	--	--	--	--	--	--	--	--	--	--	--	--	--	--	--	--	--	--	--	--	--	--	--	--	--	--	--	--	--	--	--	--	--	--	--	--	--	--	--	--	--	--	--	--	--	--	--	--	--	--	--	--	--	--	--	--	--	--	--	--	--	--	--	--	--	--	--	--	--	--	--	--	--	--	--	--	--	--	--	--	--	--	--	--	--	--	--	--	--	--	--	--	--	--	--	--	--	--	--	--	--	--	--	--	--	--	--	--	--	--	--	--	--	--	--	--	--	--	--	--	--	--	--	--	--	--	--	--	--	--	--	--	--	--	--	--	--	--	--	--	--	--	--	--	--	--	--	--	--	--	--	--	--	--	--	--	--	--	--	--	--	--	--	--	--	--	--	--	--	--	--	--	--	--	--	--	--	--	--	--	--	--	--	--	--	--	--	--	--	--	--	--	--	--	--	--	--	--	--	--	--	--	--	--	--	--	--	--	--	--	--	--	--	--	--	--	--	--	--	--	--	--	--	--	--	--	--	--	--	--	--	--	--	--	--	--	--	--	--	--	--

	10	20	30	40	50
<i>Lycopersion esculentum</i> POM34	-----	-MGKGP GL	Y T E I GKKARDLL	Y K D Y Q S D H K F	S I T T Y S P T G V
<i>Lycopersion esculentum</i> POM34	-----	-MGKGP GL	Y S D I GKKTRDLL	Y R D Y Q T D H K F	T I T T Y S A T G V
<i>Solanum tuberosum</i> POM34	-----	-MGKGP GL	Y S D I GKKTRDLL	Y R D Y Q T D H K F	T I T T Y S P T G V
<i>Lotus corniculatus</i> VDAC1.1	-----	--AKGP GL	Y T D I GKKARDLL	F K D Y H S D Q K F	T I T T F S P T G V
<i>Glycine max</i> VDAC1.1	-----	--AKGP GL	Y S D I GKKARDLL	F K D Y H S D Q K F	T I T T Y S P T G V
<i>Lotus corniculatus</i> VDAC1.2	-----	--AKGP GL	Y T D I GKKARDLL	F K D Y H S D Q K F	T I T T Y S P T G V
<i>Medicago truncatula</i> VDAC1.1	-----	--SKGP GL	Y S D I GKKARDLL	Y K D Y N T D Q K F	T L T T Y S P T G V
<i>Picea glauca</i>	-----	-MGKGP GL	Y S D I GKKTRDLL	N K D Y N F D Q K F	S F T S Y T S T G L
<i>Pinus pinus</i>	-----	-MGKGP GL	Y S D I GKKTRDLL	N K D Y N F D Q K F	S F T S Y T S T G L
<i>Pinus pinus</i>	-----	-MVKGP GL	F S D I GKKSRLDL	Y K D F L V D Q K F	S L T T Y T P T G L
<i>Populus trichocarpa</i>	-----	-MVKGP GL	Y S E I GKKARDLL	Y K D Y Q T D H K F	T L N T S S P T G V
<i>Glycine max</i> VDAC1.3	-----	--VKGP GL	Y S D I GKKARDLL	F K D Y Q N D H K F	T I T T Y T S T G V
<i>Medicago truncatula</i> VDAC1.3	-----	-MVKGP GL	Y S D I GKKARDLL	F K D Y Q N D H K F	T I T T Q T L A G V
<i>Arabidopsis thaliana</i> VDAC3	-----	--VKGP GL	Y T E I GKKARDLL	Y K D H N S D Q K F	S I T T F S P A G V
<i>Pisum sativum</i> plastid porin	-----	--VKGP GL	Y T D I GKKARDLL	Y K D Y H S D Q K F	T I S T Y S P T G V
<i>Pisum sativum</i> plastid porin	-----	--VKGP GL	Y T D I GKKARDLL	Y K D Y H S D Q K F	T I S T Y S P T G V
<i>Arabidopsis thaliana</i> VDAC3	-----	--VKGP GL	Y T E I GKKARDLL	Y R D Y Q G D Q K F	S V T T Y S S T G V
<i>Brassica rapa</i>	-----	--GKGP GL	Y T E I GKKARDLL	Y K D Y Q G D Q K L	S I T A Y S S T G V
<i>Solanum habrochaites</i> VDAC1	-----	-----	GP GL Y T E I GKKARDLL	Y K D Y Q S D H K F	S I T T Y S P T G V
<i>Citrus reticulata</i> VDAC1	-----	-----	I GP GL Y S E I GKKARDLL	Y K D Y Q S D H K F	T V T T Y S A G V
<i>Gossypium raimondii</i> VDAC3.1	-----	--MAGP AP	F V D L GKKAKDLL	T K D Y N F D Q K F	T L S M L S T T G M
<i>Vitis vinifera</i> VDAC3.1	-----	--GNGP AP	F S D I GKKTRDLL	N K D Y N F D H K F	T L L M Q S P G G M
<i>Solanum tuberosum</i> VDAC3	-----	--MEQP AP	F S E I GRRARDLL	T K D Y N Y D Q K F	T F S I P S S S G V
<i>Lotus corniculatus</i> VDAC3.1	-----	--ANGP AL	Y P E I GKKARDLL	Y K D Y N F D Q K F	N L S I P S S T G L
<i>Glycine max</i> VDAC3.1	-----	--ANGP AP	F S E I GKKAKDLL	Y K D Y N F D H K F	S L S I P N S T G L
<i>Medicago truncatula</i> VDAC3.1	-----	--ANGP AP	F S E I GKKARDLL	Y K D Y N F D H K F	S L S I P S S T G L
<i>Allium cepa</i>	-----	--GSGP AP	F S E I GKKARDLL	T R D Y N F D H K F	S L S T Y S K D G L
<i>Pinus pinus</i>	-----	--GKGP GL	F S D I GKKAKDLL	T K D Y N Y D Q K F	T V T T F S E T G L
<i>Pinus taeda</i>	-----	-----	GP GL F S N I GKKARDLL	T K D Y S Y D Q K F	A V A T Y S D D G L
<i>Hordeum vulgare</i> VDAC3.1	-----	--SKGP VP	F P I F GKKARDLL	Y K D Y N F D Q K F	S W S T T S E F G L
<i>Sorghum bicolor</i> VDAC3.1	-----	--SKGP VP	F E V N I GKKAKDLL	Y K D Y N F D Q K F	S L S T S S S S G L
<i>Oryza sativa</i> POM36	-----	--SKGP AP	F L N I GKKAKDLL	Y K D Y N F D Q K F	S L T T T S N S G L
<i>Arabidopsis thaliana</i> POM36	-----	--GSSP AP	F A D I GKKAKDLL	N K D Y I F D H K F	T L T M L S A T G T
<i>Pennisetum glaucum</i>	-----	--MKGP GL	F S D I GKKAKDLL	T R D Y T Y D Q K L	T V S T Y S S S G V
<i>Zea mays</i>	-----	--MKGP GL	F S D I GKKAKDLL	S K D Y T Y D Q K L	T I S T A S A S G L
<i>Triticum aestivum</i>	-----	MAMKGP GL	F T D I GKKAKDLL	T R D Y T Y D Q K L	S V S T V S S S G V
<i>Vitis vinifera</i> VDAC2.1	-----	--SKGP GL	F A D I GKKAKDLL	T R D Y I S D Q K F	T V S T Y S D T G V
<i>Solanum tuberosum</i> VDAC2	-----	-MSKGP GL	F A D I GKKARDLL	T K D Y I S D Q K L	S I S T Y S D T G V
<i>Glycine max</i> VDAC2.1	-----	--SKGP GL	F T D I GKKSRLDL	T K D Y N S D Q K L	T I S S Y S I S G V
<i>Lotus corniculatus</i> VDAC2.1	-----	--SKGP GL	F S D I GKKPRDLL	T K D Y S S D Q K L	T V S S Y S T A G V
<i>Gossypium raimondii</i> VDAC2.1	-----	--SKGP GL	F V D I GKKAKDLL	T K D Y T S D Q K F	T V S T Y T A G V
<i>Medicago truncatula</i> VDAC2.1	-----	--SKGP GL	Y S D I GKKAKDLL	T K D Y N S D Q K L	T V S S Y S T T G V
<i>Arabidopsis thaliana</i> VDAC3	-----	--SKGP GL	F T D I GKKAKDLL	T R D Y N S D Q K F	S I S T Y S A S G V
<i>Ananas comosus</i>	-----	--MGP GL	Y S E I GKKARDLL	Y K D Y H T D Q K F	T I T T Y T S T G V
<i>Saccharum officinarum</i> VDAC3.1	-----	-----	AKD -----	L L Y K D Y N F D Q K F	S L S T S S S S G L
<i>Antirrhinum majus</i>	-----	-----	GP GL Y S D I GKKARDLL	N K D Y Q S D Q K F	T I T T Y S P T G V
<i>Welwitschia mirabilis</i>	-----	-----	S D -----	I GKGARDLL	Y K D Y N F D H K I
<i>Allium cepa</i>	-----	-----	MGP GL Y S E I GKKARDLL	Y R D Y P Y D Q K F	S I T T V T P Y G A
<i>Zantedeschia aethiopica</i>	-----	-----	MGP GL Y S E I GKKARDLL	Y K D Y Q T D H K F	S I T T Y T A N G I
<i>Lycopersion esculentum</i> VDAC3.1	-----	E Q S P A P	-----	F S E I GRRARDLL	T K D Y S Y D Q K F
<i>Triphysaria versicolor</i>	-----	-----	-----	-----	T L -----
<i>Picea sitchensis</i>	-----	-----	GP GL Y S D I GKKTRDLL	N K D Y N F D Q K F	S F T S Y T S T G L
<i>Gossypium raimondii</i> VDAC1.1	-----	--GKGP GL	Y T E I GKKARDLL	Y K D Y Q T D H K F	T L T T S S P T G V
<i>Saruma henryi</i>	-----	-----	Y S -----	D I GKKARDLL	Y R D Y Q P D Q K F
<i>Brassica rapa</i>	-----	--MGKGP GL	Y T D I GKKARDLL	Y K D H N S D Q K L	S I T T H S P A G V
<i>Liriodendron tulipifera</i>	-----	--MSKGP GL	Y S D I GKKARDLL	C K D Y Q S D H K F	T I T T Y T S T G V
<i>Saccharum officinarum</i> VDAC1	-----	--MVG GP	GL Y T E I GKKTRDLL	Y K D Y Q T D H K F	T V T T Y T S H G V
<i>Panicum virgatum</i>	-----	-----	VGP GL Y T E I GKKTRDLL	Y R D Y Q T D H K F	T L T T Y T S N G V
<i>Lactuca sativa</i>	-----	--GKGP GL	Y P D I GKKARDLL	Y R D Y Q G D H K F	S L T T Y T A N G V
<i>Nicotiana tabacum</i> POM34	-----	--GKGP GL	Y S D I GKKARDLL	Y R D Y Q T D H K F	T I T T Y S P T G V
<i>Eschscholzia californica</i>	-----	--MGKGP GL	Y T D I GKKARDLL	Y R D Y Q S D Q K F	T V T T Y T S T G V
<i>Beta vulgaris</i>	-----	-----	VNGP GL F S D I GKKAKDLL	S K D Y V L D Q K F	T I S S C S E T G V
<i>Cycas rumphii</i>	-----	--MGP GL	F S D I GKKTRDLL	Y K D Y L I D Q K F	S L T T Y T S T G L
<i>Glycine max</i> VDAC1.2	-----	--MSKGP GL	Y S D I GKKARDLL	F K D Y H S D Q K F	T I T T Y S P T G V
<i>Hordeum vulgare</i>	-----	-----	MAP GL	-----	Y T D I GKKTR
<i>Lycopersion esculentum</i> VDAC2	-----	-----	MP GL	-----	F S D I GKKAK
<i>Citrus sinensis</i>	-----	-----	GP GL	-----	Y T D I GKKAR
<i>Gossypium raimondii</i> VDAC1.3	-----	-----	GK GP GL	-----	Y T D I GKKAR
<i>Picea glauca</i>	-----	-----	-----	-----	Y S D I GKKTR
<i>Welwitschia mirabilis</i>	-----	-----	GP GL	-----	F S E I GKKTR
<i>Acorus americanus</i>	-----	-----	-----	-----	-----
<i>Selaginella moellendorffii</i>	-----	-----	-----	-----	F S D I GRNTR

		60	70	80	90	100																																																		
<i>Oryza sativa</i> VDAC1	A	I	T	A	T	S	T	K	K	A	D	L	I	F	G	E	I	Q	S	Q	I	K	N	-	N	T	V	D	V	K	A	N	S	D	S	N	V	T	T	V	T	-	D	E	L	-	-									
<i>Triticum aestivum</i> VDAC1	A	I	T	A	T	S	T	K	K	A	D	L	I	V	G	E	I	Q	S	Q	I	K	N	N	-	I	K	N	N	T	V	D	V	K	A	N	S	A	S	N	V	T	T	I	A	D	D	L	A	-	-					
<i>Triticum aestivum</i>	A	I	T	A	T	S	T	K	K	A	D	L	I	L	G	E	I	Q	S	Q	I	K	N	K	N	-	I	K	N	N	T	V	D	V	K	A	N	S	A	S	N	V	T	T	I	A	D	D	L	A	-	-				
<i>Hordeum vulgare</i>	A	I	T	A	T	S	T	K	K	A	D	L	I	L	G	E	I	Q	S	Q	I	K	N	K	N	-	I	K	N	N	T	V	D	V	K	A	N	S	A	S	N	V	T	T	I	A	D	D	L	A	-	-				
<i>Zea mays</i> VDAC2	A	I	T	A	A	S	T	R	K	D	E	A	I	F	N	E	I	Q	S	Q	L	K	H	-	N	-	N	T	V	D	V	K	A	T	S	E	S	N	V	T	T	I	T	V	H	E	L	G	-	-						
<i>Oryza sativa</i> VDAC2	A	I	T	V	A	G	T	K	K	N	E	S	I	F	G	E	I	Q	S	Q	V	K	N	-	N	-	N	S	V	D	V	K	A	T	S	D	S	K	L	T	T	F	V	H	D	L	G	-	-							
<i>Triticum aestivum</i> VDAC2	T	I	T	S	S	T	K	K	N	E	A	I	L	A	D	L	Q	T	Q	V	K	I	-	N	-	N	T	V	D	V	K	A	T	S	D	S	S	V	T	T	I	T	V	P	E	L	-	-								
<i>Hordeum vulgare</i>	T	I	T	S	S	T	K	K	N	E	A	I	L	S	D	L	Q	T	Q	V	K	I	-	N	-	N	T	V	D	V	K	A	T	S	D	S	S	V	T	T	I	T	I	P	E	L	-	-								
<i>Triticum aestivum</i>	T	I	T	S	S	T	K	K	N	E	A	I	L	A	D	L	Q	T	Q	V	K	I	-	N	-	N	T	V	D	V	K	A	T	S	D	S	S	V	T	T	I	T	V	P	E	L	-	-								
<i>Asparagus officinalis</i> VDAC1	A	I	T	A	S	T	R	K	N	E	M	I	F	G	E	I	Q	S	Q	L	K	N	K	N	-	I	K	N	N	T	V	D	V	K	A	N	S	D	S	N	L	T	T	V	T	I	D	E	L	A	-	-				
<i>Triticum aestivum</i> VDAC3	A	I	T	A	A	G	T	R	K	N	E	S	I	F	G	E	L	Q	T	Q	L	K	N	-	N	-	N	T	V	D	I	K	A	N	S	E	S	D	L	L	T	T	F	T	V	D	E	L	A	-	-					
<i>Triticum aestivum</i>	A	I	T	A	A	G	T	R	K	N	E	S	I	F	G	E	L	Q	T	Q	L	K	N	K	N	-	I	K	N	N	T	V	D	I	K	A	N	S	E	S	D	L	L	T	T	F	T	V	D	E	L	A	-	-		
<i>Zea mays</i> plastid porin	A	I	T	A	A	G	T	R	K	N	E	S	I	F	G	E	L	H	T	Q	I	K	N	-	K	-	N	-	K	T	V	D	V	K	A	N	S	E	S	D	L	L	T	T	I	T	V	D	E	F	G	-	-			
<i>Zea mays</i> plastid porin	A	I	T	A	A	G	T	R	K	N	E	S	I	F	G	E	L	H	T	Q	I	K	N	K	K	-	I	K	N	K	K	L	T	V	D	V	K	A	N	S	E	S	D	L	L	T	T	I	T	V	D	E	F	G	-	-
<i>Sorghum bicolor</i> plastid porin	A	I	T	A	A	G	T	R	K	N	E	S	I	F	G	E	L	H	T	Q	I	K	N	K	K	-	I	K	N	K	K	L	T	V	D	I	K	A	N	S	E	S	D	L	L	T	T	I	T	V	D	E	L	G	-	-
<i>Saccharum officinarum</i> plastid porin	A	I	T	A	A	G	T	R	K	N	E	S	I	F	G	E	L	H	T	Q	I	K	N	K	K	-	I	K	N	K	K	L	T	V	D	V	K	A	N	S	E	S	D	L	L	T	T	I	T	A	D	E	F	G	-	-
<i>Oryza sativa</i> VDAC3	T	I	T	A	A	G	T	R	K	N	E	S	V	F	G	E	L	Q	T	Q	L	K	N	K	L	-	I	-	N	T	V	D	V	K	A	N	S	E	S	D	L	L	T	T	V	T	V	D	E	F	G	-	-			
<i>Zea mays</i> VDAC1a	A	V	T	A	S	T	K	K	A	D	L	I	L	G	E	I	Q	S	Q	I	-	K	N	N	-	N	-	N	T	I	D	V	K	A	N	S	E	S	N	I	T	T	I	T	V	D	E	I	A	-	-					
<i>Zea mays</i> VDAC1b	A	V	T	A	S	T	K	K	A	D	L	I	F	S	E	I	H	S	Q	I	-	K	N	N	-	N	-	N	T	I	D	V	K	A	N	S	E	S	N	I	T	T	V	T	V	N	E	I	A	-	-					
<i>Citrus paradisi</i> VDAC1	A	I	T	S	S	G	V	K	K	G	E	L	F	L	A	D	V	S	T	Q	L	K	N	K	N	-	I	-	N	T	D	V	K	V	D	T	S	N	-	L	F	T	T	I	T	V	D	E	P	-	-					
<i>Nicotiana tabacum</i> POM36	A	I	T	S	S	G	L	K	K	G	E	L	F	L	A	D	V	N	T	Q	L	K	N	K	N	-	I	-	N	T	D	V	K	V	D	T	S	N	-	V	T	T	I	T	V	D	E	P	-	-						
<i>Spinacia oleracea</i> VDAC1	A	I	T	S	T	G	T	K	K	G	E	L	F	L	A	D	V	S	T	Q	L	-	T	N	N	-	I	-	N	T	D	V	K	V	D	T	S	N	-	L	F	T	T	I	T	V	D	E	P	-	-					
<i>Mesembryanthemum crystallinum</i>	A	I	T	S	S	G	T	K	K	G	E	L	F	L	A	D	V	N	T	Q	L	-	K	N	N	-	I	-	N	T	D	V	K	V	D	T	S	N	-	L	L	T	T	I	T	V	D	E	A	-	-					
<i>Lycopersion esculentum</i> VDAC1.3	E	I	T	S	T	G	V	K	K	G	E	I	Y	L	A	D	V	S	T	Q	L	-	K	N	N	-	I	-	N	T	D	V	K	V	D	T	S	N	-	L	H	T	T	I	T	V	D	E	P	-	-					
<i>Prunus armeniaca</i>	A	I	S	S	T	G	I	R	K	G	E	L	Y	L	A	D	V	S	T	Q	L	-	K	N	N	-	I	-	N	T	D	V	K	V	D	T	S	N	-	L	R	T	T	I	T	I	D	E	P	-	-					
<i>Solanum tuberosum</i> VDAC1	A	I	T	A	S	G	L	K	K	G	E	L	F	L	A	D	V	S	T	Q	L	K	N	-	N	-	I	-	N	T	D	V	K	V	D	A	N	S	N	-	V	T	T	I	T	V	D	E	P	-	-					
<i>Lycopersion esculentum</i> POM36	A	I	T	S	S	G	L	K	K	G	E	L	F	L	A	D	V	S	T	Q	L	K	N	K	N	-	I	-	N	T	D	V	K	V	D	T	S	N	-	L	Y	T	T	I	T	V	D	E	P	-	-					
<i>Populus trichocarpa</i>	A	I	T	S	T	G	I	K	K	G	E	L	F	L	A	D	I	S	S	Q	L	K	N	K	N	-	I	-	N	T	D	V	K	V	D	T	S	N	-	L	L	T	T	I	T	V	D	E	P	-	-					
<i>Vitis vinifera</i> VDAC1.1	A	I	T	S	S	G	T	K	K	G	E	L	F	V	A	D	V	N	T	Q	L	K	N	K	N	-	I	-	N	T	D	V	K	V	D	T	S	N	-	L	F	V	T	V	T	V	D	E	P	-	-					
<i>Helianthus annuus</i> POM34	A	I	T	S	S	G	T	K	K	G	E	L	F	L	A	D	V	N	T	Q	L	K	R	N	N	-	I	-	N	T	D	V	K	V	D	T	S	N	-	L	S	T	T	I	V	V	D	E	P	-	-					
<i>Solanum tuberosum</i> POM34	V	I	T	S	S	G	S	K	K	G	E	L	F	L	A	D	V	N	T	Q	L	-	K	N	N	-	I	-	N	T	D	I	K	V	D	T	S	N	-	L	F	T	T	I	T	V	D	E	A	-	-					
<i>Lycopersion esculentum</i> POM34	V	I	T	S	S	G	S	K	K	G	E	L	F	L	A	D	V	N	T	Q	L	K	N	K	N	-	I	-	N	T	D	I	K	V	D	T	S	N	-	L	F	T	T	I	T	V	D	E	A	-	-					
<i>Lycopersion esculentum</i> POM34	A	I	T	S	S	G	L	K	K	G	E	L	F	L	A	D	V	N	T	Q	L	K	N	K	N	-	I	-	N	T	D	I	K	V	D	T	S	N	-	L	L	A	T	V	T	V	D	E	A	-	-					
<i>Solanum tuberosum</i> POM34	A	I	T	S	S	G	L	K	K	G	E	L	F	L	A	D	V	N	T	Q	L	K	N	K	N	-	I	-	N	T	D	I	K	V	D	T	S	N	-	L	A	T	V	T	V	D	E	A	-	-						
<i>Lotus corniculatus</i> VDAC1.1	A	I	T	S	S	G	T	K	K	G	E	L	F	V	A	D	V	N	T	Q	L	-	K	N	N	-	I	-	N	T	D	I	K	V	D	T	S	N	-	L	F	T	T	I	A	V	N	D	P	-	-					
<i>Glycine max</i> VDAC1.1	A	I	T	A	S	G	T	R	K	S	E	L	F	L	A	D	V	N	T	Q	L	K	N	K	N	-	I	-	N	T	D	I	K	V	D	T	S	N	-	L	F	T	T	I	T	V	N	E	P	-	-					
<i>Lotus corniculatus</i> VDAC1.2	A	I	T	S	S	G	I	K	K	G	E	L	F	V	A	D	V	N	T	Q	L	-	K	-	N	N	-	I	-	N	T	D	L	K	V	D	T	S	N	-	L	F	T	T	V	T	V	D	E	P	-	-				
<i>Medicago truncatula</i> VDAC1.1	A	L	T	A	S	S	T	K	K	G	E	L	F	L	A	D	I	N	T	Q	L	K	H	K	N	-	I	-	N	T	D	I	K	V	D	T	S	N	-	L	F	T	T	I	T	V	T	E	P	-	-					
<i>Picea glauca</i>	A	F	T	S	T	G	I	K	K	G	E	F	F	L	G	D	L	N	T	Q	L	K	N	N	N	-	I	-	N	T	D	I	K	V	D	T	S	N	-	L	F	A	T	V	T	I	D	E	P	-	-					
<i>Pinus pinus</i>	A	F	T	S	T	G	I	K	K	G	E	F	F	L	G	D	L	N	T	Q	L	K	N	N	N	-	I	-	N	T	D	I	K	V	D	T	S	N	-	L	F	A	T	V	T	I	D	E	P	-	-					
<i>Pinus pinus</i>	V	F	T	S	T	G	T	K	K	G	E	F	F	L	G	D	L	T	T	Q	L	K	N	K	N	-	I	-	N	T	D	I	K	V	D	T	S	N	-	L	F	A	T	V	T	I	D	E	P	-	-					
<i>Populus trichocarpa</i>	T	I	T	S	S	G	T	K	K	G	E	L	L	A	D	V	N	T	Q	L	K	N	K	N	-	I	-	N	T	D	I	K	V	D	T	S	N	-	L	F	T	T	I	T	V	D	E	P	-	-						
<i>Glycine max</i> VDAC1.3	E	I	T	S	T	G	V	R	K	G	E	I	Y	L	A	D	V	S	T	Q	L	K	N	K	N	-	I	-	N	T	D	V	K	V	D	T	S	N	-	L	R	T	T	I	T	V	D	E	P	-	-					
<i>Medicago truncatula</i> VDAC1.3	E	I	T	S	A	G	V	R	K	G	E	A	F	L	A	D	V	S	T	Q	L	K	N	K	N	-	I	-	N	T	D	I	K	V	D	T	S	N	-	L	R	T	T	I												

		60	70	80	90	100
<i>Antirrhinum majus</i>	T L T S S	G T K K G	E F L A D V N T Q	L K N K N I T T D I	K V D T S S N - L F	T T I T V D E P - -
<i>Welwitschia mirabilis</i>	E F S S T	G I K K G	D L F L G D I K T Q	L K S S R V T T D L	K V D T G S N - L	T T V T S D E L - -
<i>Allium cepa</i>	A I T A S	S T K K N	D L I G E I Q S R	L K N K N V T V D V	K A N S D S N - L	T T I T V D E L - -
<i>Zantedeschia aethiopica</i>	A I T S S	G T K K N	D L I G E I Q A Q	Q K S N G I T T D V	K V N S D S N - L F	T T I T V D E L - -
<i>Lycopersion esculentum</i> VDAC3.1	G I T A T	G V K K D	Q I F I G D I S T Q	Y K L G S T V V D I	K V D T Y S N - V S	T K V T L V D V - -
<i>Triphysaria versicolor</i>	V L T S T	G T K K G	D L F L A D V N T Q	L K N K N I T T D I	K V D T S S N - L F	T T I T V D E P - -
<i>Picea sitchensis</i>	A F T S T	G I K K G	E F L G D L N T Q	L K N N N V T T D I	K V D T S S N - L F	A T V T I D E P - -
<i>Gossypium raimondii</i> VDAC1.1	A I T S A	G T K K G	E L F L A D V N T Q	L K N K N V T T D I	K V D T Y S N - L Y	T T I T V D Q P - -
<i>Saruma henryi</i>	T I T S T	G L K K G	E L F L A D V N T Q	L K S R N F T T D I	K V D T N S N - L F	T T I T V D E P - -
<i>Brassica rapa</i>	A I T S T	G T K K G	D S L L G D V S L Q	L K Q K N I T T D L	K V S T D S T - V L	I A T A T V D E A - -
<i>Liriodendron tulipifera</i>	A I T S T	G I K K G	E L F L A D I N T Q	L K N K N I T T D I	K V D T N S N - L F	T T I T V N E P - -
<i>Saccharum officinarum</i> VDAC1	A V T A S	S T K K A	D L I F G E I Q S Q	I K N K N I T V D V	K A N S E S N I T T	T V T V D E I A - -
<i>Panicum virgatum</i>	A V T A T	S T K K A	D L I F G E I Q S Q	I K N K N V T I D V	K A N S G S N V I T	T V T V D E I A - -
<i>Lactuca sativa</i>	S I T S S	G A K K G	E L F L A D V N T K	L I N K N I T T D V	K V D T N S K V E T	T I T I D E A - -
<i>Nicotiana tabacum</i> POM34	A I T S S	G L K K G	D L F L A D V N T Q	L K N K N V T T D I	K V D T N S N - L	A T V T V D E A - -
<i>Eschscholzia californica</i>	A I T S S	G T K K G	E L F L A D V N T Q	L K N K N I T T D V	K V D T N S R - V F	T T I T V D E P - -
<i>Beta vulgaris</i>	A F T S T	A V K N G	G L S A G D V G A L	Y K Y K N V M A D V	K L H T E S S - I S	T T F T I A D I - -
<i>Cycas rumphii</i>	V F T S T	G T K K G	E L F V G E L N T Q	L K N N N I T T D I	K V D T S S N - L F	T T V T I D E P - -
<i>Glycine max</i> VDAC1.2	A I T S S	G T K K G	D L F V A D V N T Q	L K N K N I T T D I	K V D T G S N - L	F T T I T V N E P - -
<i>Hordeum vulgare</i>	D L L Y R D Y	C T H Q K	F T L T T C T P	E - G V A I T A A - -	- - - - -	G T R K N E S I F - -
<i>Lycopersion esculentum</i> VDAC2	D L L T K D Y	- - - - -	- - - - -	I A D Q - - - - -	- - - - -	- - - - - K L S - -
<i>Citrus sinensis</i>	D L L Y K D Y	Q S D H K	F T I T T - - - -	Y S P - T G V A I T S - -	- - - - -	S G T K K G E L F - -
<i>Gossypium raimondii</i> VDAC1.3	D L L Y K D Y	Q A D H K	F T L T T - - - -	Y T S - N G V A I T S - -	- - - - -	T G T K K G E L L - -
<i>Picea glauca</i>	D L L N K D Y	N F D Q K	F S F T S - - - -	Y T S - T G L A F T S - -	- - - - -	T G I K K G E F F - -
<i>Welwitschia mirabilis</i>	D L L Y K D Y	L V D Q K	F S V T T - - - -	Y T S - S G L A F T S - -	- - - - -	T G V K K G D L F - -
<i>Acorus americanus</i>	- - - - -	- - - - -	- - - - -	- - - - -	T A - - N G V A I T S - -	- - - - - T G T K K G D I T - -
<i>Selaginella moellendorffii</i>	D L L N X D Y	I Y N H K	F T V T T - - - -	T T S - S G L T F T S - -	- - - - -	T G T R K G E S L - -
		110	120	130	140	150
<i>Oryza sativa</i> VDAC1	T P G L K S I L S F	A V P D Q R S G - -	K F E L Q Y S H D Y	A G V S A S I G L T	A S P V V N L S S V	
<i>Triticum aestivum</i> VDAC1	A P G L K T I L S F	A V P D Q K S G - -	K V E L Q Y L H D Y	A G I N A S I G L T	A N P V V N L S G A	
<i>Triticum aestivum</i>	A P G L K T I L S F	A V P D Q K S G - -	K V E L Q Y L H D Y	A G I N A S I G L T	A N P V V N L S G A	
<i>Hordeum vulgare</i>	A P G L K T I L S F	A V P D Q K S G - -	K V E L Q Y L H D Y	A G I N A S I G L T	A N P V V N L S A A	
<i>Zea mays</i> VDAC2	T P G L K A I L C V	P F P Y Q K S A - -	K A E L Q Y L H H H	A G V A A S V G L N	A N P V V N L S G V	
<i>Oryza sativa</i> VDAC2	T P G L K G I L S I	P F P Y Q K S A - -	K A E V Q Y L H P H	A G L N A I V G L N	A N P L V S F S G V	
<i>Triticum aestivum</i> VDAC2	T P G L K G V L S L	P F P Y Q K S T P G	K A E L Q Y L H P H	L G I N G S V G L N	S N P L V N F S G V	
<i>Hordeum vulgare</i>	K P G L K G V L S L	P F P Y Q K S T P G	K A E L Q Y L H P H	L G I N G S V G L N	P N P L V N I S G V	
<i>Triticum aestivum</i>	T P G L K G V L S L	P F P Y Q K S T P G	K A E L Q Y L H P H	L G I N G S V G L N	P N P L V N F S G V	
<i>Asparagus officinalis</i> VDAC1	T P G L K S I L S F	V V P D Q K S G - -	K V E L Q Y F H E Y	A G V N A S I G L T	A N P V V N L A G V	
<i>Triticum aestivum</i> VDAC3	T P G L K S I L S L	V V P D Q R S G - -	K L E L Q Y L H E F	A G I N A S V G L N	P N P M V N L S G V	
<i>Triticum aestivum</i>	T P G L K S I L S L	V V P D Q R S G - -	K L E L Q Y L H E F	A G I N A S V G L N	P N P M V N L S G V	
<i>Zea mays</i> plastid porin	T P G L K S I I N L	V V P D Q R S G - -	K L E F Q Y L H E Y	A G V N A S V G L N	S N P M V N L S G A	
<i>Zea mays</i> plastid porin	T P G L K S I I N L	V V P D Q R S G - -	K L E F Q Y L H E Y	A G V N A S V G L N	S N P M V N L S G A	
<i>Sorghum bicolor</i> plastid porin	T P G L K S I L S L	V V P D Q R S G - -	K F E L Q Y L H E Y	A G V N A S I G L N	P N P M V N I S G V	
<i>Saccharum officinarum</i> plastid porin	A P G L K S I L S L	V V P D Q R S G - -	K L E L Q Y L H K Y	A G V N A S I G L N	P N P M V N L S G V	
<i>Oryza sativa</i> VDAC3	T P G L K S I L S L	V V P D Q R S G - -	K L E L Q Y L H E Y	A G I N A S V G L N	S N P M V N L S G V	
<i>Zea mays</i> VDAC1a	T P G L K T I L S F	A V P D Q R S G - -	K V E L Q Y L H D Y	A G V N A S I G L T	A N P V V N L S A A	
<i>Zea mays</i> VDAC1b	T P G L K T I L S F	A V P D Q R S G - -	K V E L Q Y L H D Y	A G V N A S V S L T	A N P V A N L S A G	
<i>Citrus paradisi</i> VDAC1	A P G L K S I F S F	I V P D Q R S G - -	K V E L Q Y Q H E Y	A G I S T G I G F T	A N P I V N F S G V	
<i>Nicotiana tabacum</i> POM36	A P G L K T I V S F	V L P D Q R S G - -	K V E L Q Y L H E Y	A G I S T G I G L T	A S P L V N F S G V	
<i>Spinacia oleracea</i> VDAC1	A P G L K A I F S F	R V P D Q R S G - -	K V E L Q Y L H E Y	A G I S T S L G L T	A N P I V N F S G V	
<i>Mesembryanthemum crystallinum</i>	A P G L K T I L S F	R V P D Q R S G - -	K L E L Q Y L H D Y	A G I C T S V G L T	A N P I V N F S G V	
<i>Lycopersion esculentum</i> VDAC1.3	A P G L K T I F S F	I F P D Q S A - -	K V E L Q Y Q H E Y	A G I S T S I G L T	A S P I V N F S G I	
<i>Prunus armeniaca</i>	A P G L K A I F S F	I V P D Q R S G - -	K V E L Q Y Q H E Y	A G I S T S I G L T	A N P I V N F S G V	
<i>Solanum tuberosum</i> VDAC1	A P G L K T I F S F	V V P D Q K S G - -	K V E L Q Y L H E Y	A G I N T S I G L T	A S P L V N F S G V	
<i>Lycopersion esculentum</i> POM36	A P G L K T I F S F	V V P D Q K S G - -	K V E L Q Y L H E Y	A G I N T S I G L T	A S P L V N F S G V	
<i>Populus trichocarpa</i>	A P G L K T I F S F	K V P D Q R S G - -	K V E L Q Y Q H E Y	A G I S T S L G L T	A N P I V N F S G V	
<i>Vitis vinifera</i> VDAC1.1	A P G L K S I F N F	K V P D Q R S G - -	K V E L Q Y L H D Y	A G I S T S I G L T	A N P I V N F S G T	
<i>Helianthus annuus</i> POM34	A P G L K A I F S F	K V P D Q R S G - -	K L E L Q Y L H D Y	A G I A T S I G L T	A N P I V N F S G V	
<i>Solanum tuberosum</i> POM34	A P G L K T I L S F	R V P D Q R S G - -	K L E V Q Y L H D Y	A G I C T S V G L T	A N P I V N F S G V	
<i>Lycopersion esculentum</i> POM34	A P G L K T I L S F	R V P D Q R S G - -	K L E V Q Y L H D Y	A G I C T S V G L T	A N P I V N F S G V	
<i>Lycopersion esculentum</i> POM34	A P G L K T I F S C	R I P D Q S A - -	K M E L Q Y L H D Y	A G I C T S V G L T	A N P I V N F S G V	
<i>Solanum tuberosum</i> POM34	A P G L K T I F S C	R I P D Q S A - -	K M E L Q Y L H D Y	A G I C T S V G L T	A N P I V N F S G V	
<i>Lotus corniculatus</i> VDAC1.1	A P G L K A I F S F	K V P D Q R S G - -	K V E L Q Y L H D Y	A G I S S S I G L T	A N P I V N F S G V	
<i>Glycine max</i> VDAC1.1	A P G L K A I F S F	K V P D Q R S G - -	K V E V Q Y L H D Y	A G I S T S V G L T	A N P I V N F S G V	
<i>Lotus corniculatus</i> VDAC1.2	A P G L K A I F S F	R V P D Q R S G - -	K V E L Q Y L H D Y	A G I S T S V G L T	P N P I V N F S G V	
<i>Medicago truncatula</i> VDAC1.1	A P G L K T I L S F	R I P E P L K S G	K A E V Q Y L H D Y	A G I S A S I G L T	A N P V A N F S G V	
<i>Picea glauca</i>	A P G L K T I L S F	T V P D Q R S G - -	K V E L Q Y L H D Y	A G V S T S I G L T	P S P I T H F S G V	
<i>Pinus pinus</i>	A P G V K A I F S F	T V P D Q R S G - -	K V E L Q Y L H D Y	A G V S A S I G L T	P S P I T H F S G A	
<i>Pinus pinus</i>	A P G L K A I L N F	T V P D Q R S G - -	K V E L Q Y L H D Y	A G I S T S I G L T	A T P V V E S S V V	
<i>Populus trichocarpa</i>	A P G L K T I F S F	K V P D Q R S G - -	K V E I Q Y L H D Y	A A V S S S V G L T	V N P T V N F S G V	
<i>Glycine max</i> VDAC1.3	A P G L K T I F S F	N F P D Q K S G - -	K V E L Q Y Q H E Y	A G I N T S I G L T	A N P V V N F S G V	
<i>Medicago truncatula</i> VDAC1.3	V P G L K T I F S F	I Y P E Q K S G - -	K V E L Q Y L H D Y	A G I S T S I G L T	A T P T V N I S A V	
<i>Arabidopsis thaliana</i> VDAC3	A P G L R S I F S F	K V P D Q N S G - -	K V E L Q Y L H E Y	A G I S T S M G L T	Q N P T V N F S G V	
<i>Pisum sativum</i> plastid porin	A P G V K A I L S E	K V P E Q R S G - -	K L E F Q Y L H E Y	A G V N A S V G L N	S N P M V N L S G A	

		110	120	130	140	150																																											
<i>Pisum sativum</i> plastid porin	A	P	G	V	K	A	I	L	S	F	K	V	P	E	Q	T	S	G	--	K	V	E	L	Q	Y	L	H	E	Y	A	G	I	S	S	S	V	G	L	K	A	N	P	I	V	N	F	S	S	V
<i>Arabidopsis thaliana</i> VDAC3	A	P	G	L	K	V	I	V	Q	A	K	L	P	D	H	K	S	G	--	K	A	E	V	Q	Y	F	H	D	Y	A	G	I	S	T	S	V	G	F	T	A	P	I	V	N	F	S	S	V	
<i>Brassica rapa</i>	T	F	G	L	K	A	I	V	S	A	K	V	P	D	Q	K	S	A	--	K	V	E	L	Q	Y	M	H	P	H	A	G	I	C	T	S	V	G	L	T	A	N	P	V	N	F	S	S	V	
<i>Solanum habrochaites</i> VDAC1	A	P	G	L	K	I	L	S	F	R	V	P	D	Q	R	S	G	--	K	L	E	V	Q	Y	L	H	D	Y	A	G	I	C	T	S	V	G	L	T	A	N	P	I	V	N	F	S	S	V	
<i>Citrus reticulata</i> VDAC1	A	P	G	L	K	S	I	F	S	F	I	V	P	D	Q	R	S	G	--	K	V	E	L	Q	Y	Q	H	E	Y	A	G	I	S	T	G	I	G	F	T	A	N	P	I	V	N	F	S	S	V
<i>Gossypium raimondii</i> VDAC3.1	W	P	C	S	K	A	A	L	S	F	R	I	P	D	H	K	S	G	--	K	L	D	V	Q	Y	L	H	P	H	A	A	I	D	S	S	I	G	L	N	P	T	P	L	L	E	L	S	A	
<i>Vitis vinifera</i> VDAC3.1	L	P	C	T	K	V	A	C	S	F	K	I	P	D	H	K	S	G	--	K	L	D	V	Q	Y	L	H	P	H	A	A	I	D	S	S	I	G	L	N	P	T	P	L	L	E	L	S	A	
<i>Solanum tuberosum</i> VDAC3	F	R	S	T	K	V	S	L	G	F	N	I	P	D	H	K	S	G	--	K	L	D	V	Q	Y	L	H	Q	H	A	A	I	N	S	S	I	G	L	N	P	S	P	L	L	E	L	S	A	
<i>Lotus corniculatus</i> VDAC3.1	F	R	C	K	V	A	L	S	F	N	I	P	D	H	K	S	G	--	K	L	D	V	Q	Y	L	H	P	H	A	A	I	D	S	S	I	G	L	N	P	S	P	L	L	E	L	S	A		
<i>Glycine max</i> VDAC3.1	L	H	G	T	K	A	A	L	S	F	N	I	P	D	H	K	S	G	--	K	L	D	V	Q	Y	L	H	P	H	A	A	I	D	S	S	I	G	L	N	P	S	P	L	L	E	L	S	A	
<i>Medicago truncatula</i> VDAC3.1	S	H	S	K	V	A	L	S	F	N	I	P	D	H	K	S	G	--	K	L	D	V	Q	Y	L	H	P	H	A	A	I	D	S	S	I	G	L	N	P	A	P	K	L	E	L	S	A		
<i>Allium cepa</i>	V	D	G	G	K	A	I	L	S	F	K	L	P	D	H	K	S	G	--	K	L	D	L	H	Y	A	N	G	Y	A	A	V	S	S	T	G	L	T	A	P	A	L	L	E	F	S	A		
<i>Pinus pinus</i>	I	F	H	A	K	T	I	F	S	F	K	I	P	D	Q	K	S	G	--	K	V	D	L	Q	Y	F	H	D	H	V	L	S	S	S	I	G	L	T	P	T	I	V	E	V	S	G			
<i>Pinus taeda</i>	I	P	G	A	T	V	F	S	F	K	L	P	D	D	K	S	G	--	K	L	E	V	Q	Y	L	H	E	H	V	L	S	S	S	I	G	L	T	P	K	P	V	V	D	F	S	T			
<i>Hordeum vulgare</i> VDAC3.1	V	P	G	L	K	T	S	F	G	F	K	V	P	D	Q	R	S	G	--	K	L	D	L	Q	Y	L	H	D	R	F	A	L	N	S	T	I	G	L	T	S	A	P	V	I	E	L	A	T	
<i>Sorghum bicolor</i> VDAC3.1	L	T	G	L	K	T	S	F	A	F	K	V	P	D	H	K	S	G	--	K	L	D	L	Q	Y	A	H	N	R	F	S	L	N	S	T	I	G	L	T	S	T	P	L	V	E	L	A	A	
<i>Oryza sativa</i> POM36	L	T	G	L	K	T	S	F	S	F	R	V	P	D	Q	K	S	G	--	K	L	D	L	Q	Y	L	H	D	H	F	A	L	N	S	T	I	G	L	T	S	T	P	L	I	E	L	A	A	
<i>Arabidopsis thaliana</i> POM36	L	P	S	A	K	A	V	I	S	F	K	I	P	D	H	K	S	G	--	K	L	D	V	Q	Y	V	H	P	H	A	L	N	S	S	I	G	L	N	P	T	P	L	L	D	L	S	A		
<i>Pennisetum glaucum</i>	L	P	S	T	K	V	T	S	V	K	L	P	D	Y	N	S	G	--	K	V	E	L	H	Y	F	H	E	N	A	S	L	A	T	V	V	G	T	K	P	S	P	V	V	E	L	S	G		
<i>Zea mays</i>	L	P	C	T	K	V	T	S	V	K	L	P	D	Y	N	S	G	--	K	V	E	L	Q	Y	F	H	E	N	A	T	F	A	T	V	V	G	T	K	P	S	P	V	I	D	L	S	G		
<i>Triticum aestivum</i>	L	P	S	T	K	V	T	S	I	K	F	P	D	Y	N	A	G	--	K	V	E	V	Q	Y	F	H	D	H	A	T	F	A	A	A	V	G	M	K	P	S	P	V	D	F	S	L	V		
<i>Vitis vinifera</i> VDAC2.1	I	P	S	T	K	T	I	A	S	F	K	F	P	D	Y	N	S	G	--	K	L	E	V	Q	Y	F	H	D	H	A	T	L	T	T	S	V	A	L	N	P	S	P	A	V	D	L	S	V	
<i>Solanum tuberosum</i> VDAC2	A	P	S	T	K	T	I	A	S	L	K	F	P	D	Y	S	G	--	K	L	E	V	Q	Y	H	H	H	A	A	F	S	T	A	V	G	L	K	Q	S	P	I	V	D	L	S	V			
<i>Glycine max</i> VDAC2.1	L	P	S	T	K	T	I	A	S	F	K	L	P	D	Y	N	S	G	--	K	L	E	V	Q	Y	F	H	D	H	A	T	L	T	A	V	A	L	N	P	S	P	I	D	V	S	A			
<i>Lotus corniculatus</i> VDAC2.1	L	P	S	T	K	T	I	A	S	F	K	L	P	D	Y	N	S	G	--	K	L	E	V	Q	Y	F	H	D	H	A	T	L	T	A	V	A	L	N	P	S	P	I	D	V	S	A			
<i>Gossypium raimondii</i> VDAC2.1	L	P	S	T	K	T	I	A	S	F	K	V	P	D	Y	N	A	G	--	K	L	E	V	Q	Y	F	H	H	A	T	F	T	T	T	I	A	L	Y	K	T	P	V	V	D	A	T			
<i>Medicago truncatula</i> VDAC2.1	F	P	S	T	K	T	I	A	S	I	K	L	P	D	Y	S	G	--	K	L	E	V	Q	Y	F	H	D	H	A	T	L	T	S	V	A	L	K	Q	S	P	I	F	D	V	S	A			
<i>Arabidopsis thaliana</i> VDAC3	L	P	S	T	K	A	I	A	S	F	K	V	P	D	Y	N	S	A	--	K	L	E	V	Q	Y	F	H	D	H	A	T	V	T	A	A	A	L	N	Q	P	L	I	D	T	A	T			
<i>Ananas comosus</i>	T	F	G	L	K	T	I	F	S	F	V	V	P	D	Q	R	S	G	--	K	V	E	L	Q	Y	L	H	D	Y	A	G	V	N	A	S	I	G	L	T	A	N	P	V	V	N	L	A	G	
<i>Saccharum officinarum</i> VDAC3.1	L	T	G	L	K	T	S	F	A	F	K	V	P	D	H	K	S	G	--	K	L	D	L	Q	Y	A	H	N	R	F	S	L	N	S	T	I	G	L	T	S	T	P	L	V	E	L	A	A	
<i>Antirrhinum majus</i>	A	P	G	L	K	T	I	L	S	F	R	V	P	D	Q	R	S	G	--	K	L	E	L	Q	Y	L	H	E	Y	A	G	I	C	S	S	V	G	L	T	A	N	P	I	V	N	F	S	S	V
<i>Welwitschia mirabilis</i>	A	P	G	L	K	S	I	L	N	F	T	F	P	D	Q	K	S	G	--	K	V	E	V	Q	Y	K	H	D	Y	A	G	I	S	S	S	I	G	L	T	A	P	V	A	N	F	S	S	V	
<i>Allium cepa</i>	T	F	G	L	K	S	I	L	T	F	V	V	P	D	Q	K	S	G	--	K	V	E	L	Q	Y	F	H	D	Y	A	G	I	N	A	S	I	G	L	T	A	S	P	I	V	N	L	S	G	
<i>Zantedeschia aethiopica</i>	A	P	G	F	K	T	I	L	S	F	V	V	P	V	Q	K	Y	G	--	K	V	E	L	Q	Y	L	H	D	Y	A	G	I	S	A	S	F	G	L	T	A	N	P	I	V	N	F	A	S	V
<i>Lycopersion esculentum</i> VDAC3.1	F	R	S	T	K	V	S	L	G	F	N	I	P	D	H	K	S	G	--	K	L	D	V	Q	Y	L	H	Q	H	A	A	I	N	S	S	I	G	L	N	P	S	P	L	L	E	L	S	V	
<i>Triphysaria versicolor</i>	T	F	G	L	K	A	I	L	G	F	R	V	P	D	Q	R	S	G	--	K	L	E	L	Q	Y	L	H	E	Y	A	G	V	S	S	S	V	G	L	T	A	N	P	I	V	N	F	S	S	V
<i>Picea sitchensis</i>	A	P	G	L	K	T	I	L	S	F	T	V	P	D	Q	R	S	G	--	K	V	E	L	Q	Y	L	H	D	Y	A	G	V	S	T	S	I	G	L	T	P	S	P	I	T	H	S	S	V	
<i>Gossypium raimondii</i> VDAC1.1	A	P	G	L	K	A	I	F	S	F	R	V	P	D	Q	R	S	G	--	K	V	E	L	Q	Y	L	H	E	Y	A	G	I	S	S	S	I	G	L	T	A	N	P	I	V	N	F	S	S	V
<i>Saruma henryi</i>	T	F	G	L	K	A	I	F	N	F	V	V	P	D	Q	R	S	G	--	K	V	E	L	Q	Y	L	H	D	N	A	G	I	N	T	S	V	G	L	T	S	N	P	T	I	N	F	A	G	V
<i>Brassica rapa</i>	A	P	G	L	K	S	I	F	S	F	R	A	P	D	Q	K	S	G	--	K	I	E	L	Q	Y	L	H	E	Y	A	G	I	S	T	S	M	G	L	T	Q	N	P	T	V	N	F	S	S	V
<i>Liriodendron tulipifera</i>	A	P	G	L	K	T	I	V	S	F	I	V	P	D	Q	K	S	G	--	K	V	E	L	Q	Y	L	H	D	Y	A	G	I	A	T	S	I	G	L	T	A	N	P	V	N	F	S	S	V	
<i>Saccharum officinarum</i> VDAC1	T	F	G	L	K	T	I	L	S	F	A	V	P	D	Q	R	S	G	--	K	V	E	L	Q	Y	L	H	D	Y	A	G	V	N	A	S	I	G	L	T	A	N	P	V	V	N	L	S	A	
<i>Panicum virgatum</i>	T	F	G	L	K	T	I	L	S	F	A	V	P	D	Q	R	S	G	--	K	F	E	L	Q	Y	L	H	D	H	A	G	V	N	A	S	I	G	L	T	A	N	P	V	V	N	L	S	A	
<i>Lactuca sativa</i>	A	P	G	L	K	T	I	F	S	F	V	V	P	D	Q	R	S	G	--	K	V	E	L	Q	Y	L	H	E	H	A	G	I	S	T	S	I	G	L	T	A	N	P	I	V	N	F	S	S	V
<i>Nicotiana tabacum</i> POM34	A	P	G	L	K	T	I	L	S	F	R	I	P	D	Q	S	A	--	K	L	E	V	Q	Y	L	H	D	Y	A	G	I	S	T	S	L	G	L	T	A	N	P	I	V	N	F	S	S	V	
<i>Eschscholzia californica</i>	A	P	G	L	K	T	I	F	N	F	V	V	P	D	Q	R	S	G	--	K	V	E	L	Q	Y	Q	H	E	Y	A	G	I	T	T	S	I	G	L	T	A	N	P	I	V	N	F	S	S	V
<i>Beta vulgaris</i>	L	P	S	T	K	A	I	A	S	F	K	I	P	N	Y	S	S	G																															

		160	170	180	190	200																																											
<i>Oryza sativa</i> VDAC3	F	G	S	K	E	L	S	V	G	V	D	V	A	F	D	--	T	A	T	S	N	F	T	K	Y	N	A	A	L	S	L	T	N	S	D	L	I	A	S	L	H	L	N	N	H	G	D	T	L
<i>Zea mays</i> VDAC1a	F	G	T	K	A	V	A	L	G	A	D	I	S	L	D	--	T	A	T	G	N	L	T	K	Y	N	A	A	L	R	F	T	H	E	D	L	I	A	S	L	N	L	N	N	K	G	D	S	L
<i>Zea mays</i> VDAC1b	F	G	T	K	A	V	A	L	G	A	E	I	S	F	D	--	S	A	T	G	N	F	T	K	Y	N	A	G	L	M	F	T	H	E	D	L	I	A	S	L	N	M	N	K	G	D	N	L	
<i>Citrus paradisi</i> VDAC1	V	G	N	N	S	V	A	L	G	T	D	L	S	F	D	--	T	A	T	G	N	F	T	K	C	N	A	G	L	S	Y	T	H	T	D	L	I	A	S	L	T	L	N	D	K	G	D	T	L
<i>Nicotiana tabacum</i> POM36	A	G	N	N	T	V	A	L	G	T	D	L	S	F	D	--	T	A	S	G	N	F	T	K	C	N	A	G	L	S	F	S	T	S	D	L	I	A	S	L	A	L	N	D	K	G	D	T	L
<i>Spinacia oleracea</i> VDAC1	F	G	N	S	T	L	A	L	G	T	D	L	S	F	D	--	T	A	S	G	N	F	T	K	C	N	A	G	L	S	F	T	N	D	D	L	I	A	S	V	N	V	N	D	K	L	D	I	L
<i>Mesembryanthemum crystallinum</i>	L	G	T	N	L	L	A	F	G	T	D	V	S	F	D	--	S	K	T	G	N	F	T	K	C	N	A	G	L	S	F	A	N	A	D	L	I	A	S	L	T	L	N	D	K	G	D	T	L
<i>Lycopersion esculentum</i> VDAC1.3	I	G	N	N	L	V	A	V	G	T	D	L	S	F	D	--	T	A	S	G	N	F	T	K	Y	N	A	G	L	N	V	T	H	A	D	L	I	A	S	L	T	L	N	D	K	G	D	S	L
<i>Prunus armeniaca</i>	V	G	N	N	L	S	L	G	T	D	L	S	F	D	--	T	A	S	G	N	F	T	K	C	N	A	G	L	N	F	T	H	T	D	L	I	A	S	L	I	L	N	D	K	A	D	T	V	
<i>Solanum tuberosum</i> VDAC1	A	G	N	N	T	V	A	L	G	T	D	L	S	F	D	--	T	A	T	G	N	F	T	K	C	N	A	G	L	S	F	S	S	S	D	L	I	A	S	L	A	L	N	D	K	G	D	T	V
<i>Lycopersion esculentum</i> POM36	A	G	N	N	I	V	A	L	G	T	D	V	S	F	D	--	T	A	T	G	N	F	T	K	C	N	A	G	L	S	F	S	S	S	D	L	I	A	S	L	A	L	N	D	K	G	D	T	V
<i>Populus trichocarpa</i>	V	G	S	N	V	A	L	G	T	D	L	S	F	D	--	T	A	T	G	N	F	T	K	C	N	A	G	L	S	Y	T	N	S	D	L	I	A	S	L	T	V	N	D	K	G	D	T	L	
<i>Vitis vinifera</i> VDAC1.1	I	G	T	N	V	A	L	G	T	D	L	S	F	D	--	T	K	S	G	N	F	T	K	C	N	A	G	V	S	F	C	N	A	D	L	I	A	S	L	T	V	N	D	K	G	D	A	V	
<i>Helianthus annuus</i> POM34	V	G	T	N	L	A	A	I	G	T	D	V	S	F	D	--	T	K	T	G	N	F	T	K	C	N	A	G	I	S	F	S	N	A	D	L	I	A	S	L	T	L	N	D	K	G	E	T	L
<i>Solanum tuberosum</i> POM34	I	G	T	N	I	L	A	L	G	T	D	V	S	F	D	--	T	K	T	G	D	E	T	K	C	N	A	G	L	S	F	T	N	A	D	L	V	A	S	L	N	L	N	N	K	G	D	N	L
<i>Lycopersion esculentum</i> POM34	L	G	T	N	V	L	A	L	G	T	D	V	S	F	D	--	T	K	A	G	A	I	T	K	C	N	A	G	L	R	F	T	N	A	D	L	I	T	S	L	N	L	N	N	K	G	D	S	L
<i>Solanum tuberosum</i> POM34	L	G	T	N	V	L	A	L	G	T	D	V	S	F	D	--	T	K	A	G	A	I	T	K	C	N	A	G	L	S	F	T	N	A	D	L	I	T	S	L	N	L	N	N	K	G	D	S	L
<i>Lotus corniculatus</i> VDAC1.1	I	G	T	N	V	L	A	L	G	A	D	L	T	F	D	--	T	K	I	G	E	L	T	K	S	N	A	G	L	S	F	T	K	D	D	L	I	A	S	L	T	L	N	D	K	G	D	A	L
<i>Glycine max</i> VDAC1.1	I	G	T	N	V	L	A	L	G	A	D	L	S	F	D	--	T	K	I	G	E	L	T	K	S	N	A	G	L	S	F	T	K	D	D	L	I	A	S	L	T	L	N	D	K	G	D	A	L
<i>Lotus corniculatus</i> VDAC1.2	V	G	T	N	A	L	A	V	G	T	D	L	S	F	D	--	T	K	I	G	E	L	T	K	F	N	A	G	L	N	F	T	K	A	D	L	I	A	S	L	T	V	N	D	K	G	D	A	L
<i>Medicago truncatula</i> VDAC1.1	I	G	N	N	V	A	L	G	G	D	L	S	Y	D	--	T	K	T	G	V	E	T	R	L	N	A	G	L	N	F	T	K	D	D	L	I	A	S	L	T	L	N	E	K	A	N	A	L	
<i>Picea glauca</i>	I	G	N	D	T	F	S	V	G	G	E	V	S	F	D	--	T	A	S	G	N	F	L	K	Y	D	A	G	L	S	F	S	K	P	D	F	V	S	S	L	T	L	T	G	K	G	D	T	L
<i>Pinus pinus</i>	I	G	N	D	T	F	A	V	G	G	E	V	S	F	D	--	T	A	S	G	N	F	L	K	Y	D	A	G	L	S	F	S	K	P	D	F	V	S	S	L	T	L	T	G	K	G	D	T	L
<i>Pinus pinus</i>	I	G	N	E	S	V	A	L	G	G	E	F	A	F	D	--	T	A	S	G	N	F	T	K	Y	N	A	G	L	N	F	V	Q	P	D	F	I	S	S	L	N	L	T	D	R	G	D	T	L
<i>Populus trichocarpa</i>	I	G	T	N	V	A	S	L	G	T	D	L	S	F	D	--	T	K	T	G	D	F	I	K	C	N	A	G	V	S	L	S	K	V	D	L	I	A	S	L	T	L	N	D	K	G	D	S	L
<i>Glycine max</i> VDAC1.3	V	G	N	N	L	V	A	V	G	T	D	L	S	F	D	--	T	A	S	G	N	F	T	K	Y	N	A	G	L	N	I	T	H	A	D	L	I	A	S	L	T	L	N	D	K	G	D	N	L
<i>Medicago truncatula</i> VDAC1.3	L	G	N	N	L	V	S	V	G	S	D	V	S	F	E	--	T	S	S	G	S	L	N	K	C	N	F	G	L	N	V	T	H	A	D	L	I	A	S	L	T	V	N	D	R	G	D	S	L
<i>Arabidopsis thaliana</i> VDAC3	I	G	S	N	V	L	A	V	G	T	D	V	S	F	D	--	T	K	S	G	N	F	T	K	I	N	A	G	L	S	F	T	K	E	D	L	I	A	S	L	T	V	N	D	K	G	D	L	L
<i>Pisum sativum</i> plastid porin	F	G	S	K	A	L	S	V	G	V	D	V	S	F	D	--	T	A	T	S	D	F	T	K	Y	N	A	A	V	N	F	V	K	D	S	L	I	G	S	L	T	L	N	E	K	G	D	L	L
<i>Pisum sativum</i> plastid porin	I	G	T	N	A	L	A	F	G	A	D	I	S	F	D	--	T	K	L	G	E	L	T	K	S	N	A	A	V	N	F	V	K	D	L	I	G	S	L	T	L	N	E	K	G	D	L	L	
<i>Arabidopsis thaliana</i> VDAC3	V	G	T	N	G	L	S	L	G	T	D	V	A	Y	N	--	T	E	S	G	N	F	K	H	F	N	A	G	F	N	F	T	K	D	D	L	I	A	S	L	I	N	D	K	G	E	L	L	
<i>Brassica rapa</i>	I	G	T	S	V	L	A	L	G	T	D	V	S	F	D	--	T	E	S	G	N	F	K	H	F	N	T	G	V	S	F	T	K	D	D	L	I	A	S	L	T	L	N	D	K	G	E	L	L
<i>Solanum habrochaites</i> VDAC1	V	G	T	N	I	V	A	L	G	T	D	V	S	F	D	--	T	K	T	G	D	F	T	K	C	N	A	G	L	S	F	T	N	A	D	L	V	A	S	L	N	L	N	N	K	G	D	N	L
<i>Citrus reticulata</i> VDAC1	V	G	N	N	S	V	A	L	G	T	D	L	S	F	D	--	T	A	T	G	N	F	T	K	C	N	A	G	L	S	Y	T	H	T	D	L	I	A	S	L	T	L	N	D	K	G	D	T	L
<i>Gossypium raimondii</i> VDAC3.1	I	G	S	K	E	L	A	L	G	G	E	I	G	F	D	--	T	A	S	A	S	F	T	E	Y	T	A	G	I	N	L	N	K	P	D	F	S	V	A	L	L	L	T	D	K	G	Q	A	L
<i>Vitis vinifera</i> VDAC3.1	I	G	S	K	D	L	S	L	G	G	E	V	G	L	N	--	T	A	S	A	S	F	T	K	Y	N	A	G	I	G	I	T	K	P	D	F	S	V	A	L	L	T	D	K	G	E	T	L	
<i>Solanum tuberosum</i> VDAC3	I	G	S	K	D	L	A	L	G	G	E	I	G	F	N	--	T	A	S	S	S	I	T	K	C	N	A	G	I	S	F	N	K	P	D	F	S	A	A	L	M	L	T	D	R	G	O	A	V
<i>Lotus corniculatus</i> VDAC3.1	I	G	S	K	D	L	C	M	G	A	E	V	G	F	N	--	T	T	S	A	S	F	T	K	Y	N	A	G	I	T	F	N	R	P	D	F	S	A	A	L	M	L	V	D	K	G	K	S	L
<i>Glycine max</i> VDAC3.1	I	G	S	K	D	L	C	L	G	A	E	V	G	F	N	--	T	T	S	A	S	F	T	K	Y	N	A	G	V	A	F	N	K	P	D	F	S	V	A	L	M	L	A	D	K	G	Q	T	L
<i>Medicago truncatula</i> VDAC3.1	I	G	S	K	D	I	S	M	G	A	E	V	G	F	D	--	T	T	S	A	S	F	S	I	Y	N	A	G	I	A	F	N	K	P	D	F	S	A	T	L	M	L	A	D	K	G	S	L	
<i>Allium cepa</i>	T	G	T	K	D	I	T	L	G	A	E	I	A	F	D	--	T	A	S	A	S	F	S	K	Y	N	A	G	V	M	L	T	K	P	D	F	S	A	S	L	I	L	A	D	K	G	E	T	L
<i>Pinus pinus</i>	L	G	Y	D	E	I	S	V	G	G	E	M	A	F	D	--	T	A	S	G	T	E	L	K	Y	N	A	G	I	G	L	S	K	P	E	Y	T	A	A	V	I	L	A	D	K	G	D	T	V
<i>Pinus taeda</i>	I	G	S	D	V	F	T	V	G	G	E	V	G	F	D	--	T	S	S	G	L	I	T	K	Y	N	A	A	I	G	I	T	K	P	E	F	S	A	A	V	I	F	A	D	K	G	D	T	L
<i>Hordeum vulgare</i> VDAC3.1	I	G	T	N	E	L	A	V	G	G	E	V	G	F	D	--	T	S	S	A	S	V	T	K	Y	N	S	G	I	S	Y	T	K	D	D	F	S	A	A	L	L	A	D	K	G	E	T	L	
<i>Sorghum bicolor</i> VDAC3.1	V	G	T	S	E	L	T	I	G	A	E	V	G	F	D	--	T	S	S	A	A	V	T	K	Y	N	S	G	I	G	Y	N	K	S	D	F	S	A	S	L	L	L	A	D	K	G	E	T	L
<i>Oryza sativa</i> POM36	I	G	T	N	E	L	S	A	G	A	E	V	G	F	D	--	T	S	S	A	S	V	T	K	Y	N	S	G	I	C	Y	N	K	H	D	F	S	A	A	V	L								

		160	170	180	190	200
<i>Beta vulgaris</i>		LGTPTAFGV	EAGVD--ANS	GNFTKYTAGV	NVSKPE	SCASILLGDKGDTI
<i>Cycas rumphii</i>		IGNESLAFGG	EVAFD--TAS	GNFTKYNAGL	SPVKPDFISS	LILTODKGDILL
<i>Glycine max</i> VDAC1.2		VGTNVLAALGT	DVSFD--TKI	GELTKFNAGL	NFTKDDL	VASLTVNTKV---
<i>Hordeum vulgare</i>		LKSLLSLVVP	DQRSGK--LEL	QYLHEFASVN	ASVGLNPS	SPMVNLSGVF--GS
<i>Lycopersion esculentum</i> VDAC2		PLIDVKVDTR	IKFLAG--XRL	NI FTITPTFT	TAVALKQCPA	VDLSITL--GT
<i>Citrus sinensis</i>		LKTLISFKVP	DQRS--GKV	ELOYLHDYAG	ISTSVGLTAN	PIVNFSA--VI
<i>Gossypium raimondii</i> VDAC1.3		LKTLISFIAP	DQRSGKVELQ	YQHEYAGIST	SIGLTANPLV	NFSGVVG--NN
<i>Picea glauca</i>		LKTLISFTVP	DQRSGK--VEL	QYLHDYAGVS	TSIGLTPSPI	THESGVI--GN
<i>Welwitschia mirabilis</i>		LKALISFTIP	DQRSGK--VEL	QYYHDYAGVS	AVGMTASPV	VETSVAV--GN
<i>Acorus americanus</i>		LKTLISFVVP	DQKSGK--AEI	QYLHDYAGIT	SSIGLTANPV	VNMSGVI--GS
<i>Selaginella moellendorffii</i>		VKALIGVNL	NVSTGK--VEV	HYVHDNVGLT	SAVGLTASPP	VDVTAAF--GN
		210	220	230	240	250
<i>Oryza sativa</i> VDAC1		TASYHHVNH	S--ATAVGAEL	THSFSSNEN	SLTFGTQHTLD	P-----
<i>Triticum aestivum</i> VDAC1		TASYHHVEK	S--GTAVGAEL	THSFSSNEN	SLTFGTQHTLD	P-----
<i>Triticum aestivum</i>		TASYHHVEK	S--GTAVGAEL	THSFSSNEN	SLTFGTQHTLD	P-----
<i>Hordeum vulgare</i>		TASYHHVEK	S--STAVGAEL	THSFSSNEN	SLTFGTQHTLD	P-----
<i>Zea mays</i> VDAC2		AASYHHVSP	T--TAVGGEL	SHSFSTNGNT	ITFGTQHALD	P-----
<i>Oryza sativa</i> VDAC2		AASYHHVSK	T--SAVGAEL	AHSFSSNENT	LTFGTQHALD	E-----
<i>Triticum aestivum</i> VDAC2		AASYHHVQR	T--TAVGAEL	AHSFSSNENT	ITIGTQHELD	P-----
<i>Hordeum vulgare</i>		AASYHHVQL	T--TAVGAEL	AHSFSSNENT	ITVGTQHELD	P-----
<i>Triticum aestivum</i>		AASYHHVQR	T--TAVGAEL	AHSFSSNENT	ITVGTQHELD	P-----
<i>Asparagus officinalis</i> VDAC1		SASYHHVSP	LTSTAVGAEM	THSFSSNENT	LTFGTQHALD	P-----
<i>Triticum aestivum</i> VDAC3		TASYHHVKY	TSTAVGAEL	SHMFPRNEST	LIFGSQHSLD	P-----
<i>Triticum aestivum</i>		TASYHHVKS	HSTAVGAEL	SHMFPRNEST	LIFGSQHSLD	P-----
<i>Zea mays</i> plastid porin		VASYHHVKN	HSGTAVGAEL	SHMSRNEST	LIFGSQHSLD	P-----
<i>Zea mays</i> plastid porin		VASYHHVKN	HSGTAVGAEL	SHMSRNEST	LIFGSQHSLD	P-----
<i>Sorghum bicolor</i> plastid porin		VGSYYHLVKH	HSGTAVGAEL	SHSIRNEST	LIFGSQHSLD	P-----
<i>Saccharum officinarum</i> plastid porin		VASYHHVKN	HSGTAVGAEL	SHSVSRNEST	LIFGSQHSLD	P-----
<i>Oryza sativa</i> VDAC3		IASYHHVKN	HNTAVGAEL	SHSFSSNENT	LIFGSQHSLD	P-----
<i>Zea mays</i> VDAC1a		TGAYHHVSE	LNTAVGAEL	THSFSTNENT	LTFGGQHALD	P-----
<i>Zea mays</i> VDAC1b		TGAYHHVSE	LNTAVGAEL	THSFSTNENT	LTFGGQHALD	P-----
<i>Citrus paradisi</i> VDAC1		NASYHHVSP	LNTAVGAEL	THSFSSNENT	LTIGTQHALD	P-----
<i>Nicotiana tabacum</i> POM36		SASYHHVVKP	VNTAVGAEL	THSFSSNENT	LTIGTQHALD	P-----
<i>Spinacia oleracea</i> VDAC1		NASYHHVSP	LNTAVGAEL	SHSFSSNENT	LNI GTQHALD	P-----
<i>Mesembryanthemum crystallinum</i>		NASYHHVSP	LNTAVGAEL	SHSFSSNENT	LNI GTQHALD	P-----
<i>Lycopersion esculentum</i> VDAC1.3		NASYHHVSP	LNTAVGAEL	SHSFSSNENT	LTIGTQHALD	P-----
<i>Prunus armeniaca</i>		TASYHHVSP	LNTAVGAEL	SHSFSSNENT	LTIGTQHALD	P-----
<i>Solanum tuberosum</i> VDAC1		SASYHHVVKP	VNTAVGAEL	THSFSSNENT	LTIGTQHALD	P-----
<i>Lycopersion esculentum</i> POM36		SASYHHVVKP	VNTAVGAEL	THSFSSNENT	LTIGTQHALD	P-----
<i>Populus trichocarpa</i>		SASYHHVSP	LNTAVGAEL	THSFSSNENT	LTIGTQHALD	P-----
<i>Vitis vinifera</i> VDAC1.1		NASYHHVNL	LNTAVGAEL	THSFSTNENT	LTLGAQHLLD	P-----
<i>Helianthus annuus</i> POM34		NASYHHVVKP	LNTAVGAEL	RHNFSTNENT	ITVGTQHALD	P-----
<i>Solanum tuberosum</i> POM34		TASYHHVSP	LNTAVGAEL	NHSFSTNENT	ITVGTQHALD	P-----
<i>Lycopersion esculentum</i> POM34		TASYHHVSP	LNTAVGAEL	NHSFSTNENT	ITVGTQHALD	P-----
<i>Lycopersion esculentum</i> POM34		SASYHHVSP	LNTAVGAEL	THSFSTNENT	ITVGTQHALD	P-----
<i>Solanum tuberosum</i> POM34		SASYHHVTP	LNTAVGAEL	THSFSTNENT	ITVGTQHALD	P-----
<i>Lotus corniculatus</i> VDAC1.1		NASYHHVSP	LNTAVGAEL	THRFSTNENT	LTLGTQHALD	P-----
<i>Glycine max</i> VDAC1.1		NAAYHHVNP	LNTAVGAEL	THRFSTNENT	LTLGTQHALD	P-----
<i>Lotus corniculatus</i> VDAC1.2		NASYHHVNP	LNTAVGAEL	THRFSTNENT	LTLGTQHALD	P-----
<i>Medicago truncatula</i> VDAC1.1		NASYHHVNP	VTKTAVGAEL	SHRFSTKENT	LTLGTQHALD	S-----
<i>Picea glauca</i>		KASYLHTVSP	LTKTAVGAEL	SHSFSSNENT	FTIGTQHALD	P-----
<i>Pinus pinus</i>		KASYLHTVSP	LTKTAVGAEL	SHSFSSNENT	FTIGTQHALD	P-----
<i>Pinus pinus</i>		KASYLHTVSP	LTKTAVGAEL	SHSFSSNENT	FTIGTQHALD	P-----
<i>Populus trichocarpa</i>		NASYHHVNP	LNTAVGAEL	SHSFSSNENT	ITVGAQHALLD	P-----
<i>Glycine max</i> VDAC1.3		TASYHHVNP	LNTAVGAEL	SHSFSSNENT	LTFGTQHALD	P-----
<i>Medicago truncatula</i> VDAC1.3		NASYHHVSP	LNTAVGAEL	SHSFSSNENT	LTIGTQHALD	P-----
<i>Arabidopsis thaliana</i> VDAC3		NASYHHVNP	LNTAVGAEL	SHKLSSKDS	ITVGTQHALD	P-----
<i>Pisum sativum</i> plastid porin		SASYHHVNP	LNTAVGVDI	SHRFSTKENT	FTLGTQHALD	P-----
<i>Pisum sativum</i> plastid porin		SASYHHVNP	LNTAVGVDI	SHRFSTKENT	FTLGTQHALD	P-----
<i>Arabidopsis thaliana</i> VDAC3		NASYHHVNP	LNTAVGAEL	SHNFSTKENT	ITVGTQHALD	P-----
<i>Brassica rapa</i>		NASYHHVNP	LNTAVGAEL	SHNLKSSQVNS	ITVGTQHALD	P-----
<i>Solanum habrochaites</i> VDAC1		TASYHHVSP	LNTAVGAEL	NHSFSTNENT	ITVGTQHALD	P-----
<i>Citrus reticulata</i> VDAC1		NASYHHVSP	LNTAVGAEL	THSFSSNENT	LTIGTQHALD	P-----
<i>Gossypium raimondii</i> VDAC3.1		KASYIHSVNP	F--LCVAAEM	AHRFSTYENT	FTIGSSHAVD	P-----
<i>Vitis vinifera</i> VDAC3.1		KASYIHSVNP	PGGTTVAAL	THKFNTYENT	FTIGSAHVVD	P-----
<i>Solanum tuberosum</i> VDAC3		KASYVHSVDP	ANGTEVGAEM	IHRLSTYENT	FSIGSSHKVD	P-----
<i>Lotus corniculatus</i> VDAC3.1		KASYIHHVDR	PDGFTVAAEI	NHRFSSFE	FTIGSSQLD	P-----
<i>Glycine max</i> VDAC3.1		KASYIHHVDR	PDGFTVAAEI	SHRFSSLEN	FTIGSSQSD	P-----
<i>Medicago truncatula</i> VDAC3.1		KASYIHHVDR	PDGLTVAAEL	AHKLSSSEN	FTFGTSQSD	P-----
<i>Allium cepa</i>		KASYIHLVNP	ASENAVAAEM	VHRFNTFENT	FTIGSSHKD	T-----
<i>Pinus pinus</i>		KASYTHVNP	ISKTAVAAEF	THKFSTNENT	YTVGSSHAID	Q-----
<i>Pinus taeda</i>		KASYLHELNP	ITKTCFAAEI	SRKFSANQNT	FTVGSYYALD	P-----

	210	220	230	240	250
<i>Hordeum vulgare</i> VDAC3.1	KASYIHLFSP	T--SAVAAEV	MHLKTKENY	FTIGSSHALD	P-----
<i>Sorghum bicolor</i> VDAC3.1	KASYIHLFNP	TNGATVAAEV	THKFKTKENY	FTVGSSHALD	P-----
<i>Oryza sativa</i> POM36	KASYIHLFNE	TNGATVAAEV	THKLKTKENY	FTIGSSHALD	S-----
<i>Arabidopsis thaliana</i> POM36	RATYVHTVNP	T--SFGAEL	IRRFSNYNNS	FTVGSSHSVD	Q-----
<i>Pennisetum glaucum</i>	KVSGVYHLDE	KOKASAVAEI	TRRLSTNVNT	LTVGGLYKID	P-----
<i>Zea mays</i>	KVSGVYHLDE	KOKASAVAEI	TRRLSTNQNT	LTVGGLYTVD	P-----
<i>Triticum aestivum</i>	KVSGVYHLDE	KOKASAVAEI	TRKLSTNENT	LTVGGLYTVD	P-----
<i>Vitis vinifera</i> VDAC2.1	RASYVHHLDS	LKKSAAVGEI	SRRFSTNDNT	FTVGGSYALD	P-----
<i>Solanum tuberosum</i> VDAC2	KASYIHLHDE	LKKSAAVGEI	TRRFSTNENT	FTVGGSYAVD	N-----
<i>Glycine max</i> VDAC2.1	KASYLHHLDL	LKKSAAVAEI	TRKFSTNENI	FTVGGSFAYD	P-----
<i>Lotus corniculatus</i> VDAC2.1	KASYLHHLDD	LKKSAAVAEI	TRKFSTNENT	FTVGGSFAYD	H-----
<i>Gossypium raimondii</i> VDAC2.1	KASYVHYLDN	LKKSAAVGEI	SRRFSTNENT	FTVGGSYAVD	H-----
<i>Medicago truncatula</i> VDAC2.1	KVSYLHHLDD	LKKSAAVVDI	TRRFSTNQNT	ITVGGSFAYD	P-----
<i>Arabidopsis thaliana</i> VDAC3	KASYLHHLDE	FKRTAAVGEV	YRKFSSTNENT	ITVGGLYALD	H-----
<i>Ananas comosus</i>	GASYYYHLVSP	L--SAVGAEL	THSFASSENT	LTFGTQHQLD	P-----
<i>Saccharum officinarum</i> VDAC3.1	KASYIHLFNP	TNGATVAAEV	THKFKTKENY	FTIGSSHALD	P-----
<i>Antirrhinum majus</i>	SASYYYHTVSP	FTNTAVSAEV	THSFSSNENT	ITVGTOHSLD	P-----
<i>Welwitschia mirabilis</i>	KASYLHTVSP	LTKTAVGAEL	QHSCKSKSENT	LTIGTQHALLD	P-----
<i>Allium cepa</i>	SASYYYHLVNP	LSNTAVGAEM	THSFTTNENT	LTFGTQHVLD	P-----
<i>Zantedeschia aethiopica</i>	TAAYYYHLVSP	LMSAVGAEL	AHCFSSNENT	LTFGTQHALLD	P-----
<i>Lycopersion esculentum</i> VDAC3.1	KASYVHLVDP	TNGTEVGAEM	IHRLSTYENS	FSIGSAHVVD	S-----
<i>Triphysaria versicolor</i>	SASYYYHVNP	LNTAVGAEV	THSFSSNENT	ITVGTOHTLD	P-----
<i>Picea sitchensis</i>	KASYLHTVSP	LTKTAVGAEL	SHSFSRSSENT	FTIGTQHALLD	P-----
<i>Gossypium raimondii</i> VDAC1.1	NASYYYHIVNP	MTNTAVGAEV	THSFTSNENT	ITIGTQHALLD	P-----
<i>Saruma henryi</i>	TASYFHI VSP	LNTAVGAEL	SHCFSSNDNT	LTIGTQHALLD	P-----
<i>Brassica rapa</i>	NASYYYHIVNP	LFNTAVGAEV	NHKFSTNVNT	ITVGTOHSLD	P-----
<i>Liriodendron tulipifera</i>	KASYYYHTVRP	LTSNTAVGAEL	SHSFTSNENT	LTIGTQHALLD	P-----
<i>Saccharum officinarum</i> VDAC1	TGAYYYHKVSE	LSNTAGGAEL	THSFTSNENT	LTFGTQHALLD	P-----
<i>Panicum virgatum</i>	TAAYYYHNVNL	LTSNTAVGAEL	THSFTSNENT	LTFGTQHALLD	P-----
<i>Lactuca sativa</i>	TASYYYHTVSP	LTKRIWGGEL	THGFSNENSS	VDFWDTAVVG	S-----
<i>Nicotiana tabacum</i> POM34	SASYYYHIVSP	LTYTAVSAEV	---	PTVS-	-----
<i>Eschscholzia californica</i>	NASYYYHTVSP	L---	---	TSTA-	-----
<i>Beta vulgaris</i>	KASYLHHLDD	LNKNAAVAEF	S---	RRFS-	-----
<i>Cycas rumphii</i>	KASYLHTVSP	---	---	---	P-----
<i>Glycine max</i> VDAC1.2	---	---	---	---	-----
<i>Hordeum vulgare</i>	KELSVGV DVS	FDTATSNTFK	YNAALSLAY-	PDLIASLHL	NNHGDTLTAS
<i>Lycopersion esculentum</i> VDAC2	PTFALGAEAS	YETATSKLTK	YTAGISVTK-	PDSCAAIL	GDKGDTIKAS
<i>Citrus sinensis</i>	GTNVLSLGTDL	LSFDSKSGNF	TKCNAGLSFN	NADLIASLNL	NNKGDLSAAS
<i>Gossypium raimondii</i> VDAC1.3	SVTVGTDL	LSFDTASGNFTKI	NAGLNFTHSD	LIASLIL	--VNDKGDTLNAS
<i>Picea glauca</i>	DTFSVGG EVS	F--DTASGNF	LKYDAGLSFS	KPDFVSLTL	TGKGDTLKAS
<i>Welwitschia mirabilis</i>	ENVALGG EIA	F--DTTSSNL	TKYNAGISYI	KPDFILGVNW	TDKGDVAKAS
<i>Acorus americanus</i>	NVLSVGLHVS	F--DTATGNF	LKYNAGLSFT	NADLIAALNL	NNKGDTLVAS
<i>Selaginella moellendorffii</i>	KEYSLGGAVS	L--DTAAGTV	KKYEAGLGIT	KPDFTAALL	CDKGDTVKVS
	260	270	280	290	300
<i>Oryza sativa</i> VDAC1	---	---	---	LT	VVKARFNNSG
<i>Triticum aestivum</i> VDAC1	---	---	---	LT	LVKARFNNSG
<i>Triticum aestivum</i>	---	---	---	LT	LVKARFNNSG
<i>Hordeum vulgare</i>	---	---	---	LT	LVKARFNNSG
<i>Zea mays</i> VDAC2	---	---	---	LT	TVKARFNNYG
<i>Oryza sativa</i> VDAC2	---	---	---	LT	TVKARFNNFG
<i>Triticum aestivum</i> VDAC2	---	---	---	LT	TVKGRYNNFG
<i>Horeum vulgare</i>	---	---	---	LT	TLKGRYNNFG
<i>Triticum aestivum</i>	---	---	---	LT	TVKGRYNNFG
<i>Asparagus officinalis</i> VDAC1	---	---	---	LT	TVKARFNNYG
<i>Triticum aestivum</i> VDAC3	---	---	---	HT	SVKARFNNYG
<i>Triticum aestivum</i>	---	---	---	HT	SVKARFNNYG
<i>Zea mays</i> plastid porin	---	---	---	HT	TIKTRFNNYG
<i>Zea mays</i> plastid porin	---	---	---	HT	TIKTRFNNYG
<i>Sorghum bicolor</i> plastid porin	---	---	---	HT	TVKARFNNYG
<i>Saccharum officinarum</i> plastid porin	---	---	---	HT	TVKARFNNYG
<i>Oryza sativa</i> VDAC3	---	---	---	HT	TVKARFNNYG
<i>Zea mays</i> VDAC1a	---	---	---	LT	VLKARFNNSG
<i>Zea mays</i> VDAC1b	---	---	---	LT	VLKARFNNSG
<i>Citrus paradisi</i> VDAC1	---	---	---	LT	SVKARFNNYG
<i>Nicotiana tabacum</i> POM36	---	---	---	LT	TVKARFNNYG
<i>Spinacia oleracea</i> VDAC1	---	---	---	LT	SVKARFNNYG
<i>Mesembryanthemum crystallinum</i>	---	---	---	LT	NLKGRYNNFG
<i>Lycopersion esculentum</i> VDAC1.3	---	---	---	IT	LLKARFNNYG
<i>Prunus armeniaca</i>	---	---	---	LT	TVKGRYNNYG
<i>Solanum tuberosum</i> VDAC1	---	---	---	LT	TVKARFNNYG
<i>Lycopersion esculentum</i> POM36	---	---	---	LT	TVKARFNNYG
<i>Populus trichocarpa</i>	---	---	---	LT	TVKARFNNYG
<i>Vitis vinifera</i> VDAC1.1	---	---	---	LT	TVKARFNNFG

	260	270	280	290	300
<i>Helianthus annuus</i> POM34				LT TVKAR	DNLG
<i>Solanum tuberosum</i> POM34				LT SVKAR	NNFG
<i>Lycopersion esculentum</i> POM34				LT SVKAR	NNFG
<i>Lycopersion esculentum</i> POM34				LT TVKAR	NNFG
<i>Solanum tuberosum</i> POM34				LT TVKAR	NNFG
<i>Lotus corniculatus</i> VDAC1.1				LT TLKAR	NNFG
<i>Glycine max</i> VDAC1.1				LT TLKAR	NNFG
<i>Lotus corniculatus</i> VDAC1.2				LT SVKAR	NNLG
<i>Medicago truncatula</i> VDAC1.1				LT TAKLR	NNFG
<i>Picea glauca</i>				LT TVKGR	NNYG
<i>Pinus pinus</i>				LT TVKGR	NSYG
<i>Pinus pinus</i>				FT TVKAR	NNHG
<i>Populus trichocarpa</i>				LT TLKAR	NNAG
<i>Glycine max</i> VDAC1.3				LT LLKSR	NNYG
<i>Medicago truncatula</i> VDAC1.3				VT LLKAK	NNYG
<i>Arabidopsis thaliana</i> VDAC3				LT SVKAR	VNSAG
<i>Pisum sativum</i> plastid porin				LT TVKGR	VNTSG
<i>Pisum sativum</i> plastid porin				LT TVKGR	VNTSG
<i>Arabidopsis thaliana</i> VDAC3				LT TVKAR	VNNAG
<i>Brassica rapa</i>				LT TVKAR	VNNAG
<i>Solanum habrochaetes</i> VDAC1				LT SVKAR	NNFG
<i>Citrus reticulata</i> VDAC1				LT SVKAR	NNYG
<i>Gossypium raimondii</i> VDAC3.1				FT VVKTR	FDNG
<i>Vitis vinifera</i> VDAC3.1				YT MMKTR	SNNG
<i>Solanum tuberosum</i> VDAC3				LT SLKTR	SDNG
<i>Lotus corniculatus</i> VDAC3.1				NT VLKTR	SDDG
<i>Glycine max</i> VDAC3.1				KT VLKTR	SDDG
<i>Medicago truncatula</i> VDAC3.1				KT VLKTR	SDDG
<i>Allium cepa</i>				AT MMKTR	SNNG
<i>Pinus pinus</i>				LT TMKSR	DNRG
<i>Pinus taeda</i>				LT TMKTR	NNHG
<i>Hordeum vulgare</i> VDAC3.1				ST TVKTR	SNSG
<i>Sorghum bicolor</i> VDAC3.1				ST LLKTR	SNSG
<i>Oryza sativa</i> POM36				ST LLKTR	SNGG
<i>Arabidopsis thaliana</i> POM36				FT VVKTR	SNSG
<i>Pennisetum glaucum</i>				QT AVKAR	NNTG
<i>Zea mays</i>				QT ALKAR	NNTG
<i>Triticum aestivum</i>				QT AVKAR	NNTG
<i>Vitis vinifera</i> VDAC2.1				LT NVKAR	NNHG
<i>Solanum tuberosum</i> VDAC2				LT IVKLK	NNHG
<i>Glycine max</i> VDAC2.1				LT QVKAR	NNHG
<i>Lotus corniculatus</i> VDAC2.1				LT QVRAR	NNHG
<i>Gossypium raimondii</i> VDAC2.1				LT LIKAR	NNHG
<i>Medicago truncatula</i> VDAC2.1				LT QIKAR	NNQG
<i>Arabidopsis thaliana</i> VDAC3				ST AVKAR	NNHG
<i>Ananas comosus</i>				LT TVKAR	NNYG
<i>Saccharum officinarum</i> VDAC3.1				ST LLKTR	SNSG
<i>Antirrhinum majus</i>				LT TVKAR	NNFG
<i>Welwitschia mirabilis</i>				LT TVRAR	DNYG
<i>Allium cepa</i>				LT MVKAR	NNYG
<i>Zantedeschia aethiopica</i>				LT SVKAR	NNFG
<i>Lycopersion esculentum</i> VDAC3.1				LT SLKTR	SDNG
<i>Triphysaria versicolor</i>				LT SVKAR	NNFG
<i>Picea sitchensis</i>				LT TVKGR	NNYG
<i>Gossypium raimondii</i> VDAC1.1				LT MVKAR	VNNAG
<i>Saruma henryi</i>				LT SVKAR	NNFG
<i>Brassica rapa</i>				LT TVKAR	VNS--
<i>Liriodendron tulipifera</i>				LT SVKAR	-V--
<i>Saccharum officinarum</i> VDAC1				-R-	
<i>Panicum virgatum</i>				LT	
<i>Lactuca sativa</i>				VD	Y-
<i>Nicotiana tabacum</i> POM34					
<i>Eschscholzia californica</i>					
<i>Beta vulgaris</i>					
<i>Cycas rumphii</i>				LT	RLQLE-
<i>Glycine max</i> VDAC1.2					
<i>Hordeum vulgare</i>	YYHLVKSHSS	TAVGAELSHN	FPRNESTLIF	GSQHS	SLDPHT SVKARFNNYG
<i>Lycopersion esculentum</i> VDAC2	YIHHMDALKT	TAATGEITRR	FSTNENTFTV	GGSYAVDCLT	IVKLKLNHHG
<i>Citrus sinensis</i>	YYHFNPLT-	-AVGAEVIHS	FSTTDNTITV	GTQHILDPLT	TLKARVNNAG
<i>Gossypium raimondii</i> VDAC1.3	YYHIVSPLTN	PTVGAELSHS	FSSNENPFPI	GTQHAFDPLT	TVKAXLNNYG
<i>Picea glauca</i>	YLHTVSP LTK	TAVGAELSHS	FSSSENTFTI	GTQHAXXXLT	TVXXRLNNYG
<i>Welwitschia mirabilis</i>	YLQHI DPSKN	TTVGVEACHS	ISXNENTFTL	GAQHALDPLT	MVKVRCNSHG
<i>Acorus americanus</i>	YYHLVSP LTS	TAVGVE MTHS	FSTNENTLTI	GTQHAXLPLT	TVKGRVNNYG
<i>Selaginella moellendorffii</i>	YSHTVSP LTK	ATVGAEEVHS	ISKKLNTFTH	RGAYNLDLLT	TVKARLNNXG

		310	320	330	340
<i>Oryza sativa</i> VDAC1	KASALQHEW	RPKSVWTISA	EVDT-KAIDK	SSKVGIAVAL	KP
<i>Triticum aestivum</i> VDAC1	KASALQHEF	MPKSLCTISA	EVDT-KAIEK	SSKVGIAIAL	KP
<i>Triticum aestivum</i>	KASALQHEF	MPKSLCTISA	EVDT-KAIEK	SSKVGIAIAL	KP
<i>Hordeum vulgare</i>	KASALQHEF	RPKSLCTISA	EVDT-KAIEK	SSKVGIAIAL	KP
<i>Zea mays</i> VDAC2	MASALQHEW	RPKSLVTIST	EVDT-KAIEK	SSKVGLSLVL	KP
<i>Oryza sativa</i> VDAC2	MASALQHEF	RPKSLVTIST	EVDT-KAIDK	SSKVGLSLVL	KP
<i>Triticum aestivum</i> VDAC2	VASALQHAW	RPKSLITFST	EVDT-KAIEK	SPKFGALALS	KP
<i>Horeum vulgare</i>	IASALQHAW	RPKSVITFST	EVDT-KAVEK	SPKFGALALS	KP
<i>Triticum aestivum</i>	IANALQHAW	RPKSLITFST	EVDT-KAIEK	SPKFGALALS	KP
<i>Asparagus officinalis</i> VDAC1	RASALQHQW	RPKSFVTISG	EVDT-KAIEK	SSKVGLSLVL	KP
<i>Triticum aestivum</i> VDAC3	MASALVQHEW	RAKSLVTISG	EVDT-KAIEK	STKVGLSLVL	KP
<i>Triticum aestivum</i>	MASALVQHEW	RAKSLVTISG	EVDT-KAIEK	STKVGLSLVL	KP
<i>Zea mays</i> plastid porin	MASALVQHEW	RPKSFVTISG	DVDT-KAIEK	STKVGLSLVL	KH
<i>Zea mays</i> plastid porin	MASALVQHEW	RPKSFVTISG	DVDT-KAIEK	STKVGLSLVL	KH
<i>Sorghum bicolor</i> plastid porin	MASALVQHEW	RPKSFVTISG	EVDT-KAIEK	STKVGLSLVL	KH
<i>Saccharum officinarum</i> plastid porin	MASALVQHEW	RPKSFVTISG	EVDT-KAIEK	STKVGLSLVL	KH
<i>Oryza sativa</i> VDAC3	MASALVQHEW	RPKSLITISG	EVDT-KAIEK	STKVGLSLVL	KH
<i>Zea mays</i> VDAC1a	KASALQHEW	RPKSLVTISA	EVDT-KTIEK	SSKVGIAVAL	KP
<i>Zea mays</i> VDAC1b	KASVLTQHEW	RPKSLVTISA	EVDT-KTIEK	SSKVGIAVAL	KP
<i>Citrus paradisi</i> VDAC1	RASALQHEW	RPKSLFTISG	EVDT-RAIEK	SAKIGLALAL	KP
<i>Nicotiana tabacum</i> POM36	KASALQHEW	RPKSLFTISG	EVDT-RAIEK	SAKIGLALAL	KP
<i>Spinacia oleracea</i> VDAC1	KASALQHEW	RPKSLVTISG	EVDT-SAIEK	SAKIGLALAL	KP
<i>Mesembryanthemum crystallinum</i>	KATALQHEW	RPKSLVTISG	EVDT-KAIEK	SAKIGLALAL	KP
<i>Lycopersion esculentum</i> VDAC1.3	RASALQHEW	NPRTRVSLVG	EVDT-GAIEK	SAKIGLALAL	KP
<i>Prunus armeniaca</i>	RASALQHEW	RPKSFFTISG	EVDT-RAIEK	SAKIGLALAL	KP
<i>Solanum tuberosum</i> VDAC1	KASALQHEW	RPKSLFTISG	EVDT-RAIEK	SAKIGLALAL	KP
<i>Lycopersion esculentum</i> POM36	KASALQHEW	RPKSLFTISG	EVDT-RAIEK	SAKIGLALAL	KP
<i>Populus trichocarpa</i>	KVSALQHEW	RPKSLFTISG	EVDT-KAIEK	SAKIGLALAL	KP
<i>Vitis vinifera</i> VDAC1.1	KASALQHEW	RPKSLFTISG	EVDT-KAVDK	TAKVGLALAL	KP
<i>Helianthus annuus</i> POM34	KANALQHEW	RPKSLFTISG	EVDT-KAVDK	SAKFGALALAL	KP
<i>Solanum tuberosum</i> POM34	KASALQHEW	RPKSLFTVSG	EVDT-KSVDK	GAKFGALALAL	KP
<i>Lycopersion esculentum</i> POM34	KASALQHEW	RPKSLFTVSG	EVDT-KSVDK	GAKFGALALAL	KP
<i>Lycopersion esculentum</i> POM34	MATALQHEW	RPKSLFTISG	EVDT-KAVDK	SAKFGALALAL	KP
<i>Solanum tuberosum</i> POM34	TATALQHEW	RPKSLFTISG	EVDT-KAVDK	SAKFGALALAL	KP
<i>Lotus corniculatus</i> VDAC1.1	KASALQHEW	RPKSFFTISG	EVDT-KAIEK	SAKIGLALAL	KP
<i>Glycine max</i> VDAC1.1	RTSALQHEW	RPKSFFTISG	EVDT-KAIEK	SAKVGGLGLVL	KP
<i>Lotus corniculatus</i> VDAC1.2	KANALQHEW	RAKSFFTISG	EVDT-KAIEK	SAKIGLGLAL	KP
<i>Medicago truncatula</i> VDAC1.1	LASGLQHEW	RPKSFFTISG	EVDT-KAIEK	SARI GLALAL	K-
<i>Picea glauca</i>	KAAALQHEW	RPKSFVTLTG	EVDT-KALHN	SAKVGLSLIL	KP
<i>Pinus pinus</i>	RAAALQHEW	RPKSFVNLTG	EVDT-KALHN	SAKVGLSLVL	KP
<i>Pinus pinus</i>	KIAALVQHEW	RPKSLITLST	EVDS-KALDN	SSKIGLSLVL	KP
<i>Populus trichocarpa</i>	KASALVQHQW	RPKSFFTVSG	EVDT-KAIEK	TAKVGLALAL	KP
<i>Gycine max</i> VDAC1.3	RASALQHDW	TPRTRFSLVG	EVDT-GAIEK	SAKVGLAVAL	KP
<i>Medicago truncatula</i> VDAC1.3	KASALQHDW	SRQARFSLVG	EVDT-AAIQK	TAKVGLALAL	KP
<i>Arabidopsis thaliana</i> VDAC3	IASALQHEW	KPKSFFTISG	EVDT-KSIDK	SAKVGLAVAL	KP
<i>Pisum sativum</i> plastid porin	KASALQHEW	RPKSLITISS	EVDT-KAIEK	SAKIGLSLAL	K-
<i>Pisum sativum</i> plastid porin	KASALQHEW	RPKSLITISS	EVDT-KAIEK	SAKIGLSLAL	KP
<i>Arabidopsis thaliana</i> VDAC3	VANALQHEW	RPKSFFTVSG	EVDS-KAIDK	SAKVGIAVAL	KP
<i>Brassica rapa</i>	IANALQHEW	RPKSFITISG	EVDS-KAIEK	SAKVGIALAL	KP
<i>Solanum habrochaites</i> VDAC1	KASALQHEW	RPKSLFTISG	EVDT-KSVD-	-----	--
<i>Citrus reticulata</i> VDAC1	RASALQHEW	RPQSLFTISG	EVDT-RAIE-	-----	--
<i>Gossypium raimondii</i> VDAC3.1	KVAMLQREW	RPKSLVTISG	EYDS-KAINA	SPKMGALALAF	KP
<i>Vitis vinifera</i> VDAC3.1	KFVMLQREW	RPKSLITVSG	EYDP-KANNG	ATKLGALALAL	KP
<i>Solanum tuberosum</i> VDAC3	KVAMLQREW	RPKSLITISG	EYDT-KANNS	VPKLGALALAL	KP
<i>Lotus corniculatus</i> VDAC3.1	KAAFLQRAW	RPKSLITLST	EYDSTKIFGS	STKLGALALAL	QP
<i>Glycine max</i> VDAC3.1	KAAFLQRAW	RPNSLITLST	EYDSTKIFGS	STKFGALALAL	KP
<i>Medicago truncatula</i> VDAC3.1	KAAFLQRAW	RPNSLITLST	EYDSKKIIGS	PAKFGALALS	KP
<i>Allium cepa</i>	KFGVDVSMNG	RPKSLATVSA	EYDC-KAVGA	TPKVGVALAL	KW
<i>Pinus pinus</i>	KL GALQHEW	RPKSLVTISG	EFDT-KALDK	SAKIGLSLAL	KP
<i>Pinus taeda</i>	KL GTVLQHEW	KPKSLITLSS	EFDT-KALDK	SPKIGLALAY	KP
<i>Hordeum vulgare</i> VDAC3.1	KAGLLQHEW	RPKSYVTLSA	EYDP-KVVSS	PARFGVAVAL	SP
<i>Sorghum bicolor</i> VDAC3.1	KVGLLQHEW	RPKSLVTLSA	EYDP-KVVSA	PSRIGVAISL	KP
<i>Oryza sativa</i> POM36	KVGVLQHEW	RPKSTVTSISA	EYDP-KVVSS	PSRFGVAIAL	KP
<i>Arabidopsis thaliana</i> POM36	KAGMVLQREW	RPKSHITFSA	EYDS-KAVTS	SPKLGALALAL	KP
<i>Pennisetum glaucum</i>	T LAALQHEL	KPKSLITISG	EFDT-KALDR	APKFGALALAL	KP
<i>Zea mays</i>	T LAALQHEL	KPKSLITISG	EFDT-KALDR	SPKFGALALAL	KP
<i>Triticum aestivum</i>	KL AALQHEV	KPKSLITISG	EFDT-KALDR	APKFGALSAL	KP
<i>Vitis vinifera</i> VDAC2.1	NL GALQHEI	IPKSLITLST	EFDT-KALDK	TPRFGALALAL	KP
<i>Solanum tuberosum</i> VDAC2	NL GALQHEL	IPKSLITISS	EFDT-KALEK	TPKFGVALAL	KP
<i>Glycine max</i> VDAC2.1	KL GALQHEI	IPKSVFTVSG	EIDT-KALDK	KPRFGALIAL	KP
<i>Lotus corniculatus</i> VDAC2.1	KL GALQHEI	IPKSVLTISS	EVDT-KALDK	NPRFGALIAL	KP
<i>Gossypium raimondii</i> VDAC2.1	RL GALQHEV	IPKSLITVSG	EIDT-KSLDK	SPRLGLALAFAL	KP
<i>Medicago truncatula</i> VDAC2.1	KVGGLLQHEL	FPKSVLTISG	EVDT-KALEK	KPKFGALIAL	KP
<i>Arabidopsis thaliana</i> VDAC3	TL GALQHEV	LPRSLVTVSS	EIDT-KALEK	HPRFGLSLAL	KP
<i>Ananas comosus</i>	KASALQHEW	RPKSLFTIST	EVDT-KAIEK	APR-----SA	YL
<i>Saccharum officinarum</i> VDAC3.1	KVGLLQHEW	RPKSLVTLSA	EYDP-KVVSA	PSRIGVAISL	KP

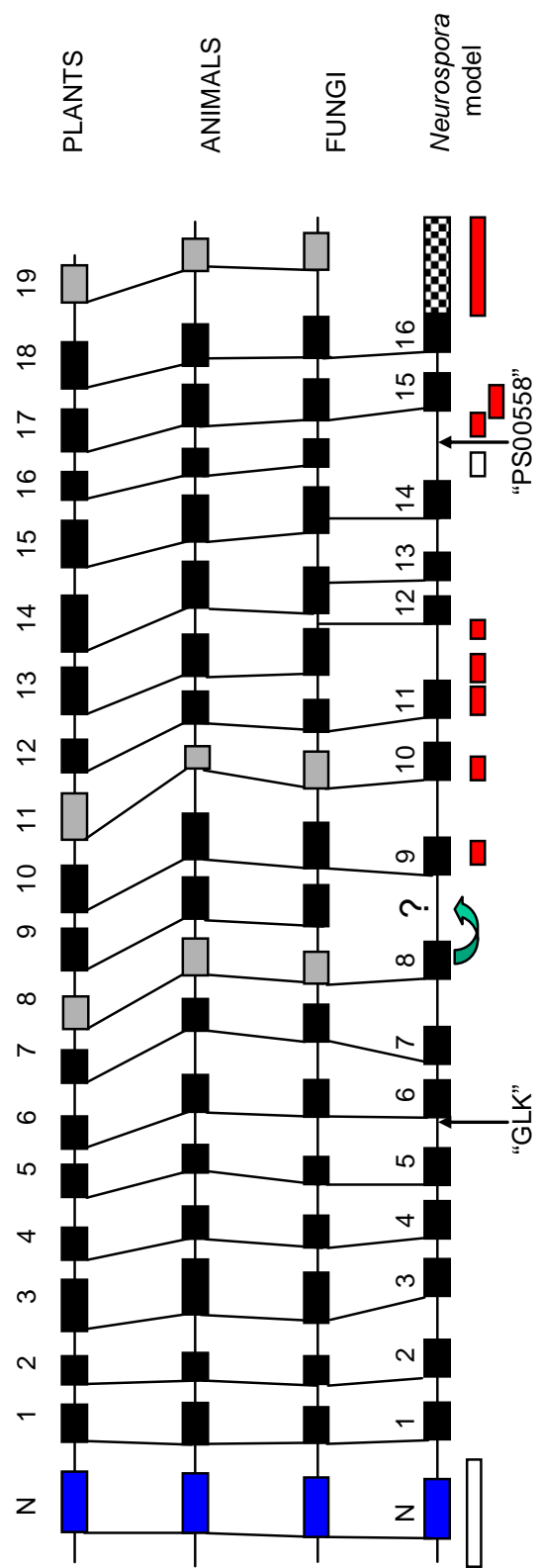
					310					320						330					340	
<i>Antirrhinum majus</i>	K	A	N	A	L	Q	H	E	W	R	P	K	S	L	T	V	S	-	-	-	-	-
<i>Welwitschia mirabilis</i>	K	A	A	A	L	Q	H	E	W	R	P	K	S	F	I	T	S	G	E	V	D	-
<i>Allium cepa</i>	K	A	S	G	L	Q	H	P	W	R	A	N	S	F	V	T	L	S	-	-	-	-
<i>Zantedeschia aethiopica</i>	K	A	S	A	L	P	Q	E	W	R	P	K	-	-	-	-	-	-	-	-	-	-
<i>Lycopersion esculentum</i> VDAC3.1	K	V	A	M	L	Q	R	E	W	R	P	K	S	L	V	T	F	S	A	E	Y	D
<i>Triphysaria versicolor</i>	K	A	S	A	L	Q	H	E	W	R	P	K	S	L	I	T	L	S	S	E	V	D
<i>Picea sitchensis</i>	K	A	A	A	L	Q	-	-	-	H	E	-	-	-	-	-	-	-	-	-	-	-
<i>Gossypium raimondii</i> VDAC1.1	N	A	-	-	-	-	-	-	-	S	A	L	-	-	-	-	-	-	-	-	-	-
<i>Saruma henryi</i>	K	A	S	A	L	Q	-	-	-	-	-	-	-	-	-	-	-	-	-	-	-	-
<i>Brassica rapa</i>	-	-	-	-	-	-	-	-	-	-	-	-	-	-	-	-	-	-	-	-	-	-
<i>Liriodendron tulipifera</i>	-	-	-	-	-	-	-	-	-	-	-	-	-	-	-	-	-	-	-	-	-	-
<i>Saccharum officinarum</i> VDAC1	-	-	-	-	-	-	-	-	-	-	-	-	-	-	-	-	-	-	-	-	-	-
<i>Panicum virgatum</i>	-	-	-	-	-	-	-	-	-	-	-	-	-	-	-	-	-	-	-	-	-	-
<i>Lactuca sativa</i>	-	-	-	-	-	-	-	-	-	-	-	-	-	-	-	-	-	-	-	-	-	-
<i>Nicotiana tabacum</i> POM34	-	-	-	-	-	-	-	-	-	-	-	-	-	-	-	-	-	-	-	-	-	-
<i>Eschscholzia californica</i>	-	-	-	-	-	-	-	-	-	-	-	-	-	-	-	-	-	-	-	-	-	-
<i>Beta vulgaris</i>	-	-	-	-	-	-	-	-	-	-	-	-	-	-	-	-	-	-	-	-	-	-
<i>Cycas rumphii</i>	-	-	-	-	-	-	-	-	-	-	-	-	-	-	-	-	-	-	-	-	-	-
<i>Glycine max</i> VDAC1.2	-	-	-	-	-	-	-	-	-	-	-	-	-	-	-	-	-	-	-	-	-	-
<i>Hordeum vulgare</i>	M	A	S	A	L	Q	H	E	W	R	P	K	S	L	V	T	I	S	G	E	V	D
<i>Lycopersion esculentum</i> VDAC2	S	L	G	A	V	L	Q	H	E	V	I	P	K	S	L	L	T	I	S	S	E	F
<i>Citrus sinensis</i>	I	A	S	A	L	Q	H	E	W	R	P	K	S	L	F	T	I	S	G	E	V	X
<i>Gossypium raimondii</i> VDAC1.3	R	A	S	A	L	Q	H	E	W	R	P	K	S	L	I	S	I	F	G	E	V	D
<i>Picea glauca</i>	K	A	A	A	L	Q	H	E	X	X	P	K	S	F	-	-	-	-	-	-	-	-
<i>Welwitschia mirabilis</i>	K	V	A	G	L	Q	H	E	W	R	P	K	S	L	I	T	I	S	-	-	-	-
<i>Acorus americanus</i>	K	A	S	A	L	Q	H	Q	W	R	P	K	S	-	-	-	-	-	-	-	-	-
<i>Selaginella moellendorffii</i>	K	L	A	A	L	Q	-	-	-	-	-	-	-	-	-	-	-	-	-	-	-	-

As shown in Fig. 6.1, a segment located 5-6 residues from the amino-terminus predicts an α -helix similar to previous secondary structure prediction methods (see Chapter 1, section 1.5). The primary sequences of these putative α -helices are highly conserved within the major phylogenetic groups, and based on the high level of primary sequence conservation are likely the best candidates for refining eukaryotic porin signature motifs.

In all cases, the remainder of the protein is predicted to be rich in β -strands, in agreement with existing models of porin structure (reviewed in Mannella 1997, Benz 1994, De Pinto and Palmieri 1992, Bay and Court 2002, Song *et al.* 1998, Runke *et al.* 2006, Chapter 1). Nineteen regions with β -strand propensity are predicted in the majority of porin sequences (Fig. 6.1), these are numbered 1-19 in Fig. 6.2 and for simplicity will be referred to as β 1, β 2 etc. for the subsequent discussion. Remarkably, each of these regions corresponds to an aligned segment in the multiple sequence analysis, although the spacing between individual putative β -strands varies between the major phylogenetic groups (Fig. 6.2).

It is unlikely that 19 TM β -strands predicted by SSPRO reflect the true porin TM topology. As discussed in Chapter 1, regions including β 1- β 7 are in agreement with previous prediction algorithms and models. Interestingly, in an alignment of all 244 sequences, the region including β 8 is not always predicted to form a β -strand (data not shown). However, when the plant or fungal sequences are aligned alone, a 6-residue β -strand is predicted in some sequences (residues, 114-119 of *Oryza sativa* VDAC1, and 122-129 of *N. crassa* porin); in others this β -strand region is shorter (3-5 aa) (Fig. 6.1). Six residues are the minimum proposed to be sufficient for the β -strands in bacterial porins to span the thickness of a lipid bilayer (Koebnik *et al.* 2000) but a shorter strand may be possible if two short β -strands or perhaps a short β -strand/ α -helix were to occur in this region. β 8 (residues 125-

Figure 6.2. Summary of the secondary structure prediction and analysis. Predicted secondary structure elements in VDAC from the crown groups of plants, animals, and fungi. Predictions were made as described in Materials and Methods. For each summary diagram, the putative N-terminal α -helix is indicated by a blue rectangle labelled “N” on the top, subsequent β -strands are indicated by black filled rectangles, and the intervening loops are shown as thin lines. Boxes in grey indicate β -strands that are weakly supported by experimental data (see text). According to the models described in Chapter 1, the N-terminal α -helix resides in the intermembrane space, and the subsequent loops and turns alternate between exposure to the cytosol and to the intermembrane space. The lower panel shows the model for *Neurospora crassa* VDAC structure derived in (Runke *et al.* 2006). Structural elements are as described for the plant, animal and fungal models, except that the hatched region indicates a C-terminal segment that does not form a TM β -strand (see text for discussion). Below the model of *N. crassa* VDAC structure, rectangles indicate segments, that when absent in porin variants, create VDAC able (white), or unable (red), to form pores in artificial membranes. The arrow indicates that the multiple alignment supports a different placement of β 8 in the Runke *et al.* model to the position occupied by β 9 in the current predictions. Positions of the GLK and porin signature motifs are also noted.



132 in *Homo sapiens* VDAC1) in the animal sequences also contains some α -helical propensity and is unlikely to satisfy this minimum TM β -strand requirement. Furthermore, this region contains a cysteine residue, which is absent from all β -strands in bacterial porins (Koebnik *et al.* 2000). Therefore, if all porins have a common structure, the region including putative β 8 may not form a β -strand (Fig. 6.2).

The situation described for β 8 in animals is also pertinent for β 11 from all three groups, since this TM strand also has some α -helical propensity in some sequences. If these two putative β -strands are “disregarded” in this prediction, another β -strand should be omitted to maintain an even number of β -strands within the barrel (Koebnik *et al.* 2000). As discussed previously, in Chapter 1 (see also Bay and Court 2002, Runke *et al.* 2006), deletion of the β -strand predicted at the C-terminus of *N. crassa* porin resulted in pore formation (Popp *et al.* 1996) and suggests that a β -strand within this region is not critical for pore formation. Hence, β 19 may also be omitted from the model (Fig. 6.2).

Based on the size of the data set and representation from all three crown groups, a common structural framework exists amongst the various porins and isoforms (Fig. 6.2). These data support a common, 16 β -strand pore structure, in which the interstrand loops and turns vary in size.

In spite of the predicted structural similarities, there is a great deal of variation in the amino acid sequences that make up the putative strands and the intervening regions. For example, pairwise sequence comparisons between the sequences of predicted β -strands reveal average sequence identity of around 47-61% for each phylogenetic crown group. To demonstrate this sequence diversity, when the regions encoding the predicted β -strands from

one representative of the animals (*Homo sapiens* VDAC1), the fungi (*Neurospora crassa*), the plants (*Oryza sativa* VDAC1) and the stramenopiles (*Phytophthora sojae*) were followed in the alignments of Fig. 6.1. Very few positions were conserved. Considering identical and chemically similar residues, there are at most three positions that are related in three β -strands among all four sequences ($\beta 7$, $\beta 11$, $\beta 13$), and in $\beta 8$, $\beta 14$, $\beta 17$ there are no positions consistently occupied by chemically similar residues. As observed for bacterial porins, structural similarity rather than sequence similarity is favoured in mitochondrial porins (Jap and Walian 1996, Koebnik *et al.* 2000).

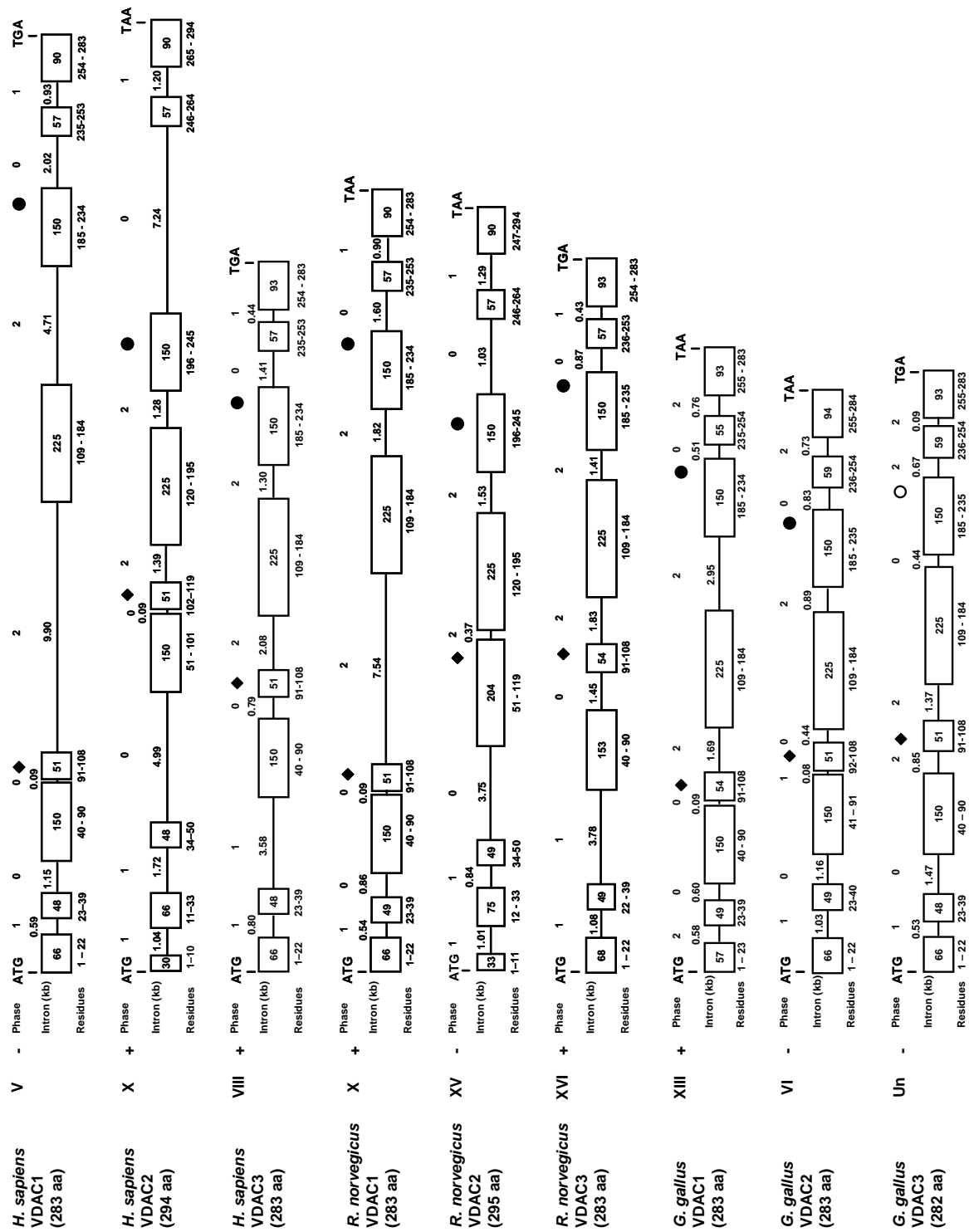
6.3.2. Comparison of VDAC gene structure

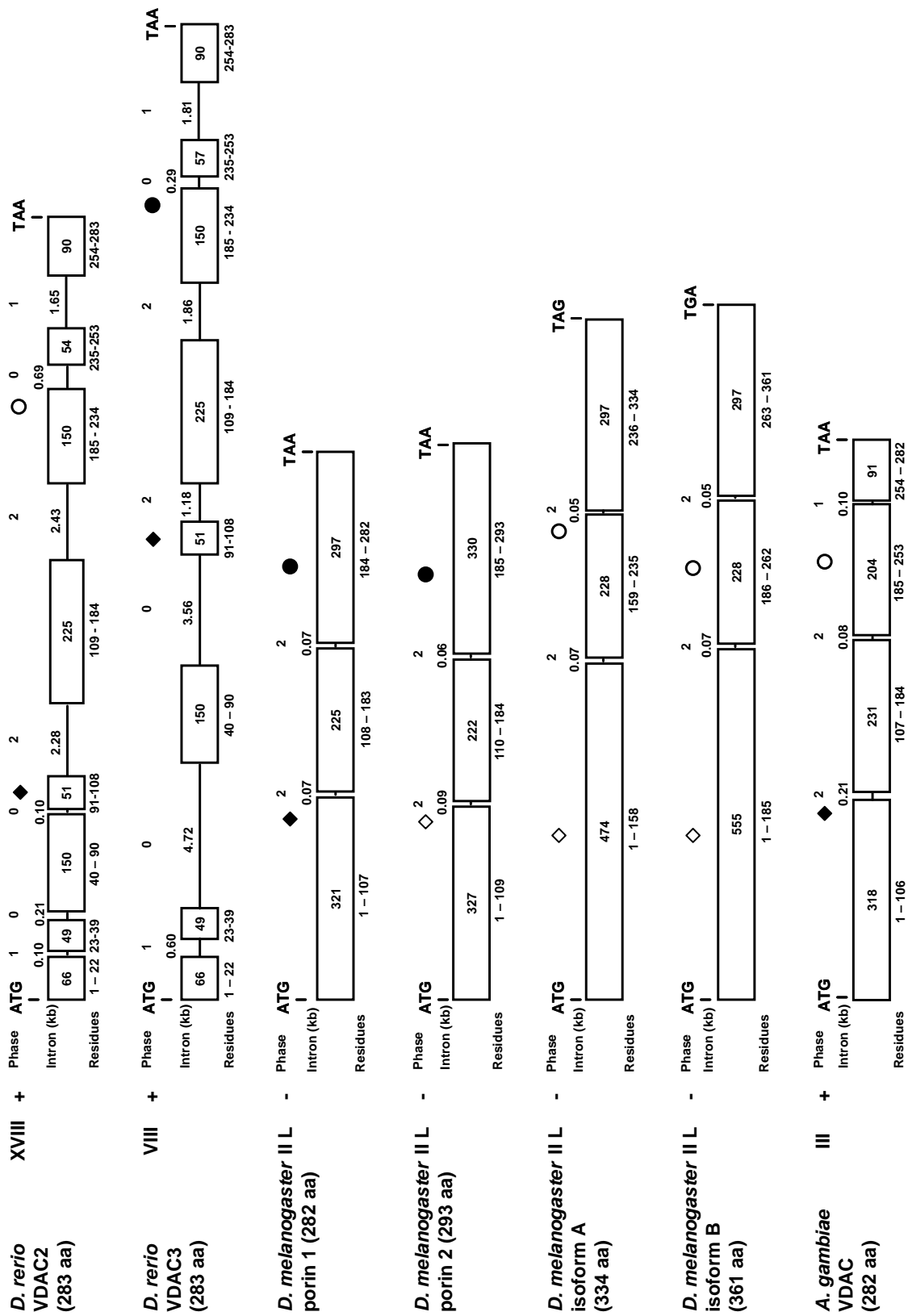
Given the shared predicted structural and primary sequence elements in mitochondrial porins, it was of interest to examine representative animal, plant, and fungal VDAC genes (including paralogs) for the number of introns present, intron phasing, and the position of introns with respect to functional and structural motifs (Fig. 6.3). The comparative VDAC gene maps show that the vertebrate VDAC open reading frames usually consist of 8 exons and 7 introns, a pattern also observed within the sea urchin (*Strongylocentrotus purpuratus*) VDAC gene. The *Caenorhabditis elegans* VDAC gene has 4 introns and the *Drosophila melanogaster* paralogs contain 2 introns. Thus, the number of introns appears to decrease and the introns get shorter as one goes from the vertebrates/echinoderms/nematodes to the arthropods. The plant VDAC paralogs examined typically had 4 to 5 short introns.

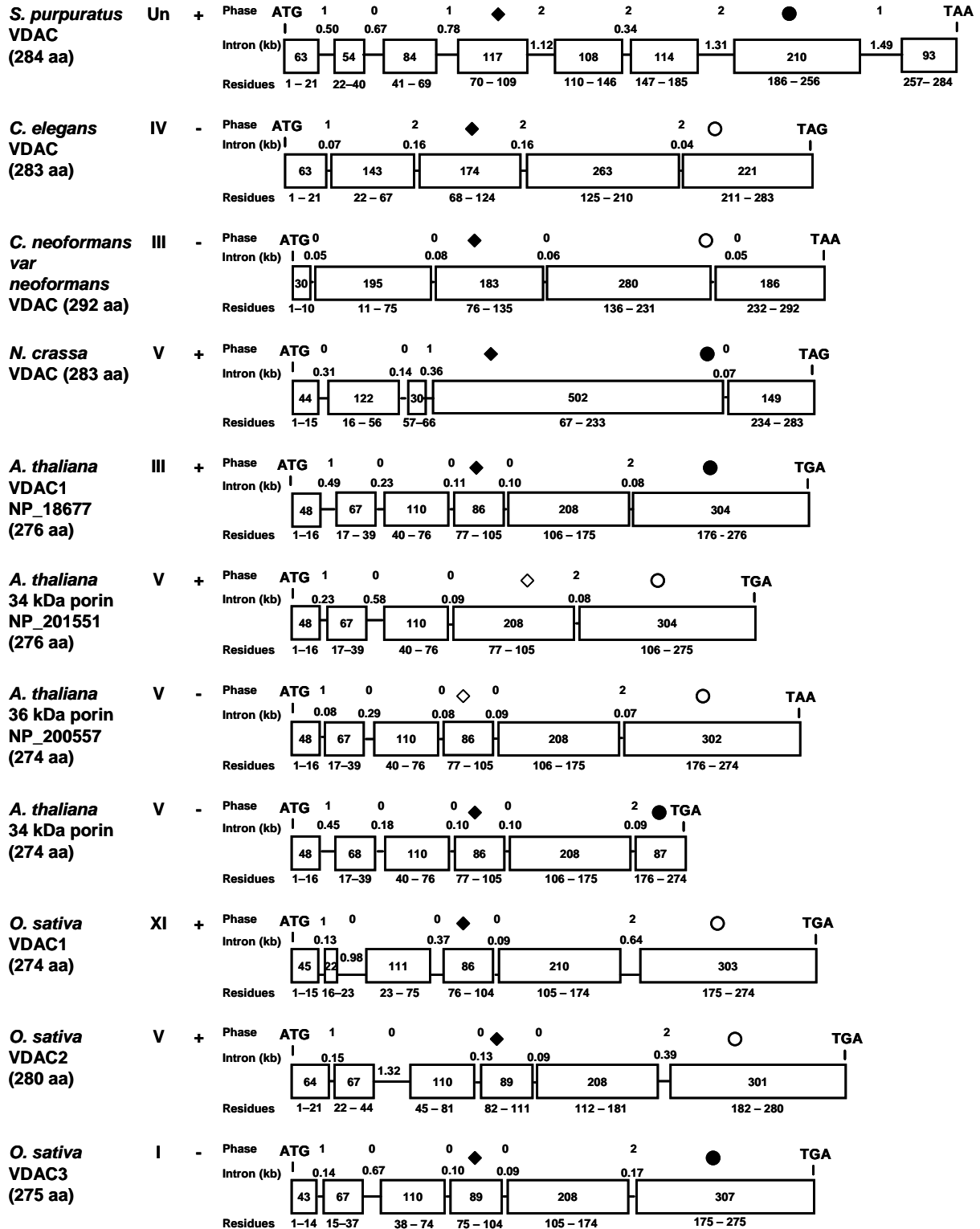
Figure 6.3. A) Comparison of the mitochondrial porin gene structure. The exonic and intronic regions of mitochondrial porin open reading frames were mapped for a variety of organisms. The gene structure for all species was retrieved from the NCBI genome database using BLASTN or map viewer programs to analyze the ORF of each porin cDNA. Only regions of the gene containing ORFs are shown; chromosome number is indicated beside the species in Roman numerals and plus (+) or minus (-) strand reading frames are indicated beside chromosome number. Where multiple spliceoforms exist, as for human VDAC2, the form not listed as a splice variant was used. Loci of unknown location are indicated by “Un”. Lengths of exons in bp are indicated inside the boxes representing the exons; the numbers of the corresponding amino acid residues are indicated below the boxes. Lines indicate introns, the sizes of which are indicated in kb above the line; the intron phase (0, 1, or 2) is indicated directly above the intron size. The positions of the coding sequence for the GLK (diamonds) and the eukaryotic porin (circles) motifs are shown above the intron/exon map. Filled and open symbols indicate matches and imperfect matches to these motifs, respectively. **B)** Intron placement with respect to coding sequences for conserved structural elements. Intron placement is indicated by vertical bars in the rows above the structural model for each crown group of organisms (see Fig. 6.2 for symbol descriptions). Patterns of intron location that are found in several VDAC genes are shown only once. The positions of the N-terminal motifs derived in this study, and the eukaryotic signature motif (PS00558) near the C-terminal of the protein are indicated by open boxes. Triangles indicate the GLK motif. Upper panel: Animal sequences. Hs, *Homo sapiens* VDAC1 (NP_003365), VDAC2 (NP_003366) and VDAC3 (NP_005653); Rn, *Rattus norvegicus* VDAC1 (NP_112643), VDAC2 (NP_112644) and VDAC3 (NP_112645); Gg, *Gallus gallus* VDAC1 (TC10222), VDAC2 (NM_204741),

VDAC3 (TC9741): Dr, *Danio rerio* accession numbers NM_199585 and BC065468; Dm, *Drosophila melanogaster* VDAC1 (CG6647-PA), VDAC2 (609462), and isoform B of CG31722 (CG31722_PB); Dm-2; *D. melanogaster* isoform A (CG31722_PA); Sp, *Strongylocentrotus purpuratus* (sea urchin, XM_775173); Ag, *Anopheles gambiae* (XM_318947). Middle panel: Fungal sequences. Cn, *Cryptococcus neoformans* (XM_569804.1); Nc, *Neurospora crassa* (XP_323644). Lower panel: Plant sequences. At, *Arabidopsis thaliana*, (NP_186777, NP_201551, NP_200057, NP_197013); At-2 *A. thaliana* NP_190561; Os, *Oryza sativa* (CAB82853_VDAC1, CAC80850_VDAC2, CAC80851_VDAC3).

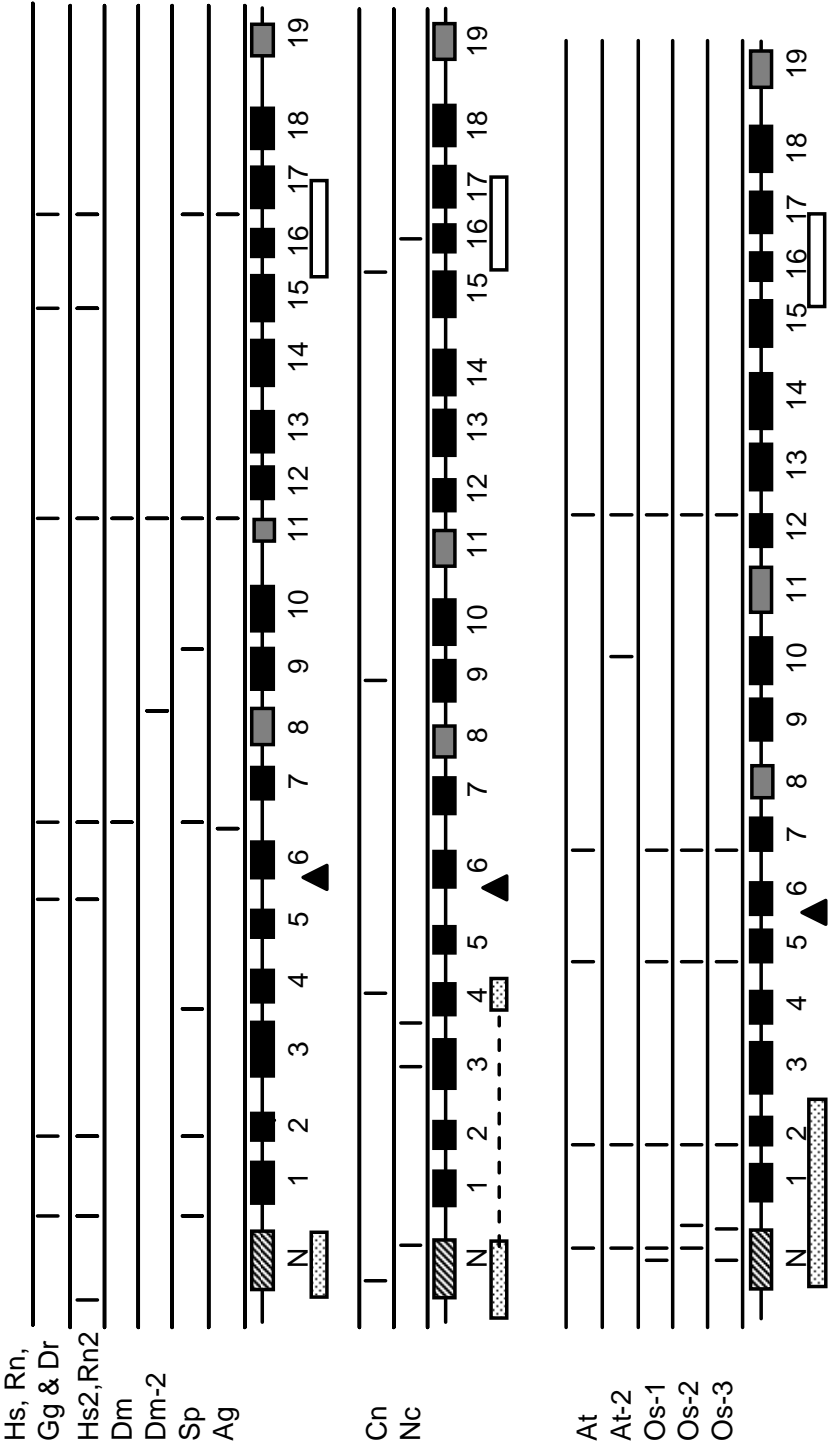
A







B



In general, introns were longest within the mammalian sequences sampled and shorter in the invertebrate, plant and fungal taxa (Fig. 6.3A). This contrasts with the shorter exons noted within the chordate sequences, as exemplified by the human, rat, zebra fish and bird (*Gallus gallus*) VDAC genes in which exons range in size from 30 bp (human VDAC2) to 225 bps. There is a general trend among the vertebrate and echinoderm VDACs that, relative to the internal exons, the 5' terminal exons 1 and 2 are very short (30 to 75 bps), as are the 3' terminal exons 7 and 8. However, the echinoderm is an exception, with a relatively longer exon 7 (210 bp).

In the chordates, the largest exon (exon 5) appears to be quite ancient as its size is conserved from zebra fish to humans. Also, exon 5 appears to be flanked by introns that both are in phase 2, *i.e.* intron phase correlation exists, where flanking introns are in the same phase, or are found as a combination of a phase 0 and a phase 2 intron. Intron phase correlation has been viewed as evidence of non-random insertion of an intron and thus interpreted by some as the presence of an ancient intron (reviewed by Fedorova and Fedorov 2003). These observations further suggest that exon 5 and its flanking introns might have been present in the ancestor to the vertebrate lineage. Exon 6 also appears to be quite conserved both in terms of size (150 bp) and in that it is flanked downstream by a phase 0 intron.

Likewise, phase 0 introns are viewed as old by some authors (reviewed by Fedorova and Fedorov 2003). The fungal VDAC genes examined either lack introns (*S. cerevisiae* VDAC1 and VDAC2, *Ustilago maydis*) or show a bias towards phase 0 introns; overall it was noted among the fungal VDAC paralogs displayed in Fig. 6.3 seven phase 0 introns and one phase 1 intron. The plant VDACs appear to have more phase 0 introns with a ratio of 21:9:8

for phase 0, 1 and 2 introns respectively. In contrast, there are 29 phase 0, 26 phase 1, and 28 phase 2 introns in vertebrate VDAC paralogs; thus there is not a strong bias towards one category of intron. In contrast to this general trend, the *C. elegans* and Arthropod porin gene sequences appear to be devoid of phase 0 introns and the ratio of phase 1 to phase 2 introns is 2 to 13.

The coding sequences for the sequence motifs discussed above are also conserved with respect to exonic location (Fig. 6.3B). In the animal sequences presented, the N-terminal motif is encoded by sequence within the first exon; the only exceptions are VDAC2 in *H. sapiens* and *Rattus norvegicus*, in which an intron is located near the middle of the coding sequence. The 42-residue plant motif begins near residue six and includes the predicted α -helix, which is encoded by a single exon, and in most cases the coding region extends through exon 2 into exon 3. The exception is the *O. sativa* VDAC1 gene, in which an additional intron is inserted past the codon for amino acid residue 15. The fungal motif also begins about six residues from the N-terminus of the protein and the N-terminal portion of the motif (see Chapter 1) spans 14-18 residues. In both fungal sequences in Fig. 6.3, this portion of the motif is encoded by exons 1 and 2. The C-terminal part of the motif is encoded by sequence including the junction between exons 2 and 3 in *Cryptococcus neoformans*, and entirely by exon 2 in *N. crassa*. In the sequences examined, the entire coding sequence for the GLK motif is in Exon 4, with the exception of VDAC2 of human and rat, in which it resides in Exon 5; VDAC2 has an additional N-terminal intron (see Fig. 6.3A). Exon 6 contains the eukaryotic porin signature motif (PS00558, Fig. 6.3A).

6.3.3 Intron location with respect to functional and structural motifs of VDAC

A more detailed examination of the position of introns with respect to the position of protein domains/or modules, such as the β -strands that are important components of the VDAC structure, showed that these modules appear to correlate with the position of introns. The introns in general do not interrupt β -strand modules or the GLK and eukaryotic porin motifs (Fig. 6.3B). This observation is most pronounced in the vertebrate, sea urchin, *Drosophila* and plant VDAC genes; for example, there appears to be an intron conserved between $\beta 6$ and $\beta 7$ and between $\beta 11$ and $\beta 12$. Other introns are frequently located between the coding sequences for the N-terminal α -helix and the first β -strand module, between $\beta 1$ and $\beta 2$, and between $\beta 16$ and $\beta 17$.

Within the plant VDAC genes examined there was a bias towards introns being located between β -strand modules (see Fig. 6.3B). Introns were located between the coding sequences for putative $\beta 1$ and $\beta 2$, $\beta 4$ and $\beta 5$, $\beta 6$ and $\beta 7$, and $\beta 12$ and $\beta 13$ strands. In addition, there is generally an intron within the coding region for the N-terminal α -helix as well. Based on the limited data for *C. elegans* and the fungal VDAC genes did not allow conclusions to be made; as more complete sequences become available a more detailed examination of these groups of organisms can be carried out.

6.4 Conclusions

Amongst members of the three groups, and isoforms within individual organisms, the lengths and positions of putative β -strands predicted by PRALINE/ SSPO appear to be highly conserved. These data support the 16 stranded model of *N. crassa* as a candidate for

porin TM topology, assuming TM β -strand arrangements are as highly conserved within plants, animals and fungi as observed.

Analysis of the porin gene structures in the metazoans in particular has demonstrated that both the GLK and eukaryotic signature motif are located within conserved exons flanked by introns of the same phase (phase correlation). Furthermore, it appears that in general introns do not disrupt exons encoding the structural framework of porin in this case the predicted β -strands. The relevance of these observations will become clearer as more genomic sequences and structural data become available for mitochondrial porins and other β -barrel, membrane spanning proteins.

References

- Abrecht, H., E. Goormaghtigh, J. M. Ruyschaert and F. Homble (2000). "Structure and orientation of two voltage-dependent anion-selective channel isoforms. An attenuated total reflection fourier-transform infrared spectroscopy study." J Biol Chem **275**(52): 40992-9.
- Abrecht, H., R. Wattiez, J. M. Ruyschaert and F. Homble (2000). "Purification and characterization of two voltage-dependent anion channel isoforms from plant seeds." Plant Physiol **124**(3): 1181-90.
- Ahting, U., C. Thun, R. Hegerl, D. Typke, F. E. Nargang, W. Neupert and S. Nussberger (1999). "The TOM core complex: the general protein import pore of the outer membrane of mitochondria." J Cell Biol **147**(5): 959-68.
- Aiello, R., A. Messina, B. Schiffler, R. Benz, G. Tasco, R. Casadio and V. De Pinto (2004). "Functional characterization of a second porin isoform in *Drosophila melanogaster*. DmPorin2 forms voltage-independent cation-selective pores." J Biol Chem **279**(24): 25364-73.
- Al Bitar, F., N. Roosens, J. V. Boxtel, E. Dewaele, M. Jacobs and F. Homble (2002). "Expression of the rice vdac isoform2: histochemical localization and expression level." Biochim Biophys Acta **1579**(2-3): 133-41.
- Al Bitar, F., N. Roosens, M. Smeyers, M. Vauterin, J. Van Boxtel, M. Jacobs and F. Homble (2003). "Sequence analysis, transcriptional and posttranscriptional regulation of the rice vdac family." Biochim Biophys Acta **1625**(1): 43-51.
- Aljamal, J. A., G. Genchi, V. De Pinto, L. Stefanizzi, A. De Santis, R. Benz and F. Palmieri (1993). "Purification and characterization of porin from corn (*Zea mays* L.) mitochondria." Plant Physiol **102**(2): 615-621.
- Anflous, K., O. Blondel, A. Bernard, M. Khrestchatisky and R. Ventura-Clapier (1998). "Characterization of rat porin isoforms: cloning of a cardiac type-3 variant encoding an additional methionine at its putative N-terminal region." Biochim Biophys Acta **1399**(1): 47-50.
- Angeles, R., J. Devine, R. Barret, D. Goebel, E. Blachyl-Dyson, M. Forte and R. McCauley (1999). "Mutations in the voltage-dependent anion channel of the mitochondrial outer membrane cause a dominant nonlethal growth impairment." J Bioenerg Biomembr **31**(2): 143-51.

- Arora, A., F. Abildgaard, J. H. Bushweller and L. K. Tamm (2001). "Structure of outer membrane protein A transmembrane domain by NMR spectroscopy." Nat Struct Biol **8**(4): 334-8.
- Arora, A., D. Rinehart, G. Szabo and L. K. Tamm (2000). "Refolded outer membrane protein A of Escherichia coli forms ion channels with two conductance states in planar lipid bilayers." J Biol Chem **275**(3): 1594-600.
- Arora, K. K., C. R. Filburn and P. L. Pedersen (1993). "Structure/function relationships in hexokinase. Site-directed mutational analyses and characterization of overexpressed fragments implicate different functions for the N- and C-terminal halves of the enzyme." J Biol Chem **268**(24): 18259-66.
- Arthington-Skaggs, B. A., H. Jradi, T. Desai and C. J. Morrison (1999). "Quantitation of ergosterol content: novel method for determination of fluconazole susceptibility of Candida albicans." J Clin Microbiol **37**(10): 3332-7.
- Asworth, L. A. E. and C. Green (1966). "Cholesterol is the major sterol in mammalian organisms." Science **151**: 210-211.
- Bangham, A. D. (1978). "Properties and uses of lipid vesicles: an overview." Ann N Y Acad Sci **308**: 2-7.
- Baker, M. A., D. J. Lane, J. D. Ly, V. De Pinto and A. Lawen (2004). "VDAC1 is a transplasma membrane NADH-ferricyanide reductase." J Biol Chem **279**(6): 4811-9.
- Bathori, G., G. Csordas, C. Garcia-Perez, E. Davies and G. Hajnoczky (2006). "Ca²⁺-dependent control of the permeability properties of the mitochondrial outer membrane and VDAC." J Biol Chem. epub ahead of print.
- Bathori, G., M. Sahin-Toth, A. Fonyo and E. Ligeti (1993). "Transport properties and inhibitor sensitivity of isolated and reconstituted porin differ from those of intact mitochondria." Biochim Biophys Acta **1145**(1): 168-76.
- Bay, D. C. and D. A. Court (2002). "Origami in the outer membrane: the transmembrane arrangement of mitochondrial porins." Biochem Cell Biol **80**(5): 551-62.
- Benz, R. (1994). "Permeation of hydrophilic solutes through mitochondrial outer membranes: review on mitochondrial porins." Biochim Biophys Acta **1197**(2): 167-96.
- Beutner, G., A. Ruck, B. Riede, W. Welte and D. Brdiczka (1996). "Complexes between kinases, mitochondrial porin and adenylate translocator in rat brain resemble the permeability transition pore." FEBS Lett **396**(2-3): 189-95.

- Blachly-Dyson, E., A. Baldini, M. Litt, E. R. McCabe and M. Forte (1994). "Human genes encoding the voltage-dependent anion channel (VDAC) of the outer mitochondrial membrane: mapping and identification of two new isoforms." Genomics **20**(1): 62-7.
- Blachly-Dyson, E. and M. Forte (2001). "VDAC channels." IUBMB Life **52**(3-5): 113-8.
- Blachly-Dyson, E., S. Peng, M. Colombini and M. Forte (1990). "Selectivity changes in site-directed mutants of the VDAC ion channel: structural implications." Science **247**(4947): 1233-6.
- Blachly-Dyson, E., S. Z. Peng, M. Colombini and M. Forte (1989). "Probing the structure of the mitochondrial channel, VDAC, by site-directed mutagenesis: a progress report." J Bioenerg Biomembr **21**(4): 471-83.
- Blachly-Dyson, E., J. Song, W. J. Wolfgang, M. Colombini and M. Forte (1997). "Multicopy suppressors of phenotypes resulting from the absence of yeast VDAC encode a VDAC-like protein." Mol Cell Biol **17**(10): 5727-38.
- Blachly-Dyson, E., E. B. Zambronicz, W. H. Yu, V. Adams, E. R. McCabe, J. Adelman, M. Colombini and M. Forte (1993). "Cloning and functional expression in yeast of two human isoforms of the outer mitochondrial membrane channel, the voltage-dependent anion channel." J Biol Chem **268**(3): 1835-41.
- Bousquet, J. A., C. Garbay, B. P. Roques and Y. Mely (2000). "Circular dichroic investigation of the native and non-native conformational states of the growth factor receptor-binding protein 2 N-terminal src homology domain 3: effect of binding to a proline-rich peptide from guanine nucleotide exchange factor." Biochemistry **39**(26): 7722-35.
- Brdiczka, D. (1990). "Interaction of mitochondrial porin with cytosolic proteins." Experientia **46**(2): 161-7.
- Brdiczka, D., K. Bucheler, M. Kottke, V. Adams and V. K. Nalam (1990). "Characterization and metabolic function of mitochondrial contact sites." Biochim Biophys Acta **1018**(2-3): 234-8.
- Brdiczka, D., P. Kaldis and T. Wallimann (1994). "In vitro complex formation between the octamer of mitochondrial creatine kinase and porin." J Biol Chem **269**(44): 27640-4.
- Buettner, R., G. Papoutsoglou, E. Scemes, D. C. Spray and R. Dermietzel (2000). "Evidence for secretory pathway localization of a voltage-dependent anion channel isoform." Proc Natl Acad Sci U S A **97**(7): 3201-6.
- Burstein, E. A., E. A. Permyakov, V. A. Yashin, S. A. Burkhanov and A. Finazzi Agro (1977). "The fine structure of luminescence spectra of azurin." Biochim Biophys Acta **491**(1): 155-9.

- Burstein, E. A., N. S. Vedenkina and M. N. Ivkova (1973). "Fluorescence and the location of tryptophan residues in protein molecules." Photochem Photobiol **18**(4): 263-79.
- Casadio, R., I. Jacoboni, A. Messina and V. De Pinto (2002). "A 3D model of the voltage-dependent anion channel (VDAC)." FEBS Lett **520**(1-3): 1-7.
- Cesar Mde, C. and J. E. Wilson (2004). "All three isoforms of the voltage-dependent anion channel (VDAC1, VDAC2, and VDAC3) are present in mitochondria from bovine, rabbit, and rat brain." Arch Biochem Biophys **422**(2): 191-6.
- Chang, C. T., C. S. Wu and J. T. Yang (1978). "Circular dichroic analysis of protein conformation: inclusion of the beta-turns." Anal Biochem **91**(1): 13-31.
- Cheng, E. H., T. V. Sheiko, J. K. Fisher, W. J. Craigen and S. J. Korsmeyer (2003). "VDAC2 inhibits BAK activation and mitochondrial apoptosis." Science **301**(5632): 513-7.
- Chuang, J. Z., T. Y. Yeh, F. Bollati, C. Conde, F. Canavosio, A. Caceres and C. H. Sung (2005). "The dynein light chain Tctex-1 has a dynein-independent role in actin remodeling during neurite outgrowth." Dev Cell **9**(1): 75-86.
- Colombini, M. (1980). "Structure and mode of action of a voltage dependent anion-selective channel (VDAC) located in the outer mitochondrial membrane." Ann N Y Acad Sci **341**: 552-63.
- Colombini, M., C. L. Yeung, J. Tung and T. Konig (1987). "The mitochondrial outer membrane channel, VDAC, is regulated by a synthetic polyanion." Biochim Biophys Acta **905**(2): 279-86.
- Compton, L. A. and W. C. Johnson, Jr. (1986). "Analysis of protein circular dichroism spectra for secondary structure using a simple matrix multiplication." Anal Biochem **155**(1): 155-67.
- Conlan, S. and H. Bayley (2003). "Folding of a monomeric porin, OmpG, in detergent solution." Biochemistry **42**(31): 9453-65.
- Court, D. A., R. Kleene, W. Neupert and R. Lill (1996). "Role of the N- and C-termini of porin in import into the outer membrane of *Neurospora* mitochondria." FEBS Lett **390**(1): 73-7.
- Court, D. A., F. E. Nargang, H. Steiner, R. S. Hodges, W. Neupert and R. Lill (1996). "Role of the intermembrane-space domain of the preprotein receptor Tom22 in protein import into mitochondria." Mol Cell Biol **16**(8): 4035-42.
- Cowan, S. W., R. M. Garavito, J. N. Jansonius, J. A. Jenkins, R. Karlsson, N. Konig, E. F. Pai, R. A. Paupit, P. J. Rizkallah, J. P. Rosenbusch and et al. (1995). "The structure of OmpF porin in a tetragonal crystal form." Structure **3**(10): 1041-50.

- Cowan, S. W., T. Schirmer, G. Rummel, M. Steiert, R. Ghosh, R. A. Paupit, J. N. Jansonius and J. P. Rosenbusch (1992). "Crystal structures explain functional properties of two *E. coli* porins." Nature **358**(6389): 727-33.
- Cowgill, R. W. (1966). "Fluorescence and protein structure. IX. Relationship between tyrosine fluorescence and various stages in denaturation of ribonuclease." Biochim Biophys Acta **120**(2): 196-211.
- Cowgill, R. W. (1967). "Fluorescence and protein structure. X. Reappraisal of solvent and structural effects." Biochim Biophys Acta **133**(1): 6-18.
- Cowgill, R. W. (1968). "Fluorescence and protein structure. XIV. Tyrosine fluorescence in helical muscle proteins." Biochim Biophys Acta **168**(3): 417-30.
- Cowgill, R. W. (1968). "Fluorescence and protein structure. XV. Tryptophan fluorescence in helical muscle protein." Biochim Biophys Acta **168**(3): 431-8.
- Cowgill, R. W. (1968). "Fluorescence and protein structure. XVI. Detergents bound to muscle proteins." Biochim Biophys Acta **168**(3): 439-46.
- Cowgill, R. W. (1970). "Fluorescence and protein structure. XVII. On the mechanism of peptide quenching." Biochim Biophys Acta **200**(1): 18-25.
- Crompton, M., E. Barksby, N. Johnson and M. Capano (2002). "Mitochondrial intermembrane junctional complexes and their involvement in cell death." Biochimie **84**(2-3): 143-52.
- Crompton, M., S. Virji, V. Doyle, N. Johnson and J. M. Ward (1999). "The mitochondrial permeability transition pore." Biochem Soc Symp **66**: 167-79.
- Crompton, M., S. Virji and J. M. Ward (1998). "Cyclophilin-D binds strongly to complexes of the voltage-dependent anion channel and the adenine nucleotide translocase to form the permeability transition pore." Eur J Biochem **258**(2): 729-35.
- Czub, J. and M. Baginski (2006). "Comparative molecular dynamics study of lipid membranes containing cholesterol and ergosterol." Biophys J **90**(7): 2368-82.
- de Kroon, A. I. P. M., D. Dolis, A. Mayer, R. Lill and B. de Kruijff (1997). "Phospholipid composition of highly purified mitochondrial outer membranes of rat liver and *Neurospora crassa*. Is cardiolipin present in the mitochondrial outer membrane?" Biochim Biophys Acta **1325**: 108-116.
- de la Maza, A. and J. L. Parra (1996). "Alterations in phospholipid bilayers caused by oxyethylenated nonylphenol surfactants." Arch Biochem Biophys **329**(1): 1-8.

- de la Maza, A. and J. L. Parra (1996). "Changes in phosphatidylcholine liposomes caused by a mixture of Triton X-100 and sodium dodecyl sulfate." Biochim Biophys Acta **1300**(2): 125-34.
- De Pinto, V., J. A. al Jamal and F. Palmieri (1993). "Location of the dicyclohexylcarbodiimide-reactive glutamate residue in the bovine heart mitochondrial porin." J Biol Chem **268**(17): 12977-82.
- De Pinto, V., R. Benz and F. Palmieri (1989). "Interaction of non-classical detergents with the mitochondrial porin. A new purification procedure and characterization of the pore-forming unit." Eur J Biochem **183**(1): 179-87.
- De Pinto, V. D. and F. Palmieri (1992). "Transmembrane arrangement of mitochondrial porin or voltage-dependent anion channel (VDAC)." J Bioenerg Biomembr **24**(1): 21-6.
- Decker, W. K. and W. J. Craigen (2000). "The tissue-specific, alternatively spliced single ATG exon of the type 3 voltage-dependent anion channel gene does not create a truncated protein isoform in vivo." Mol Genet Metab **70**(1): 69-74.
- Diederichs, K., J. Freigang, S. Umhau, K. Zeth and J. Breed (1998). "Prediction by a neural network of outer membrane beta-strand protein topology." Protein Sci **7**(11): 2413-20.
- Dolder, M., K. Zeth, P. Tittmann, H. Gross, W. Welte and T. Wallimann (1999). "Crystallization of the human, mitochondrial voltage-dependent anion-selective channel in the presence of phospholipids." J Struct Biol **127**(1): 64-71.
- Dornmair, K., H. Kiefer and F. Jahnig (1990). "Refolding of an integral membrane protein. OmpA of *Escherichia coli*." J Biol Chem **265**(31): 18907-11.
- Eftink, M. R. (1994). "The use of fluorescence methods to monitor unfolding transitions in proteins." Biophys J **66**(2 Pt 1): 482-501.
- Eisele, J. L. and J. P. Rosenbusch (1990). "In vitro folding and oligomerization of a membrane protein. Transition of bacterial porin from random coil to native conformation." J Biol Chem **265**(18): 10217-20.
- Elkeles, A., A. Breiman and M. Zizi (1997). "Functional differences among wheat voltage-dependent anion channel (VDAC) isoforms expressed in yeast. Indication for the presence of a novel VDAC-modulating protein?" J Biol Chem **272**(10): 6252-60.
- Elkeles, A., K. M. Devos, D. Graur, M. Zizi and A. Breiman (1995). "Multiple cDNAs of wheat voltage-dependent anion channels (VDAC): isolation, differential expression, mapping and evolution." Plant Mol Biol **29**(1): 109-24.

- Engelman, D. M., Y. H. Chen, C. N. Chin, A. R. Curran, A. M. Dixon, A. D. Dupuy, A. S. Lee, U. Lehnert, E. E. Matthews, Y. K. Reshetnyak, A. Senes and P. J. L. (2003). "Membrane protein folding: beyond the two stage model." FEBS Lett **555**(1): 122-5.
- Fasman, G. D. (1989). "Protein conformational prediction." Trends Biochem Sci **14**(7): 295-9.
- Fedorova, L. and A. Fedorov (2003). "Introns in gene evolution." Genetica **118**(2-3): 123-31.
- Ferguson, A. D., E. Hofmann, J. W. Coulton, K. Diederichs and W. Welte (1998). "Siderophore-mediated iron transport: crystal structure of FhuA with bound lipopolysaccharide." Science **282**(5397): 2215-20.
- Fernández, C., K. Adeishvili and K. Wüthrich (2001). "Transverse relaxation-optimized NMR spectroscopy with the outer membrane protein OmpX in dihexanoyl phosphatidylcholine micelles." Proc Natl Acad Sci U S A **98**(5): 2358-63.
- Fernández, C., C. Hilty, S. Bonjour, K. Adeishvili, K. Pervushin and K. Wüthrich (2001). "Solution NMR studies of the integral membrane proteins OmpX and OmpA from *Escherichia coli*." FEBS Lett **504**(3): 173-8.
- Fernández, C., C. Hilty, G. Wider, P. Guntert and K. Wüthrich (2004). "NMR structure of the integral membrane protein OmpX." J Mol Biol **336**(5): 1211-21.
- Fischer, K., A. Weber, S. Brink, B. Arbinger, D. Schunemann, S. Borchert, H. W. Heldt, B. Popp, R. Benz, T. A. Link and et al. (1994). "Porins from plants. Molecular cloning and functional characterization of two new members of the porin family." J Biol Chem **269**(41): 25754-60.
- Forst, D., W. Welte, T. Wacker and K. Diederichs (1998). "Structure of the sucrose-specific porin ScrY from *Salmonella typhimurium* and its complex with sucrose." Nat Struct Biol **5**(1): 37-46.
- Forte, M., D. Adelsberger-Mangan and M. Colombini (1987). "Purification and characterization of the voltage-dependent anion channel from the outer mitochondrial membrane of yeast." J Membr Biol **99**(1): 65-72.
- Freitag, H., G. Genchi, R. Benz, F. Palmieri and W. Neupert (1982). "Isolation of mitochondrial porin from *Neurospora crassa*." FEBS Lett **145**(1): 72-6.
- Freitag, H., M. Janes and W. Neupert (1982). "Biosynthesis of mitochondrial porin and insertion into the outer mitochondrial membrane of *Neurospora crassa*." Eur J Biochem **126**(1): 197-202.

- Freitag, H., W. Neupert and R. Benz (1982). "Purification and characterisation of a pore protein of the outer mitochondrial membrane from *Neurospora crassa*." Eur J Biochem **123**(3): 629-36.
- Freudl, R., S. MacIntyre, M. Degen and U. Henning (1988). "Alterations to the signal peptide of an outer membrane protein (OmpA) of *Escherichia coli* K-12 can promote either the cotranslational or the posttranslational mode of processing." J Biol Chem **263**(1): 344-9.
- Garavito, R. M. and S. Ferguson-Miller (2001). "Detergents as tools in membrane biochemistry." J Biol Chem **278**: 32403-32406.
- Garcia-Borron, J. C., J. Escribano, M. Jimenez and J. L. Iborra (1982). "Quantitative determination of tryptophanyl and tyrosyl residues of proteins by second-derivative fluorescence spectroscopy." Anal Biochem **125**(2): 277-85.
- Gentle, I., K. Gabriel, P. Beech, R. Waller and T. Lithgow (2004). "The Omp85 family of proteins is essential for outer membrane biogenesis in mitochondria and bacteria." J Cell Biol **164**(1): 19-24.
- Gilbert, R. J. (2002). "Pore-forming toxins." Cell Mol Life Sci **59**(5): 832-44.
- Gincel, D., H. Zaid and V. Shoshan-Barmatz (2001). "Calcium binding and translocation by the voltage-dependent anion channel: a possible regulatory mechanism in mitochondrial function." Biochem J **358**(Pt 1): 147-55.
- Gonzalez-Gronow, M., T. Kalfa, C. E. Johnson, G. Gawdi and S. V. Pizzo (2003). "The voltage-dependent anion channel is a receptor for plasminogen kringle 5 on human endothelial cells." J Biol Chem **278**(29): 27312-8.
- Graham, B. H. and W. J. Craigen (2005). "Mitochondrial Voltage-dependent anion channel gene family in *Drosophila melanogaster*: Complex patterns of evolution, genomic organization, and developmental expression." Mol Genet Metab.
- Guo, X. W. and C. A. Mannella (1993). "Conformational change in the mitochondrial channel, VDAC, detected by electron cryo-microscopy." Biophys J **64**(2): 545-9.
- Guo, X. W., P. R. Smith, B. Cognon, D. D'Arcangelis, E. Dolginova and C. A. Mannella (1995). "Molecular design of the voltage-dependent, anion-selective channel in the mitochondrial outer membrane." J Struct Biol **114**(1): 41-59.
- Guzow, K., A. Rzeska, J. Mrozek, J. Karolczak, R. Majewski, M. Szabelski, T. Ossowski and W. Wiczk (2005). "Photophysical properties of tyrosine and its simple derivatives in organic solvents studied by time-resolved fluorescence spectroscopy and global analysis." Photochem Photobiol **81**(3): 697-704.

- Ha, H., P. Hajek, D. M. Bedwell and P. D. Burrows (1993). "A mitochondrial porin cDNA predicts the existence of multiple human porins." J Biol Chem **268**(16): 12143-9.
- Harkness, T. A., F. E. Nargang, I. van der Klei, W. Neupert and R. Lill (1994). "A crucial role of the mitochondrial protein import receptor MOM19 for the biogenesis of mitochondria." J Cell Biol **124**(5): 637-48.
- Harms, N., G. Koningstein, W. Dontje, M. Muller, B. Oudega, J. Luirink and H. de Cock (2001). "The early interaction of the outer membrane protein phoe with the periplasmic chaperone Skp occurs at the cytoplasmic membrane." J Biol Chem **276**(22): 18804-11.
- Havel, H. A. (1996). Derivative near-ultraviolet absorption techniques for investigating protein structure. Spectroscopic methods for determining protein structure in solution. H. A. Havel. New York, VCH Publishers, Inc.: 62-68.
- Havel, H. A., E. W. Kauffman, S. M. Plaisted and D. N. Brems (1986). "Reversible self-association of bovine growth hormone during equilibrium unfolding." Biochemistry **25**(21): 6533-8.
- Heins, L., H. Mentzel, A. Schmid, R. Benz and U. K. Schmitz (1994). "Biochemical, molecular, and functional characterization of porin isoforms from potato mitochondria." J Biol Chem **269**(42): 26402-10.
- Heringa, J. (2000). "Computational methods for protein secondary structure prediction using multiple sequence alignments." Curr Protein Pept Sci **1**(3): 273-301.
- Heringa, J. (2002). "Local weighting schemes for protein multiple sequence alignment." Comput Chem **26**(5): 459-77.
- Hoppins, S. C. and F. E. Nargang (2004). "The Tim8-Tim13 complex of *Neurospora crassa* functions in the assembly of proteins into both mitochondrial membranes." J Biol Chem **279**(13): 12396-405.
- Jacotot, E., K. F. Ferri, C. El Hamel, C. Brenner, S. Druillennec, J. Hoebeke, P. Rustin, D. Metivier, C. Lenoir, M. Geuskens, H. L. Vieira, M. Loeffler, A. S. Belzacq, J. P. Briand, N. Zamzami, L. Edelman, Z. H. Xie, J. C. Reed, B. P. Roques and G. Kroemer (2001). "Control of mitochondrial membrane permeabilization by adenine nucleotide translocator interacting with HIV-1 viral protein rR and Bcl-2." J Exp Med **193**(4): 509-19.
- Jacotot, E., L. Ravagnan, M. Loeffler, K. F. Ferri, H. L. Vieira, N. Zamzami, P. Costantini, S. Druillennec, J. Hoebeke, J. P. Briand, T. Irinopoulou, E. Daugas, S. A. Susin, D. Cointe, Z. H. Xie, J. C. Reed, B. P. Roques and G. Kroemer (2000). "The HIV-1 viral protein R induces apoptosis via a direct effect on the mitochondrial permeability transition pore." J Exp Med **191**(1): 33-46.

- Jansen, C., M. Heutink, J. Tommassen and H. de Cock (2000). "The assembly pathway of outer membrane protein PhoE of *Escherichia coli*." Eur J Biochem **267**(12): 3792-800.
- Jap, B. K. and P. J. Walian (1996). "Structure and functional mechanism of porins." Physiol Rev **76**(4): 1073-88.
- Johnson, W. C., Jr. (1990). "Protein secondary structure and circular dichroism: a practical guide." Proteins **7**(3): 205-14.
- Kakorin, S., U. Brinkmann and E. Neumann (2005). "Cholesterol reduces membrane electroporation and electric deformation of small bilayer vesicles." Biophys Chem **117**(2): 155-71.
- Kawahara, K. and C. Tanford (1966). "Viscosity and density of aqueous solutions of urea and guanidine hydrochloride." J Biol Chem **241**(13): 3228-32.
- Kayser, H., H. D. Kratzin, F. P. Thinner, H. Gotz, W. E. Schmidt, K. Eckart and N. Hilschmann (1989). "[Identification of human porins. II. Characterization and primary structure of a 31-kDa porin from human B lymphocytes (Porin 31HL).]" Biol Chem Hoppe Seyler **370**(12): 1265-78.
- Kim, R., M. Emi, K. Tanabe, S. Murakami, Y. Uchida and K. Arihiro (2006). "Regulation and interplay of apoptotic and non-apoptotic cell death." J Pathol **208**(3): 319-26.
- Kleene, R., N. Pfanner, R. Pfaller, T. A. Link, W. Sebald, W. Neupert and M. Tropschug (1987). "Mitochondrial porin of *Neurospora crassa*: cDNA cloning, in vitro expression and import into mitochondria." EMBO J **6**(9): 2627-33.
- Kleinschmidt, J. H. (2003). "Membrane protein folding on the example of outer membrane protein A of *Escherichia coli*." Cell Mol Life Sci **60**(8): 1547-58.
- Kleinschmidt, J. H. (2006). "Folding kinetics of the outer membrane proteins OmpA and FomA into phospholipid bilayers." Chem Phys Lipids **141**(1-2): 30-47.
- Kleinschmidt, J. H., T. den Blaauwen, A. J. Driessen and L. K. Tamm (1999). "Outer membrane protein A of *Escherichia coli* inserts and folds into lipid bilayers by a concerted mechanism." Biochemistry **38**(16): 5006-16.
- Kleinschmidt, J. H. and L. K. Tamm (1996). "Folding intermediates of a beta-barrel membrane protein. Kinetic evidence for a multi-step membrane insertion mechanism." Biochemistry **35**(40): 12993-3000.

- Kleinschmidt, J. H. and L. K. Tamm (1999). "Time-resolved distance determination by tryptophan fluorescence quenching: probing intermediates in membrane protein folding." Biochemistry **38**(16): 4996-5005.
- Kleinschmidt, J. H. and L. K. Tamm (2002). "Secondary and tertiary structure formation of the beta-barrel membrane protein OmpA is synchronized and depends on membrane thickness." J Mol Biol **324**(2): 319-30.
- Kleinschmidt, J. H., M. C. Wiener and L. K. Tamm (1999). "Outer membrane protein A of *E. coli* folds into detergent micelles, but not in the presence of monomeric detergent." Protein Sci **8**(10): 2065-71.
- Koebnik, R. (1995). "Proposal for a peptidoglycan-associating alpha-helical motif in the C-terminal regions of some bacterial cell-surface proteins." Mol Microbiol **16**(6): 1269-70.
- Koebnik, R., K. P. Locher and P. Van Gelder (2000). "Structure and function of bacterial outer membrane proteins: barrels in a nutshell." Mol Microbiol **37**(2): 239-53.
- Komarov, A. G., B. H. Graham, W. J. Craigen and M. Colombini (2004). "The physiological properties of a novel family of VDAC-like proteins from *Drosophila melanogaster*." Biophys J **86**(1 Pt 1): 152-62.
- Konstantinova, S. A., C. A. Mannella, V. P. Skulachev and D. B. Zorov (1995). "Immunoelectron microscopic study of the distribution of porin on outer membranes of rat heart mitochondria." J Bioenerg Biomembr **27**(1): 93-9.
- Konstantinova, S. A., K. A. Mannella, V. P. Skulachev and D. B. Zorov (1994). "[Detection of porin in inter-mitochondrial contacts]." Biokhimiia **59**(8): 1109-21.
- Koppel, D. A., K. W. Kinnally, P. Masters, M. Forte, E. Blachly-Dyson and C. A. Mannella (1998). "Bacterial expression and characterization of the mitochondrial outer membrane channel. Effects of n-terminal modifications." J Biol Chem **273**(22): 13794-800.
- Krimmer, T., D. Rapaport, M. T. Ryan, C. Meisinger, C. K. Kassenbrock, E. Blachly-Dyson, M. Forte, M. G. Douglas, W. Neupert, F. E. Nargang and N. Pfanner (2001). "Biogenesis of porin of the outer mitochondrial membrane involves an import pathway via receptors and the general import pore of the TOM complex." J Cell Biol **152**(2): 289-300.
- Kumar, T. K., G. Jayaraman, C. S. Lee, T. Sivaraman, W. Y. Lin and C. Yu (1995). "Identification of 'molten globule'-like state in all beta-sheet protein." Biochem Biophys Res Commun **207**(2): 536-43.

- Künkele, K. P., P. Juin, C. Pompa, F. E. Nargang, J. P. Henry, W. Neupert, R. Lill and M. Thieffry (1998). "The isolated complex of the translocase of the outer membrane of mitochondria. Characterization of the cation-selective and voltage-gated preprotein-conducting pore." J Biol Chem **273**(47): 31032-9.
- Kyte, J. and R. F. Doolittle (1982). "A simple method for displaying the hydropathic character of a protein." J Mol Biol **157**(1): 105-32.
- Ladokhin, A. S. (2000). Fluorescence spectroscopy in peptide and protein analysis. Encyclopedia of analytical chemistry. R. A. Meyers. Chichester, John Wiley and Sons Ltd.: 5762-5779.
- Laemmli, U. K. (1970). "Cleavage of structural proteins during the assembly of the head of bacteriophage T4." Nature **227**(5259): 680-5.
- Lau, F. W. and J. U. Bowie (1997). "A method for assessing the stability of a membrane protein." Biochemistry **36**(19): 5884-92.
- Lazar, S. W. and R. Kolter (1996). "SurA assists the folding of Escherichia coli outer membrane proteins." J Bacteriol **178**(6): 1770-3.
- Lee, J. and R. Ross (1998). "Absorption and fluorescence of tyrosine hydrogen-bonded to amide-like ligands." J Phys Chem B **102**: 4612-18.
- Lemasters, J. J. and E. Holmuhamedov (2006). "Voltage-dependent anion channel (VDAC) as mitochondrial governor--thinking outside the box." Biochim Biophys Acta **1762**(2): 181-90.
- Lemeshko, S. V. and V. V. Lemeshko (2000). "Metabolically derived potential on the outer membrane of mitochondria: a computational model." Biophys J **79**(6): 2785-800.
- Lemeshko, S. V. and V. V. Lemeshko (2004). "Energy flux modulation on the outer membrane of mitochondria by metabolically-derived potential." Mol Cell Biochem **256-257**(1-2): 127-39.
- Lemeshko, V. V. and S. V. Lemeshko (2004). "The voltage-dependent anion channel as a biological transistor: theoretical considerations." Eur Biophys J **33**(4): 352-9.
- Li, X. X. and M. Colombini (2002). "Catalyzed insertion of proteins into phospholipid membranes: specificity of the process." Biophys J **83**(5): 2550-9.
- Lin, K., V. A. Simossis, W. R. Taylor and J. Heringa (2005). "A simple and fast secondary structure prediction method using hidden neural networks." Bioinformatics **21**(2): 152-9.

- Linke, D., J. Frank, J. F. Holzwarth, J. Soll, C. Boettcher and P. Fromme (2000). "In vitro reconstitution and biophysical characterization of OEP16, an outer envelope pore protein of pea chloroplasts." Biochemistry **39**(36): 11050-6.
- Liu, M. Y. and M. Colombini (1991). "Voltage gating of the mitochondrial outer membrane channel VDAC is regulated by a very conserved protein." Am J Physiol **260**(2 Pt 1): C371-4.
- Liu, M. Y. and M. Colombini (1992). "Regulation of mitochondrial respiration by controlling the permeability of the outer membrane through the mitochondrial channel, VDAC." Biochim Biophys Acta **1098**(2): 255-60.
- Liu, M. Y. and M. Colombini (1992). "A soluble mitochondrial protein increases the voltage dependence of the mitochondrial channel, VDAC." J Bioenerg Biomembr **24**(1): 41-6.
- Liu, M. Y., A. Torgrimson and M. Colombini (1994). "Characterization and partial purification of the VDAC-channel-modulating protein from calf liver mitochondria." Biochim Biophys Acta **1185**(2): 203-12.
- Lopez-Llano, J., S. Maldonado, S. Jain, A. Lostao, R. Godoy-Ruiz, J. M. Sanchez-Ruiz, M. Cortijo, J. Fernandez-Recio and J. Sancho (2004). "The long and short flavodoxins: II. The role of the differentiating loop in apoflavodoxin stability and folding mechanism." J Biol Chem **279**(45): 47184-91.
- Madesh, M. and G. Hajnoczky (2001). "VDAC-dependent permeabilization of the outer mitochondrial membrane by superoxide induces rapid and massive cytochrome c release." J Cell Biol **155**(6): 1003-15.
- Manavalan, P. and W. C. Johnson, Jr. (1987). "Variable selection method improves the prediction of protein secondary structure from circular dichroism spectra." Anal Biochem **167**(1): 76-85.
- Manley, D. and J. D. O'Neil (2003). "Preparation of glycerol facilitator for protein structure and folding studies in solution." Methods Mol Biol **228**: 89-101.
- Mannella, C. A. (1989). "Fusion of the mitochondrial outer membrane: use in forming large, two-dimensional crystals of the voltage-dependent, anion-selective channel protein." Biochim Biophys Acta **981**(1): 15-20.
- Mannella, C. A. (1997). "Minireview: on the structure and gating mechanism of the mitochondrial channel, VDAC." J Bioenerg Biomembr **29**(6): 525-31.
- Mannella, C. A. (1998). "Conformational changes in the mitochondrial channel protein, VDAC, and their functional implications." J Struct Biol **121**(2): 207-18.

- Mannella, C. A., M. Forte and M. Colombini (1992). "Toward the molecular structure of the mitochondrial channel, VDAC." J Bioenerg Biomembr **24**(1): 7-19.
- Mannella, C. A. and J. Frank (1984). "Negative staining characteristics of arrays of mitochondrial pore protein: use of correspondence analysis to classify different staining patterns." Ultramicroscopy **13**(1-2): 93-102.
- Mannella, C. A., X. W. Guo and J. Dias (1992). "Binding of a synthetic targeting peptide to a mitochondrial channel protein." J Bioenerg Biomembr **24**(1): 55-61.
- Mannella, C. A., A. F. Neuwald and C. E. Lawrence (1996). "Detection of likely transmembrane beta strand regions in sequences of mitochondrial pore proteins using the Gibbs sampler." J Bioenerg Biomembr **28**(2): 163-9.
- Manting, E. H. and A. J. Driessen (2000). "Escherichia coli translocase: the unravelling of a molecular machine." Mol Microbiol **37**(2): 226-38.
- Mao, D. and B. A. Wallace (1984). "Differential light scattering and absorption flattening optical effects are minimal in the circular dichroism spectra of small unilamellar vesicles." Biochemistry **23**(12): 2667-73.
- Marsh, D., B. Shanmugavadivu and J. H. Kleinschmidt (2006). "Membrane elastic fluctuations and the insertion and tilt of beta-barrel proteins." Biophys J **91**(1): 227-32.
- Martin, N. L., E. G. Rawling, R. S. Wong, M. Rosok and R. E. Hancock (1993). "Conservation of surface epitopes in Pseudomonas aeruginosa outer membrane porin protein OprF." FEMS Microbiol Lett **113**(3): 261-6.
- Masui, R., T. Mikawa and S. Kuramitsu (1997). "Local folding of the N-terminal domain of *Escherichia coli* RecA controls protein-protein interaction." J Biol Chem **272**(44): 27707-15.
- Matsuura, J. E., A. E. Morris, R. R. Ketchum, E. H. Braswell, R. Klinke, W. R. Gombotz and R. L. Remmele, Jr. (2001). "Biophysical characterization of a soluble CD40 ligand (CD154) coiled-coil trimer: evidence of a reversible acid-denatured molten globule." Arch Biochem Biophys **392**(2): 208-18.
- Mayer, A., R. Lill and W. Neupert (1993). "Translocation and insertion of precursor proteins into isolated outer membranes of mitochondria." J Cell Biol **121**(6): 1233-43.
- McEnery, M. W. (1992). "The mitochondrial benzodiazepine receptor: evidence for association with the voltage-dependent anion channel (VDAC)." J Bioenerg Biomembr **24**(1): 63-9.

- McGuire, R. and I. Feldman (1973). "The quenching of tyrosine and tryptophan fluorescence by H₂O and D₂O." Photochem Photobiol **18**(2): 119-24.
- Messina, A., M. Oliva, C. Rosato, M. Huizing, W. Ruitenbeek, L. P. van den Heuvel, M. Forte, M. Rocchi and V. De Pinto (1999). "Mapping of the human Voltage-Dependent Anion Channel isoforms 1 and 2 reconsidered." Biochem Biophys Res Commun **255**(3): 707-10.
- Mihara, K., G. Blobel and R. Sato (1982). "In vitro synthesis and integration into mitochondria of porin, a major protein of the outer mitochondrial membrane of *Saccharomyces cerevisiae*." Proc Natl Acad Sci U S A **79**(23): 7102-6.
- Mihara, K. and R. Sato (1985). "Molecular cloning and sequencing of cDNA for yeast porin, an outer mitochondrial membrane protein: a search for targeting signal in the primary structure." EMBO J **4**(3): 769-74.
- Minetti, C. A., M. S. Blake and D. P. Remeta (1998). "Characterization of the structure, function, and conformational stability of PorB class 3 protein from *Neisseria meningitidis*. A porin with unusual physicochemical properties." J Biol Chem **273**(39): 25329-38.
- Minetti, C. A., J. Y. Tai, M. S. Blake, J. K. Pullen, S. M. Liang and D. P. Remeta (1997). "Structural and functional characterization of a recombinant PorB class 2 protein from *Neisseria meningitidis*. Conformational stability and porin activity." J Biol Chem **272**(16): 10710-20.
- Muller, A., D. Gunther, V. Brinkmann, R. Hurwitz, T. F. Meyer and T. Rudel (2000). "Targeting of the pro-apoptotic VDAC-like porin (PorB) of *Neisseria gonorrhoeae* to mitochondria of infected cells." Embo J **19**(20): 5332-43.
- Muller, A., J. Rassow, J. Grimm, N. Machuy, T. F. Meyer and T. Rudel (2002). "VDAC and the bacterial porin PorB of *Neisseria gonorrhoeae* share mitochondrial import pathways." Embo J **21**(8): 1916-29.
- Murzin, A. G., A. M. Lesk and C. Chothia (1994). "Principles determining the structure of beta-sheet barrels in proteins. I. A theoretical analysis." J Mol Biol **236**(5): 1369-81.
- Narhi, L. O., J. S. Philo, T. Li, M. Zhang, B. Samal and T. Arakawa (1996). "Induction of alpha-helix in the beta-sheet protein tumor necrosis factor-alpha: thermal- and trifluoroethanol-induced denaturation at neutral pH." Biochemistry **35**(35): 11447-53.
- Nayar, S., A. Brahma, C. Mukherjee and D. Bhattacharyya (2002). "Second derivative fluorescence spectra of indole compounds." J Biochem (Tokyo) **131**(3): 427-35.

- Ninomiya, Y., K. Suzuki, C. Ishii and H. Inoue (2004). "Highly efficient gene replacements in *Neurospora* strains deficient for nonhomologous end-joining." Proc Natl Acad Sci U S A **101**(33): 12248-53.
- Noronha, M., J. Lima, P. Lamosa, H. Santos, C. Maycock, R. Ventura and A. Macanita (2004). "Intramolecular fluorescence quenching of tyrosine by the peptide α -carbonyl group revisited." J Phys Chem A **108**: 2155-66.
- Ohnishi, S. and K. Kameyama (2001). "*Escherichia coli* OmpA retains a folded structure in the presence of sodium dodecyl sulfate due to a high kinetic barrier to unfolding." Biochim Biophys Acta **1515**(2): 159-66.
- Ohnishi, S., K. Kameyama and T. Takagi (1998). "Characterization of a heat modifiable protein, *Escherichia coli* outer membrane protein OmpA in binary surfactant system of sodium dodecyl sulfate and octylglucoside." Biochim Biophys Acta **1375**(1-2): 101-9.
- Otzen, D. E. (2003). "Folding of DsbB in mixed micelles: a kinetic analysis of the stability of a bacterial membrane protein." J Mol Biol **330**(4): 641-9.
- Park, K., A. Perczel and G. D. Fasman (1992). "Differentiation between transmembrane helices and peripheral helices by the deconvolution of circular dichroism spectra of membrane proteins." Protein Sci **1**(8): 1032-49.
- Paschen, S. A. and W. Neupert (2001). "Protein import into mitochondria." IUBMB Life **52**(3-5): 101-12.
- Paschen, S. A., W. Neupert and D. Rapaport (2005). "Biogenesis of beta-barrel membrane proteins of mitochondria." Trends Biochem Sci **30**(10): 575-82.
- Paschen, S. A., T. Waizenegger, T. Stan, M. Preuss, M. Cyrklaff, K. Hell, D. Rapaport and W. Neupert (2003). "Evolutionary conservation of biogenesis of beta-barrel membrane proteins." Nature **426**(6968): 862-6.
- Pautsch, A. and G. E. Schulz (1998). "Structure of the outer membrane protein A transmembrane domain." Nat Struct Biol **5**(11): 1013-7.
- Pavlica, R. J., C. B. Hesler, L. Lipfert, I. N. Hirshfield and D. Haldar (1990). "Two-dimensional gel electrophoretic resolution of the polypeptides of rat liver mitochondria and the outer membrane." Biochim Biophys Acta **1022**(1): 115-25.
- Peng, S., E. Blachly-Dyson, M. Forte and M. Colombini (1992). "Large scale rearrangement of protein domains is associated with voltage gating of the VDAC channel." Biophys J **62**(1): 123-31; discussion 131-5.

- Perczel, A., K. Park and G. D. Fasman (1992). "Analysis of the circular dichroism spectrum of proteins using the convex constraint algorithm: a practical guide." Anal Biochem **203**(1): 83-93.
- Pfaller, R., H. Freitag, M. A. Harmey, R. Benz and W. Neupert (1985). "A water-soluble form of porin from the mitochondrial outer membrane of *Neurospora crassa*. Properties and relationship to the biosynthetic precursor form." J Biol Chem **260**(13): 8188-93.
- Pocanschi, C. L., H. J. Apell, P. Puntervoll, B. Hogh, H. B. Jensen, W. Welte and J. H. Kleinschmidt (2006). "The major outer membrane protein of *Fusobacterium nucleatum* (FomA) folds and inserts into lipid bilayers via parallel folding pathways." J Mol Biol **355**(3): 548-61.
- Pocanschi, C. L., G. J. Patel, D. Marsh and J. H. Kleinschmidt (2006). "Curvature elasticity and refolding of OmpA in large unilamellar vesicles." Biophys J.
- Pollastri, G., D. Przybylski, B. Rost and P. Baldi (2002). "Improving the prediction of protein secondary structure in three and eight classes using recurrent neural networks and profiles." Proteins **47**(2): 228-35.
- Popot, J. L. and D. M. Engelman (1990). "Membrane protein folding and oligomerization: the two-stage model." Biochemistry **29**(17): 4031-7.
- Popot, J. L. and D. M. Engelman (2000). "Helical membrane protein folding, stability, and evolution." Annu Rev Biochem **69**: 881-922.
- Popp, B., D. A. Court, R. Benz, W. Neupert and R. Lill (1996). "The role of the N and C termini of recombinant *Neurospora* mitochondrial porin in channel formation and voltage-dependent gating." J Biol Chem **271**(23): 13593-9.
- Popp, B., S. Gebauer, K. Fischer, U. I. Flügge and R. Benz (1997). "Study of structure and function of recombinant pea root plastid porin by biophysical methods." Biochemistry **36**(10): 2844-52.
- Popp, B., A. Schmid and R. Benz (1995). "Role of sterols in the functional reconstitution of water-soluble mitochondrial porins from different organisms." Biochemistry **34**(10): 3352-61.
- Privalov, P. L. and S. A. Potekhin (1986). "Scanning microcalorimetry in studying temperature-induced changes in proteins." Methods Enzymol **131**: 4-51.
- Proulx, P., H. Aubry, I. Brglez and D. G. Williamson (1984). "Studies on the mechanism of cholesterol uptake and on the effects of bile salts on this uptake by brush-border membranes isolated from rabbit small intestine." Biochim Biophys Acta **778**(3): 586-93.

- Provencher, S. W. and J. Glockner (1981). "Estimation of globular protein secondary structure from circular dichroism." Biochemistry **20**(1): 33-7.
- Przybylski, M., M. O. Glocker, U. Nestel, V. Schnaible, M. Bluggel, K. Diederichs, J. Weckesser, M. Schad, A. Schmid, W. Welte and R. Benz (1996). "X-ray crystallographic and mass spectrometric structure determination and functional characterization of succinylated porin from *Rhodobacter capsulatus*: implications for ion selectivity and single-channel conductance." Protein Sci **5**(8): 1477-89.
- Ragone, G., G. Colonna, L. Servillo and G. Irace (1985). "Resolution of overlapping bands in the near-UV absorption spectrum of indole derivatives." Photochem. Photobiol. **42**: 505-8.
- Ragone, R., G. Colonna, C. Balestrieri, L. Servillo and G. Irace (1984). "Determination of tyrosine exposure in proteins by second-derivative spectroscopy." Biochemistry **23**(8): 1871-5.
- Rahmani, Z., C. Maunoury and A. Siddiqui (1998). "Isolation of a novel human voltage-dependent anion channel gene." Eur J Hum Genet **6**(4): 337-40.
- Rapaport, D. (2005). "How does the TOM complex mediate insertion of precursor proteins into the mitochondrial outer membrane?" J Cell Biol **171**(3): 419-23.
- Rauch, G. and O. Moran (1994). "On the structure of mitochondrial porins and its homologies with bacterial porins." Biochem Biophys Res Commun **200**(2): 908-15.
- Rawling, E. G., N. L. Martin and R. E. Hancock (1995). "Epitope mapping of the *Pseudomonas aeruginosa* major outer membrane porin protein OprF." Infect Immun **63**(1): 38-42.
- Reader, J. S., N. A. Van Nuland, G. S. Thompson, S. J. Ferguson, C. M. Dobson and S. E. Radford (2001). "A partially folded intermediate species of the beta-sheet protein apopseudoazurin is trapped during proline-limited folding." Protein Sci **10**(6): 1216-24.
- Reshetnyak, Y. K., Y. Koshevnik and E. A. Burstein (2001). "Decomposition of protein tryptophan fluorescence spectra into log-normal components. III. Correlation between fluorescence and microenvironment parameters of individual tryptophan residues." Biophys J **81**(3): 1735-58.
- Roman, I., J. Figys, G. Steurs and M. Zizi (2006). "Hunting interactomes of a membrane protein: obtaining the largest set of VDAC-interacting protein epitopes." Mol Cell Proteomics.

- Roos, N., R. Benz and D. Brdiczka (1982). "Identification and characterization of the pore-forming protein in the outer membrane of rat liver mitochondria." Biochim Biophys Acta **686**(2): 204-14.
- Rostovtseva, T. and M. Colombini (1996). "ATP flux is controlled by a voltage-gated channel from the mitochondrial outer membrane." J Biol Chem **271**(45): 28006-8.
- Rostovtseva, T. and M. Colombini (1997). "VDAC channels mediate and gate the flow of ATP: implications for the regulation of mitochondrial function." Biophys J **72**(5): 1954-62.
- Rostovtseva, T. K., B. Antonsson, M. Suzuki, R. J. Youle, M. Colombini and S. M. Bezrukov (2004). "Bid, but not Bax, regulates VDAC channels." J Biol Chem **279**(14): 13575-83.
- Runke, G., E. Maier, J. D. O'Neil, R. Benz and D. A. Court (2000). "Functional characterization of the conserved "GLK" motif in mitochondrial porin from *Neurospora crassa*." J Bioenerg Biomembr **32**(6): 563-70.
- Runke, G., E. Maier, W. A. Summers, D. C. Bay, R. Benz and D. A. Court (2006). "Deletion variants of *Neurospora* mitochondrial porin: electrophysiological and spectroscopic analysis." Biophys J **90**(9): 3155-64.
- Sampson, M. J., W. K. Decker, A. L. Beaudet, W. Ruitenbeek, D. Armstrong, M. J. Hicks and W. J. Craigen (2001). "Immotile sperm and infertility in mice lacking mitochondrial voltage-dependent anion channel type 3." J Biol Chem **276**(42): 39206-12.
- Sampson, M. J., R. S. Lovell and W. J. Craigen (1996). "Isolation, characterization, and mapping of two mouse mitochondrial voltage-dependent anion channel isoforms." Genomics **33**(2): 283-8.
- Sampson, M. J., R. S. Lovell and W. J. Craigen (1997). "The murine voltage-dependent anion channel gene family. Conserved structure and function." J Biol Chem **272**(30): 18966-73.
- Sampson, M. J., L. Ross, W. K. Decker and W. J. Craigen (1998). "A novel isoform of the mitochondrial outer membrane protein VDAC3 via alternative splicing of a 3-base exon. Functional characteristics and subcellular localization." J Biol Chem **273**(46): 30482-6.
- Schein, S. J., M. Colombini and A. Finkelstein (1976). "Reconstitution in planar lipid bilayers of a voltage-dependent anion-selective channel obtained from paramecium mitochondria." J Membr Biol **30**(2): 99-120.

- Schleiff, E., G. C. Shore and I. S. Goping (1997). "Human mitochondrial import receptor, Tom20p. Use of glutathione to reveal specific interactions between Tom20-glutathione S-transferase and mitochondrial precursor proteins." FEBS Lett **404**(2-3): 314-8.
- Schleiff, E., J. R. Silvius and G. C. Shore (1999). "Direct membrane insertion of voltage-dependent anion-selective channel protein catalyzed by mitochondrial Tom20." J Cell Biol **145**(5): 973-8.
- Schmidt, S., A. Strub, K. Rottgers, N. Zufall and W. Voos (2001). "The two mitochondrial heat shock proteins 70, Ssc1 and Ssq1, compete for the cochaperone Mge1." J Mol Biol **313**(1): 13-26.
- Schulz, G. E. (2000). "beta-Barrel membrane proteins." Curr Opin Struct Biol **10**(4): 443-7.
- Schwarzer, C., S. Barnikol-Watanabe, F. P. Thinnes and N. Hilschmann (2002). "Voltage-dependent anion-selective channel (VDAC) interacts with the dynein light chain Tctex1 and the heat-shock protein PBP74." Int J Biochem Cell Biol **34**(9): 1059-70.
- Schweizer, M., I. Hindennach, W. Garten and U. Henning (1978). "Major proteins of the Escherichia coli outer cell envelope membrane. Interaction of protein II with lipopolysaccharide." Eur J Biochem **82**(1): 211-7.
- Scotto, A. W. and D. Zakim (1988). "Reconstitution of membrane proteins. Spontaneous incorporation of integral membrane proteins into preformed bilayers of pure phospholipid." J Biol Chem **263**(34): 18500-6.
- Shao, L., K. W. Kinnally and C. A. Mannella (1996). "Circular dichroism studies of the mitochondrial channel, VDAC, from *Neurospora crassa*." Biophys J **71**(2): 778-86.
- Sherman, E. L., N. E. Go and F. E. Nargang (2005). "Functions of the small proteins in the TOM complex of *Neurospora crassa*." Mol Biol Cell **16**(9): 4172-82.
- Sherman, E. L., R. D. Taylor, N. E. Go and F. E. Nargang (2006). "Effect of mutations in Tom40 on stability of the translocase of the outer mitochondrial membrane (TOM) complex, assembly of Tom40, and import of mitochondrial preproteins." J Biol Chem **281**(32): 22554-65.
- Shimizu, S., T. Ide, T. Yanagida and Y. Tsujimoto (2000). "Electrophysiological study of a novel large pore formed by Bax and the voltage-dependent anion channel that is permeable to cytochrome c." J Biol Chem **275**(16): 12321-5.
- Shimizu, S., A. Konishi, T. Kodama and Y. Tsujimoto (2000). "BH4 domain of antiapoptotic Bcl-2 family members closes voltage-dependent anion channel and inhibits apoptotic mitochondrial changes and cell death." Proc Natl Acad Sci U S A **97**(7): 3100-5.

- Shimizu, S., M. Narita and Y. Tsujimoto (1999). "Bcl-2 family proteins regulate the release of apoptogenic cytochrome c by the mitochondrial channel VDAC." Nature **399**(6735): 483-7.
- Shimizu, S. and Y. Tsujimoto (2000). "Proapoptotic BH3-only Bcl-2 family members induce cytochrome c release, but not mitochondrial membrane potential loss, and do not directly modulate voltage-dependent anion channel activity." Proc Natl Acad Sci U S A **97**(2): 577-82.
- Shoshan-Barmatz, V., A. Israelson, D. Brdiczka and S. S. Sheu (2006). "The voltage-dependent anion channel (VDAC): function in intracellular signalling, cell life and cell death." Curr Pharm Des **12**(18): 2249-70.
- Simons, K. and E. Ikonen (2000). "How cells handle cholesterol." Science **290**(5497): 1721-6.
- Simossis, V. A. and J. Heringa (2003). "The PRALINE online server: optimising progressive multiple alignment on the web." Comput Biol Chem **27**(4-5): 511-9.
- Simossis, V. A. and J. Heringa (2005). "PRALINE: a multiple sequence alignment toolbox that integrates homology-extended and secondary structure information." Nucleic Acids Res **33**(Web Server issue): W289-94.
- Singh, S. P., Y. U. Williams, S. Miller and H. Nikaido (2003). "The C-terminal domain of Salmonella enterica serovar typhimurium OmpA is an immunodominant antigen in mice but appears to be only partially exposed on the bacterial cell surface." Infect Immun **71**(7): 3937-46.
- Sivaraman, T., T. K. Kumar, G. Jayaraman, C. C. Han and C. Yu (1997). "Characterization of a partially structured state in an all-beta-sheet protein." Biochem J **321** (Pt 2): 457-64.
- Smith, M. D., M. Petrak, P. D. Boucher, K. N. Barton, L. Carter, G. Reddy, E. Blachly-Dyson, M. Forte, J. Price, K. Verner and et al. (1995). "Lysine residues at positions 234 and 236 in yeast porin are involved in its assembly into the mitochondrial outer membrane." J Biol Chem **270**(47): 28331-6.
- Song, J., C. Midson, E. Blachly-Dyson, M. Forte and M. Colombini (1998). "The sensor regions of VDAC are translocated from within the membrane to the surface during the gating processes." Biophys J **74**(6): 2926-44.
- Song, J., C. Midson, E. Blachly-Dyson, M. Forte and M. Colombini (1998). "The topology of VDAC as probed by biotin modification." J Biol Chem **273**(38): 24406-13.

- Spyroacopoulos, L. and J. D. O'Neil (1994). "Effect of a hydrophobic environment on the hydrogen exchange kinetics of model amides determined by ^1H -NMR spectroscopy." J Am Chem Soc **116**: 1395-1402.
- Sreerama, N., S. Y. Venyaminov and R. W. Woody (2000). "Estimation of protein secondary structure from circular dichroism spectra: inclusion of denatured proteins with native proteins in the analysis." Anal Biochem **287**(2): 243-51.
- Stanley, S., J. A. Dias, D. D'Arcangelis and C. A. Mannella (1995). "Peptide-specific antibodies as probes of the topography of the voltage-gated channel in the mitochondrial outer membrane of *Neurospora crassa*." J Biol Chem **270**(28): 16694-700.
- Sugawara, E. and H. Nikaido (1992). "Pore-forming activity of OmpA protein of *Escherichia coli*." J Biol Chem **267**(4): 2507-11.
- Sugawara, E. and H. Nikaido (1994). "OmpA protein of *Escherichia coli* outer membrane occurs in open and closed channel forms." J Biol Chem **269**(27): 17981-7.
- Surrey, T. and F. Jahnig (1992). "Refolding and oriented insertion of a membrane protein into a lipid bilayer." Proc Natl Acad Sci U S A **89**(16): 7457-61.
- Surrey, T. and F. Jahnig (1995). "Kinetics of folding and membrane insertion of a beta-barrel membrane protein." J Biol Chem **270**(47): 28199-203.
- Surrey, T., A. Schmid and F. Jahnig (1996). "Folding and membrane insertion of the trimeric beta-barrel protein OmpF." Biochemistry **35**(7): 2283-8.
- Tamm, L. K., F. Abildgaard, A. Arora, H. Blad and J. H. Bushweller (2003). "Structure, dynamics and function of the outer membrane protein A (OmpA) and influenza hemagglutinin fusion domain in detergent micelles by solution NMR." FEBS Lett **555**(1): 139-43.
- Tamm, L. K., H. Hong and B. Liang (2004). "Folding and assembly of beta-barrel membrane proteins." Biochim Biophys Acta **1666**(1-2): 250-63.
- Thomas, L., E. Blachly-Dyson, M. Colombini and M. Forte (1993). "Mapping of residues forming the voltage sensor of the voltage-dependent anion-selective channel." Proc Natl Acad Sci U S A **90**(12): 5446-9.
- Thomas, L., E. Kocsis, M. Colombini, E. Erbe, B. L. Trus and A. C. Steven (1991). "Surface topography and molecular stoichiometry of the mitochondrial channel, VDAC, in crystalline arrays." J Struct Biol **106**(2): 161-71.

- Thundimadathil, J., R. W. Roeske and L. Guo (2005). "A synthetic peptide forms voltage-gated porin-like ion channels in lipid bilayer membranes." Biochem Biophys Res Commun **330**(2): 585-90.
- Thundimadathil, J., R. W. Roeske and L. Guo (2006). "Conversion of a porin-like peptide channel into a gramicidin-like channel by glycine to D-alanine substitutions." Biophys J **90**(3): 947-55.
- Thundimadathil, J., R. W. Roeske and L. Guo (2006). "Effect of membrane mimicking environment on the conformation of a pore-forming (xSxG)₆ peptide." Biopolymers **84**(3): 317-28.
- Thundimadathil, J., R. W. Roeske, H. Y. Jiang and L. Guo (2005). "Aggregation and porin-like channel activity of a beta sheet peptide." Biochemistry **44**(30): 10259-70.
- Traikia, M., D. B. Langlais, G. M. Cannarozzi and P. F. Devaux (1997). "High-resolution spectra of liposomes using MAS NMR. The case of intermediate-size vesicles." J Magn Reson **125**(1): 140-4.
- Traikia, M., D. E. Warschawski, M. Recouvreur, J. Cartaud and P. F. Devaux (2000). "Formation of unilamellar vesicles by repetitive freeze-thaw cycles: characterization by electron microscopy and ³¹P-nuclear magnetic resonance." Eur Biophys J **29**(3): 184-95.
- Traurig, M. and R. Misra (1999). "Identification of bacteriophage K20 binding regions of OmpF and lipopolysaccharide in *Escherichia coli* K-12." FEMS Microbiol Lett **181**(1): 101-8.
- Troll, H., D. Malchow, A. Muller-Taubenberger, B. Humbel, F. Lottspeich, M. Ecke, G. Gerisch, A. Schmid and R. Benz (1992). "Purification, functional characterization, and cDNA sequencing of mitochondrial porin from *Dictyostelium discoideum*." J Biol Chem **267**(29): 21072-9.
- Tsujimoto, Y. and S. Shimizu (2002). "The voltage-dependent anion channel: an essential player in apoptosis." Biochimie **84**(2-3): 187-93.
- van Stokkum, I. H., H. J. Spoelder, M. Bloemendal, R. van Grondelle and F. C. Groen (1990). "Estimation of protein secondary structure and error analysis from circular dichroism spectra." Anal Biochem **191**(1): 110-8.
- Vander Heiden, M. G., X. X. Li, E. Gottleib, R. B. Hill, C. B. Thompson and M. Colombini (2001). "Bcl-xL promotes the open configuration of the voltage-dependent anion channel and metabolite passage through the outer mitochondrial membrane." J Biol Chem **276**(22): 19414-9.

- Verschoor, A., W. F. Tivol and C. A. Mannella (2001). "Single-particle approaches in the analysis of small 2D crystals of the mitochondrial channel VDAC." J Struct Biol **133**(2-3): 254-65.
- Visser, L. and E. R. Blout (1971). "Elastase. II. Optical properties and the effects of sodium dodecyl sulfate." Biochemistry **10**(5): 743-52.
- Visudtiphole, V., M. B. Thomas, D. A. Chalton and J. H. Lakey (2005). "Refolding of Escherichia coli outer membrane protein F in detergent creates LPS-free trimers and asymmetric dimers." Biochem J **392**(Pt 2): 375-81.
- Vogel, H. and F. Jahnig (1986). "Models for the structure of outer-membrane proteins of Escherichia coli derived from raman spectroscopy and prediction methods." J Mol Biol **190**(2): 191-9.
- Voos, W. and K. Rottgers (2002). "Molecular chaperones as essential mediators of mitochondrial biogenesis." Biochim Biophys Acta **1592**(1): 51-62.
- Voulhoux, R., M. P. Bos, J. Geurtsen, M. Mols and J. Tommassen (2003). "Role of a highly conserved bacterial protein in outer membrane protein assembly." Science **299**(5604): 262-5.
- Waldispuhl, J., B. Berger, P. Clote and J. M. Steyaert (2006). "Predicting transmembrane beta-barrels and interstrand residue interactions from sequence." Proteins **65**(1): 61-74.
- Waldispuhl, J., B. Berger, P. Clote and J. M. Steyaert (2006). "transFold: a web server for predicting the structure and residue contacts of transmembrane beta-barrels." Nucleic Acids Res **34**(Web Server issue): W189-93.
- Wallace, B. A. and D. Mao (1984). "Circular dichroism analyses of membrane proteins: an examination of differential light scattering and absorption flattening effects in large membrane vesicles and membrane sheets." Anal Biochem **142**(2): 317-28.
- Wandrey, M., B. Trevaskis, N. Brewin and M. K. Udvardi (2004). "Molecular and cell biology of a family of voltage-dependent anion channel porins in Lotus japonicus." Plant Physiol **134**(1): 182-93.
- Webb, D. C. and A. W. Cripps (1999). "A method for the purification and refolding of a recombinant form of the nontypeable Haemophilus influenzae P5 outer membrane protein fused to polyhistidine." Protein Expr Purif **15**(1): 1-7.
- Weiss, M. S., U. Abele, J. Weckesser, W. Welte, E. Schiltz and G. E. Schulz (1991). "Molecular architecture and electrostatic properties of a bacterial porin." Science **254**(5038): 1627-30.

- Whitmore, L. and B. A. Wallace (2004). "DICHROWEB, an online server for protein secondary structure analyses from circular dichroism spectroscopic data." Nucleic Acids Res **32**(Web Server issue): W668-73.
- Whittington, S. J., B. W. Chellgren, V. M. Hermann and T. P. Creamer (2005). "Urea promotes polyproline II helix formation: implications for protein denatured states." Biochemistry **44**(16): 6269-75.
- Woodfield, K., A. Ruck, D. Brdiczka and A. P. Halestrap (1998). "Direct demonstration of a specific interaction between cyclophilin-D and the adenine nucleotide translocase confirms their role in the mitochondrial permeability transition." Biochem J **336** (Pt 2): 287-90.
- Xu, X. and M. Colombini (1996). "Self-catalyzed insertion of proteins into phospholipid membranes." J Biol Chem **271**(39): 23675-82.
- Xu, X. and M. Colombini (1997). "Autodirected insertion: preinserted VDAC channels greatly shorten the delay to the insertion of new channels." Biophys J **72**(5): 2129-36.
- Xu, X., W. Decker, M. J. Sampson, W. J. Craigen and M. Colombini (1999). "Mouse VDAC isoforms expressed in yeast: channel properties and their roles in mitochondrial outer membrane permeability." J Membr Biol **170**(2): 89-102.
- Yang, J. T., C. S. Wu and H. M. Martinez (1986). "Calculation of protein conformation from circular dichroism." Methods Enzymol **130**: 208-69.
- Yeh, T. Y., D. Peretti, J. Z. Chuang, E. Rodriguez-Boulan and C. H. Sung (2006). "Regulatory Dissociation of Tctex-1 Light Chain from Dynein Complex Is Essential for the Apical Delivery of Rhodopsin." Traffic.
- Zaid, H., S. Abu-Hamad, A. Israelson, I. Nathan and V. Shoshan-Barmatz (2005). "The voltage-dependent anion channel-1 modulates apoptotic cell death." Cell Death Differ **12**(7): 751-60.
- Zakharian, E. and R. N. Reusch (2003). "Outer membrane protein A of Escherichia coli forms temperature-sensitive channels in planar lipid bilayers." FEBS Lett **555**(2): 229-35.
- Zakharian, E. and R. N. Reusch (2005). "Kinetics of folding of Escherichia coli OmpA from narrow to large pore conformation in a planar bilayer." Biochemistry **44**(17): 6701-7.
- Zalk, R., A. Israelson, E. S. Garty, H. Azoulay-Zohar and V. Shoshan-Barmatz (2005). "Oligomeric states of the voltage-dependent anion channel and cytochrome c release from mitochondria." Biochem J **386**(Pt 1): 73-83.

- Zizi, M., M. Forte, E. Blachly-Dyson and M. Colombini (1994). "NADH regulates the gating of VDAC, the mitochondrial outer membrane channel." J Biol Chem **269**(3): 1614-6.
- Zizi, M., L. Thomas, E. Blachly-Dyson, M. Forte and M. Colombini (1995). "Oriented channel insertion reveals the motion of a transmembrane beta strand during voltage gating of VDAC." J Membr Biol **144**(2): 121-9.